Studies on formation, oxidative stability and plausible applications of food-grade ‘droplet-stabilised’ oil-in-water emulsions

A thesis presented in partial fulfilment of the requirements for the degree of

Doctor of Philosophy
in
Food Technology

at
Riddet Institute, Massey University
Palmerston North, New Zealand.

Okubanjo Samantha Sewuese

2019

MASSEY UNIVERSITY
TE KUNENGA KI PŪREHUROA
UNIVERSITY OF NEW ZEALAND

Riddet Institute
ADVANCING FRONTIERS IN FOOD SCIENCE

Abstract

This research was aimed at studying the structural characteristics, chemical stability and plausible functional applications of droplet-stabilised oil-in-water emulsions (DSEs). DSEs consist of oil-in-water droplets (the core) stabilised by submicron protein-stabilised oil droplets (the shell).

The first objective was to increase our understanding of their structural properties and processing factors that contribute to DSE formation using food grade ingredients. To achieve this objective, milk protein concentrate (MPC) was chosen as the emulsifier. Four MPCs with different levels of calcium were used. The surface lipid (20 %) consisted of either a low (olive oil), medium (palmolein oil) or high (trimyristin) melting surface lipid. The core lipid (20 %) consisted of either a triglyceride (soybean oil) or pure fatty acid (linoleic acid). Protein-stabilised shell emulsions were processed either via the microfluidizer (170 MPa) or two-stage homogeniser (1st stage-20 MPa; 2nd stage-4 MPa). Results of the study showed that aggregated structure of protein emulsifier, shell droplet concentration, surface and core lipid types influenced the formation and structural properties of DSEs.

The second objective focused on investigating the chemical stability of DSEs by evaluating their stability to oxidation and ability of its interfacial structure to protect polyunsaturated lipids incorporated within from oxidation. To achieve this objective, oxidative stability of high linoleic acid oil (safflower oil) stabilised by protein-coated low (olive oil), medium (palmolein oil) and high (trimyristin) melting lipid droplets was evaluated and compared with composition-matched conventional protein-stabilised safflower oil-in-water emulsion as well as a

conventional protein-stabilised safflower oil-in-water emulsion (reference emulsions). Influence of physical state of high melting lipid droplets on oxidative stability of droplet-stabilised safflower oil emulsion was also evaluated. High linoleic acid (72.54% of total fatty acids) safflower oil (20%) was used because of its high susceptibility to oxidation. Olive oil (low acidity), palmolein oil and trimyristin were chosen because of their low susceptibility to oxidation. The study showed that safflower oil oxidation in DSEs was reduced by about 40-55% in comparison to conventional emulsions. High melting surface lipid DSEs provided better protection for safflower oil than low and medium melting surface lipid DSEs.

The third objective aimed at improving our understanding of the influence of antioxidant's location in emulsions on antioxidant performance. The study was also focused on exploring a plausible functional application of DSEs by incorporating a hydrophobic antioxidant in shell droplets (at the interface) of DSEs rather than in the interior of the core unsaturated lipid. To achieve this objective, butylated hydroxyanisole (BHA) a common commercially used synthetic hydrophobic antioxidant was chosen. BHA was incorporated either in shell droplets or core droplets of DSEs. The ability of BHA to counteract oxidation when incorporated in low (olive oil) and high melting (trimyristin) shell droplets of DSEs was evaluated and compared with BHA's anti-oxidation performance when incorporated directly in core droplets (safflower oil) stabilised by low (olive oil) and high melting (trimyristin) shell droplets without BHA. Results of the study indicate that ability of BHA-in-shell DSEs to counteract oxidation of core safflower oil better than BHA-in-core DSEs is influenced by BHA's concentration and transfer mechanism to reaction sites.

The fourth and final objective was aimed at investigating mobility of a hydrophobic antioxidant incorporated at the interface of DSEs to establish their location after emulsification. The study focused on determining if a hydrophobic antioxidant incorporated in shell droplets remained localised within or migrated overtime to core droplets. The study also investigated the use of two techniques (saturated transfer difference (STD)-nuclear magnetic resonance and confocal Raman microscopy) to determine partitioning of antioxidants in DSE. To achieve this objective, confocal Raman spectroscopy technique was employed to probe antioxidant location without phase separation or destruction of DSE structure. Beta-carotene was chosen for the study for its excellent Raman scattering property. Beta-carotene was incorporated either in shell droplets (olive oil and trimyristin) or core droplets (safflower oil) of DSEs. Location and mobility of beta-carotene was evaluated after three days production. Beta-carotene migration from low (olive) and high melting shell droplets to core safflower oil was minimal.

The present study provides processing conditions and structural characteristics required to form food-grade DSEs. The study confirms and establishes the potential of DSEs to effectively protect oxidation-sensitive lipophilic bioactives incorporated within from degradation and confirms the viability of concurrent incorporation of two different bioactives in DSEs emulsions by locating one bioactive in shell droplets and the second within the core.

Acknowledgements

I am extremely grateful to my main supervisor Dr Simon Loveday for his guidance, patience and encouragement during the entire period of my research. I am profoundly grateful to him for constantly pushing me in the right direction and ensuring I did not lose focus of the main objectives.

I am very grateful to my co-supervisors Associate Professor Aiqian Ye, Professor Peter Wilde, and Distinguished Professor Harjinder Singh for their support, guidance and for sharing their vast knowledge and expertise with me. I enjoyed my discussions with each one of them and the expert insights they always provided. A special thank you to Professor Peter Wilde for his committed supervision, contributions, and guidance miles away from New Zealand. I am very grateful to him for attending all my meetings via video conference and for very prompt responses to my emails and questions.

A huge thank you to Niki Minards for training on confocal and DIC microscopy and for answering all my questions which ensured I got very clear images. I am also grateful to Sushila Pillai of Victoria University, Wellington for training on how to use Victoria University's confocal microscope when the confocal at Massey University was unavailable.

A huge thanks to Mr. Chris Hall, Dr. Peter Zhu, Ms. Janiene Gilliland and Ms. Maggie Zou for equipment trainings, assistance, advice, and co-operation in my experimental work. I wish to thank Ms. Janine Gilliland and Ms. Maggie Zou specifically for helping with chemicals, reagents and consumable orders and purchases.

I will like to particularly acknowledge and thank the following for their contribution to this research work

- Associate Professor Mark Waterland for his expertise on Raman spectroscopy and for the training on using python to analyse the Raman data and introducing me to Anaconda. I am equally grateful to him for checking the python codes and going over the data analysis.

- Sam Brooke also for his expertise on Raman spectroscopy and especially for accompanying me to Auckland university of Technology to collect the Confocal Raman data.

- Nic Mostert for writing the python codes used for Confocal Raman data analysis.

- Rob Ward for his expertise on microfluidics and for providing the microfluidic channel used for Confocal Raman spectroscopy. Also, for designing and producing the microfluidic channel holder.

- Pat Edward for his expertise on Nuclear Magnetic Resonance (NMR) and for data collection and analysis.

- Dr. Simon Loveday for oxidation data integration.

I will like to acknowledge Massey University and Riddet Institute for providing scholarships to financially support my research. I am particularly grateful to Riddet institute for travel grants to present at international conferences in Australia. I also wish to express my gratitude to Riddet institute staff Ms. Ansley Te Hiwi, Ms. Terri Palmer and Mr. John Henley-King for their administrative

support throughout the period of my research. A huge thank you to Mr. Matt Levin for providing technology support throughout the period of my research.

I am most grateful to my life-group family for the spiritual and emotional support. To my lovely friends Mr. & Dr. Fong and Maria Au-young for their emotional and spiritual support, for all the times my daughter Ana stayed with you while I attended conferences or worked in the laboratory I am extremely grateful, for all the times you had me and my family over for meals I am sincerely thankful, your support has been tremendously amazing and I really do not have the right words to express my gratitude. To my lovely friend Dr. Adeyinka for always opening your home to my daughter and I, I am sincerely grateful for all the times Ana stayed with you so I could attend conferences, work in the laboratory or focus on my research. Your love, support, and encouragement has been fantastic, and I can never thank you enough. I am also grateful to Prof. Adeyinka for the training on R statistical software and for allowing your wife Dr. Adeyinka support me throughout my PhD. To Ms. Oyelere and family I am very grateful for your support and encouragement, for all the times you helped with Ana I am so grateful. To Ms. Rowena Brown and Family, thank you so much for the encouragements and all the time you had my family over for dinner. To Mr. & Mrs. Brian and Shirley Pegler I am sincerely thankful for the emotional and spiritual support, for all the times you took my family out for lunch and for all the gifts for my daughter. I also acknowledge the emotional support of close friends who have made my stay in Palmerston North enjoyable.

This journey could never have been possible without the love and support of my family. To my parents Mr. and Mrs. Jonathan Ichaver, your words of

encouragement kept me going on this journey and I am forever grateful for the training and love. To my lovely sister Ier Jonathan-Ichaver, you have been an amazing pillar of support, for all the times we spent talking and you kept cheering me on and your words of encouragement I am extremely grateful, I always came off those calls feeling energized and ready to finish what I started, thank you so much for sharing my dream, you are indeed a priceless sister, To my sisters, Ms Doosuur Tor-anyiin and Ms. Kashimana Ichaver thank you for the emotional support and love. To my dear brother Mr. Bem Ichaver thank you for the love and words of encouragement. To my brothers-in-law Prof. Yinka Okubanjo and Mr. Yemi Okubanjo thank you so much for your love, encouragement and support, for all the chats and words of encouragement I am sincerely grateful.

Finally, I will like to acknowledge the tremendous love and support of my best friend and husband, without you Mr. Tosin Okubanjo this journey could not have been successful, thank you for sharing and living this dream with me, thank you for supporting me all the way and for the huge sacrifices you have made to ensure I accomplish this dream. To my beautiful and lovely daughter Ms. Ana Okubanjo, you are the most beautiful gift I have ever received and thank you for embarking on this long, bitter-sweet journey with me, your sweet words of encouragement motivated me every day, I looked forward to your hugs and laughter after each difficult day or moment, My darling Ana I dedicate this thesis to you and I hope that it will inspire you in future and help you accomplish your dream of becoming a scientist and inventor.

Table of Contents

List of Figures

List of Tables

List of Publications

Okubanjo, S. S., Loveday, S. M., Ye, A., Wilde, P. J., & Singh, H. (2019). Droplet-Stabilized Oil-in-Water Emulsions Protect Unsaturated Lipids from Oxidation. *Journal of Agricultural and Food Chemistry, 67*(9), 2626-2636.

Conference Presentations

Okubanjo, S. S., Loveday, S. M., Ye, A., Wilde, P. J., & Singh, H. (2019). Droplet-stabilised emulsions: colloidal and oxidative stability advantages. Presented at the 9th Australian Colloid and Interface Symposium. Hobart, Tasmania.

Okubanjo, S. S., Loveday, S. M., Ye, A., Wilde, P. J., & Singh, H. (2017). Droplet-stabilized emulsions: formulation and processing effects on structure. Presented at the 7th international symposium on delivery of functionality in complex food systems. Auckland, New Zealand.

Okubanjo, S. S., Loveday, S. M., Ye, A., Wilde, P. J., & Singh, H. (2017). Anti-oxidative properties of droplet-stabilized emulsions. Presented at the 4th international food structures, digestion and health conference. Sydney, Australia.

Chapter 1: Introduction

1.1 General Introduction

Over the years, efforts are been made to provide food solutions that deliver health benefits beyond basic nutrition. This concept birthed the functional food industry. The functional food centre in Dallas recently proposed a unique definition of functional foods as ‘’natural or processed foods containing known or unknown bioactive compounds which if present in effective, non-toxic amounts provide a clinically proven and recorded health benefit for the prevention and treatment of chronic diseases’’ (Martirosyan & Singh, 2015).

Food bioactives are defined as naturally occurring compounds in the food chain which are capable of conferring a health benefit (Biesalski et al., 2009). The biological activities of many bioactive compounds have been researched and documented, but these compounds are prone to degradations that result in a loss in their bioactive functionality. Conventional, micro/nano and multi-layered emulsions can improve the stability, solubility and bioavailability of lipid-soluble bioactives.

Over the years, a lot of research has been focused on the stability of food emulsions (C. Berton, Ropers, Bertrand, Viau, & Genot, 2012; Mezdour, Lepine, Erazo-Majewicz, Ducept, & Michon, 2008; Phan, Le, Van de Walle, Van der Meeren, & Dewettinck, 2016; Singh, Tamehana, Hemar, & Munro, 2003), and their applications (Aditya et al., 2015; Piorkowski & McClements, 2013).

The use of emulsions as carriers of active ingredients in the food industry is also on the rise. Increased protection, stability and efficient delivery of various lipophilic, hydrophilic and amphiphilic bioactives such as vitamin E, ß-carotene, ascorbic acid, resveratrol, omega 3 fatty acids etc. within emulsion-based carrier systems have been explored for applications in the food industry (Hategekirnana, Masamba, Ma, & Zhong, 2015; Hemar, Cheng, Oliver, Sanguansri, & Augustin, 2010; Tan & Nakajima, 2005; Tokle, Mao, & McClements, 2013; L. Wang et al., 2016; Yang & McClements, 2013; Yi, Li, Zhong, & Yokoyama, 2015).

Recently, a novel emulsion structure made up of oil droplets stabilised by protein-stabilised nano-droplets was reported (Ye, Zhu, & Singh, 2013). This novel emulsion which is referred to as a 'droplet-stabilised' emulsion consists of 'core lipid' stabilised by protein-coated smaller lipid droplets that are referred to as 'shell droplets'. The structure of this novel emulsion has the potential to protect and enhance the delivery and bioavailability of bioactive compounds, thus maximising their health benefits.

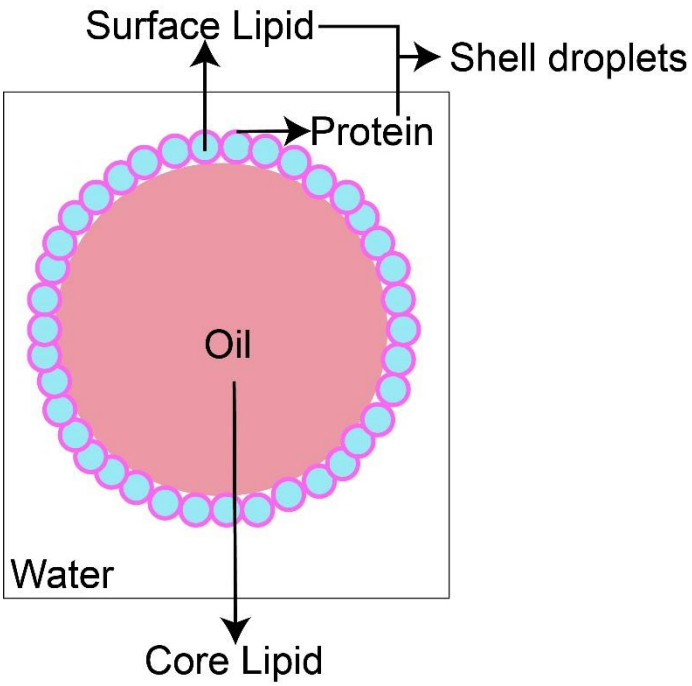

Figure 1.1: *Schematic diagram of 'droplet-stabilised' emulsion*

These functionalities if successfully explored, studied, and understood will positively contribute to the growth of the functional food industry; therefore, it is necessary to fully understand the structure, stability and plausible applications of this novel emulsion. This research sought to answer the following questions:

1. How do the emulsion composition and emulsification conditions of droplet-stabilised emulsions affect their formation and properties?

2. How does the unique interfacial structure and composition of droplet-stabilised emulsions affect their stability to oxidation in comparison to conventional emulsion?

3. How does incorporating antioxidants in the shell droplets of droplet-stabilised emulsions rather than in the core lipid affect their stability to oxidation?

4. Can droplet-stabilised emulsions be used for concurrent encapsulation of lipophilic bioactives by incorporating one bioactive in the shell droplets and another in the core droplets?

To achieve these objectives, four studies were conducted. These studies are organized into chapters in the form of manuscripts.

Chapter 2 is a detailed literature review carried out to establish current knowledge on the subject matter.

Chapter 3 describes the materials and methods used in this research as well as some of the challenges experienced with some methods and how they were overcome.

Chapter 4 (research question 1) details the structural characteristics of droplet-stabilised emulsions as affected by varying the type of emulsifier (milk protein concentrate), homogenisation conditions, surface lipid and core lipid. The aims of the study were to explore the production of droplet-stabilised emulsions with food-grade ingredients and examine the effect of formulation and processing conditions on formation and structural characteristics of DSEs. The study tested the hypothesis that the ‘formation and structural characteristics of DSEs emulsions could be greatly influenced by its composition (interfacial and core)

and processing conditions'. The study provided critical and insightful knowledge about the structural characteristics of DSEs.

Chapter 5 (research question 2) details the impact of 'droplet-stabilised emulsions' structure and interfacial composition on oxidative stability of polyunsaturated rich oil incorporated within. The aim was to examine the influence of the emulsions' interfacial structure and varied interfacial composition on the oxidative stability of PUFA rich oil. The study also investigated the effect of physical state of surface lipid on oxidative stability. The study tested the hypothesis that 'droplet-stabilised emulsions could provide greater oxidative stability than conventional emulsions and core droplets stabilised by high melting surface lipid may provide greater oxidative stability than low melting surface lipid'. The study confirmed the potential oxidation resistance of droplet-stabilised emulsions.

Chapter 6 (research question 3) describes the effect of locating antioxidants at the interface of droplet-stabilised emulsions on oxidative stability of PUFA rich oil incorporated within in comparison with locating antioxidants in the core PUFA rich oil. The aim was to explore the possibility of incorporating antioxidants in the surface lipid located at the interface of DSEs rather than the current practice of incorporating directly in PUFA oil. The study tested the hypothesis that locating antioxidant at the interface of DSEs could provide greater oxidative stability than locating antioxidant directly in the core unsaturated lipid. The study revealed that location-based antioxidant performance in DSEs was concentration dependent.

Chapter 7 (research question 4) describes new methods used to probe the location of antioxidants incorporated in DSEs and monitor the antioxidant's

mobility. The objective was to determine if antioxidant incorporated in the surface lipid would migrate or diffuse into the core lipid thus exploring the possibility of using DSEs for concurrent encapsulation of bioactives. The study revealed that antioxidant mobility from shell to core was minimal and the antioxidant remained mostly localized at the interface.

Chapter 8 summarizes the outcomes of this research and details the impact on applicable subject areas such as development of structured oil-in-water delivery systems, bioactive compound encapsulation and protection, oxidation of polyunsaturated rich oils, location-based antioxidant performance in oil-in-water emulsion systems, and functional food applications of emulsions. The chapter also highlights future research prospects based on this research.

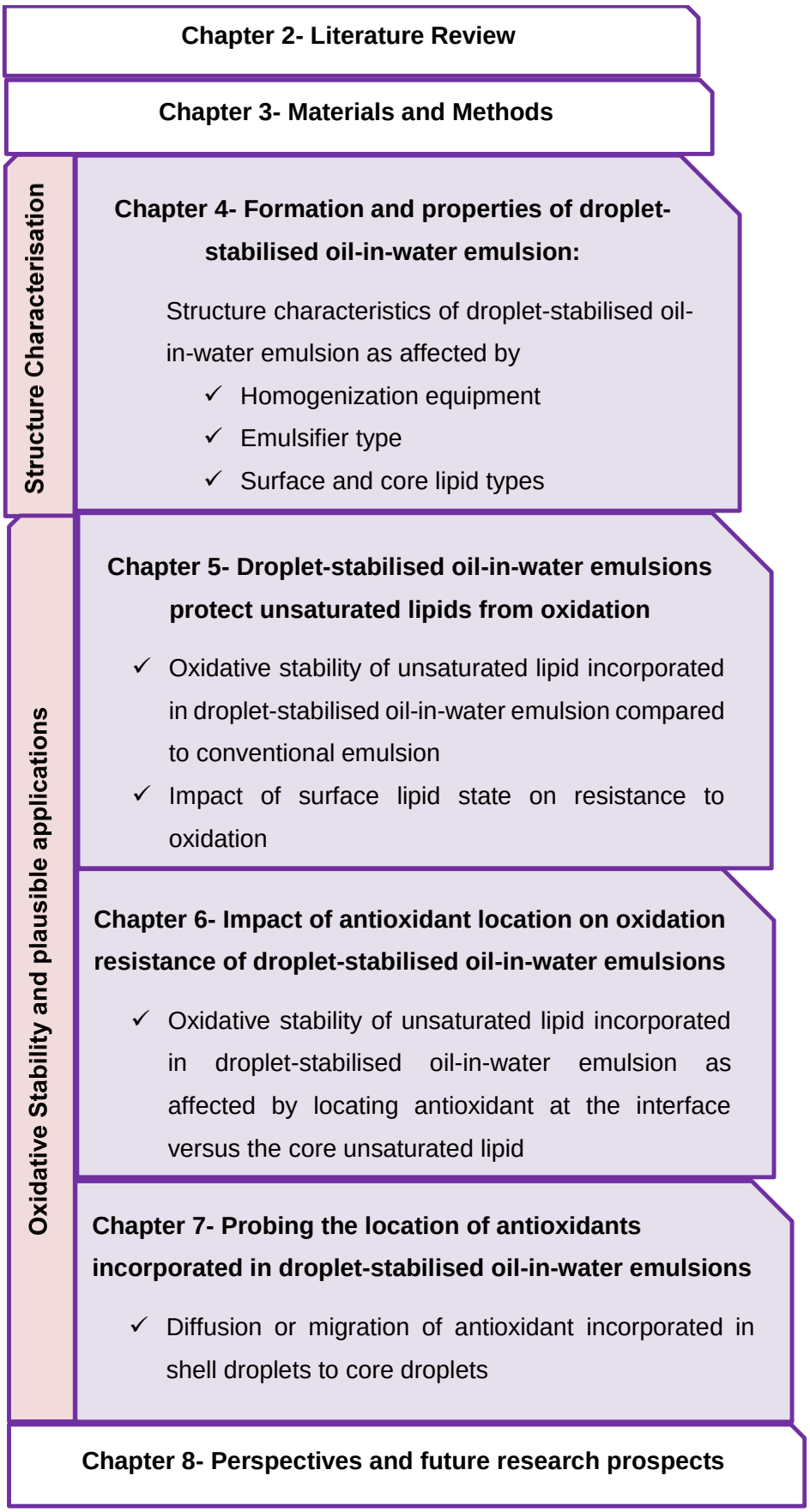

Figure 1.2 *Thesis structure*

Chapter 2: Literature Review

2.1 Classes of emulsions, preparation methods and emulsifiers

Two distinct phases are observed in an emulsion; the dispersed and continuous phase. A food system made up of oil droplets dispersed in an aqueous phase is called an oil-in-water (O/W) emulsion while water droplets dispersed in oil phase is referred to as water-in-oil emulsion (W/O). Examples of O/W food emulsions are milk, cream, mayonnaise etc. while W/O food emulsions include margarine, butter and some spreads/sauces.

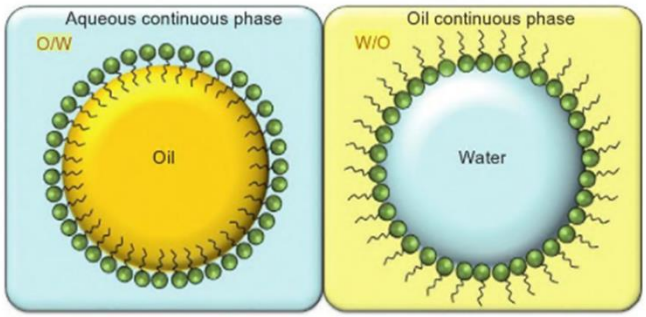

Figure 2.1 *Schematic diagram of simple (O/W & W/O).* Adapted from Chung and McClements (2015)

Generally, emulsions are classified according to the composition of their dispersed and continuous phases however, classification of emulsions have become more complex and are now also classified based on their dispersed phase size (Micro, nano, macro) or structured interfacial phase (Multi-layered, Pickering).

2.1.1 Emulsion preparation

To create an emulsion, it is usually necessary to apply mechanical energy and decrease the interfacial tension. Generally, emulsions are created by a process called homogenisation whereby the immiscible liquids are mixed by high speed or agitation (McClements, 2005). Spontaneous emulsification is another method of creating an emulsion without application of mechanical energy (Bibette, Leal-Calderon, & Schmitt, 2007; López-Montilla, Herrera-Morales, Pandey, & Shah, 2002).

2.1.2 Micro-emulsions and nano-emulsions

Micro-emulsions and nano-emulsions are terms that are sometimes used in literature without clear distinctions however; growing research involving these systems makes it necessary to provide a clear distinction. It is generally accepted that micro-emulsions are thermodynamically stable and have very small droplet sizes ($r<50nm$) whereas nano-emulsions also have small droplet sizes ($r<100nm$) but are kinetically stable (J. Rao & McClements, 2011). Anton and Vandamme (2011) in providing clarification on the differences between these systems made reference to the methods by which they are created and their resulting structure and stability. McClements (2012) in an attempt to also distinguish between the two systems highlighted the differences in their preparation, but also noted that it is often difficult to distinguish between the two systems merely by their formation methods. Both writers proposed methods such as particle size distribution that can be used to distinguish between these two systems however; the proposed methods are only indicative and not conclusive. They also emphasized that creation of nano-emulsions usually requires application of high energy.

Nano-emulsions are usually prepared by high energy methods using high pressure homogenisers. Low energy and phase inversion temperature methods have also been explored in producing nano-emulsions. T. Tadros, Izquierdo, Esquena, and Solans (2004) compared the formation of nano-emulsions using high pressure homogenisers and phase inversion temperature (PIT) methods. The emulsions produced by the homogenisers were more stable to Ostwald ripening over those made by the PIT method even though it was not clear if the composition of the nano-emulsions made with homogenisers was identical to the PIT produced nano-emulsions. On the other hand, Solans, Izquierdo, Nolla, Azemar, and Garcia-Celma (2005) emphasized that efficient formation of nano-emulsions can be achieved by low energy methods however it was evident that the size of droplets was largely dependent on the structure of the surfactant phase. The ultimate goal in selecting a method of preparing emulsions should be its stability and final application moreover, methods of overcoming high droplet polydispersity associated with oil-in-water nano-emulsions produced by low-energy methods are proposed in literature (Gutiérrez et al., 2008).

2.1.3 Double Emulsions

Over the years, more complex emulsions have emerged which consists of multiple emulsions (Figure 2.2) referred to as water-in oil-in water (W/O/W) or oil-in-water-in-oil (O/W/O). In this case, the dispersed phase is dispersed within a larger dispersed phase which is in turn dispersed in the continuous phase (Muschiolik, 2007).

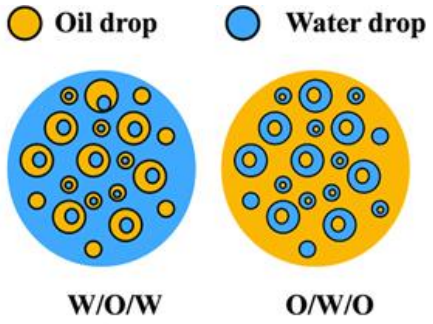

Figure 2.2: *Schematic diagram of double emulsions (W/O/W & O/W/W). Adapted from Martínez-Palou et al. (2011)*

The formation of double emulsions typically involves two stages however; other methods of preparation have been explored. Sachio Matsumoto carried out a series of studies on the preparation and stability of double emulsions specifically water-in-oil-in-water (W/O/W) emulsions and their potential applications in foods (Matsumoto, 1983, 1985, 1986; Matsumoto, Koh, & Michiura, 1985). In these studies three main methods of forming double emulsions were discussed; mechanical agitation, phase inversion and the two-stage emulsification process. The formation of W/O/W emulsions by these methods requires that attention is given to the ratio of hydrophobic and hydrophilic emulsifiers employed. It is imperative to optimize the concentration of emulsifiers, as the structure of the emulsions has a tendency to change entirely once the optimal ratio of hydrophilic to hydrophobic emulsifier is exceeded. Double emulsions formed by these methods are highly prone to instability, as the hydrophobic emulsifiers tend to migrate over time to the continuous aqueous phase leading to a breakage in the oil layer adsorbed on the surface of the aqueous phase.

Matos, Gutiérrez, Coca, and Pazos (2014) produced double emulsions for encapsulation of trans-resveratrol by mechanical agitation and membrane emulsification. The results showed higher stability with emulsions produced by

mechanical agitation over those made by membrane emulsification, but higher release of bioactive was obtained with the latter over the former. These results were not surprising as double emulsions were formed by mechanical agitation where high energy was applied therefore, it is expected that stability with membrane emulsification where low energy was applied will differ.

2.1.4 Pickering emulsions

Pickering emulsions (Figure 2.3) are emulsions stabilised by solid particles that are smaller than the emulsion droplets (Berton-Carabin & Schroën, 2015; Chevalier & Bolzinger, 2013).

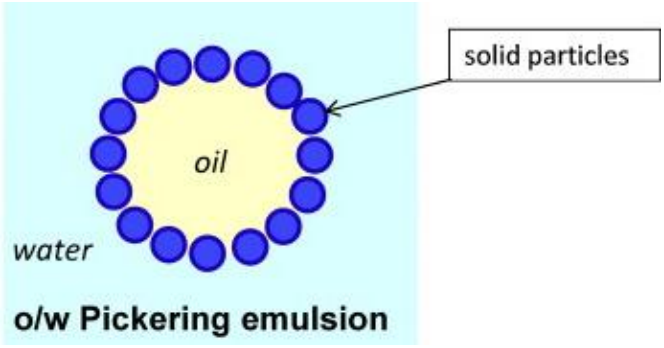

***Figure 2.3**: Schematic diagram of Pickering emulsion. Adapted from Chevalier and Bolzinger (2013)*

Pickering (1907) was the first to introduce the concept of emulsions stabilised with solid particles. He emphasized that emulsions stabilised with organic substances/surfactants separate over time or as soon as the emulsifier is destroyed by addition of acid or certain salts and highlighted the benefit of high interfacial adsorption energy of solid particles which are difficult to displace once adsorbed at the interface. Chevalier and Bolzinger (2013) reviewed the possible methods of preparing Pickering emulsions, in most methods, nanoparticles are

dispersed in either the oil or aqueous phase depending on the type of emulsion desired. The type of nanoparticle employed depends on the type of emulsion for example hydrophilic particles are dispersed in aqueous phase for O/W emulsions and both hydrophilic and hydrophobic particles are used for double emulsions (W/O/W), in all cases emulsification was achieved by high shearing except for preparation of solid particle stabilised double emulsions in which final emulsification was done by low shearing. The review revealed that Pickering emulsions can easily be used in many applications to replace classical emulsions and provide improved stability. Aveyard, Binks, and Clint (2003) also used similar methods in their study on emulsions stabilised with colloidal particles and established that hydrophilic particles create oil-in-water emulsions while hydrophobic particles create water-in-oil emulsions.

2.1.5 Multi-layered emulsions

Multi-layered emulsions (Figure 2.4) were designed as a strategy to improve emulsion stability against droplet aggregation. Multi-layered emulsions are typically made up of several layers of emulsifiers and this is achieved by a layer-by-layer (LBL) electrostatic deposition principle (Beicht, Zeeb, Gibis, Fischer, & Weiss, 2013; Gudipati, Sandra, McClements, & Decker, 2010; Jo, Chun, Kwon, Min, & Choi, 2015).

Multi-layered emulsions are typically prepared by a two stage process; first a primary emulsion stabilised by an ionic emulsifier is made by homogenisation secondly, a polymer with an opposite charge is electrostatically deposited onto the charged primary lipid droplets and this can be repeated to achieve the desired number of layers (Aoki, Decker, & McClements, 2005; Guezey & McClements,

2006; Guzey & McClements, 2006; Thanasukarn, Pongsawatmanit, & McClements, 2006).

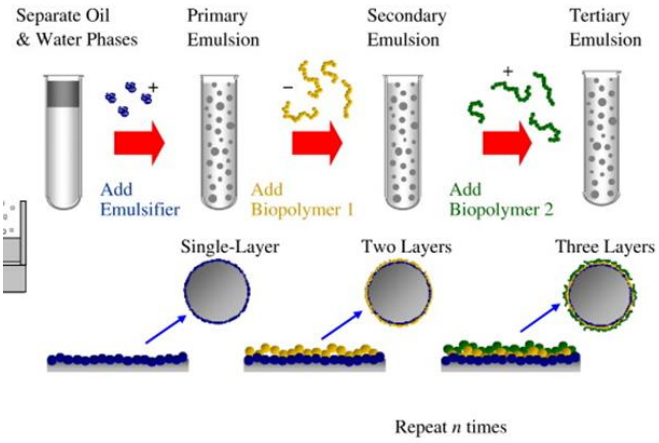

***Figure 2.4**: Schematic diagram of multi-layered emulsion and preparation steps. Adapted from McClements and Li (2010)*

2.1.6 Emulsifier types

Emulsifiers are surface-active molecules capable of stabilizing emulsions and protecting emulsion droplets from flocculation or coalescence (McClements, 2005). Surfactants are surface-active agents made up of a non-polar (hydrophobic) portion attached to a polar (hydrophilic) portion (T. F. Tadros, 2014). The oil-water interfaces in emulsions are stabilised with surfactants or emulsifiers which are both amphiphilic molecules used to modify the surface tension between two phases (Rosen & Kunjappu, 2012; T. Tadros, 2013).

Norn (2014) classified emulsifiers based on their nature or charge, and their hydrophilic-lipophilic balance (HLB). The hydrophilic-lipophilic balance is a classification system introduced by Griffin (1949) which measures the extent to which a surfactant is hydrophilic or lipophilic. On the basis of charge, Norn (2014) classified emulsifiers as non-ionic, cationic, anionic and zwitterionic. The non-

ionic emulsifiers are mostly used in foods and include monoglycerides, diglycerides, polysorbates and sorbitans etc. Anionic emulsifiers include lactylates and carboxylates however they are rarely used in foods. The most common zwitterionic emulsifier is lecithin.

***Table 2.1**: Food Emulsifiers*

Food emulsifiers	Common examples
Surfactants	Mono-diglycerides, polysorbate 60, sodium stearoyl-lactylate, lecithin, sorbitan monostearate
Biopolymers	Proteins: Milk proteins, meat proteins, egg proteins Polysaccharides: modified starch, gum Arabic, cellulose (HPMC)

It is important to note that not only surfactants are used as emulsifiers. Biopolymers which also exhibit good surface activity are used as emulsifiers. The most widely used include proteins and polysaccharides that display amphiphilic properties. Mixtures of polymers are also used to stabilise emulsions (Akhtar & Dickinson, 2007; Dickinson & Galazka, 1991; Einhorn-Stoll, Ulbrich, Sever, & Kunzek, 2005).

2.2 Structure of food emulsions

The structure of emulsions can be very complex as they are usually not just simple mixtures of lipids and water. Emulsions usually contain polysaccharides, sugars, flavouring agents, texture modifiers, proteins, and surfactant molecules etc., which contribute greatly to the complexity of their structure. These ingredients also interact in different ways with emulsion droplets giving rise to the structure of the product. For example, there is a marked difference in structure when cream dessert is produced with a polysaccharide and when it is produced without a polysaccharide.

The physical and chemical stability of an emulsion greatly depends on the structure and composition of the interfacial phase, which also has a significant influence on how effective the emulsion will be in protecting or enhancing delivery of bioactives incorporated within.

2.2.1 Physical stability

Emulsion stability refers to the potential of an emulsion to resist various forces or interactions within the system which could lead to changes in its state, structure or composition over time. When an emulsion is unable to resist changes in its physiochemical properties, it is said to be unstable.

Stability of emulsions is sometimes defined in relation to their thermodynamic or kinetic stability. An emulsion is said to be thermodynamically stable when the free energy of the droplets in aqueous phase is lower than the separate phases (oil, water and surfactants) and unstable when the free energy is higher than the separate phases. A kinetically stable emulsion has higher free energy than its

component phases, but an energy barrier inhibits droplet coalescence, thus preventing it from reverting to separate phases (McClements, 2012).

Emulsions become unstable due to physical and chemical processes that occur within the system. The physical processes responsible for emulsion instability include creaming, sedimentation, flocculation, coalescence, phase inversion, and Ostwald ripening (Figure 2.5) while the chemical processes include oxidation and hydrolysis. It is possible that two or more of these processes will occur in an emulsion at the same time.

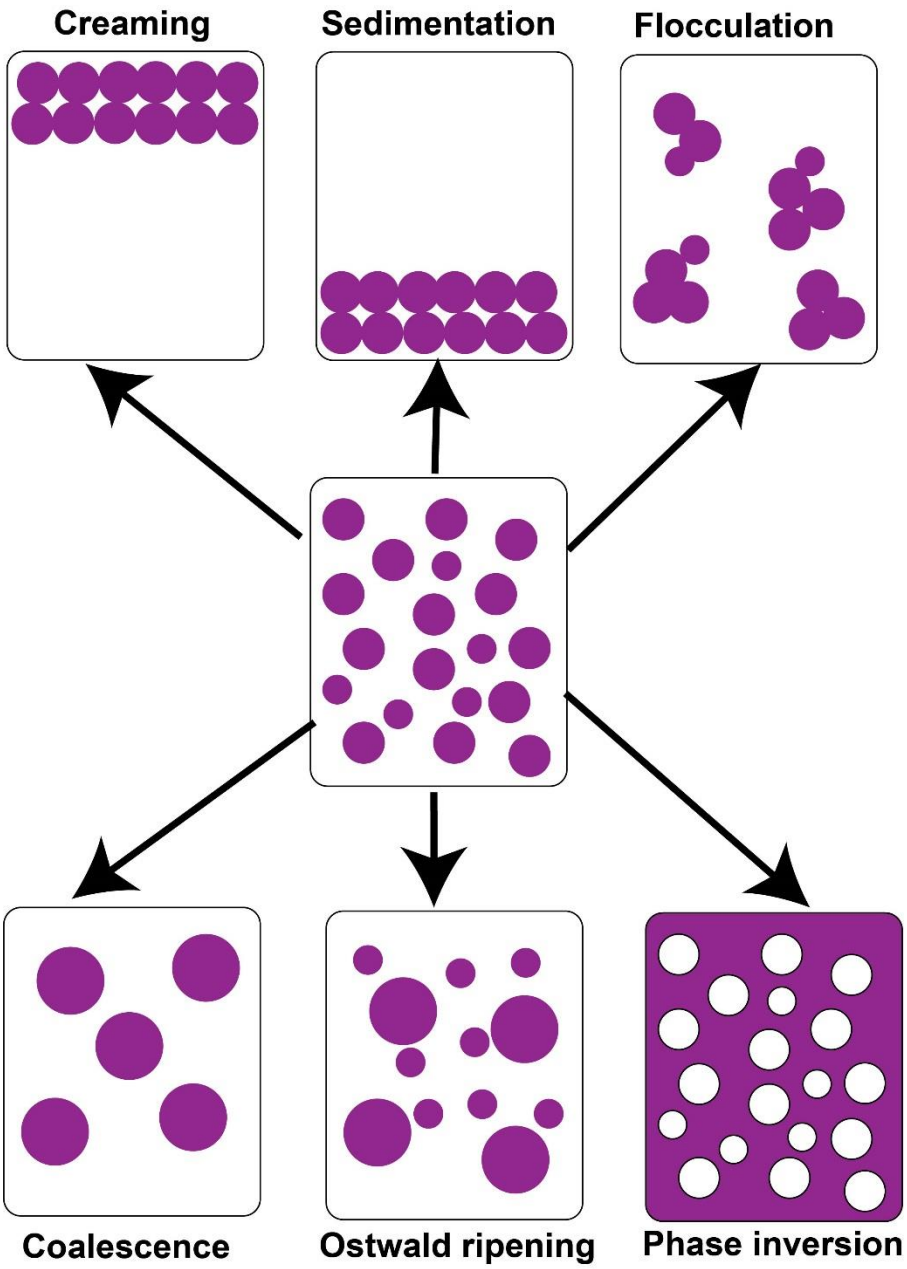

Figure 2.5 *Emulsion instability schematics.*

Oil and water have different densities hence there is usually the effect of gravitational force which leads to phase separation either by creaming or sedimentation.

1. **Creaming**: This phenomenon occurs when there is a difference in density between the droplets and the liquid in which they are dispersed

such that when the density of the droplets is lower than the liquid, the droplets travel upwards to the surface of the system. This is very common in oil-in-water emulsions because oils usually have lower densities than water, although density differences can be overcome with interfacially adsorbed ‘weighting agents’, i.e. polymers that increase the mass of droplets.

2. **Sedimentation**: This is because of a higher droplet density over that of the continuous phase. In this case the droplets settle to the bottom of the container.

Emulsion droplets are constantly in motion due to kinetic energy (Brownian motion) or gravitational forces (creaming/sedimentation). As droplets move, they tend to collide with each other. Upon collision, two droplets either move apart, flocculate or coalesce.

3. **Flocculation**: This is when droplets aggregate such that each droplet retains its individual identity. This process can be reversible or irreversible. Flocculation increases emulsion viscosity which may be undesirable in some foods as it leads to higher instability thus reducing the shelf life (Demetriades, Coupland, & McClements, 1997). Bridging flocculation is a type of flocculation that occurs when an electrically charged high molecular weight polymer adsorbs to the surface of two or more droplets through electrostatic interactions, forming bridges (Dickinson, 2003). On the other hand, depletion flocculation occurs due to osmotic effects resulting from the exclusion of non-adsorbing

polymers from regions surrounding two droplets, this leads to an increase in the attractive forces between the droplets and eventual flocculation by depletion (McClements, 2004).

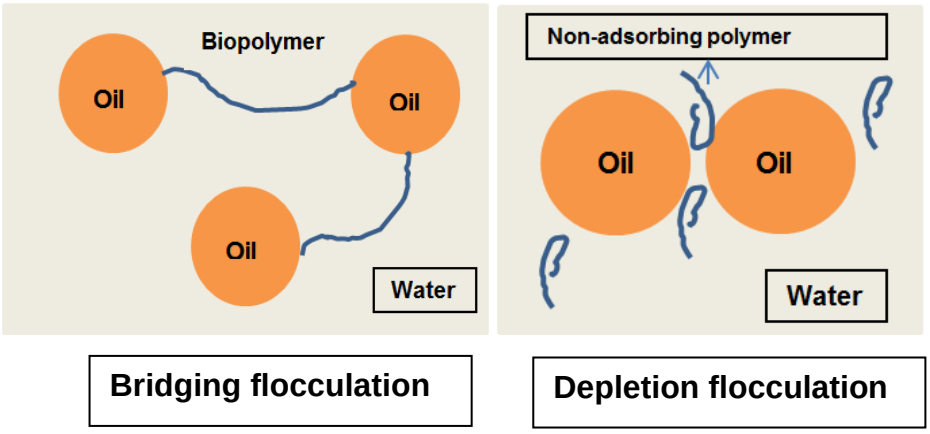

Figure 2.6 *Bridging and depletion flocculation schematics*

4. **Coalescence**: This is a process in which two or more droplets merge together into a single bigger droplet as a result of collision, and it is irreversible. This interaction results in a decrease in the area of oil-water interface. This droplet interaction is not always between the liquid of two droplets; it could also be between a solid fat crystal of one droplet and liquid of the other droplet this type of interaction is referred to as 'partial coalescence'. Partial coalescence will happen in an emulsion only when there are partially crystalline droplets. This mechanism when controlled can be desirable in the production of some foods such as ice cream where the emulsion has to be cooled thus resulting in development of fat crystals hence when coalescence occurs it improves the texture of the product (Goff, 1997).

5. **Ostwald ripening:** This is a phenomenon which has been described as occurring in solid and liquid solutions. It is described by Kabalnov (2001) as a process whereby smaller particles dissolve and larger particles grow at the expense of the smaller ones because solubility increases due to small radius of curvature.

   In emulsions, Taylor (1998) describes Ostwald ripening as the growth of a droplet at the expense of a smaller droplet arising from a difference in radius of curvature of the droplets which is inversely related to surface pressure of the dispersed phase. He states that as the smaller droplets dissolve the average radius of the droplets increases with time.

6. **Phase inversion:** This is when a system inversion occurs such that for example an oil-in-water emulsion changes to a water-in-oil emulsion or the opposite way. Phase inversion is usually caused by changes in the composition or environment of an emulsion. Phase inversion in food emulsions is reported to be induced by surfactants caused by a change in molecular geometry or induced by fat-crystallization caused by partial coalescence (McClements, 2005). This type of instability has a negative impact on the sensory properties of foods but is also very important in the production of foods like butter and margarine.

The stability of an emulsion has important consequences on the digestion and functionality of the emulsion or its components. As the utilization of emulsions as delivery systems of bioactive compounds expands, the effect of stability on their ability to perform efficiently cannot be overemphasized.

Golding and Wooster (2010) pointed out that the stability of emulsions in the digestive tract plays a role in lipid digestion and gastric emptying rate. For example, emulsions that have undergone phase separation under gastric conditions have faster gastric emptying which will subsequently affect satiety signals (Marciani et al., 2007).

The structure of emulsions can change very easily during storage, processing and digestion. These changes may result in any one of the unstable forms discussed above. According to Yao, Xiao, and McClements (2014), structure of micro-emulsions may be altered as they encounter bile salts or minerals while indigestible nano-emulsions are more likely to keep the core material intact as they pass through the gastric environment.

Table 2.2*: Factors influencing the physical stability of emulsions*

Emulsion Instability	Driving forces	Control measures	References
Gravitational separation (creaming and sedimentation)	• Difference in density between droplets and surrounding liquid. • Increased droplet poly-dispersity.	• Decrease droplet size • Increase droplet concentration and viscosity of continuous phase	McClements (2005)
Flocculation	• Droplet collisions due to Brownian motion, gravitational separation and shearing.	• Retard or decrease collision frequency. • Prevent unnecessary agitation. • Increase viscosity of continuous phase. • Increase repulsive forces (e.g. electrostatic, steric) between droplets over attractive.	McClements and Weiss (2005)
Coalescence	• Film rupture and thinning. • Emulsifier type. • Processing and storage conditions.	• Prevent interfacial membrane rupture. • Increase repulsive forces.	McClements (2005)
Ostwald ripening	• Increased solubility of molecules in droplet in continuous phase. • Increased diffusion of molecules in droplet to aqueous phase.	• Prevent solubility of dispersed phase in continuous phase. • Decrease interfacial tension. • Minimize droplet polydispersity	Walstra (2003); Weers (1998)
Phase Inversion	• Temperature • Applied mechanical energy. • Surfactant type and composition. • Fat crystallization.	• Prevent partial coalescence. • Select suitable emulsifier and concentration.	McClements and Weiss (2005)

2.2.2 Chemical Instability

Emulsions are susceptible to chemical reactions that could negatively impact their sensory and functional properties. These reactions include lipid oxidation and biopolymer hydrolysis. Lipid oxidation will be discussed extensively in the next sections.

2.3 Lipid oxidation

Lipid oxidation can be defined as the removal of one or more electrons from lipids either by the addition of oxygen or hydrogen abstraction. It is a complex process that involves the production of free radicals and hydroperoxides, alterations in the double bond arrangement of unsaturated lipids, and final breakdown of the lipid.

The rate of lipid oxidation is influenced by catalysts or factors such as light, metals, enzymes and temperature. Therefore, lipids could undergo auto-oxidation, thermal oxidation, enzymatic oxidation and photo-oxidation depending on the environmental conditions to which they are subjected.

Mechanism of lipid oxidation in emulsions differs from that in bulk oil because in emulsions, the aqueous phase may contain pro-oxidants which are not usually present in bulk oils and these pro-oxidants may partition within the different phases in emulsions. Oxidation rates in emulsions are reported to be usually faster in emulsions than bulk oils because of the large surface area of interfaces created in emulsions which allows interaction of the aqueous and oil phases (Logan, Nienaber, & Pan, 2013).

2.3.1 Auto-oxidation

Auto-oxidation as the name implies is a spontaneous reaction. It involves the reaction of atmospheric oxygen with lipids, and unsaturated lipids are very prone to these reactions. Autoxidation and thermal oxidation are chain reactions that involve three stages; initiation, propagation and termination.

Kanner, German, Kinsella, and Hultin (1987) reported three possible pathways by which lipid oxidation can be initiated as shown below.

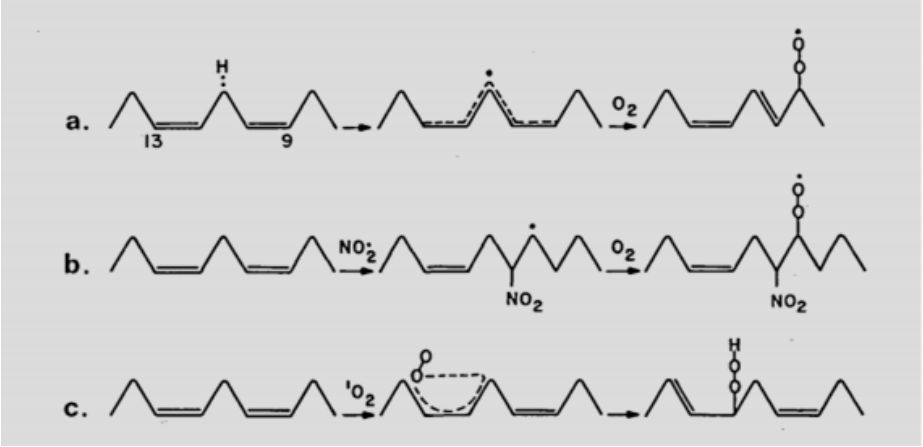

Figure 2.7 *Initiation of lipid oxidation pathways- a) Initiation by hydrogen abstraction; b) Initiation by free-radical attack on a double bond; C) Initiation by singlet oxygen. Adapted from Kanner et al. (1987).*

Initiation: Atmospheric oxygen is in the triplet ground state therefore to react with lipid molecules it requires excitation or activation. Three mechanisms by which oxygen can be activated have been identified;

1. Formation of singlet oxygen (Excited state oxygen)
2. Formation of partially reduced or activated oxygen species like hydrogen peroxide, superoxide anion, or hydroxyl radical.
3. Formation of active oxygen-iron complexes like ferric-oxygen-ferryl complexes.

At initiation, a hydrogen radical is removed from an unsaturated fatty acid (LH) resulting in a free lipid radical ($L^{\bullet}$).

$$LH \longrightarrow L^{\bullet} + H^{\bullet} \qquad (Eq.\ 2\text{-}1)$$

Propagation

During the propagation stage the free radical ($L^{\bullet}$) in turn reacts with oxygen to form an unstable lipid peroxyl radical ($LOO^{\bullet}$), which reacts with lipids by abstracting hydrogen from unsaturated fatty acid to form hydroperoxide (LOOH) and an unstable lipid radical ($L^{\bullet}$). This lipid radical again reacts with oxygen initiating another free radical resulting in a chain reaction. Propagation gives rise to the chain reaction in oxidation. It involves the following:

- Radical coupling with oxygen: $L^{\bullet} + {}^{3}O_2 \longrightarrow LOO^{\bullet}$ *(Eq. 2-2)*

- Atom or group transfer: $LOO^{\bullet} + LH \longrightarrow LOOH + L^{\bullet}$ *(Eq.2-3)*

- Fragmentation: $LOO^{\bullet} \longrightarrow L^{\bullet} + {}^{3}O_2$ *(Eq. 2-4)*

Hydroperoxides are unstable so they continue to degrade and produce radicals. According to Fereidoon Shahidi and Wanasundara (2008) there is an induction period when hydroperoxide formation is low.

Termination

To terminate the propagation chain reaction, two types of reactions are possible; radical-radical coupling and radical-radical disproportionation. These reactions

involve the formation of non-radical products such as ketones, aldehydes etc. (Erickson, 2002).

$$L^{\bullet} + L^{\bullet} \longrightarrow LL \qquad \textit{(Eq. 2-5)}$$

$$L^{\bullet} + LOO^{\bullet} \longrightarrow LOOL \qquad \textit{(Eq. 2-6)}$$

$$LOO^{\bullet} + LOO^{\bullet} \longrightarrow LOOL + {}^{3}O_2 \qquad \textit{(Eq. 2-7)}$$

Lipid oxidation pathways are not the same for every food matrix it depends on the nature of the molecules present and the environmental conditions (Erickson & Sista, 1996). The mechanisms of lipid oxidation differ for different bulk lipids so it will also not be the same for emulsions (Naz, Siddiqi, Sheikh, & Sayeed, 2005).

The rate of oxidation of fatty acids increases with an increase in their unsaturation. The rate of oxidation in terms of oxygen uptake in oleic (18:1), linoleic (18:2), and linolenic (18:3) acid is in the order of 1:50:100 with respect to oxygen consumption and 1:12:25 with respect to peroxide production (Hsieh & Kinsella, 1989). Hsieh and Kinsella also reported that the initial rate of linolenic oxidation was twice that of linoleic which is attributed to the number of double bonds present.

Triglycerides yield oxidation products that reflect their fatty acid composition. Figure 2.8 shows an example of oxidation reactions of linoleic acid producing hexanal and concentrations of the products (conjugated diene, hydroperoxide and hexanal) shown in the pathway provide a good indication of oxidative deterioration of lipids rich in linoleic acid.

Lipids when subjected to high temperatures are highly susceptible to auto-oxidation resulting in rapid formation and decomposition of hydroperoxides. Low temperature treatments does not mean there will be no oxidation, the formation of autoxidation products are just slower in this case (Choe & Min, 2006).

2.3.2 Enzymatic oxidation

Lipase enzymes present in lipids breakdown triglycerides into free fatty acids. Lipoxygenase which is an iron containing enzyme found in plants and animals is capable of catalysing (with polyunsaturated fatty acid as a suitable substrate) the reaction between free fatty acid and oxygen thus forming hydroperoxide (LOOH).

2.3.3 Photo-oxidation

Photo-oxidation occurs when there is a reaction between light-activated singlet oxygen and unsaturated fatty acids, leading to the formation of hydroperoxides. Singlet oxygen is a high-energy form of oxygen that is highly reactive with organic compounds. It is not a radical compound therefore reacts mostly with non-radical double-bonded compounds. Singlet oxygen is formed from triplet oxygen (ground state atmospheric oxygen) when photosensitizers present in foods absorb energy from light and transfer this energy to triplet oxygen. The photo-sensitization mechanisms are classified as type I and type II (Davidson, 1979; Min & Boff, 2002b).

Sensitization occurs when molecules usually called sensitizers (Sen) such as chlorophylls, riboflavin, myoglobin etc present in lipids, get sensitized by light (absorb light) and become excited (^{1}Sen*). The excited sensitizer may also be

converted to a triplet sensitizer (^{3}Sen*) by a process called intersystem crossing (Kanofsky, 2016).

$$\text{Sen} \xrightarrow{h\nu} {}^1\text{Sen}^* \xrightarrow{\text{Intersystem crossing}} {}^3\text{Sen}^* \qquad \textit{(Eq. 2-8)}$$

Type I Mechanism: The excited sensitizer (^{3}Sen*) directly abstracts hydrogen from a fatty acid and produces a free-radical this mechanism is most likely to occur under low oxygen concentrations. The free radical in turn initiates the free radical chain reaction.

$$^3\text{Sen}^* + \text{LH} \longrightarrow {}^{\bullet}\text{Sen H} + \text{L}^{\bullet} \qquad \textit{(Eq. 2-9)}$$

Type II Mechanism: When oxygen is readily available, the excited sensitizer (^{3}Sen*) is short-lived and thus they emit or transfer the energy absorbed to triplet oxygen ($^3O_2$) generating singlet oxygen ($^1O_2$). Singlet oxygen directly reacts with the double bonds of unsaturated fatty acids and produces conjugated and non-conjugated hydroperoxides (Edwin N. Frankel, 2012).

$$^3\text{Sen}^* + {}^3O_2 \longrightarrow {}^1O_2 + \text{Sen} \qquad \textit{(Eq. 2-10)}$$

$$^1O_2 + \text{LH} \longrightarrow \text{LOOH} \qquad \textit{(Eq. 2-11)}$$

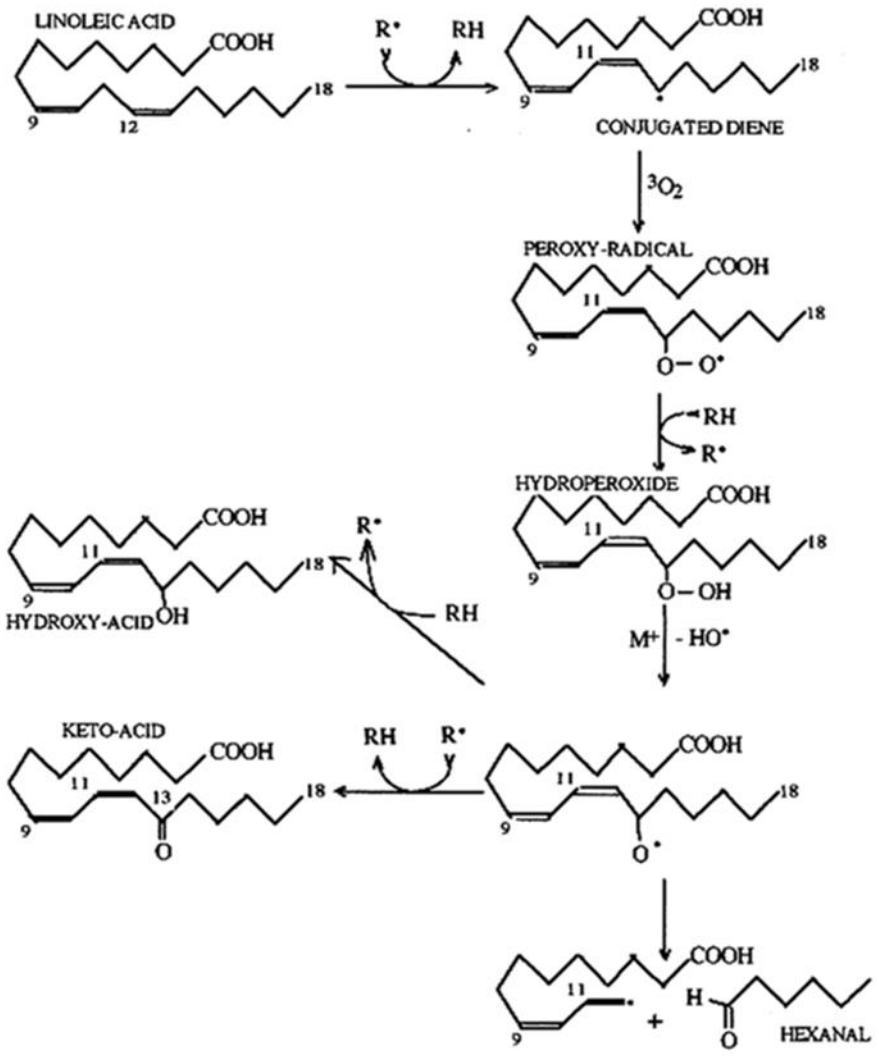

***Figure 2.8**: Oxidation pathway of linoleic acid. Adapted from Wheatley (2000)*

2.4 Structural factors affecting the oxidative stability of emulsions

The oxidative stability of emulsions must be given good attention as it has subsequent consequences on emulsion functionality.

S. J. Lee, Choi, Li, Decker, and McClements (2011) evaluated the oxidative stability of nanoemulsions and conventional emulsions stabilised by whey protein isolates. The emulsions were prepared by a two-step homogenisation process and its oxidative stability was monitored over four weeks' storage at 37°C. The rate of oxidation was higher in nano-emulsions. The authors expected slower oxidation in the nano-emulsion as a consequence of higher protein concentration (some amino acids have antioxidant effects) and attributed the observed faster oxidation to pro-oxidant impurities in the protein.

Haahr and Jacobsen (2008) compared oxidative stability of fish oil-in-water emulsions stabilised by tween 80, citrem, lecithin and caseinate. The emulsions were prepared by a two-step process and oxidation monitored over 12 days' storage in the dark at 20°C. The authors reported slightly higher oxidation rates in citrem and tween emulsions which had smaller droplet sizes over lecithin and caseinate emulsions which had larger droplets however, they emphasized that differences in oxidative stability between these emulsions could not have been solely due to differences in droplet sizes. Similarly, C. Jacobsen et al. (2000) investigated the influence of droplet size on oxidative stability of fish oil-enriched mayonnaise, and reported lower concentrations of volatile oxidation compounds in mayonnaise with large oil droplets and higher concentrations in mayonnaise with smaller droplets during storage at 20°C. The authors attributed the observed

faster oxidative deterioration in mayonnaise with smaller droplet sizes to increased interfacial area.

An opposite trend of faster oxidation in emulsions with smaller droplet sizes over larger droplet sizes was reported by Nakaya, Ushio, Matsukawa, Shimizu, and Ohshima (2005). They observed lower levels of hydroperoxides for emulsions with smaller droplet sizes (0.8μm) over bigger size (12.8μm) indicating improved oxidative stability with smaller droplets. This improved stability was attributed to a 'wedge effect' in smaller droplets which prevents mobility of lipid molecules whereas in larger droplets mobility of lipid molecules is not retarded by this effect. This wedge effect is thought to be imposed by hydrophobic residues of emulsifier thus inducing shorter oxidation chain reactions in small droplets. Walker, Decker, and McClements (2015) also examined the effect of droplet size and surfactant concentration on oxidative stability of fish oil-in-water emulsions prepared by spontaneous emulsification (low energy) and microfluidization (high energy). Additional surfactant was added to portions of the prepared emulsions to produce emulsions with large droplets and high surfactant concentration. Oxidation rate was monitored over 14days storage in the dark at 55°C. The authors expected a higher rate of oxidation in emulsions with smaller particle sizes because of increased surface area of the oil droplets but observed slightly higher hydroperoxide values in low-energy emulsions with added surfactant which had greater particle size, and attributed the observed higher oxidation rate to possible partitioning of reactants into surfactant micelles which altered the lipid oxidation rate. Lethuaut, Métro, and Genot (2002) also investigated the influence of droplet size on oxidative stability of protein stabilised emulsions and reported higher conjugated diene concentrations in emulsions with smaller droplet sizes over

emulsions with larger droplet sizes however, the authors also report that the faster oxidation rates in emulsions with smaller sizes may have been partially counteracted by antioxidant activity of adsorbed proteins which led to similar concentrations of conjugated dienes between emulsions with small and large droplet sizes at a certain point.

The effect of droplet size on oxidative stability appears to be controversial however from these literatures, it is apparent that the composition of the emulsions and methods of preparation were different even though it is possible that the structures of these emulsions were similar, it shows that the oxidative stability of an emulsion is not only dependent on the droplet size but on other factors such as the composition of the interfacial layer, emulsifier type, oil phase type and transportation mechanisms of reactants. Moreover, Osborn and Akoh (2004) investigated the influence of droplet size of emulsions on oxidative stability and reported that droplet size had no effect on lipid oxidation. Also examined effect of droplet size on oxidative stability of soybean oil and fish oil-in-water emulsions and reported reverse effects of droplet size whereby oxidative stability of fish oil-in-water emulsions increased with decreasing droplet size while the reverse effect was observed in soybean oil-in-water emulsions.

The interfacial phase plays an important role in the oxidative stability of emulsions in fact it is believed to be the gateway between pro-oxidants or hydrophobic phase and the lipid phase (C. Berton, Ropers, Viau, & Genot, 2011; Silvestre, Chaiyasit, Brannan, McClements, & Decker, 2000). Hence it is no wonder that structuring the interfacial phase of emulsions have become a popular approach in designing emulsions.

Kargar, Spyropoulos, and Norton (2011) monitored the oxidation of emulsions stabilised by tween 20 and sodium caseinate over seven days. Oxidation rates were lower for protein-stabilised emulsions over tween 20-stabilised emulsions and this was attributed to the ability of proteins to form a thicker interfacial layer. The authors also monitored oxidative stability of Pickering emulsions stabilised by silica particles and reported that the thick interfacial layer formed by Pickering particles also reduced lipid oxidation rate in Pickering emulsions compared to emulsions stabilised by tween 20. In this study, the effect of other factors such as oil-phase fraction, pH, and emulsifier concentration in the aqueous phase were assessed and all these seemed to influence the rate of lipid oxidation.

It is also interesting to note in Kargar et al's study that as the concentration of Pickering particles increased, the droplet size decreased leading to a decrease in oxidation. This signifies that contact between the lipid phase and pro-oxidants must have been minimized by the particles at the interface. Some of the factors that affect lipid oxidation in emulsions include; chemical structure of lipids, quality of ingredients, oxygen concentration, interfacial characteristics, and interactions with aqueous phase (McClements & Decker, 2000). All these factors should be taken into consideration in preventing lipid oxidation in emulsions.

Flaxseed oil-in-water emulsions stabilised by multi-layered membranes (sodium caseinate and pectin) at pH between 3 and 5 showed better oxidative stability than single layered sodium caseinate stabilised emulsion as evidenced from the levels of hydroperoxides and TBARS concentration (Kartal, Unal, & Otles, 2016). The improved oxidative stability was attributed to the limited interactions between the oil phase and pro-oxidants in the continuous phase. Addition of zein

hydrolysates (ZH) to oil-in-water emulsions stabilised by myofibrillar protein (MP) provided a more compact interface which improved oxidative stability compared to MP-stabilised emulsions without zein hydrolysates (Li, Kong, Liu, Xia, & Chen, 2017).

2.5 Antioxidants

Antioxidants are compounds capable of inhibiting or decreasing oxidation. Their mode of action has been classified into two categories; primary antioxidants and secondary antioxidants (Ingold, 1968). However, some antioxidants act via more than one mechanism thus are referred to as multiple-function antioxidants (Reische, Lillard, & Eitenmiller, 2002).

2.5.1 Primary antioxidants

They are also referred to as chain-breaking antioxidants. Their mode of action involves accepting or reacting with free radicals to form more stable products thus inhibiting the initiation stage or disrupting the propagation chain reaction of autoxidation. They do this by donating hydrogen to the free radicals (Eq.12 or 13) thus forming stable lipid products and antioxidant radicals ($A^{\bullet}$) or even reacting directly with lipid radicals (Eq.14).

$$LOO^{\bullet} + AH \longrightarrow LOOH + A^{\bullet} \qquad \textit{(Eq. 2-12)}$$

$$LO^{\bullet} + AH \longrightarrow LOH + A^{\bullet} \qquad \textit{(Eq. 2-13)}$$

$$L^{\bullet} + AH \longrightarrow LH + A^{\bullet} \qquad \textit{(Eq. 2-14)}$$

A molecule can act as a primary antioxidant if it donates hydrogen rapidly to lipid radicals and the resulting antioxidant radical ($A^{\bullet}$) is more stable than the lipid radical or is converted to more stable products (Gordon, 1990). The antioxidant radicals can react with peroxyl radicals (Eq.15) and other antioxidant radicals (Eq.16) producing non-radical products thus terminating the free radical chain reaction.

$$LOO^{\bullet} + A^{\bullet} \longrightarrow LOOA \qquad \textit{(Eq. 2-15)}$$

$$A^{\bullet} + A^{\bullet} \longrightarrow AA \qquad \textit{(Eq. 2-16)}$$

If a primary antioxidant is added to a system in which oxidation has proceeded to the propagation stage their function will be limited because their mechanism of action is free radical scavenging hence they are more effective at the initiation stage (Buck, 1991). However, primary antioxidants still have the ability to reduce hydroperoxides to hydroxyl compounds (Reische et al., 2002).

The most common primary antioxidants used in foods include BHA (butylated hydroxyanisole), BHT (butylated hydroxytoluene), PG (propyl gallate), TBHQ (tertiary butyl hydroquinone), tocopherols and carotenoids (Butnariu & Grozea, 2012)

2.5.2 Secondary Antioxidants

Secondary antioxidants do not scavenge radicals but are able to inhibit oxidation via different mechanisms. Their mode of action is through either of the following:

- Chelating and deactivating pro-oxidant metals.
- Supply hydrogen to primary antioxidants.

- Decompose hydroperoxides to non-radical molecules.
- Deactivate singlet oxygen.
- Absorb ultraviolet irradiation.
- Oxygen scavenging.

Secondary antioxidants are usually effective in the presence of the components required for their action (Gordon, 1990). For example, the chelating agents are effective in the presence of metal ions.

1. Chelators: metals that have two or more valence states increase the rate of oxidation as they catalyse free radical reactions. Two mechanisms by which metals increase oxidation rate have been proposed; they either react with hydroperoxides or directly with lipid molecules (Aust, Morehouse, & Thomas, 1985; Repetto, Boveris, & Semprine, 2012). Gordon (1990) reports that metals act as pro-oxidants by forming radicals from reactions with fatty acids or hydroperoxides (18)

$$LH + M^{n-1} \longrightarrow M^{n+} + H + L^{\bullet} \qquad \textit{(Eq. 2-17)}$$

2. Oxygen scavengers and reducing agents: These antioxidants prevent oxidation in foods by scavenging oxygen or also function as reducing agents by donating hydrogen. This functionality is very useful in foods with headspace (Jadhav, Nimbalkar, Kulkarni, & Madhavi, 1996). Ascorbic acid is reported to have strong reducing properties thus capable of reacting directly with oxygen removing it from foods (L. E. Johnson, 1995).

3. Singlet oxygen quenchers: These antioxidants act by depleting singlet oxygen of its excess energy. Carotenoids such as ß-carotene, lycopene and lutein are effective singlet oxygen quenchers (Min & Boff, 2002a). One mole of ß-carotene is said to quench about 250-1000 molecules of singlet oxygen (Deshpande, Deshpande, & Salunkhe, 1996; D. R. Johnson & Decker, 2015).

It is important to note that antioxidants are also susceptible to degradation by environmental factors (temperature, light, metal ions and enzymes) thus losing their functionality. Recent studies have recommended a blend of primary and secondary antioxidants which act in synergy such that the secondary antioxidants like chelators or oxygen scavengers complement the primary antioxidants for example by replenishing hydrogen (Rajalakshmi & Narasimhan, 1995).

2.5.3 The Polar Paradox

The polar paradox theory has been proposed and reconfirmed over the years. Porter, Black, and Drolet (1989) proposed that non-polar antioxidants or amphiphilic antioxidants with low HLB (hydrophilic-lipophilic balance) tend to be more effective in polar systems while polar antioxidants or amphiphilic antioxidants with high HLB are more effective in non-polar systems.

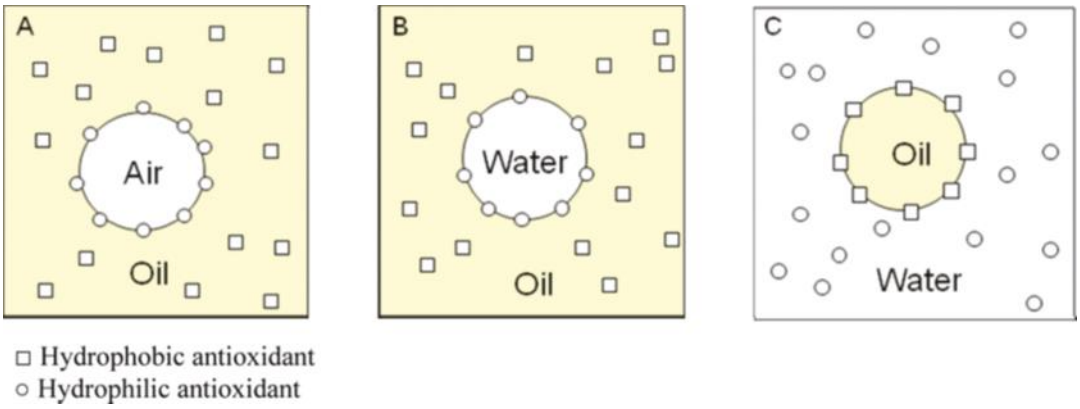

***Figure 2.9**: Schematic diagram of the polar paradox theory: partitioning of antioxidants in bulk oils (A & B) and oil-in-water emulsions (C). Adapted with permission from Fereidoon Shahidi and Zhong (2011), Copyright (2018).*

According to the theory, protective mechanisms against oxidation in oil-in-water emulsions are such that non-polar (hydrophobic) antioxidants dominate the oil-water interface surrounding the lipid droplets while the polar (hydrophilic) antioxidants dissolve within the aqueous phase (Figure 2.9C). This theory is not without challenges despite it's usefulness in selecting the most effective antioxidant for a particular system and has become controversial in recent years as some studies have contradicted this theory (Laguerre et al., 2011; Sasaki et al., 2010; Stöckmann, Schwarz, & Huynh-Ba, 2000). These contradictions indicate that polarity of antioxidants is not the only factor that contributes to the performance of antioxidants in a system it appears other factors such as antioxidant's concentration, mobility and size should be considered as well as composition of the interfacial layer.

Huang, Frankel, and German (1994) evaluated the effect of tocopherols in bulk oils and oil-in-water emulsions and reported that antioxidant activity depended on the oxidation time, method of oxidation measurement, concentration and physical state. In terms of hydroperoxide formation α-tocopherol exhibited pro-oxidant

activity in bulk oils at higher concentrations while in oil-in water emulsions, the rate of hydroperoxide formation at higher concentrations of α-tocopherol was not significantly different from rate at lower concentrations(100ppm). Interestingly, hexanal formation in both the corn oil and corn oil emulsions was prevented at all concentrations of α-tocopherol used in these studies. Overall, oxidation rates were higher in emulsions than bulk oils. This is expected due to high surface/volume ratio in emulsions proposed by Porter (as cited in Fereidoon Shahidi and Zhong (2011).

Edwin N. Frankel, Huang, Aeschbach, and Prior (1996) reported similar differences in antioxidant activity between bulk oil (Corn oil) and oil-in water emulsions. Their study, examined the antioxidant activity of rosemary extract made up of carnosol, carnosic acid and rosmarinic acid as well as α-tocopherol and showed that the more polar rosmarinic and carnosic acids were more protective in bulk oil than the emulsion system while the non-polar α-tocopherol had good activity in emulsions over bulk-oil. In this study, pH was another factor that seemed to influence antioxidant activity as it was reported that performance of carnosic acid and carnosol in emulsions improved significantly at lower pH (4-5) however, there was no information about the physical stability or droplet size of the emuslions studied hence it is not clear what other factors could have given rise to the observed differences with pH.

In studies carried out by Chaiyasit, McClements, and Decker (2005), δ-tocopherol was shown to be more surface active in bulk menhaden oil than α-tocopherol but less effective in protecting the oil from oxidation. This finding apparently contradicts the polar paradox theory but the authors pointed out that studies in

support of the polar paradox theory have mostly used antioxidants with large polarity differences while in this study δ and α-tocopherol's polarity differences are not so large, hence the antioxidant activity not significantly different in bulk oils. In terms of preventing lipid oxidation in menhaden oil-in water emulsions, δ-tocopherol performed better and this was attributed to their high surface activity which could have enabled them concentrate at the oil-water interface such that they trapped the surface active free radicals more effectively.

Interestingly the reverse was the case when comparing activity of BHT (butylated hydroxy) and 4-hydroxymethyl—2,6-ditertiary-butylphenol whereby despite BHT's lower surface activity it performed better in both Menhaden oil and oil-in-water emulsions than it's structurally related antioxidant (4-hydroxymethyl—2,6-ditertiary-butylphenol). Sørensen et al. (2011) studied antioxidant activity of compounds with different polarities in two different emulsions (O/W and W/O) and in this research, efficient performance of the antioxidants in W/O emulsions was in agreement with the polar paradox theory while in O/W emulsions their efficiency was not in accordnace with the theory.

The polar paradox theory though very useful should not be used as the sole determinant in selecting a suitable antioxidant as it is evident that there are so many driving factors that determine their optimal performance which may not be fully considered in many antioxidant activity and partitioning studies.

2.5.4 Antioxidant location

Interfacial positioning of antioxidants in emulsions has proven to be very effective in improving oxidative stability. Table 2.3 shows a summary of studies that investigated the impact of antioxidant location at the interface of oil-in-water emulsions on oxidative stability. These studies reported improved oxidative stability when antioxidants were preferentially located at the interface however, only the study of L.-J. Wang et al. (2015) compared antioxidant (curcumin) performance when located at the interface against direct location in the oil droplets. They reported improved oxidative stability when curcumin was located at the interface of zein-chitosan particle-stabilised corn oil-in-water Pickering emulsions over when curcumin was directly incorporated in corn oil before emulsification. The other studies only compared oxidative stability of emulsions with interfacially positioned antioxidant over emulsion systems without antioxidant.

Table 2.3: *Summary of research on impact of interfacial location of antioxidants on oxidative stability*

Interfacial Composition	Control emulsion	Emulsion sample	Oxidative stability compared to control	Reference
Lactoglobulin-green tea polyphenols nano-complexes	Lactoglobulin stabilised emulsion	Liver fish oil (omega-3 PUFA-38.4%) emulsion	Lower hydroperoxides	von Staszewski, Pizones Ruiz-Henestrosa, and Pilosof (2014)
Soybean protein isolate-rutin complex	Emulsions without rutin	Soybean oil emulsion	Lower hydroperoxides and hexanal	Cui, Kong, Chen, Zhang, and Hua (2014)
Soy protein isolate-resveratrol complex	SPI emulsions	Corn oil emulsions	Lower hydroperoxides and hexanal	Wan, Wang, Wang, Yuan, and Yang (2014)
Catechin-egg white protein complexes (CT-EWP)	Egg white protein and catechin- egg white protein mixture emulsions	Beta-carotene (dispersed in sunflower oil) emulsions	Slower beta-carotene degradation	Gu et al. (2017)
Zein/Chitosan complex particles (ZCPs)-shell curcumin	Zein-chitosan O/w Pickering emulsions	Corn oil-in-water Pickering emulsion	Lower hydroperoxides and malondialdehyde; no detectable hexanal (Lower oxidation values with shell curcumin than core curcumin)	L.-J. Wang et al. (2015)
Lactoferrin-chlorogenic acid and EGCG conjugates	Lactoferrin emulsions	Beta-carotene (dispersed in MCT oil) emulsions	Slower beta-carotene degradation	Liu, Wang, Sun, McClements, and Gao (2016)
Ovalbumin-catechin conjugates	Ovalbumin emulsions	Fish oil emulsions	Lower hydroperoxides and TBARS	Feng, Cai, Wang, Li, and Liu (2018)

2.6 Emulsions as delivery systems for bioactives

Emulsions have become very interesting vehicles for protection and release of lipophilic bioactives especially as the quest to enhance incorporation of various bioactives in foods increases. It is expected that an efficient delivery system will not only protect the core bioactive but will also permit incorporation of the bioactive in reasonable amounts capable of delivering the intended functionality.

The term ‘bioactive compounds’ or ‘bioactives’ can be defined as naturally occurring compounds or substances present in foods which, if consumed in sufficient amounts, will confer a health effect (positive or negative) on humans (Biesalski et al., 2009). Many of these bioactive compounds are lipophilic which means that they have poor solubility in aqueous systems thus limiting their incorporation in many foods as well as their bioavailability. These compounds can be highly sensitive to factors such as light, heat, pH, ionic strength, enzymes etc. and tend to precipitate in aqueous systems. As a result of their sensitivity to these factors, they are prone to chemical and physiochemical changes during food preparations or processing in the digestive system hence limiting their biological efficiency.

Lipids, proteins and carbohydrates contain various groups of bioactive compounds and studies on the potential health benefits of these compounds are on the rise. Protection of these bioactives is paramount for efficient delivery and improved bioavailability and bio-accessibility, which will subsequently have positive benefits on consumers’ health. Table 2.4 shows some lipophilic bioactives and their reported potential health benefits.

Table 2.4: *Bioactive compounds and their potential health benefits*

Bioactive compound Class	Types/Examples	Potential health Benefit	References (potential health benefit)
Fatty acids	Omega-3 fatty acid, conjugated linoleic acid (CLA)	• Omega-3 fatty acid: Infant visual and brain development, Prevent coronary heart diseases. • CLA: Body fat reduction, anti-cancer	- Innis and Friesen (2008); Mozaffarian and Wu (2011); Uauy, Hoffman, Peirano, Birch, and Birch (2001) - S. H. Lee et al. (2006); Yeong and So Bong (2010)
Carotenoids	Beta-carotene, Lutein, Lycopene	Coronary heart disease, cancer, cataracts	Gaziano and Hennekens (1993); V. Rao and Agarwal (2000); Ribaya-Mercado and Blumberg (2004)
Antioxidants	Tocopherols, Polyphenols	Reduction of heart disease, Anti-cancer and Alzheimer's disease prevention.	Tucker and Townsend (2005); Vauzour, Rodriguez-Mateos, Corona, Oruna-Concha, and Spencer (2010)

To protect bioactive compounds from undergoing changes in their structure which may alter or limit their functionality, it is beneficial to embed them within protective layers or coatings or delivery systems that are stable to various processing conditions and capable of maximizing their potential functionality. The ability of emulsions to protect bioactives from oxidation is greatly dependent on the emulsion matrix and stability. The protective layer surrounding oil droplet surface should form a barrier to prevent oxygen permeation. If a hydrophobic bioactive is incorporated in an emulsion, the interfacial properties of that emulsion plays a major part in preventing the bioactives degradation because at the droplet surface is where metal ions and other pro-oxidants can interact and trigger oxidation. The type of ingredients employed in emulsifying a bioactive is also important; ingredients that are low in pro-oxidants should be chosen.

In encapsulating bioactives it is necessary to understand its solubility as this will determine the type of emulsion system to be employed. Some bioactives are hydrophobic (carotenoids, fatty acids etc.) while others are hydrophilic (ascorbic acid, anthocyanins). For example, the most common emulsion system used for delivery of hydrophilic bioactives is the W/O/W and multi-layered emulsions. Typically, the bioactive is dispersed within the phase it is most soluble. Effective encapsulation of bioactives in emulsion systems also requires a good understanding of how emulsion properties (such as droplet size, interfacial structure, interfacial composition etc.) influence bioavailability and bio-accessibility of bioactives embedded within.

2.6.1 Influence of droplet size on encapsulated bioactives

Ahmed, Li, McClements, and Xiao (2012) assessed the impact of emulsion droplet size and oil phase composition on the bio-accessibility of curcumin encapsulated in emulsions. Curcumin is a polyphenol believed to have anti-oxidative and anti-inflammatory activities. In their study, physically stable curcumin emulsions comprising of various oil phases were successfully produced however, the quantity of curcumin that could be incorporated within the emulsions, curcumin's bio-accessibility and rate of lipid digestion depended greatly on the composition of the oil phase. The droplet size did not seem to have any impact on curcumin's bio-accessibility contrary to previous studies which suggest that nanoparticles are absorbed better than larger particles (Acosta, 2009; Desai, Labhasetwar, Amidon, & Levy, 1996).

On the other hand, Yi, Li, Zhong, and Yokoyama (2014) evaluated the effect of droplet size on the stability and bio-accessibility of beta-carotene incorporated within protein stabilised emulsions and showed that beta-carotene oxidation increased as droplet size decreased, this is not surprising because a decrease in droplet size means an increase in the surface area eventually giving rise to increased risks of contact between the core material and pro-oxidants (Lethuaut et al., 2002). However, this group's study showed that bio-accessibility of beta-carotene improved as droplet size decreased. Salvia-Trujillo, Qian, Martín-Belloso, and McClements (2013) also reported similar results where bio-accessibility of beta-carotene increased with nano-emulsions.

Tan and Nakajima (2005) evaluated the stability of ß-carotene nano-emulsions in relation to the particle size and the retention of ß-carotene after storage depended

greatly on the droplet size. Beta-carotene degradation increased as the mean particle diameter of nano-emulsion decreased which was attributed to increased surface area and possible generation of free radicals during high pressure homogenisation.

2.6.2 Influence of emulsion composition and interfacial structure on encapsulated bioactives

Beta-carotene degradation rate in emulsions is influenced greatly by the type of lipid used for the emulsion and initial stability of the emulsion as revealed by studies carried out by Cornacchia and Roos (2011). In this research, the physical state (solid vs liquid) of the lipid phase impacted stability of beta-carotene as emulsions made up of solid lipid (hydrogenated palm kernel oil) showed lower rates of beta-carotene degradation over those made with liquid lipid (sunflower oil), the observed effect was attributed to partial crystallinity of emulsified hydrogenated palm kernel oil (HPKO) which may have entrapped beta-carotene within liquid compartments surrounded by solid HPKO network barrier. It was also clear in this study, that the emulsifier played a role in enhancing the protection of beta-carotene whereby sodium caseinate showed better protection compared to whey protein isolate which was attributed to the ability of caseins to form thicker protein layers than those formed by whey protein isolate.

Yang and McClements (2013) examined the influence of carrier oil type on bio-accessibility of Vitamin E acetate incorporated in oil-in-water emulsions. The emulsions were prepared with lipid phases consisting of vitamin E acetate dispersed in long (LCT-corn oil) or medium (MCT) chain triglyceride oils.

Concentrations of α-tocopherol acetate and α-tocopherol were obtained after in-vitro digestion and the results showed that some α-tocopherol acetate was converted to α-tocopherol during digestion. Overall bio-accessibility of vitamin E was 17% with MCT as carrier oil and 39% with LCT. The higher bio-accessibility obtained with LCT oil was attributed to LCT's ability to form mixed micelles with greater solubilisation capacity for vitamin E. Studies carried out by (Qian, Decker, Xiao, & McClements, 2012) also reported higher beta-carotene bio-accessibility in LCT (corn oil) nanoemulsions over MCT and orange oil nanoemulsions which was also attributed to larger solubilisation capacity of micelles formed by LCT.

Feasibility of concurrent encapsulation of bioactives with different physicochemical properties (resveratrol and α-tocopherol) in oil-in-water emulsions stabilised by whey protein isolate (WPI) was explored by L. Wang et al. (2016). Decomposition of α-tocopherol was greatly dependent on emulsifier (WPI) concentration, higher WPI concentrations resulted in better protective effects but, encapsulation efficiency of α-tocopherol decreased at WPI concentrations above 0.01 % (w/w). Loss of resveratrol was faster at the oil/water interface than in the continuous phase of the emulsion and this was attributed to resveratrol's partial adsorption into WPI at the oil/water interface resulting in faster degradation. This study showed very promising results in terms of concurrent encapsulation of bioactives however, the optimal conditions (such as optimal concentrations) of both bioactives were not defined but it was clear that resveratrol provided a good protection against loss of tocopherol regardless of its concentration.

Tokle et al. (2013) encapsulated ß-carotene within multi-layered protein coated emulsions consisting of either lactoferrin or ß-lactoglobulin and evaluated the influence of protein coatings on bio-accessibility of ß-carotene after digestion in the small intestine and surprisingly obtained very low bio-accessibility in all emulsions studies, the observed low bio-accessibility was attributed to possible binding of ß-carotene to lactoferrin and/or lactoferrin digestion products. This is not conclusive since the interactions were not further investigated. Pinheiro, Coimbra, and Vicente (2016) also reported surprisingly low bio-accessibility of curcumin encapsulated in nanoemulsions stabilised by lactoferrin which they also attributed to possible binding of curcumin to lactoferrin.

Shah, Zhang, Li, and Li (2016) compared bio-accessibility of curcumin encapsulated in nanoemulsions containing an organic phase and Pickering emulsions stabilised by chitosan-tripolyphosphate nanoparticles by measuring curcumin concentrations in the micelle phase and overall digesta after in-vitro digestion. Results showed that curcumin bio-accessibility was lower in Pickering emulsions than nanoemulsions for both types of oil phases studied. The writers explained that the reason for lower bio-accessibility in Pickering emulsion was due to slow and incomplete lipid digestion in these emulsions which was attributed to inability of pancreatic lipase to access lipids within large chitosan aggregates formed during digestion at pH 7.

Lu et al. (2016) evaluated the influence of emulsion structure on cellular uptake of beta-carotene encapsulated in oil-in-water emulsions stabilised by whey protein isolate (WPI, sodium caseinate (SCN) and tween 80 (TW80). Results showed that cellular uptake of beta-carotene was highest in WPI-stabilised

emulsions followed by SCN emulsions and then TW80 emulsions. The higher cellular uptake observed with protein-stabilised emulsions over TW80 emulsions was attributed to proteins higher hydrophilicity resulting in easier interactions with caco-2 cells than TW80 which has a weaker binding to hydrophilic surfaces.

Some of the studies highlighted took into consideration the various food matrices that these emulsion systems could be incorporated thus giving good insights into the possible structural and stability changes that may be encountered. Despite the different methods employed in assessing the stability and bio-accessibility of bioactives in the studies mentioned above it is apparent that common challenges exist in these systems and it is important that an optimal balance is struck between the droplet size, emulsion stability, emulsions composition and interfacial structure to ensure efficient incorporation, stability, delivery and bio-availability/bio-accessibility of bioactives.

2.7 Pickering emulsions in food

Solid particles commonly used for Pickering stabilisation in food systems are inorganic particles such as silicon dioxide but due to concerns raised about the safety of such materials in foods, biodegradable organic particles that are carbohydrate, lipid or protein based have been explored (Gao et al., 2014; Nadin, Rousseau, & Ghosh, 2014; Rayner, Sjöö, Timgren, & Dejmek, 2012). Despite the growing exploration of food applications of Pickering emulsions, challenges exist which seem to limit applications in food.

Berton-Carabin and Schroën (2015) in their review on challenges of food applications of Pickering emulsions raised questions about the general perception and acceptability of nanoparticles in foods, lack of extensive research on stability in relation to emulsification methods employed, difficulties in determining the suitability and emulsifying efficiency of nanoparticles, and preservation of the Pickering structural network overtime. These questions raised are valid and will need to be fully addressed to facilitate widespread applications of Pickering emulsions in foods.

Tan et al. (2014); Yusoff and Murray (2011) investigated the use of hydrophobic starch particles and starch-based nano-spheres respectively to stabilise oil-in water emulsions. In the case of hydrophobic starch particles, the size of emulsion droplets was similar to the size of the starch particles (1-20µm), the starch particles aggregated and were milled to reduce their sizes however it is unlikely that big particles will stabilise droplet sizes smaller than the particles. As a result of the somewhat big droplet sizes obtained the droplets creamed rapidly. For the emulsions stabilised by starch-based nano-spheres, the oil droplets were highly unstable to flocculation on addition of salt and coalesced as salt concentration increased producing bigger droplets.

The use of cocoa particles for Pickering stabilisation has been shown (Gould, Vieira, & Wolf, 2013). The cocoa particles were of different sizes and it was shown that the emulsion was stabilised by very small fine cocoa particles while the bigger cocoa particles did not seem to have any effect on emulsion stability but rather appeared to create a network that had impact on the rheological properties of the emulsion.

Water insoluble zein proteins were studied as novel particles for Pickering stabilisation. Stable emulsions were obtained at optimal pH and ionic conditions however, at very high ionic strength zein particles aggregated resulting in droplet flocculation and subsequent formation of a gel structure (de Folter, van Ruijven, & Velikov, 2012).

It is interesting to note that most of the research carried out on Pickering stabilisation by solid particles in emulsions are mostly focused on the potential and/or benefits of improving physical stability of emulsions (as highlighted and evidenced above), very little attention has been given to their impact on the oxidative stability of these emulsions or bioactives incorporated within. Considering that lipids are one of the major ingredients in emulsions and are susceptible to degradation, investigating the oxidative stability of emulsions stabilised by particles or nano-droplets requires urgent attention.

Also worthy of investigation is the fate of Pickering emulsions on incorporation of Pickering emulsions within food system. It is also necessary to investigate the stability of Pickering emulsions under various processing conditions such as shearing, low temperature etc. The focus has been on physical stability therefore information from Pickering literature about these scenarios is scarce.

2.8 Summary and Conclusions

There are several techniques currently employed to improve protection, delivery and bioavailability of lipophilic bioactives however, several limitations such as porous structure, high cost of production, time consuming process and limited stability of these delivery systems exist. These limitations must be overcome to achieve the goal of efficient protection, delivery and enhanced bioavailability of lipophilic bioactives. Another challenge is the limitations in quantities of bioactives that can be incorporated within emulsion delivery systems. It is imperative that biologically meaningful quantities of bioactives are incorporated within delivery systems to meet the recommended daily intakes and deliver the intended functionality.

Many studies involving particle-stabilised emulsions or structured emulsion interfaces tend to focus mostly on physical stability while some studies have focused on the impact of interfacial structure on chemical stability of bioactives incorporated within, only very few studies have focused on practical potential food applications of these delivery systems.

The structure of droplet-stabilised emulsion may effectively protect any bioactive incorporated within and enable incorporation of meaningful amounts of bioactives thus the need to explore and establish these possibilities. Previous study on DSEs reported by Ye et al. (2013) mainly focused on mechanism of stabilization and formation of DSEs. To evaluate and examine ability of droplet-stabilised emulsions to effectively protect bioactives incorporated within, the following approaches which have not been previously studied will be taken:

- ✓ Potential to form DSEs with only food-grade emulsifier and lipids will be explored.
- ✓ Influence of interfacial structure, interfacial lipid phase type and state on chemical stability of core bioactive incorporated within will be examined.
- ✓ Impact of interfacial location of lipophilic antioxidants in emulsions versus direct location in unsaturated lipid will be evaluated and compared.
- ✓ Effect of antioxidant concentration on location-based performance of lipophilic antioxidant will be investigated.
- ✓ Transportation or mobility of hydrophobic antioxidant incorporated at interface (in shell droplets) of DSEs will be monitored without separation of oil and aqueous phase

Chapter 3: Materials and Methods

This chapter describes the materials, methods and equipment used in this research work. Process flow charts of experiments are also shown in this chapter. A summary of the experimental set-up used in this research work is shown in Figure 3.1.

3.1 Materials

3.1.1 Water

Except where specified all solutions were dissolved or prepared in ultrapure water produced with a Milli-Q® Q-Gard 1 purification filter (Merck KGaA, Darmstadt, Germany), hereafter referred to as 'milli Q water'. The quality of milli-Q water was monitored and tested using the in-built conductivity meter. The manufacturer's recommended cleaning process was initiated whenever water resistance was below 18.2 mΩ.

3.1.2 Milk Protein concentrate

Milk protein concentrate (MPC) was used as the emulsifier in this study. MPC is a dairy product obtained by ultrafiltration and spray-drying of skim milk. It is a complete protein that contains both caseins and whey proteins in ratios similar to that in milk and in their native state (Patel, Patel, & Agarwal, 2014).

Milk protein concentrate (MPC) was supplied by Fonterra Cooperative Ltd, Auckland, NZ. The protein, calcium and sugar composition of four MPCs used in this study as provided by the supplier are shown in Table 3.1.

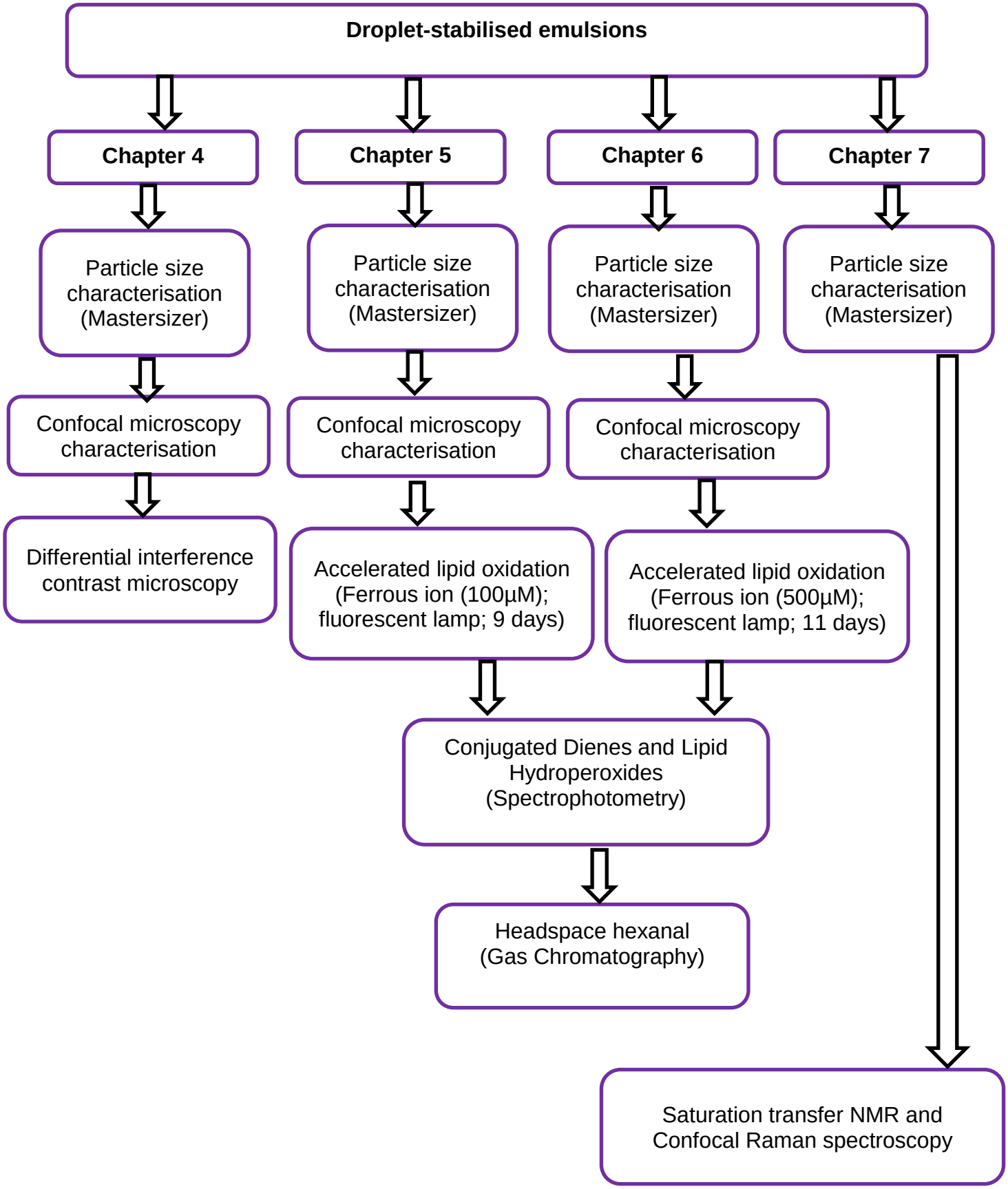

Figure 3.1 *Summary of experimental set-up*

The MPCs can be divided into three categories viz: high protein MPC (MPC-85), low protein MPC (MPC-70) and calcium-depleted MPC.

Table 3.1 *Composition of milk protein concentrate (MPC)*

MPC	Supplier's MPC details	Protein (g/100g)	Calcium (mg/100g)	Total Sugars (lactose) (g/100g)
High protein MPC				
1	MPC-4851 (22753775-22/02/2015)	82.9	2160	3.3
2	MPC-485 (CW01-17/01/2015)	81.3	2230	4.6
Low protein MPC				
3	MPC-470 (GZ20-20/02/2015)	69.9	2180	16.8
Calcium-depleted MPC				
4	MPC-4861 (GZ22-22/02/2015)	81.8	1260	4.0

Supplier's MPC details in bracket refer to the cypher number and production date

MPCs 1 (MPC-4851), 2 (MPC-485), 3 (MPC-470), and 4 (MPC-4861) were used in the study detailed in chapter 4. Only MPC 3(MPC-470) was used in the studies detailed in chapter 5, 6 and 7.

3.1.3 Surface lipids

‘Surface lipid’ refers to the lipid used in preparing the shell emulsion. Three main surface lipids were used in this study; olive oil, palmolein oil and trimyristin. The lipids were chosen based on differences in melting behaviour i.e. low, medium and high melting and low susceptibility to oxidation. The lipids were used ‘as supplied'.

Low acidity olive oil (O1515-500 mL) was purchased from Sigma-Aldrich. Palmolein oil (Tradewinds-15 L) was purchased from Davis trading, Palmerston North, New Zealand. Trimyristin (Dynasan 114) was kindly donated by IOI Oleo GmbH, Germany. Olive oil was in liquid form and stored at 5 °C in the dark, palmolein oil was in a semi-solid form (melting range 20-30 °C) and stored in the dark at room temperature (approximately 18 ˚C). Trimyristin was in solid form and stored in the dark at room temperature, the melting temperature range of trimyristin as provided by supplier was 55-58 °C.

For the saturated transfer difference study detailed in chapter 7, coconut oil (Olivado natural cooking oil, 180628-500 mL) was used as the surface lipid and it was purchased from Countdown supermarket Palmerston North, New Zealand. Coconut oil was in solid form (melting range 30-35 °C) and stored in the dark at room temperature.

3.1.4 Core Lipids

‘Core lipid’ refers to the lipid dispersed in water and stabilised by shell droplets. Three core lipids were used in this study; soybean oil, linoleic acid and safflower oil (high linoleic acid- 72.54 % of total fatty acids). Soybean oil and linoleic acid

were only used in the study detailed in chapter 4. Safflower oil was used for the studies in chapter 5, 6 and 7. High linoleic acid safflower oil was selected because of its high susceptibility to oxidation.

The lipids were used ‘as purchased’. Soybean oil (Essente-15 L) was purchased from Davis trading Palmerston North, New Zealand. Linoleic acid (62240-1L-F) was purchased from Sigma-Aldrich. Safflower oil (Kerfoot natural oils-5 L) was purchased from Pure Nature Ingredients, Auckland New Zealand.

Soybean oil was stored in the dark at room temperature, linoleic acid and safflower oil were stored in amber containers in the dark at 5 °C.

3.1.5 Antioxidants

Two types of antioxidants were used in this study; butylated hydroxyanisole (BHA) and βeta-carotene. Butylated hydroxyanisole (BHA), a common commercial primary antioxidant was used for the antioxidant study detailed in chapter 6 and 7. BHA was chosen for the study because it is readily available and for its ability to quench peroxyl radicals by donating hydrogen to free radicals. Beta-carotene was used for the study on probing the location of antioxidants detailed in chapter 7 and was chosen for the study because of its ability to exhibit very strong Raman scattering (Tschirner et al., 2008). BHA (99%, FCC, FG) and Beta-carotene (22040-5G-F) were purchased from Sigma–Aldrich.

3.1.6 Reagents/Chemicals

The following table summarises the reagents and chemicals used in this study, as well as the supplier details and grade.

Table 3.2: *Reagents and chemicals used, suppliers and grade*

Reagent/Chemical	Supplier	Grade
Cumene hydroperoxide	Sigma-Aldrich	Technical
Hexanal	Sigma-Aldrich	Standard
Iso-octane	Fischer	Optima
Methanol	Merck	ACS
1-Butanol	Merck	ACS
2-Propanol	Merck	ACS
Sodium azide	Sigma-Aldrich	ReagentPlus
Ferrous sulfate heptahydrate	Labserv	Analytical
Ammonium Thiocyanate	Labserv	Analytical
Barium chloride	Labserv	Analytical
Hydrochloric acid (HCL)	Sigma	ACS

3.2 Equipment

3.2.1 Waterbath

A temperature-controlled waterbath (Jeiotech Korea, lab companion BS-11) was used in this study to heat solutions and emulsions. A stirring waterbath (Julabo GmBH) was used to stir and heat surface and core lipid phases used in the antioxidant study detailed in chapter 6 and 7.

3.2.2 pH Meter

The same pH meter (Eutech instruments, pH510) was used for all pH measurements. All pH measurements were carried out with the temperature probe. The pH meter was calibrated using the two-point calibration technique at pH 4 and pH 7 prior to each set of measurements.

3.2.3 Centrifuge

The Thermo Scientific Heraeus Fresco 17 micro-centrifuge (24-PI rotor) was used for separation of emulsions. The samples were centrifuged at 2000 g for 5 min at 20-25 °C. The same centrifuge was used in all studies requiring centrifugation (chapters 5 & 6).

3.2.4 Spectrophotometer

The spectrophotometer used in all studies was a Thermo Scientific Genesys 10S UV-VIS spectrophotometer. The spectrophotometer was used to measure absorbance of sample extracts in all studies requiring absorbance measurements (chapter 5 & 6). The absorbance measurements were made in 4 mL plastic (polystyrene) cuvettes for readings at wavelength of 510 nm and 4 mL quartz cuvette for readings at 234 nm.

3.2.5 Gas Chromatograph

The gas chromatograph (GC) was a Shimadzu GC 2010 chromatograph coupled with a headspace and solid phase micro-extraction (SPME) GC sample injection system (AOC-5000). The AOC-5000 provided a fully automated SPME sample preparation process. SPME fibre movements, precondition, absorption and desorption were fully controlled for optimum precision. The GC 2010 was equipped with a flame ionization detector (FID). The SPME fibre was a Supelco SPME fibre assembly 75µm carboxen/Polydimethylsiloxane (CAR/PDMS) with a 23-gauge needle.

3.2.6 Homogenisers, microfluidizer and mixers

Three types of emulsification equipment were used in this study; microfluidizer, two-stage homogeniser, and high-speed mixer. The microfluidics M-110P microfluidizer was only used in the study detailed in chapter 4. A Rannie 2.5H two-stage homogeniser was used for the study in chapter 4 while a FBF Italia homolab2 two-stage homogeniser was used for the study in chapter 5, 6 and 7. The Labserv D-130 hand held homogeniser or mixer was used in all studies.

The microfluidizer and two-stage homogeniser were used to process the protein-stabilised emulsions (shell emulsions) while the high-speed mixer was used to process the final droplet-stabilised emulsion.

Figure 3.2 *Microfluidizer (microfluidics M-110P)*

Figure 3.3 *Two-stage homogeniser (Rannie 2.5H)*

Figure 3.4 *Two-stage homogeniser (FBF Italia)*

Figure 3.5 *Hand held mixer (Labserv D-130)*

3.3 Methods

3.3.1 Shell emulsion preparation

Shell emulsion refers to submicron protein-stabilised lipid droplets used to stabilise oil-in-water droplets. Preparation of shell emulsion was the first step in processing droplet-stabilised emulsions. Shell emulsions in chapter 4's study was processed by magnetic stirring of 5 g milk protein concentrate (MPC) into 95 g milli-Q water at room temperature for 1 h, after which MPC solution was heated to 55 °C and appropriate quantities of surface lipid added i.e. 80% w/w MPC solution and 20% w/w surface lipid. The mixtures were held at 55°C for 3-5 min and coarse emulsions were formed using a high-speed mixer (Labserv, D-130) at 6000 rpm for 3 min. The coarse emulsions were passed through either a micro-fluidizer (M-110P, Microfluidics) at 25000 psi (1700 bar) or a two-stage homogeniser (12.5H, Rannie, Denmark) at a first stage pressure of 200 bar and second stage pressure of 40 bar to produce a fine emulsion referred to as 'shell emulsion'.

Shell emulsions in chapter 5's study was processed as detailed above for chapter 4's study with slight modifications. In this study, coarse emulsions were made at 65 ˚C and only passed through a two-stage homogeniser (Homolab2, FBF Italia) at a first stage pressure of 400 bar and second stage pressure of 50 bar to produce shell emulsions.

Shell emulsions in chapter 6 and 7's study was processed as described for chapter 5 except that the surface lipid phase consisted of the surface lipid and antioxidant (BHA or beta-carotene) which was prepared by stirring BHA or beta-carotene into the surface lipid at 70 °C for 20 min.

3.3.2 Droplet-stabilised emulsions

Droplet-stabilised emulsion was obtained in a second step by adding the shell emulsion obtained in the first step to appropriate quantities of core lipid and potassium phosphate buffer (10mM K_2HPO_4 and KH_2PO_4, pH 6.8-7.0), i.e. 10% w/w shell emulsion, 20% w/w core lipid and 70% w/w buffer. The mixture was heated, and final emulsification achieved with a high-speed mixer.

3.3.3 Particle size characterisation

The surface area mean (Sauter mean diameter, $d_{3,2}$) and volume-weighted mean diameter ($d_{4,3}$) of emulsions were measured using a static light scattering instrument (Mastersizer 2000, Malvern instruments, Worcestershire, UK), with a sample dispersion unit (Hydro 2000S). The emulsions were dispersed in reverse osmosis-filtered water to reach obscuration index of 8 to 10% and the ratio of refractive index of emulsion droplets (1.47) to the aqueous medium (1.33) was 1.105. The measurements were taken in triplicate. The particle size of emulsions was characterised in each study within two days of preparing the emulsions or within 24 h of sample collection for the studies involving particle size characterisation during accelerated oxidation conditions (chapter 5 and 6).

3.3.4 Confocal microscopy

The structure and morphology of emulsions was studied using a confocal laser scanning microscope (DM6000B ST5, Leica Microsystems, Wetzlar, Germany). Emulsions were stained according to the method described by Gallier, Gragson, Jimenez-Flores, and Everett (2010). Lipid droplets were stained with Nile red (Sigma life science-72485-100 mg) solution prepared by dissolving Nile red in acetone (1 mg/mL), while proteins were stained with fast green (Sigma chemical-

F-7252) solution prepared by dissolving fast green in milli-Q water (1 mg/mL). Staining involved mixing 500 µl of emulsion with 10 µL and 30 µL of Nile red and fast green solutions respectively, then 25 µL of the stained emulsion was deposited on concave microscope slides and fixed with 50 µL of agarose (Sigma A9539-10G) solution (0.5%w/w dissolved in milli-Q water at 80°C). Slides were covered with coverslips and observed under the microscope with the 63X oil immersion objective lens (HCX PL APO lambda blue 63.0 x 1.40 oil UV, Leica Microsystems, Wetzlar, Germany).

Nile red was excited at 488 nm with the argon laser and the emitted fluorescence collected between 494-605 nm. Fast green was excited at 633 nm with the helium-neon laser and emission collected between 638-750 nm. The samples were scanned either between lines or sequentially between frames, and images were captured with LAS AF software (version 2.7.3.9723) at room temperature. Images were analysed using ImageJ software (Image J, National Institute of Health, Bethesda, MD, USA).

Microscopic structure of emulsions was examined within 2-3 days of preparation and within 2 days of sample collection for studies involving microscopic structure characterisation during accelerated oxidation conditions (chapter 5).

3.3.5 Differential Interference Contrast (DIC) Microscopy

The structure and morphology of emulsions processed with high melting surface lipid (trimyristin) was examined with a differential interference contrast microscope (Zeiss Axiophot, West Germany) equipped with a Leica Microsystems DFC320 camera.

3.3.6 Accelerated Lipid Oxidation

Accelerated lipid oxidation was achieved by exposure to fluorescent lamps in the presence of ferrous ion for 9 days (chapter 5) and 11 days (chapter 6). The setup involved two fluorescent lamps (

Figure ***3.6***) with light intensity of 8500-9000 lux. Oxidation of emulsions was accelerated at 20°C in 12-well cell plates sealed with parafilm and 20 mL headspace glass vials (95% or 90% headspace) for gas chromatography (Phenomenex) with rubber/Teflon septum air tight seal and magnetic crimp cap. The distance from lamp to top of plates and vials was approximately 23 cm and 22 cm respectively, and plates/vials were placed in a line directly below lamps (Figure ***3.6***B) to produce similar levels of illumination for all samples. Sodium azide (0.02% w/v) was added to the emulsions to prevent microbial growth.

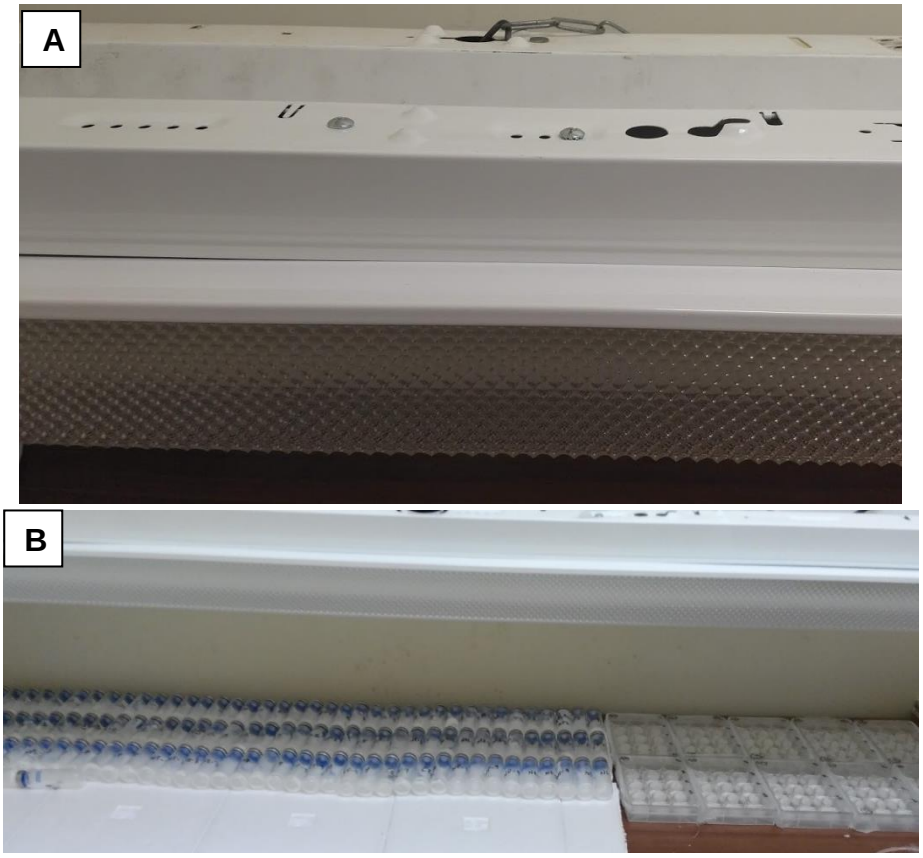

Figure 3.6: *Accelerated lipid oxidation set-up with two fluorescent lamps- A) Fluorescent lamps; B) Emulsion samples in plates and vials exposed to fluorescent lamps*

3.3.7 Preparation of Ferrous ion

Ferrous ion was prepared by dissolving iron (II) sulphate heptahydrate ($FeSO_4.7H_2O$) in 0.5 M hydrochloric acid (HCl). Ferrous ion was added to emulsions at concentrations of 100 µM (chapter 5) and 500 µM (chapter 6).

3.3.8 Lipid Oxidation Measurements

Primary (conjugated diene and lipid hydroperoxides) and secondary (hexanal) products of linoleic acid oxidation were measured using spectrophotometric and gas chromatographic techniques respectively. Emulsion samples were collected on days 1, 3, 5, 7 and 9 for the study detailed in chapter 5 and days 3, 5, 7, 9 and 11 for the study detailed in chapter 6. The samples were stored at -20°C. Samples were analysed within 1-4 weeks of freezing.

3.3.9 Sample extraction

Extraction of lipids from emulsions was carried out according to the method described by Hu, McClements, and Decker (2003). Firstly, 0.3 mL of thawed emulsion was mixed with 1.5 mL of isooctane/2-propanol (3:1 v/v) solution. The mixture was vortexed at high speed three times for 10 s each and then centrifuged (Heraeus Fresco 17, Thermo Scientific) at 2000 g for 5 min. The supernatant was collected and used for conjugated dienes and lipid hydroperoxide measurements.

3.3.10 Determination of Conjugated Dienes

Conjugated dienes (CD) are two double bonds separated by a single bond. It is an unusual structure in PUFAs therefore the presence of CD in PUFAs is a good indication of fatty acid oxidation. Conjugated dienes can be easily detected by

spectrophotometry, and they absorb in the UV region around 234nm when present in fatty acids (Corongiu & Banni, 1994).

Conjugated dienes are an initial product of linoleic acid oxidation to hexanal. This method is fast and is not dependent on the development of any colour or chemical reaction (Wanasundara, Shahidi, & Jablonski, 1995) however, the results are usually more reliable at the early stages of oxidation, when there is limited interference arising from UV absorption of other moieties present in the matrix.

Wanasundara et al. (1995) reported excellent correlation between conjugated dienes and peroxide values (PV) of oxidised canola and soybean oils. Fereidoon Shahidi, Wanasundara, and Brunet (1994) also reported excellent correlation between CD and PV for oxidised seal blubber and cod liver oils. Conjugated dienes usually accumulate at the early stage of oxidation and then CD levels plateau as they get involved in other oxidation reactions that lead to their decomposition (White, 1995). In polyunsaturated fatty acids, Jackson (1981) reported that the formation of hydroperoxides usually coincides with formation of conjugated dienes during oxidation.

In this study, conjugated dienes were determined by the methods described by Wrolstad et al. (2005), and Estévez, Kylli, Puolanne, Kivikari, and Heinonen (2008) with slight modifications. An aliquot of emulsion was mixed with extraction solvent and centrifuged as previously described in section 3.3.10, then 0.2 mL of the supernatant was diluted to 5 ml with isooctane. The solution was thoroughly mixed, and absorbance measured at 234 nm in a quartz cuvette of 1 cm path length using a spectrophotometer (Genesys 10S, Thermo Scientific). Iso-octane

was used as a blank. The concentration of conjugated dienes was calculated as follows:

$$C_{CD} = \frac{A_{234}}{(\varepsilon \times \lfloor)} \qquad \textit{(Eq. 3-1)}$$

Where

C_{CD} = Conjugated diene concentration in mmol/ml (molar concentration)

A_{234} = Absorbance of lipid at 234 nm

ε = Molar absorptivity of linoleic acid hydroperoxide (2.525 X 10^4 $M^{-1}.cm^{-1}$) (Wrolstad et al., 2005)

⌊ = Path length of cuvette in cm

The conjugated diene concentration (CD value) is expressed as µM by taking into consideration the volume of isooctane used for dilution.

3.3.11 Determination of Lipid Hydroperoxides

Lipid hydroperoxide analysis was carried out by the ferric thiocyanate method, as described by Hu et al. (2003) and Katsuda, McClements, Miglioranza, and Decker (2008). Firstly, 0.2 mL of supernatant collected after extraction (as detailed in section 3.3.10) was mixed with 2.8 mL of methanol/butanol (2:1 v/v) solution. To this solution, 15 µL of ammonium thiocyanate solution (3.94 M) and 15 µL of ferrous ion solution (prepared by mixing 0.132 M of $BaCl_2.2H_2O$ and 0.144 M $FeSO_4.7H_2O$) was added. The solution was vortexed and incubated in the dark at room temperature for 20 min (time monitored after addition of ferrous iron solution to the first reaction tube). Absorbance was read at 510 nm against a

cumene hydroperoxide standard curve (concentration range 0-20 µM) using a spectrophotometer (Genesys 10S, Thermo scientific) and peroxide values were expressed as µmol cumene hydroperoxide equivalent per litre of emulsion.

All the oxidation measurements were carried out under subdued light (sample preparation 5-6 lux; absorbance readings 6-9 lux).

3.3.12 Determination of Volatile Secondary Oxidation Product (Hexanal)

Analysis of hexanal, a major secondary breakdown product of linoleic acid, was done by solid phase micro-extraction (SPME) coupled with gas chromatography-flame ionization detection (GC-FID). Emulsion samples were placed in 20 mL vials (Phenomenex), sealed with septum crimp tops (20LLX, Phenomenex) and volatiles were extracted by the SPME method.

The SPME auto fiber assembly (AOC-5000 auto-injector, Shimadzu) consisted of a fused silica fiber coated with Carboxen®/polydimethylsiloxane (75 µm thickness). The samples were heated for 30 min in a block maintained at 50 °C and agitated at 500 rpm to enable headspace equilibration. The SPME fiber needle then penetrated the vials and the fiber was exposed to the headspace for 5 min. After extraction of volatiles, the fiber was withdrawn, and the adsorbed volatiles injected into a gas chromatograph (GC-2010, Shimadzu) port. The injection port was maintained at 230 °C and enabled thermal desorption of extracted volatiles for 2 min. The GC was equipped with a flame ionisation detector (FID). The detector temperature was 250 °C. Volatiles were separated with an Rtx-1701 column (30 m, 0.25 mm inner diameter, 1 µm film thickness). The column oven temperature was 40 °C (1 min hold) initially and then increased to 100 °C at 5 °C/min and to end temperature of 230 °C at 10 °C/min. The direct

injection mode was used. Helium was employed as the carrier gas (flow rate 1.5 mL/min). Hexanal identification and quantification in samples was determined by comparing retention time of peaks against hexanal external standard curves. To achieve this, hexanal standard was added to fresh reference emulsion in various concentrations.

3.4 Statistical Analysis

Particle size data are reported as means and standard deviation of triplicate measurements from two (chapter 6) or three (chapter 5) separate trials.

Oxidation results are reported as means and standard error of six data points: two independent trials with triplicate oxidation measurements in each. Data was analysed by two-way analysis of variance (ANOVA) and Duncan's multiple range test.

3.5 Software Packages

All confocal microscopy images were analysed with image J software (Image J, National Institute of Health, Bethesda, MD, USA). Statistical analysis was achieved with the R-statistical software (R studio- version 1.0.143). GC chromatograms were integrated with Shimadzu GC 2010 software.

Chapter 4: Formation and properties of droplet-stabilised food grade oil-in-water emulsions

4.1 Abstract

Droplet-stabilised emulsions (DSEs) consist of large lipid droplets (the core) stabilised by smaller protein-stabilised lipid droplets (the shell). This study explored the production of DSEs with food-grade ingredients and examined the effect of varying the type of milk protein concentrate (MPC), surface lipid, core lipid, homogenisation conditions and shell emulsion concentration on formation of DSEs.

Shell emulsions were prepared by homogenising MPC solutions and surface lipid using either a microfluidizer (1700 bar) or two-stage homogeniser (1st stage-200 or 400 bar; 2nd stage-40 or 50 bar). Shell emulsions were then homogenised with core lipid using a high-speed mixer to obtain droplet-stabilised emulsions.

Protective droplet layers along the interface of food grade oil droplet was formed only with shell droplets made with MPCs that were not calcium-depleted, and when shell emulsions were processed with a two-stage homogeniser. Excessive shell droplet aggregation prevented total interfacial coverage when the shell emulsions were processed through the microfluidizer. Sufficient and even interfacial coverage was obtained with lower concentrations of shell emulsion (2% & 10%).

There were observed differences in shell droplet interfacial coverage at the interfaces of soybean oil and linoleic acid as core lipid. Shell droplet stabilisation was also possible with surface lipids with varied melting points, and crystalline structures were observed in emulsions processed with high melting surface lipid. The results suggest that the aggregated structure of casein micelles which is held together by calcium phosphate bridges plays a major role in successful formation of droplet-stabilised emulsions with MPC. The study has provided very critical information to ensure consistent successful production of droplet-stabilised emulsions using food grade oils and MPC stabilised shell emulsions.

Keywords

Droplet-stabilised emulsion; Surface lipid; Shell emulsion; Core lipid; Milk protein concentrate

GRAPHICAL SUMMARY

Processing conditions	DSEs interfacial coverage
Shell emulsion made with high protein MPC (MPC-85), & contains high calcium level, & processed in microfluidizer	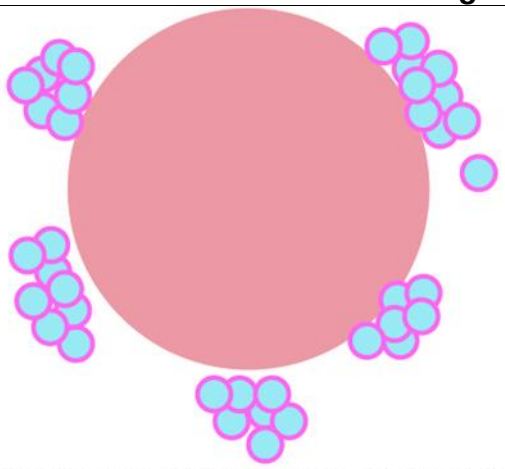 **Excessive aggregation of shell droplets prevents droplet stabilisation**
Shell emulsion processed with high (MPC-85) and low (MPC-70) protein MPCs, & contains higher calcium level, & processed in a two-stage homogeniser	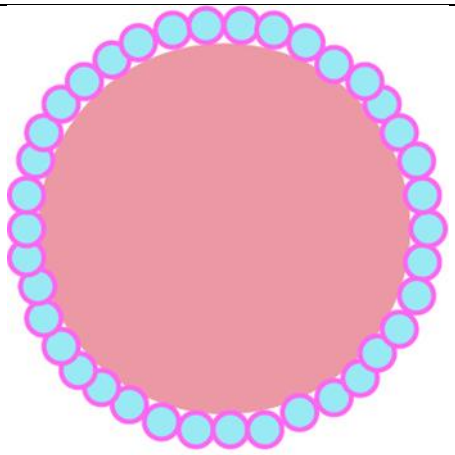 **Droplet-stabilised oil-in-water emulsion**
Core soybean oil droplets stabilised with 10% or 16% w/w shell emulsions made with MPC-85	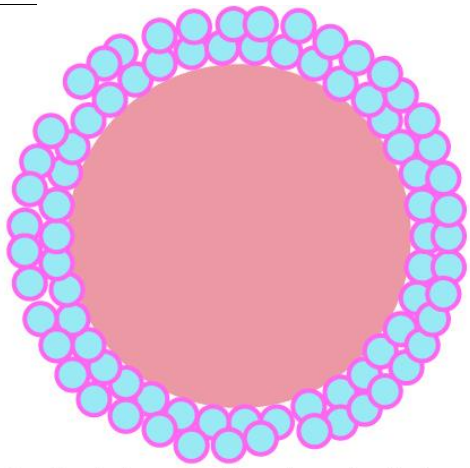 **Interfacial crowding by shell droplets prevents uniform droplet stabilisation**

Shell emulsion processed with calcium-depleted MPC either in microfluidizer or two-stage homogeniser	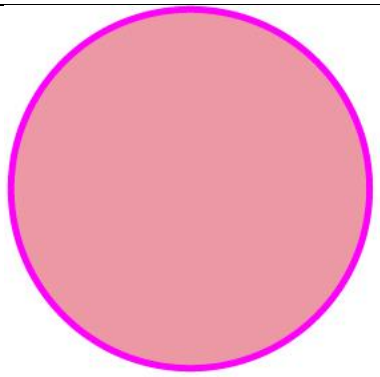 No shell droplet stabilisation

4.2 Introduction

Emulsions are classified according to the composition of their dispersed and continuous phases however, classification of emulsions has become more complex and are now also classified based on their dispersed phase size (micro, nano, macro) or structured interfacial phase (multi-layered, Pickering). Emulsions are normally created by a process called homogenisation whereby the immiscible liquids and emulsifiers are mixed by high speed mixing or agitation (McClements, 2015a).

Structural design of emulsions from food-grade ingredients to improve physical and chemical stability of emulsions has become an interesting and often challenging area of focus with many designs also aimed at effectively protecting and enhancing delivery of bioactives incorporated within. Also, of interest for many researchers is how these structured emulsions behave upon consumption in the gastro-intestinal tract (Sarkar, Goh, Singh, & Singh, 2009; Singh & Sarkar, 2011).

The final physicochemical properties of emulsions are greatly dependent on the emulsions' composition and processing conditions. One of the most critical compositional factors is the type of emulsifier employed as this has a subsequent effect on the droplet characteristics and interfacial structure (McClements, 2005).

The surface-active property of proteins facilitates their use as emulsifiers. They can adsorb to oil droplet interfaces and form a protective layer which protects the droplets against flocculation and coalescence through repulsive interactions. Milk proteins are a popular choice for emulsion stabilisation. Milk proteins are divided

into two distinct groups viz casein (β-, κ-, α_{s1}-, α_{s2}-) and whey proteins (β-lactoglobulin, α-lactalbumin). Caseins have a disordered flexible structure and the whey proteins have an ordered globular structure.

Milk proteins act as emulsifiers either as individual protein molecules or aggregates and are believed to stabilise emulsions by forming a thin, dense interfacial layer (Dickinson, 1997). During processing of milk proteins, the native casein micellar structure is disrupted to some extent based on the type of processing condition employed.

The structural conformation of proteins changes during adsorption as they rearrange and unfold due to interactions with the interface. These adsorbed conformations have been reported to differ for the disordered caseins and globular whey proteins (Dickinson, 1992) and these conformations play an important role on the final structure and stability of emulsions (Das & Kinsella, 1990).

Ye et al. (2013) reported about the design of a novel structured oil-in-water emulsion stabilised by protein coated nanoemulsion droplets. This novel food emulsion consists of a core lipid droplet stabilised by smaller, protein-coated lipid droplets. Using micellar casein, they showed the adsorption and structural conformation of casein micelle-coated oil droplets at the interface of hexadecane droplets. This novel emulsion structure proves promising in protecting and enhancing the delivery of bioactives thus a full understanding of the structure and formation will contribute significant knowledge for potential applications in the functional food industry.

In this study, formation of droplet-stabilised emulsion using food grade oils was explored and the effect of formulation and processing conditions on its formation and structural properties was examined. The potential to produce droplet-stabilised emulsions with different types of milk protein concentrates, surface lipids, core lipids and homogenisation conditions was explored with a view of providing useful critical information to ensure consistent successful production of droplet-stabilised emulsions with food grade oils and different types of milk protein concentrates.

4.3 Materials and Methods

All materials, equipment and emulsion structure characterisation methods used in this chapter are detailed in Chapter 3. Experimental set-up of this study is summarised in Figure 3.1. MPCs 1 (4851), 2 (485), 3 (470), and 4 (4861) were used in this study and except where specified, the surface and core lipids consisted of palmolein and soybean oil respectively. Protein and calcium contents of MPCs used in this study as provided by supplier are shown in Table 4.1. Calcium levels in MPC 4 were lower while calcium levels in MPC 1, 2 and 3 were similar. Protein content of MPC 3 was lower than MPC 1, 2 and 4. These MPCs can be divided into three categories viz: high protein MPC, low protein MPC, and calcium-depleted MPC.

Table 4.1 *Protein and calcium contents of MPCs*

High protein MPC (MPC-85)		
MPC	**Protein (g/100g)**	**Calcium (mg/100g)**
1	82.9	2160
2	81.3	2230
Low protein MPC (MPC-70)		
MPC	**Protein (g/100g)**	**Calcium (mg/100g)**
3	69.9	2180
Calcium-depleted MPC		
MPC	**Protein (g/100g)**	**Calcium (mg/100g)**
4	81.8	1260

4.3.1 Droplet stabilised emulsions (DSEs)

Droplet-stabilised emulsions in this study were prepared by a two-step process as shown in Figure 4.1. Firstly, MPC solutions were prepared by magnetic stirring of 5 g milk protein concentrate (MPC) into 95 g milli-Q water at room temperature for 1 h, after which MPC solution was heated to 55 °C and appropriate quantities of surface lipid added i.e. 80% w/w MPC solution and 20% w/w surface lipid. The mixtures were held at 55°C for 3-5 min and coarse emulsions were formed using a high-speed mixer (Labserv, D-130) at 6000 rpm for 3 min. The coarse emulsions were passed through either a microfluidizer (M-110P, Microfluidics) at 25000 psi (1700 bar) or a two-stage homogeniser (12.5H, Rannie, Denmark) at a first stage pressure of 200 bar and second stage pressure of 40 bar to produce

a fine emulsion referred to as ‘shell emulsion’. Droplet-stabilised emulsions were obtained in a second step by adding the shell emulsion obtained in the first step to appropriate quantities of core lipid and potassium phosphate buffer (10 mM K_2HPO_4 and KH_2PO_4, pH 6.8-7.0), i.e. 10% w/w shell emulsion, 20% w/w core lipid and 70% w/w buffer. To form droplet-stabilised emulsions, the mixture was heated to 55 °C and processed with a high-speed mixer (D-130, Labserv) at 6000 rpm for 5 min.

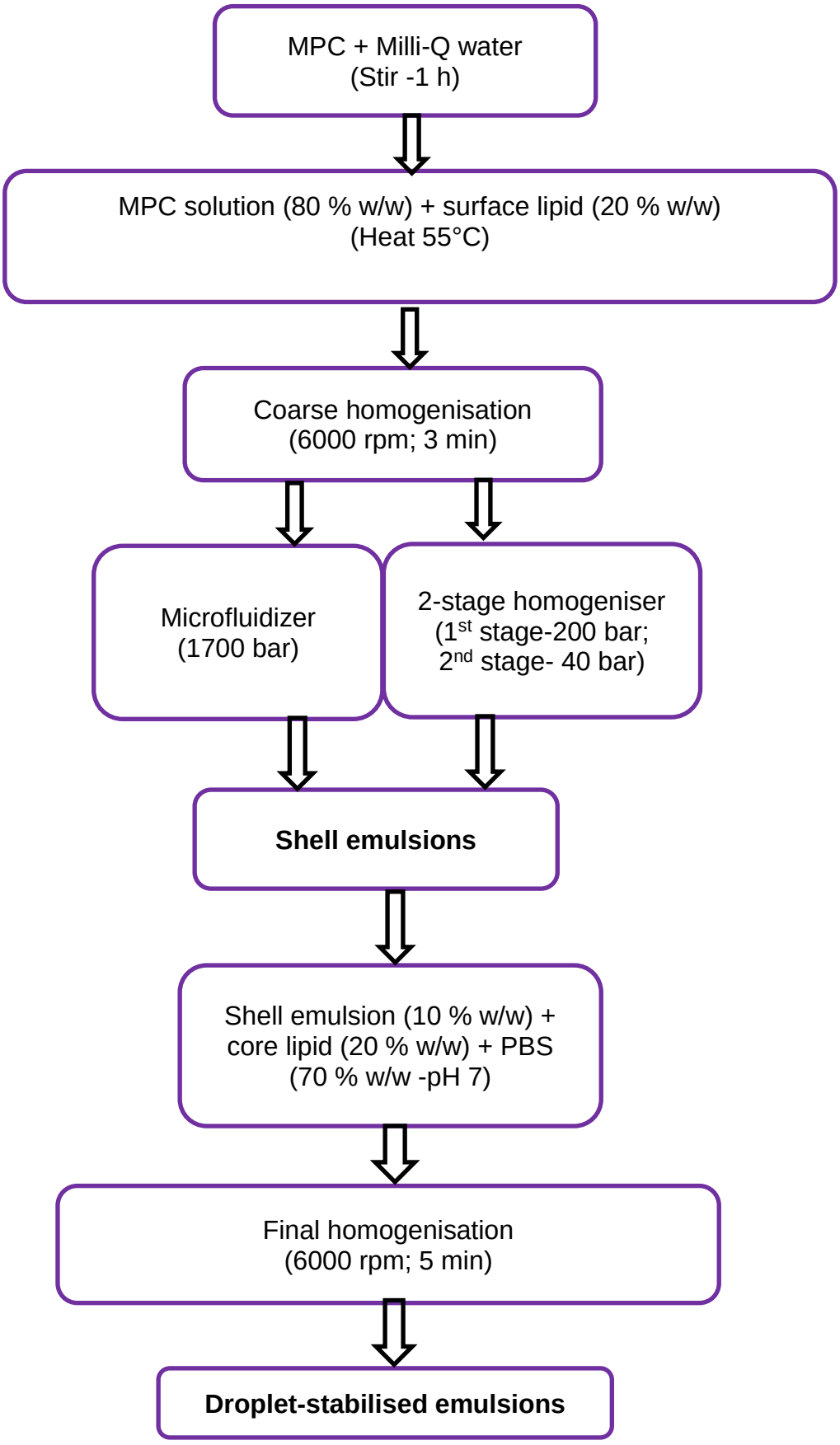

Figure 4.1 *Flow chart of droplet-stabilised oil-in-water emulsion production*

4.4 Results and Discussion

4.4.1 Formation of droplet-stabilised soybean oil-in-water emulsions with high protein MPC

The ability of MPC-85 to form droplet-stabilised emulsions (DSEs) with food-grade lipids was investigated. MPC stabilised palmolein oil shell droplets were prepared through the two-stage homogeniser and then used to stabilise soybean oil-in-water droplets. Particle size distributions of shell and droplet-stabilised soybean oil emulsions made with MPC 1 and 2 are shown in Figure 4.2. Confocal microscopy images of DSEs made with MPC 1 and 2 shell emulsions processed via the two-stage homogeniser are shown in Figure 4.3.

The average droplet diameter ($d_{3,2}$) and volume weighted mean diameter ($d_{4,3}$) of shell emulsions and droplet-stabilised emulsions made with MPC 1 and 2 were similar. Confocal micrographs of droplet-stabilised emulsions made with MPC 1 and 2 showed that shell droplets adsorbed on to the surface of soybean oil droplets and totally covered the surface area forming droplet layers (Figure 4.3 B & D). The shell droplets assembled together forming a layer along the interface of soybean oil droplets. Shell droplets at the interface did not just form a single droplet layer but connected with other shell droplets by protein interactions forming several droplet layers; these multi-droplet layers formed a thick interfacial coating at the surface of soybean oil droplets (Figure 4.3 B & D). Some soybean oil droplets were fully covered while some were not (Figure 4.3 A & C). This could be due to formation of multiple droplet layers on the fully covered interface. These interfacial structures observed are similar to those reported by Ye et al. (2013) for hexadecane droplets stabilised by casein-coated nano-droplets.

In this study, hexadecane (hydrocarbon) was replaced with palmolein and soybean oils as surface and core lipids respectively. These food grade oils have a lower interfacial tension than hexadecane (Gaonkar & Borwankar, 1991; Gurkov et al., 2005). These results show that triglyceride food grade lipids can be stabilised by MPC-coated shell droplets. The MPC-coated shell droplets act as an emulsifier by adsorbing on to the surface of oil droplets and form single or multiple droplet layers along the interface.

In the study carried out by Ye et al. (2013), casein stabilised nanoemulsions used to stabilise large hexadecane droplets were processed through the microfluidizer at a pressure of 30 MPa and, the average droplet diameter of the nanoemulsions formed was 0.15 µm. In this study, MPC shell emulsions made with MPC 1 and 2 were processed through the two-stage homogeniser at lower pressures (1^{st} stage- 20 MPa; 2^{nd} stage – 4 MPa), and the average droplet diameter of shell emulsions was > 1 µm (Figure 4.2A).

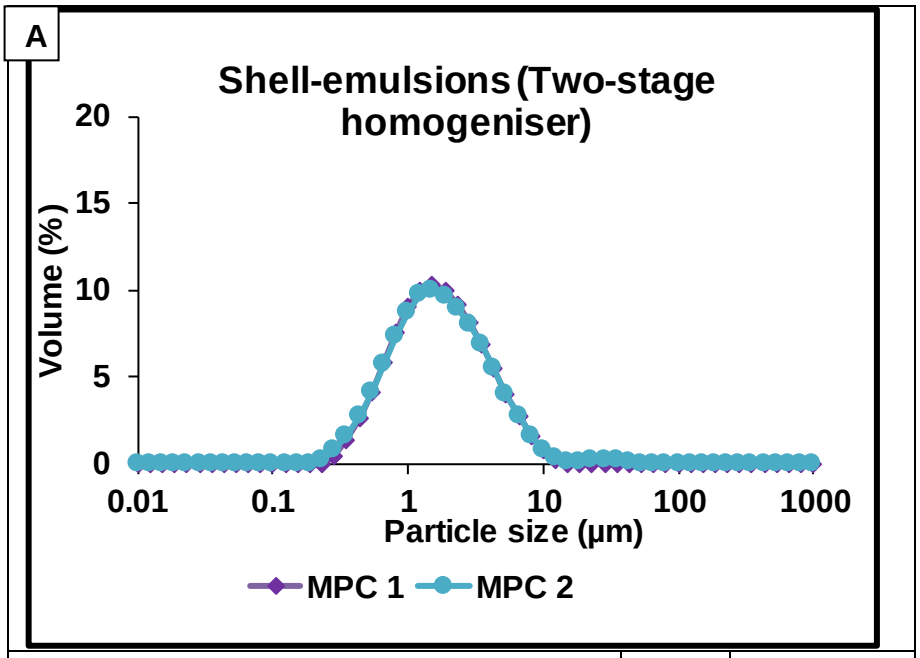

	$d_{3,2}$	$d_{4,3}$
MPC 1	1.43	2.48
MPC 2	1.40	2.71

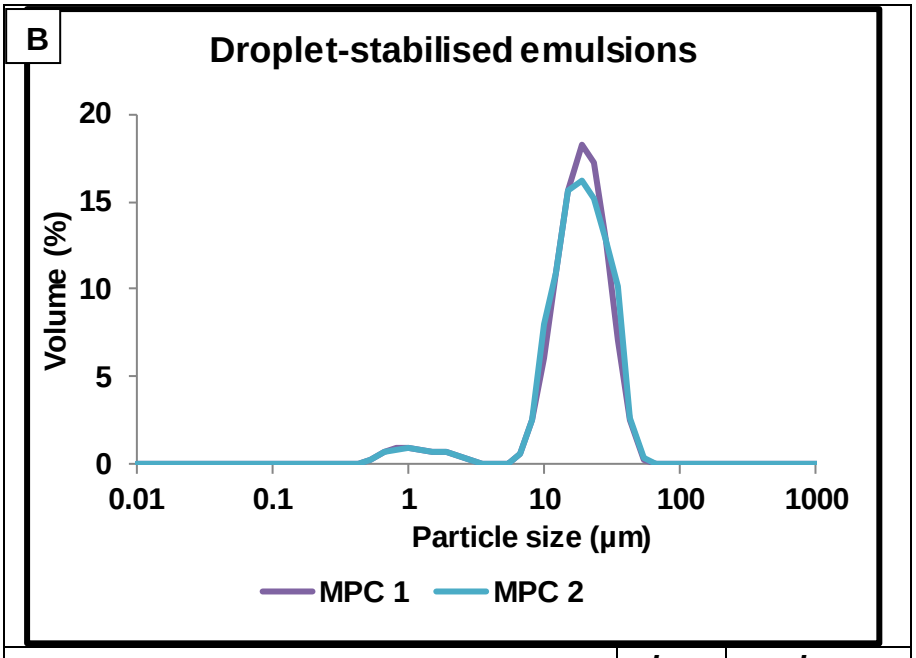

	$d_{3,2}$	$d_{4,3}$
MPC 1	10.17	21.60
MPC 2	10.20	21.64

Figure 4.2 *Particle size distribution of shell emulsions (A) and droplet-stabilised soybean oil-in-water emulsions (B) made with MPC 1 and 2*

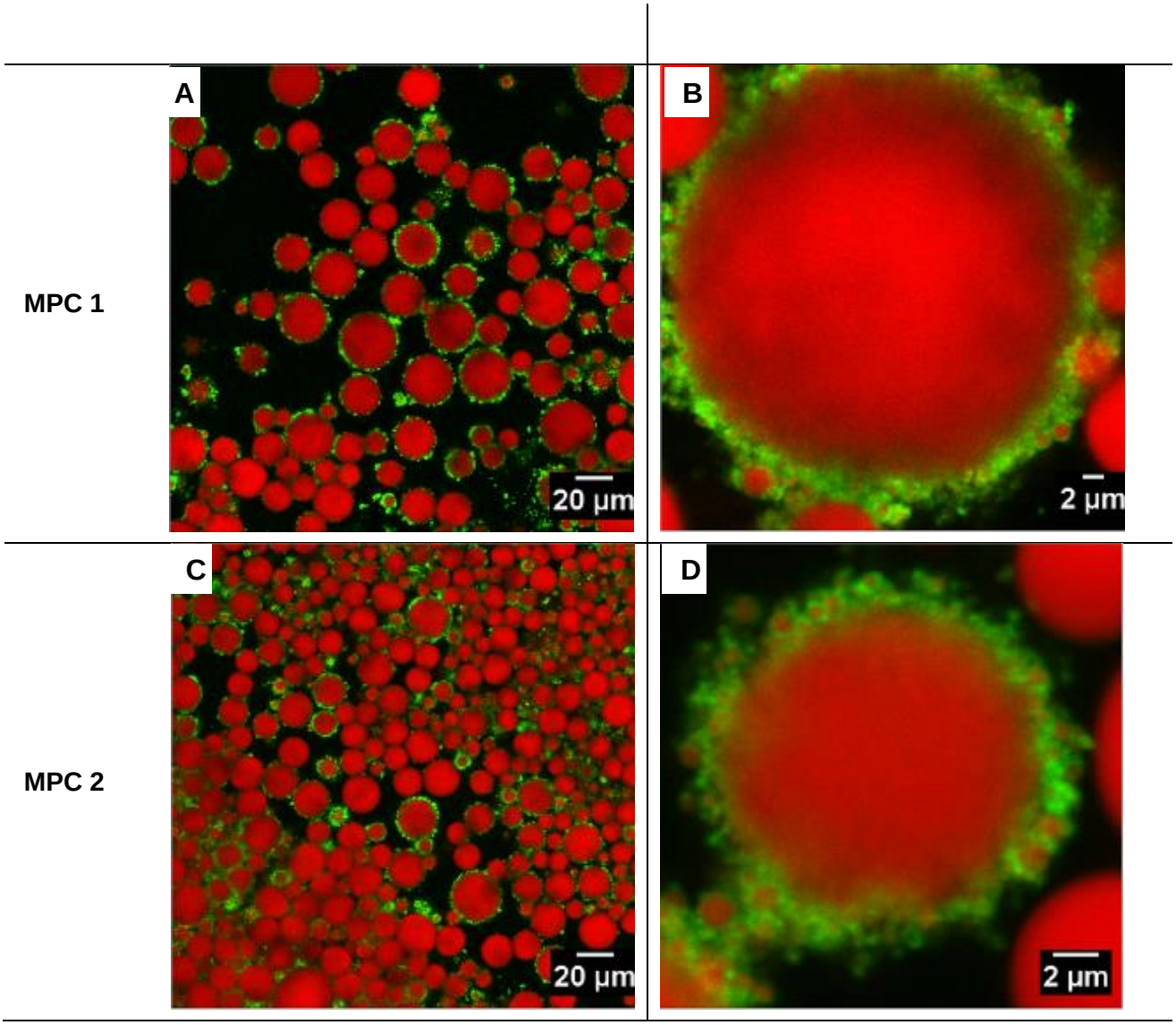

Figure 4.3 *Confocal microscopy images of droplet-stabilised emulsions made with MPC 1 and 2 shell emulsions processed via the two-stage homogeniser (B & D = zoom).*

4.4.2 Effect of shell emulsion concentration on formation of droplet-stabilised emulsions (high protein MPC)

Effect of shell emulsion concentration on DSE was investigated with MPC 1. Shell emulsion processed via the two-stage homogeniser was used to determine the effect of shell emulsion concentration (2 %, 10 % and 16 %) on formation of droplet-stabilised emulsion. Average droplet diameter ($d_{3,2}$) and volume weighted mean diameter ($d_{4,3}$) of shell emulsions made with MPC 1 and processed through the two-stage homogeniser were 1.43 µm and 2.48 µm respectively (similar results obtained with MPC 2).

Particle size distributions and confocal microscopic images of DSEs made with 2%, 10% and 16% shell emulsions made with MPC 1 are shown in Figure 4.4. Average droplet diameter ($d_{3,2}$) of final DSEs decreased from 24.33 µm to 7.17 µm as quantity of shell emulsion increased from 2 to 16% in the final emulsion. The particle size distribution became bimodal with a small peak in the size range of 0.4-1.5 µm which fell within size range of shell droplets became evident at higher shell emulsion concentrations. Volume percentage of droplets within the small peak size range of 0.4-1.5 µm also increased as shell emulsion concentration increased from 10% to 16%. These results are similar to those obtained by Ye et al. (2013) for hexadecane oil droplets stabilised with casein-coated nano-droplets, whereby the small peak in the size range of 0.05-0.8 µm observed in DSEs emulsions containing high concentrations of nanoemulsions (6%, 8%, 12% & 16%) was attributed to the presence of unadsorbed shell droplets.

DSEs made up of 2% shell emulsion was not fully coated with shell droplets (Figure 4.4 A, D & G) and this explains why the droplet size distribution curve for this emulsion did not have the shell droplet peak observed with DSEs emulsions containing higher shell emulsion concentrations. It appears all the shell droplets, though insufficient to fully cover the interface of core droplets, adsorbed to the surface of the core droplets. Again, these results confirm the observations of Ye et al. (2013).

On the other hand, confocal images showed that most of the surface of DSEs made up of 10% and 16% shell emulsion were totally covered but more even coating of core droplets was apparent with 10% shell emulsion (Figure 4.4 B, E & H). The expectation was that since shell droplet concentration was higher with DSEs containing 16% shell droplets, there would be even coating of core droplets whereby interface of most core droplets would be totally covered. However, it appeared that though most of the core droplets were coated by shell droplets, some core droplets were stabilised by multiple droplet layers forming a very thick layer of flocculated shell droplets (Figure 4.4 C, F & I). This provides a plausible explanation for why the interface of some core droplets was not evenly covered with shell droplets (Figure 4.4C).

In DSEs containing high shell droplet concentration, unadsorbed shell droplets interacted with adsorbed shell droplets to form a thick multi-droplet layer (Figure 4.4 E, F, H & I). In the work of Ye et al. (2013), transmission electron microscopy (TEM) images of droplets at the interface of hexadecane droplets containing 16 % casein micelle coated nano-droplets showed that the shape of nano-droplets adsorbed at the interface changed from a sphere to ellipse and rectangle. The

observed droplet deformation was conspicuous along the interface of the large droplets and became less pronounced toward the aqueous phase as the nano-droplet shape returned to a sphere. The TEM images also showed that nano-droplets connected together and formed multi-droplet layers as observed in this study with soybean oil droplets stabilised with MPC shell droplets.

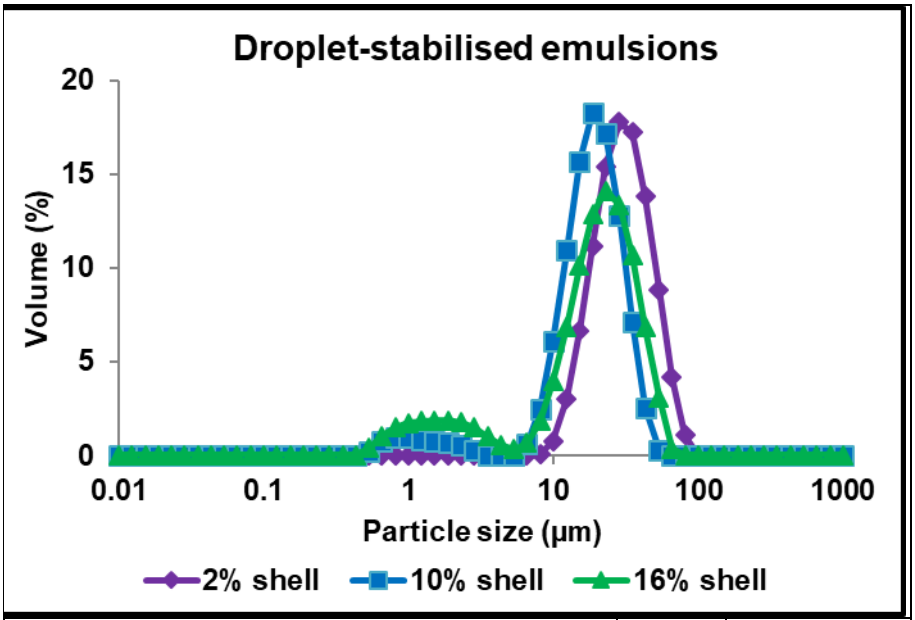

	$d_{3,2}$	$d_{4,3}$
2% shell	24.33	29.30
10% shell	10.17	21.60
16% shell	7.17	23.64

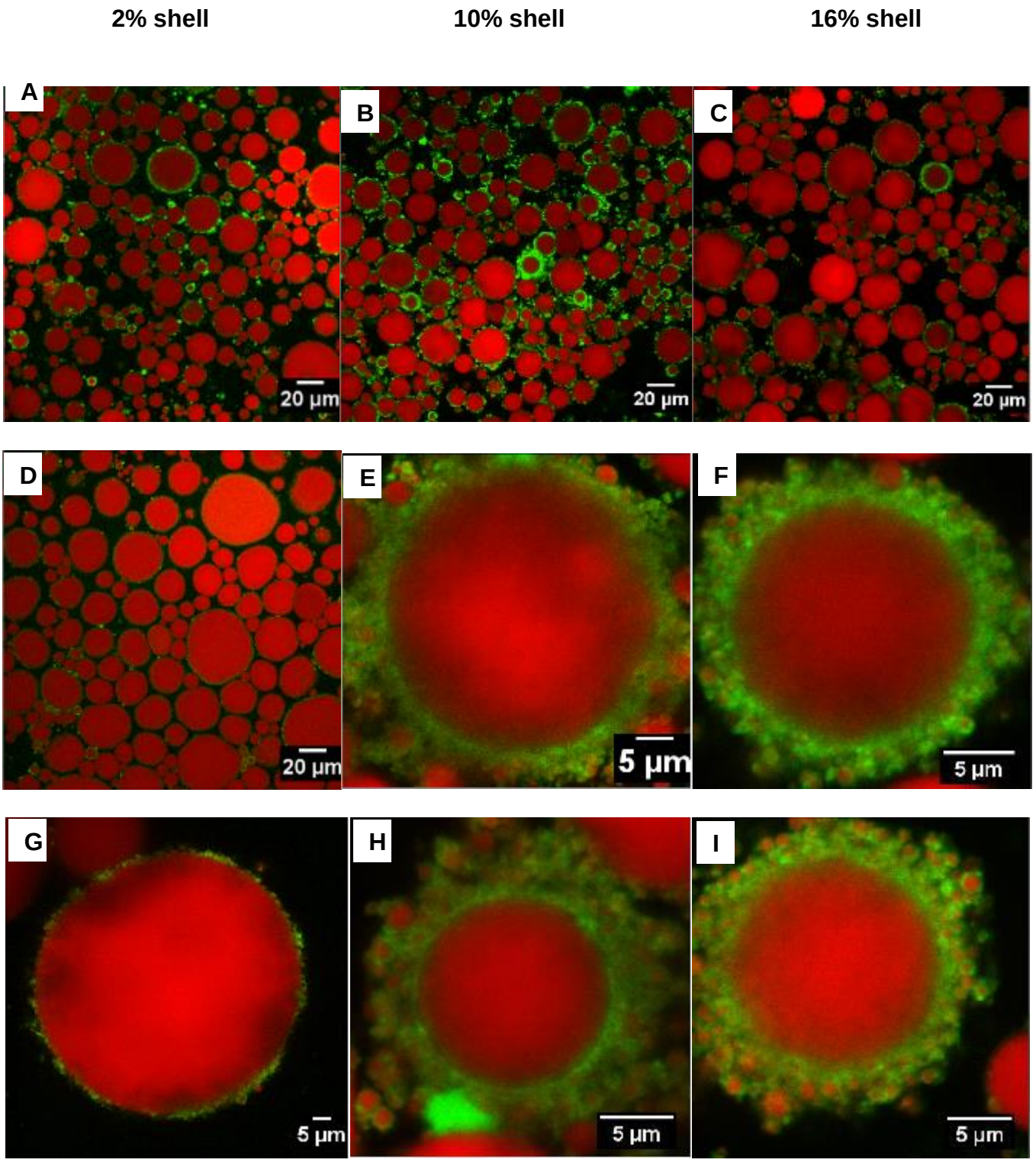

Figure 4.4: *Particle size distribution and confocal microscopy images of droplet-stabilised emulsions processed with MPC 1 and varying concentrations of shell emulsion*

4.4.3 Effect of low protein MPC on formation of droplet-stabilised emulsions

The emulsifying behaviour of lower protein MPC was investigated with MPC-70 (i.e MPC 3) at shell droplet concentration of 10%. Protein content of MPC 3 was lower than MPC 1, 2 and 4.

Particle size distribution and confocal microscopy images of DSEs made with MPC 3 shell emulsions processed with the two-stage homogeniser are shown in Figure 4.5. The average droplet diameter ($d_{3,2}$) and volume weighted mean diameter ($d_{4,3}$) of shell emulsions made with MPC 3 were 1.63 µm and 2.50 µm respectively, while that of shell emulsions made with higher protein MPC (MPC 1) was 1.79 µm and 2.69 µm respectively. Average droplet diameter ($d_{3,2}$) and volume weighted mean diameter ($d_{4,3}$) of DSEs made with MPC 3 was similar to those made with MPC 1 at the same shell emulsion concentration of 10% (Figure 4.5B).

Confocal micrographs of DSEs made with MPC 3 showed that shell droplets adsorbed to the interface of soybean oil and formed a droplet layer along the interface just as observed with DSEs made with MPC 1 (Figure 4.5 E & F). Emulsifying behaviour of shell droplets made with MPC 3 at the interface of soybean oil droplets was similar to that of shell emulsions made with MPC 1 and 2.

Calcium content of MPC 3 was similar to that of MPC 1 and 2 but protein content was lower. Emulsifying capacity of aggregated milk proteins like MPC is reported to be much lower than that of non-aggregated proteins implying that much higher

concentrations of MPC are required to form stable emulsions (Euston & Hirst, 1999; Ye, 2011). The expectation was that since protein content of MPC 3 was lower than MPC 1 and 2, higher protein and hence shell droplet concentrations would be required to form droplets layers and totally cover the interface. However, this was not the case because protein (4% w/w) and shell droplet concentrations (10% w/w) used to form MPC 3 DSEs were the same as that used for MPC 1 and 2 DSEs. Interestingly, average droplet diameter ($d_{3,2}$) and volume weighted mean diameter of DSEs made with MPC 1 and 3 were also similar (Figure 4.5B). In the study reported by Ye et al. (2013), micellar casein-coated droplet layers were also formed with 8% and 12% nano-droplets, this concentration range is similar to that used for MPC 1, 2 and 3 DSEs in this study, although in Ye et al's study, the average diameter ($d_{3,2}$) of droplets used for stabilisation are in the nano-scale range (0.15µm) while in this study the shell droplets are bigger (1.63 µm for MPC 3 & 1.79 µm for MPC 1).

These results indicate that ability of MPC stabilised shell emulsions to adsorb to the interface of soybean oil droplets, totally cover the interface and form droplet layers is greatly dependent on MPC's intact casein micelle structure. The fact that shell emulsions made with MPC 3 which contains a lower protein content than MPC 1 and 2 sufficiently formed a droplet layer at the interface of soybean oil droplets like MPC 1 and 2 shell droplets did indicate that for shell droplet emulsification with MPC, aggregated casein micellar structure is a more important factor than the protein content.

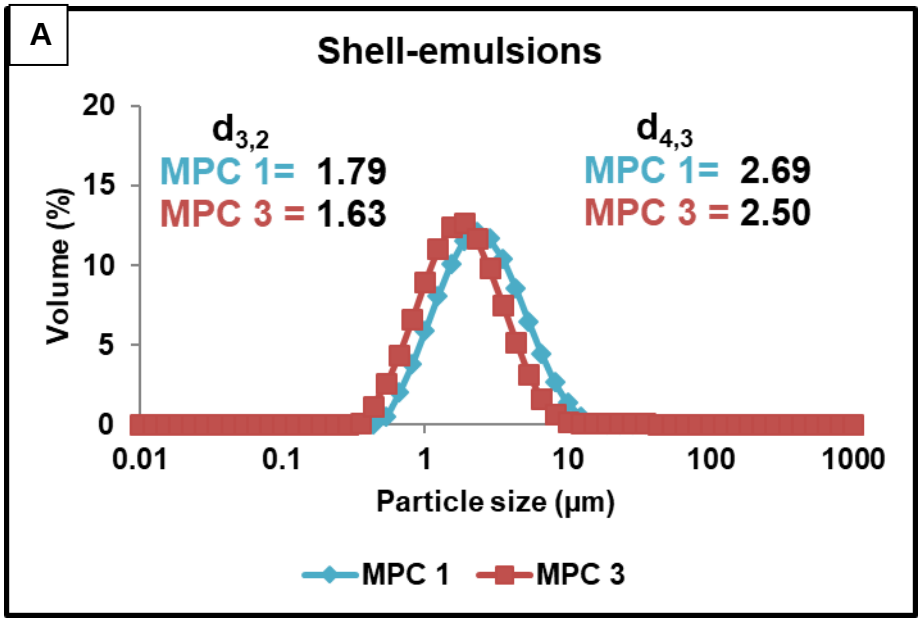
A
Shell-emulsions
$d_{3,2}$
MPC 1= 1.79
MPC 3 = 1.63
$d_{4,3}$
MPC 1= 2.69
MPC 3 = 2.50
Volume (%)
20
15
10
5
0
0.01
0.1
1
10
100
1000
Particle size (µm)
MPC 1
MPC 3

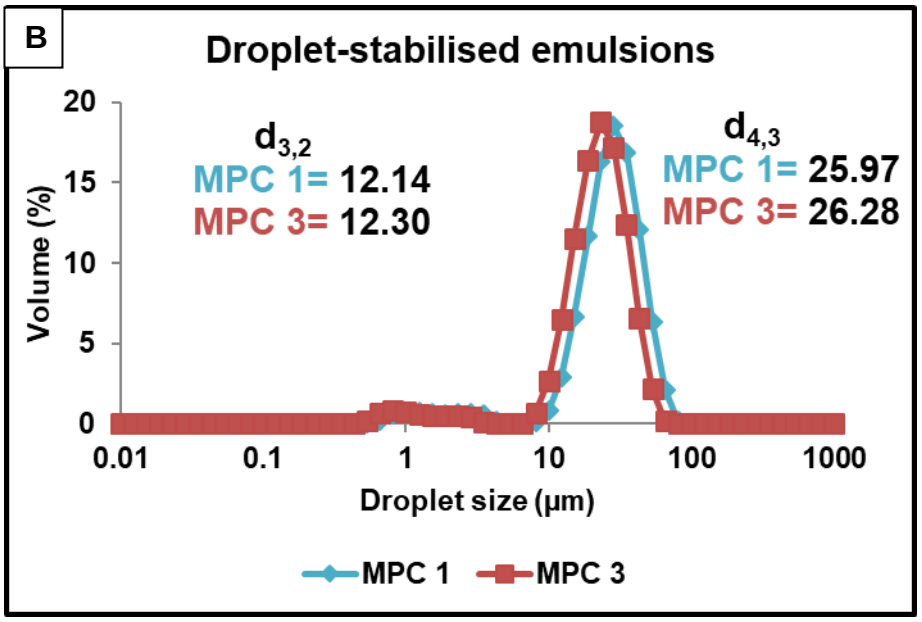
B
Droplet-stabilised emulsions
$d_{3,2}$
MPC 1= 12.14
MPC 3= 12.30
$d_{4,3}$
MPC 1= 25.97
MPC 3= 26.28
Volume (%)
20
15
10
5
0
0.01
0.1
1
10
100
1000
Droplet size (µm)
MPC 1
MPC 3

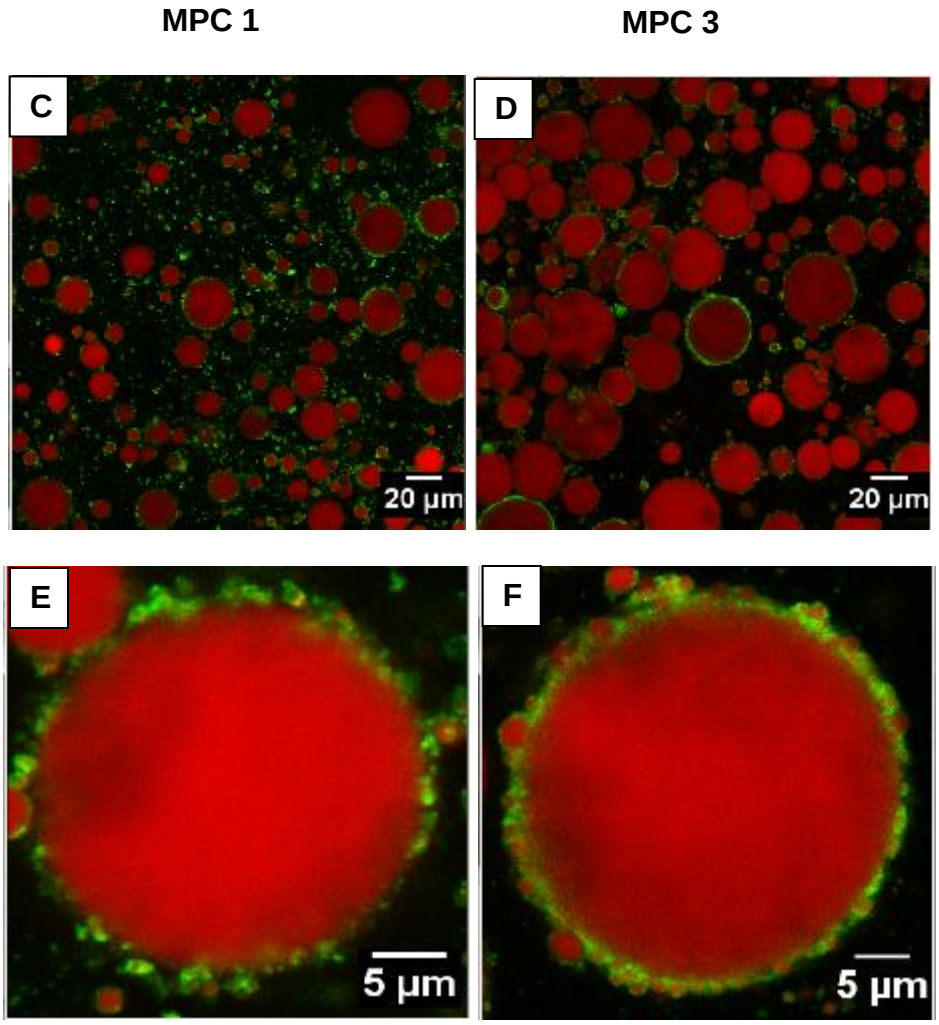

Figure 4.5: *Particle size distribution (A & B) and confocal microscopy images (C, D, E & F) of droplet-stabilised emulsions processed with MPC 1 and 3.*

4.4.4 Effect of calcium-depleted MPC on the formation of droplet-stabilised emulsions

Particle size distribution of shell and droplet-stabilised emulsions made with MPC 4 are shown in Figure 4.6. Average droplet diameter ($d_{3,2}$) of shell emulsion made with MPC 4 was smaller (<1 µm) than that of MPC 1 and 2 processed using the two-stage homogeniser (Figure 4.2A) under the same pressure conditions.

Average droplet diameter ($d_{3,2}$) of droplet-stabilised emulsions made with MPC 4 shell emulsion processed via the two-stage homogeniser was larger (>10µm) than that of MPC 1 and 2 shell emulsions (Figure 4.2B).

Confocal microscopic images of DSEs produced with MPC 4 shell emulsions processed via the two stage homogeniser are shown in Figure 4.7. Interfacial layers formed at the surface of DSEs made with MPC 4 differed from that observed with DSEs made with MPC 1, 2 and 3. Confocal micrographs of DSEs made with MPC 4 showed that the interface was stabilised by a single protein layer formed along the interface, adsorption of shell droplets was not evident at the interface of core droplets (Figure 4.7B). In DSEs made with MPC 1 and 2, when the shell droplets were processed via the two-stage homogeniser, shell droplets adsorbed to the interface of soybean oil and formed single or multiple droplet layers along the interface (Figure 4.3) but droplet layers were not observed with DSEs made with MPC 4.

MPC contains both caseins and whey proteins in ratios similar to milk and the caseins are in the micellar form. Aggregated structure of casein micelles is held together by calcium-phosphate bridges and a reduction in calcium content implies

dissociation of casein micelles to some extent (Ye, 2011). Calcium content of MPC 4 was lower than that of MPC 1, 2 and 3 which implies calcium depletion in MPC 4 and some dissociation of casein micelles. While calcium contents of MPC 1, 2 and 3 were in the range 2160-2280 mg /100g that of MPC 4 was 1260 mg/100g.

Shell droplets made with MPC 1, 2 and 3 processed through the two-stage homogeniser sufficiently stabilised soybean oil droplets while shell droplets made with MPC 4 processed under the same conditions did not form a droplet layer but, formed a single protein layer. It is possible that there was some competitive adsorption between free proteins and shell droplets for the surface of soybean oil droplets, whereby free proteins adsorbed on to the surface instead of protein-coated shell droplets.

The observed differences in the shell droplet emulsification behavior between MPC 4 and MPC 1, 2 and 3 indicate that calcium depletion in MPC 4 disrupted aggregated structure of micellar casein arising from reduced calcium levels, casein molecules became more flexible, adsorbed and spread at the interface of soybean oil droplets as single layers. These results are in agreement with Ye (2011) who reported that dissociation of casein micelles in MPCs because of reduction in calcium content improved their emulsifying ability over MPCs with higher calcium contents. Moreover, improved emulsifying properties with individual casein molecules over aggregated caseins have also been reported (Euston & Hirst, 1999; Mulvihill & Murphy, 1991) so this is not surprising.

These results substantiate the hypothesis that native micellar structure of caseins in MPC influences the ability of MPC shell droplets to sufficiently stabilise the interfaces of larger oil droplets by forming droplet layers along the interface.

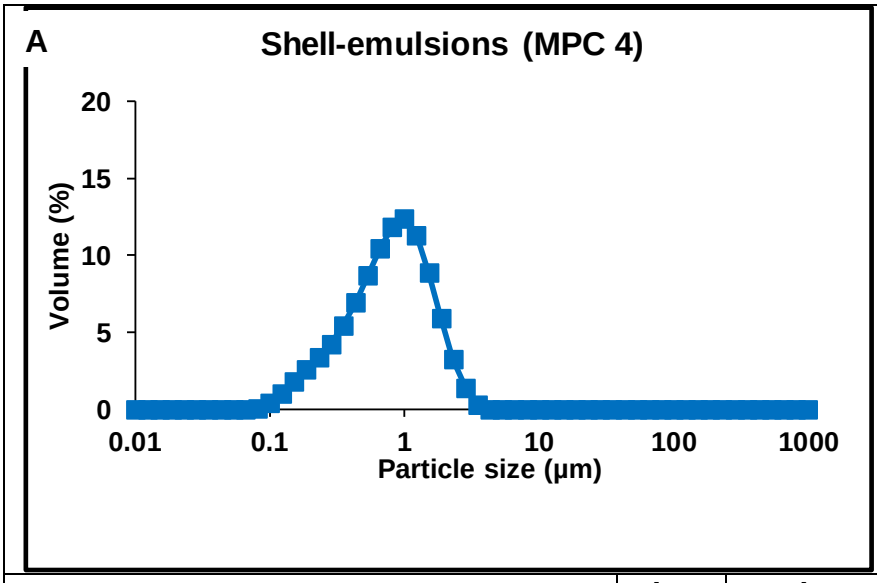

	$d_{3,2}$	$d_{4,3}$
Homogeniser	0.62	1.02

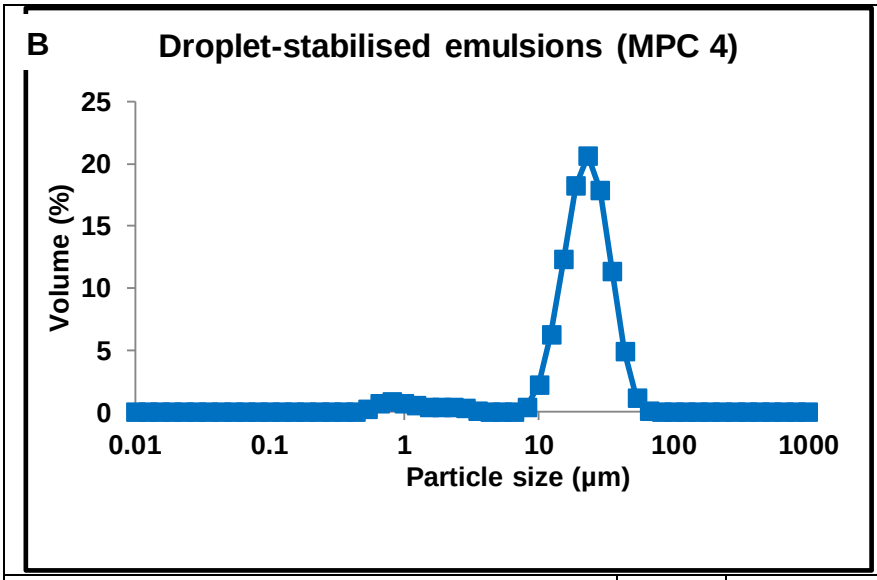

	$d_{3,2}$	$d_{4,3}$
Homogeniser	12.28	25.50

Figure 4.6: *Particle size distribution of shell (A) and droplet-stabilised (B) emulsions made with MPC 4 shell emulsion processed via the two-stage homogeniser*

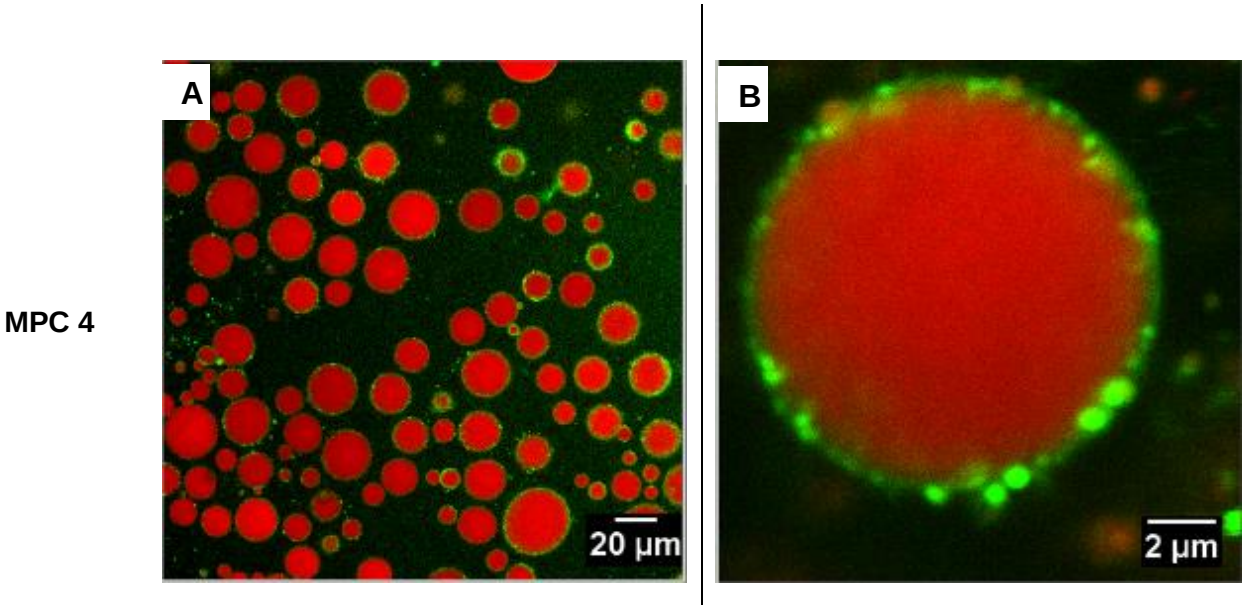

Figure 4.7: *Confocal microscopy images of droplet-stabilised emulsions made with MPC 4 shell emulsions processed via the two-stage homogeniser*

4.4.5 Effect of microfluidization on formation of droplet-stabilised emulsions with high protein and calcium-depleted MPC

The ability of shell emulsions processed via the microfluidizer with MPC 1 and 4 to form droplet-stabilised emulsions (DSEs) was investigated.

Particle size distributions of shell and droplet-stabilised soybean oil emulsions made with MPC 1 and 4 are shown in Figure 4.8.There was no rise in temperature during processing via the microfluidizer. Confocal microscopy images of DSEs made with MPC 1, 2 and 4 shell emulsions processed via the microfluidizer are shown in Figure 4.9.

The average droplet diameter ($d_{3,2}$) and volume weighted mean diameter ($d_{4,3}$) of shell emulsions made via the microfluidizer with MPC 4 were smaller (<1 µm) than shell emulsions processed with MPC 1 (Figure 4.8A). Average droplet diameter ($d_{3,2}$) of shell emulsions processed with MPC 4 via the microfluidizer was similar to results obtained by Ye et al. (2013) for micellar casein stabilised nanoemulsions (0.15 µm) processed via the microfluidizer at similar protein concentrations.

Shell emulsions prepared with MPC 1 and 4 and processed through the microfluidizer were used to stabilise soybean oil. Average droplet diameter ($d_{3,2}$) of droplet-stabilised emulsions made with MPC 4 shell emulsion processed via the microfluidizer was smaller (<10µm) than that of MPC 1 shell emulsions (Figure 4.8B).

Confocal micrographs showed that the surface of soybean oil droplets stabilised with shell emulsions made with MPC 1 and 2 processed through the microfluidizer

was not totally covered with shell droplets; a few shell droplets adsorbed to the interface but adsorption of most shell droplets at the interface appeared to be restricted by aggregation of shell droplets into flocs (Figure 4.9 A, B, C & D).

Confocal micrographs of DSEs made with MPC 4 showed that the interface was stabilised by a single protein layer formed along the interface (Figure 4.9 E & F). Adsorption of shell droplets was not evident at the interface of core droplets just as droplet layers were not observed with DSEs made with MPC 4 shell emulsions processed via the two-stage homogeniser (Figure 4.7 A & B).

In a study carried out by Jafari, He, and Bhandari (2007) to optimize the production of nanoemulsions by microfluidization, evidence of droplet coalescence at higher pressures and cycles in the microfluidizer was shown with optical microscopy and this resulted in bigger emulsion droplet size. These observed effects were attributed to the possibility of competitive processes between droplet disruption and droplet coalescence whereby droplet coalescence may have preceded droplet disruption or possible changes in the emulsifying properties of the emulsifier due to high-pressure emulsification.

Mahdi Jafari, He, and Bhandari (2006) compared droplet size of nanoemulsions produced by microfluidization and found that droplet diameter only decreased up to 70 MPa, and when pressure increased above 70 MPa, droplet diameter increased with increasing pressure. Similar results were also observed by Robin, Blanchot, Vuillemard, and Paquin (1992) and Desrumaux and Marcand (2002) where droplet diameter also increased above certain pressures. This phenomenon of increasing particle size with increasing pressure has been

described as ‘over-processing’ by Tornberg (1980) and has been observed by other writers (Kolb, Viardot, Wagner, & Ulrich, 2001; Marie, Perrier-Cornet, & Gervais, 2002; Olson, White, & Richter, 2004).

It appears that processing MPC 1 and 2 in the microfluidizer at the pressure conditions employed i.e. 25,000 Psi (~170 MPa) induced shell droplet aggregation into large aggregates (over-processing). This aggregation effect was also evident in the physical appearance of these shell emulsions which tended to be very viscous compared to those processed with the two-stage homogeniser. To enable adsorption of most MPC 1 and 2 shell droplets, optimal pressure conditions are required to process MPC 1 and 2 shell emulsions via the microfluidizer to prevent over-processing.

MPC 4 shell emulsions were finer than MPC 1 and 2 shell emulsions. This was expected because of the reduction in calcium levels in MPC 4. Ye (2011) also reported that MPC with calcium content similar to MPC 4 formed smaller droplet sizes than MPC with similar calcium content to MPC 1 and 2. These results are also in agreement with the hypothesis that native micellar structure of caseins in MPC influences their emulsifying ability.

These results indicate that shell emulsification via the microfluidizer influences the ability of shell droplets formed with MPC-85 to sufficiently stabilise oil-in-water emulsions therefore, shell emulsification conditions should be carefully chosen or optimized to ensure total droplet interfacial coverage.

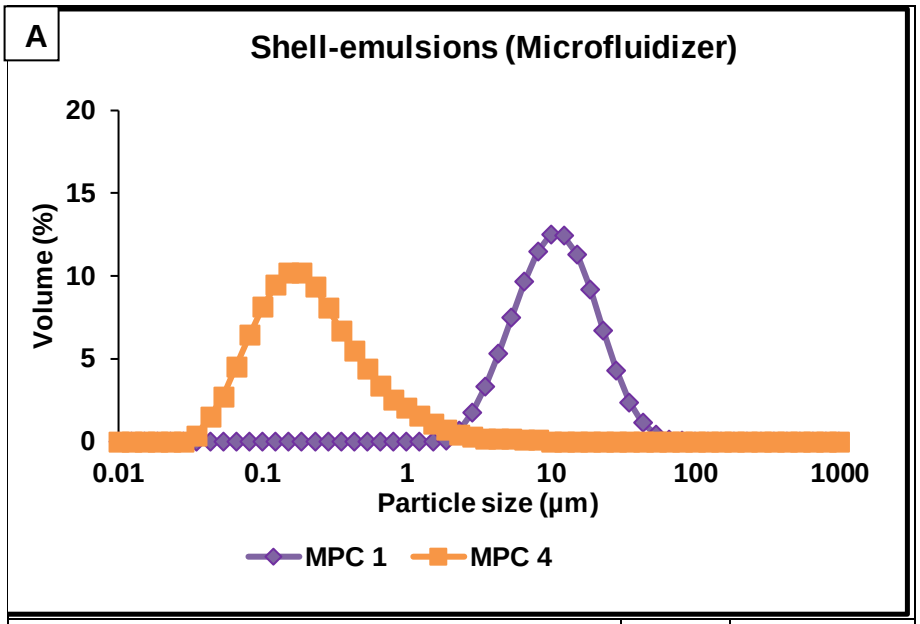

	$d_{3,2}$	$d_{4,3}$
MPC 1	9.75	14.40
MPC 4	0.17	0.38

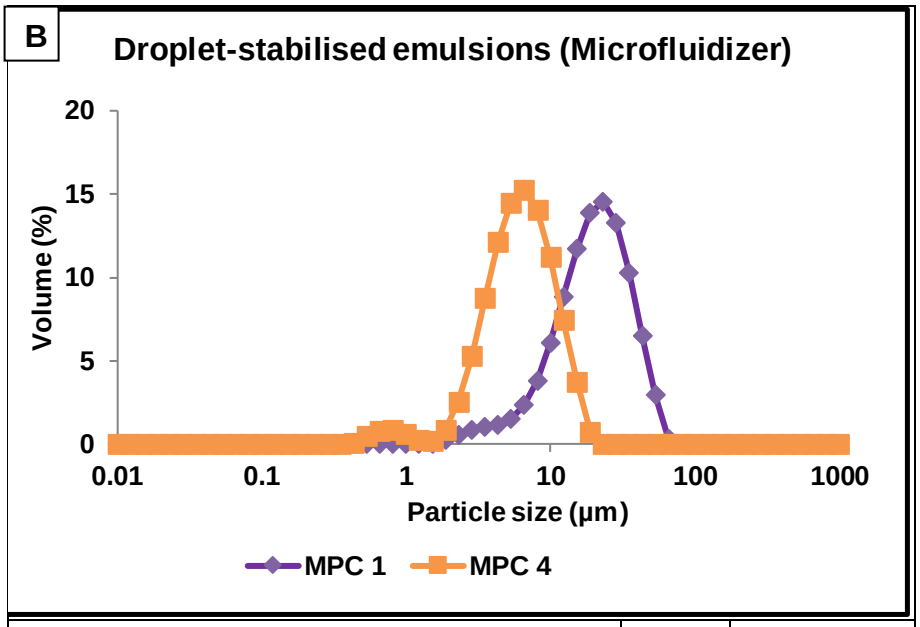

	$d_{3,2}$	$d_{4,3}$
MPC 1	16.34	24.55
MPC 4	5.09	7.50

Figure 4.8 *Particle size distribution of shell (A) and droplet-stabilised (B) emulsions made with MPC 1 and 4 shell emulsion processed via the microfluidizer*

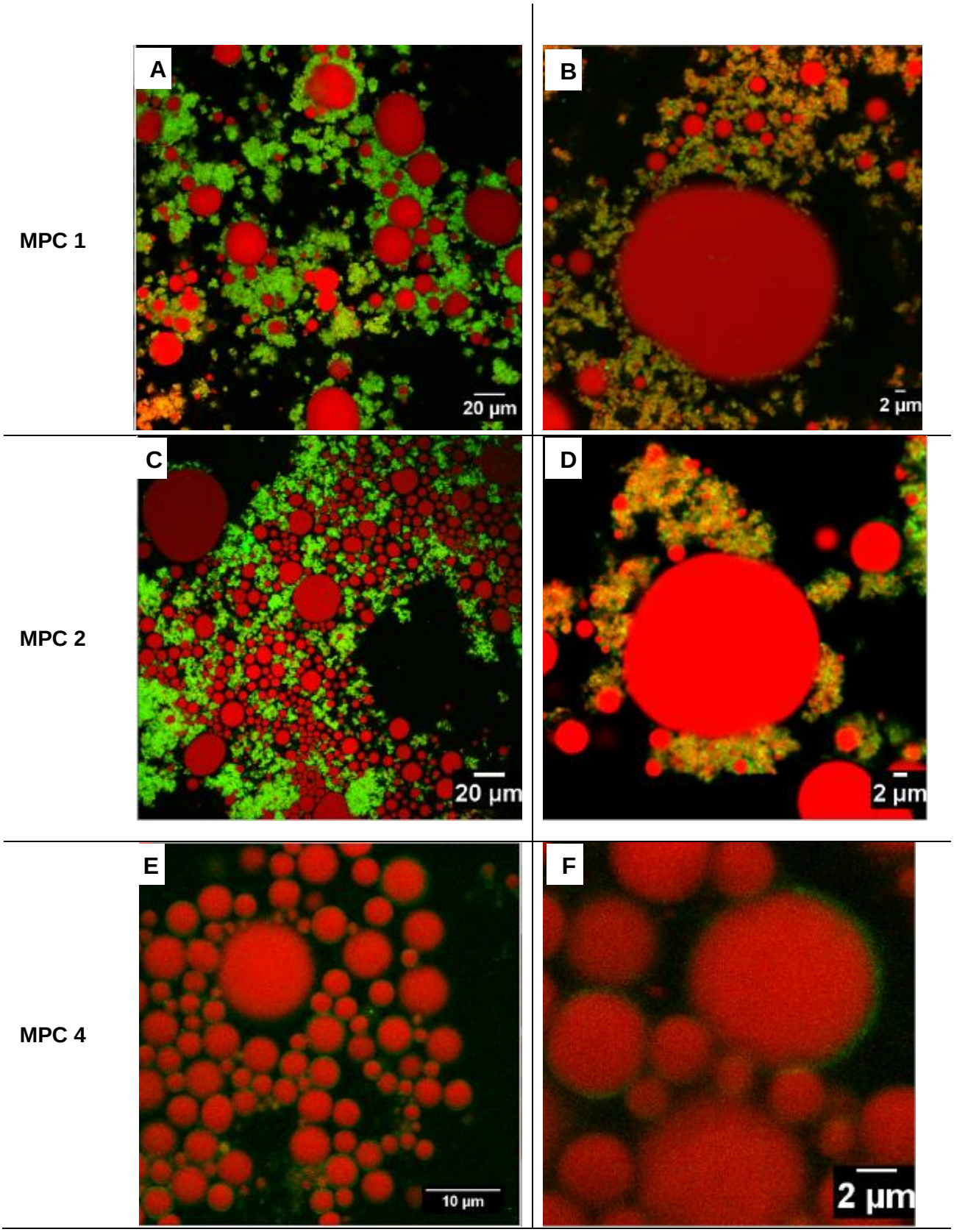

Figure 4.9 *Confocal microscopy images of droplet-stabilised emulsions made with MPC 1, 2 and 4 shell emulsions processed via the microfluidizer*

4.4.6 Effect of core lipid type on formation of droplet-stabilised emulsions

Food-grade triglyceride oil (soybean) was replaced with linoleic acid as core lipid, and MPC 1 was used as the protein source. MPC 1 shell emulsions were processed via the two-stage homogeniser. Figure 4.10 shows the particle size distribution of droplet-stabilised emulsions made with soybean oil and linoleic acid as core lipids at shell droplet concentrations of 10% (Figure 4.10A) and 16% (Figure 4.10B). Confocal micrographs of droplet-stabilised emulsions processed with linoleic acid as core lipid at shell droplet concetrations of 10% and 16% are shown in Figure 4.11.

There was significant difference ($p<0.05$) between average droplet size ($d_{3,2}$ and $d_{4,3}$) of emulsions made with soybean oil and linoleic acid as core lipids. Droplet size of core linoleic acid emulsions was smaller than that of soybean oil. Particle size distribution (PSD) of DSEs made with soybean oil core lipid was bimodal with a small peak that fell within the size range of 0.5-1.5 µm which was particularly evident in DSEs containing 16% shell droplets. PSD of DSEs made with linoleic acid core was mostly monomodal; the small bimodal peak evident in soybean oil DSEs was hardly evident in linoleic acid DSEs.

Confocal micrographs of linoleic acid DSEs containing 10% shell droplets showed that the interface of linoleic acid droplets appeared to be stabilised by a single protein layer formed along the interface (Figure 4.11B) just as observed with DSEs made with MPC 4 (i.e. calcium-depleted MPC).The micrographs of DSEs containing 16% shell droplets showed that the interface of some linoleic acid droplets was stabilised by a droplet layer formed along the interface (Figure

4.11D) while the interface of some linoleic acid droplets appeared to be stabilised by a single protein layer (Figure 4.11 E & H).

Confocal micrographs of DSEs containing 16% shell droplets also showed that the interface of some linoleic acid droplets appeared to be stabilised by a single protein layer with shell droplets connected to the single protein layer forming an outer droplet layer along the interface (Figure 4.11G). Overall, droplet stabilisation was more evident at the interfaces of soybean oil DSEs made with MPC 1 (Figure 4.3B; Figure 4.4 E,F,H & I; Figure 4.5E) than linoleic acid DSEs also made with MPC 1.

Droplet disruption is usually easier with lower interfacial tension (Walstra, 1993). Droplet disruption also becomes more difficult with increased viscosity of the dispersed phase and droplet size can be reduced by decreasing the viscosity ratio of the dispersed phase (McClements, 2015b). Viscosity of the dispersed phase has been shown to influence efficiency of droplet disruption (Jafari, Assadpoor, He, & Bhandari, 2008). Qian and McClements (2011) varied dispersed phase viscosity of nanoemulsion by using different concentrations of corn oil and octadecane; an increase in octadecane concentrations resulted in a decrease in the dispersed phase viscosity and this had an influence on the droplet diameter reduction. This effect was also dependent on the type of emulsifier used, in agreement with Wooster, Golding, and Sanguansri (2008) who also showed smaller nano-droplet sizes with low viscosity oils over higher viscosity long chain triglycerides.

In this study, since core linoleic acid droplets were smaller, it is possible that droplet disruption was easier which means that interface creation was faster resulting in adsorption of the more flexible free proteins which may have adsorbed faster to the interface than the more aggregated shell droplets resulting in the observed differences in droplet stabilisation between linoleic acid and soybean oil emulsions. These results indicate that the physicochemical properties of core lipid can influence the formation and structural properties of droplet-stabilised emulsions.

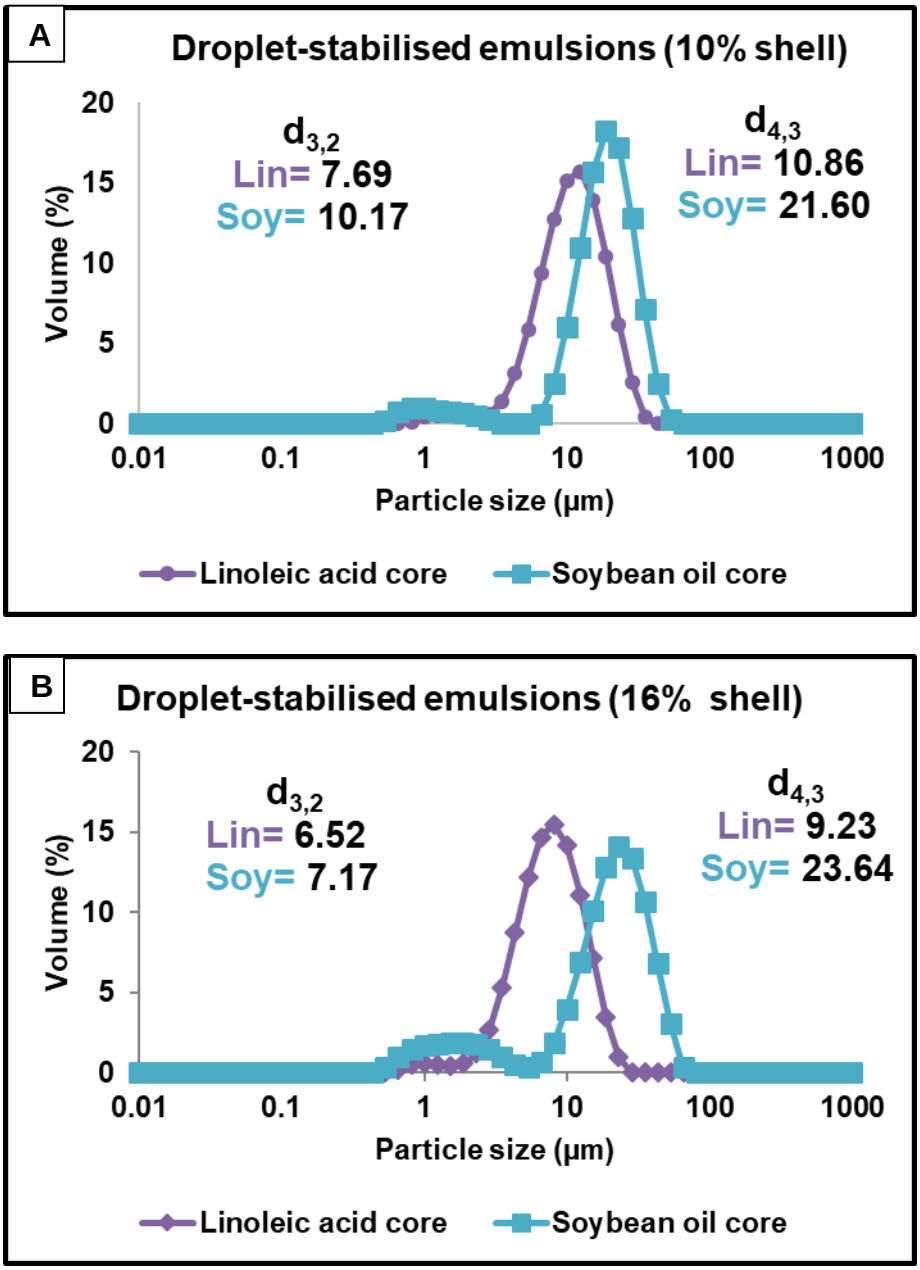

Figure 4.10: *Particle size distribution of droplet-stabilised soybean oil and linoleic acid core emulsions prepared with MPC 1 at 10% (A) and 16% (B) shell emulsion concentrations*

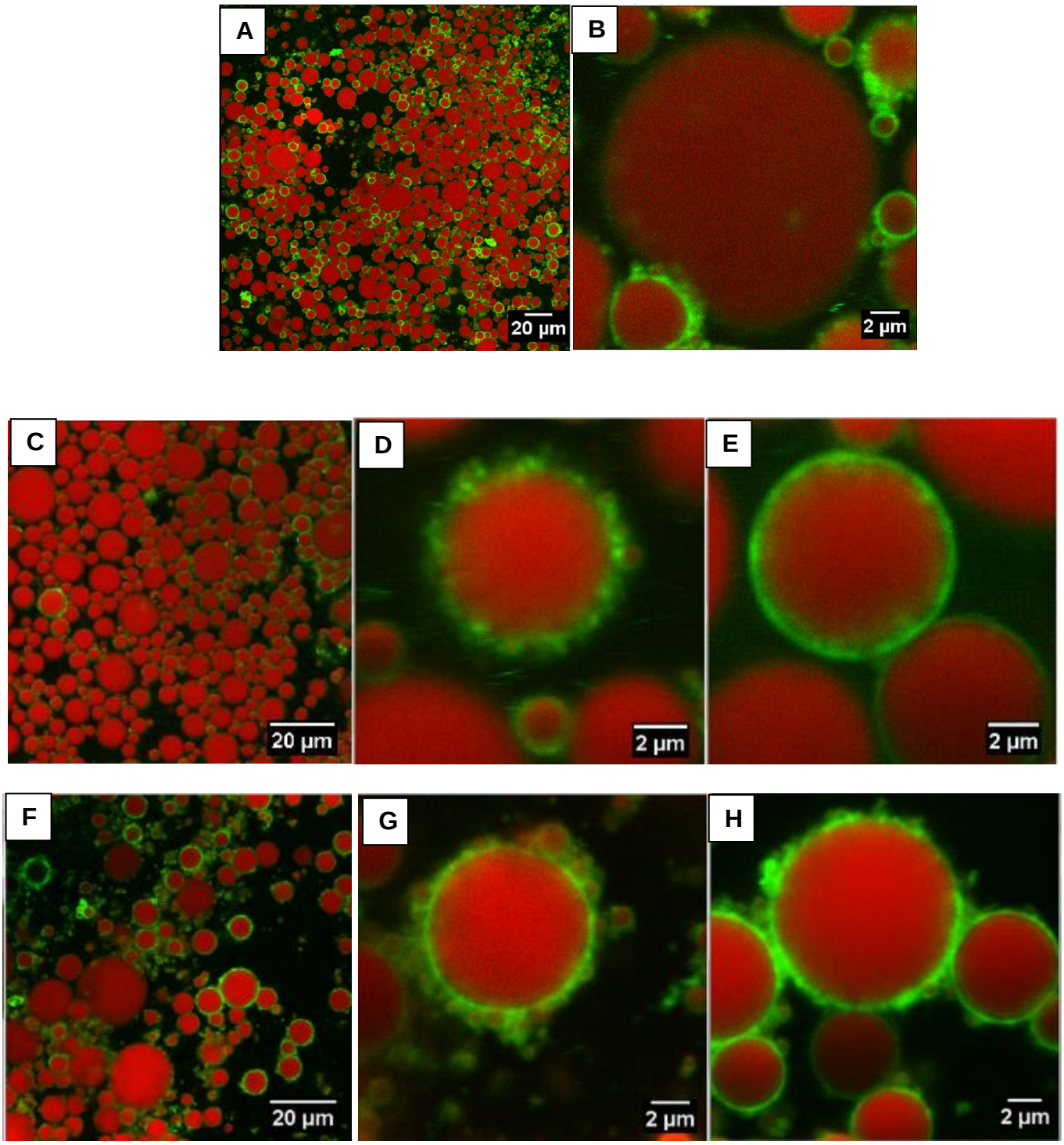

Figure 4.11: *Confocal microscopy images of droplet-stabilised linoleic acid core emulsions made with MPC 1 (A & B= 10% shell emulsion; C, D, E, F, G & H= 16% shell emulsion)*

4.4.7 Effect of surface lipid type and state on formation of droplet-stabilised emulsions

Formation of droplet-stabilised emulsions with surface lipids of varying melting points (low, medium and high) was investigated with MPC 3 (i.e. MPC 70) at 10% shell emulsion concentration. MPC-stabilised low (olive oil), medium (palmolein oil) and high (trimyristin) melting lipids were used to stabilise safflower oil-in-water droplets. Table 4.2 shows details of the DSEs processed.

Figure 4.12 shows the particle size distribution of shell and droplet stabilised emulsions made up of low (olive), medium (palmolein) and high (trimyristin) melting surface lipids. Figure 4.13 shows confocal microscopy images of droplet-stabilised emulsions made with these lipids. There were no significant differences ($p<0.05$) in the average droplet diameter ($d_{3,2}$) between shell and droplet-stabilised emulsions of low, medium and high melting lipids.

Table 4.2 *Emulsion formulations*

Samples	Description	Surface lipid	Core Lipid
NO	droplet-stabilised emulsion	Olive oil	Safflower oil
NP	droplet-stabilised emulsion	Palmolein oil	Safflower oil
NT	droplet-stabilised emulsion processed at temperature above 56°C	Trimyristin	Safflower oil
NT2	droplet-stabilised emulsion processed at temperature below 56°C	Trimyristin	Safflower oil

Confocal microscopy images of DSEs made with surface lipid of low (NO), medium (NP) and high melting points (NT & NT2) showed that the interface of safflower oil droplets was stabilised by droplet layers formed along the interface. Crystalline structures were observed in droplet stabilised emulsions of high melting surface lipid (NT & NT2).

Figure 4.14 shows confocal microscopy images of droplet-stabilised emulsions made up of trimyristin surface lipid heated above (NT) and below (NT2) melting temperature (56 °C). The crystalline structures observed were either individual crystals or crystal aggregates. For the emulsions processed above melting temperature (NT), the crystals were mostly 'needle-like' shaped and in some cases spherulites (Panel NT in Figure 4.14) while for the emulsions processed at ambient temperature and below melting temperature similar structures to the emulsion processed above 56 °C were observed. However, spherical shaped crystal-like grain structures were also observed, and the structures are referred to as 'crystal-like' structures because even though these structures resembled crystalline structures they appeared to have quite an irregular shape.

In some cases 'non-stained' coated droplets (panel NT2 in Figure 4.14) were observed where it appears that there has been some migration of the core material but, it does not seem to be the case because some partly stained droplets (Panels NT2 in Figure 4.14) were also observed indicating the presence of liquid and crystalline material.

To further understand and investigate the 'crystal-like' grain structure observed, a mixture of trimyristin and safflower oil was made and observed under the

confocal microscope. This lipid mixture was also used to process coarse emulsions at temperature above trimyristin's melting point (56°C) and ambient temperature. Figure 4.15 shows the confocal microscopy images of mixed trimyristin and safflower oil heated above 56°C, upon cooling, crystalline structures similar to those observed with trimyristin droplet-stabilised emulsions processed above melting temperature (Panels NT in Figure 4.13) were also observed with the mixtures (Figure 4.15 A & B).

Figure 4.15 also shows confocal images of mixed trimyristin and safflower oil coarse emulsion homogenised below trimyristin's melting temperature. The 'crystal-like' structures similar to those observed with trimyristin droplet-stabilised emulsions processed below melting temperature (Panels NT2 in Figure 4.14) were also observed with the coarse emulsions (Figure 4.15 C, D & E).

Trimyristin droplet-stabilised emulsions processed below melting temperature were treated in two different ways in terms of the cooling method; in the first process, after shell emulsion was processed above trimyristin's melting temperature, the emulsion was rapidly cooled to ambient temperature and then homogenised with the core lipid at ambient temperature (panels NT2 in Figure 4.14). In the second process, after shell emulsion was processed above melting temperature, the emulsion was slowly cooled to 4 °C and then heated to 25 °C prior to final homogenisation with the core lipid at 25 °C. Irregularly shaped 'crystal-like' structures were also observed with the latter process, but no 'non-stained' shells were observed as found with the former process where the emulsions were rapidly cooled to ambient temperature. This could be because the cooling rate was controlled in the second process.

Spicer and Hartel (2005) examined the effect of dewetting on crystallization of emulsion droplets and showed that molten tristearin droplet dewetted its own solid phase as it crystallized. They reported differences in crystal morphology between emulsion systems based on the dewetting and crystallization rate. When the dewetting rate was negligible in comparison to crystallization rate, tristearin crystals grew to the initial size of the molten droplet, i.e. the crystals were contained by the oil-water interface, and the reported crystal grain in this instance was similar to that observed with trimyristin droplet-stabilised emulsion processed at ambient temperature (Panels NT2 in Figure 4.14) in this study.

On the other hand, when dewetting became dominant, the crystals either caused droplet elongation into a semi-solid ellipsoidal shape or were ejected out of the droplet. The reported droplet elongation during crystal growth was also similar to that observed in this study with some trimyristin emulsions, where some droplets were partially stained and elongated (Panels NT2 in Figure 4.14). Their study explained that crystal shape is governed by competition between dewetting and crystallization rate and hence rapid cooling can lead to formation of high aspect ratio crystal shapes while controlled cooling produces discrete crystals.

Shi, Liang, and Hartel (2005) also investigated crystal structure formation in mixed lipid systems and showed that the type and characteristics of low melting lipid had an influence on the morphology of high melting lipid crystals formed. They also emphasised that processing conditions can influence the morphology and final microstructure even though these factors were not the focus of their study.

It is not clear what the non-stained protein-coated shells observed in the emulsions processed below melting temperature represent but, the differences in crystal shape or morphology observed with the mixed lipids indicates that upon cooling, trimyristin crystals exhibit different morphologies which is dependent on the rate of cooling. This explains the observed differences in crystal morphology between trimyristin droplet-stabilised emulsions processed above melting temperature (NT) and below melting temperature (NT2) and also differences between NT2 rapidly cooled to ambient temperature and NT2 slowly cooled to 4 °C and then heated to 25 °C.

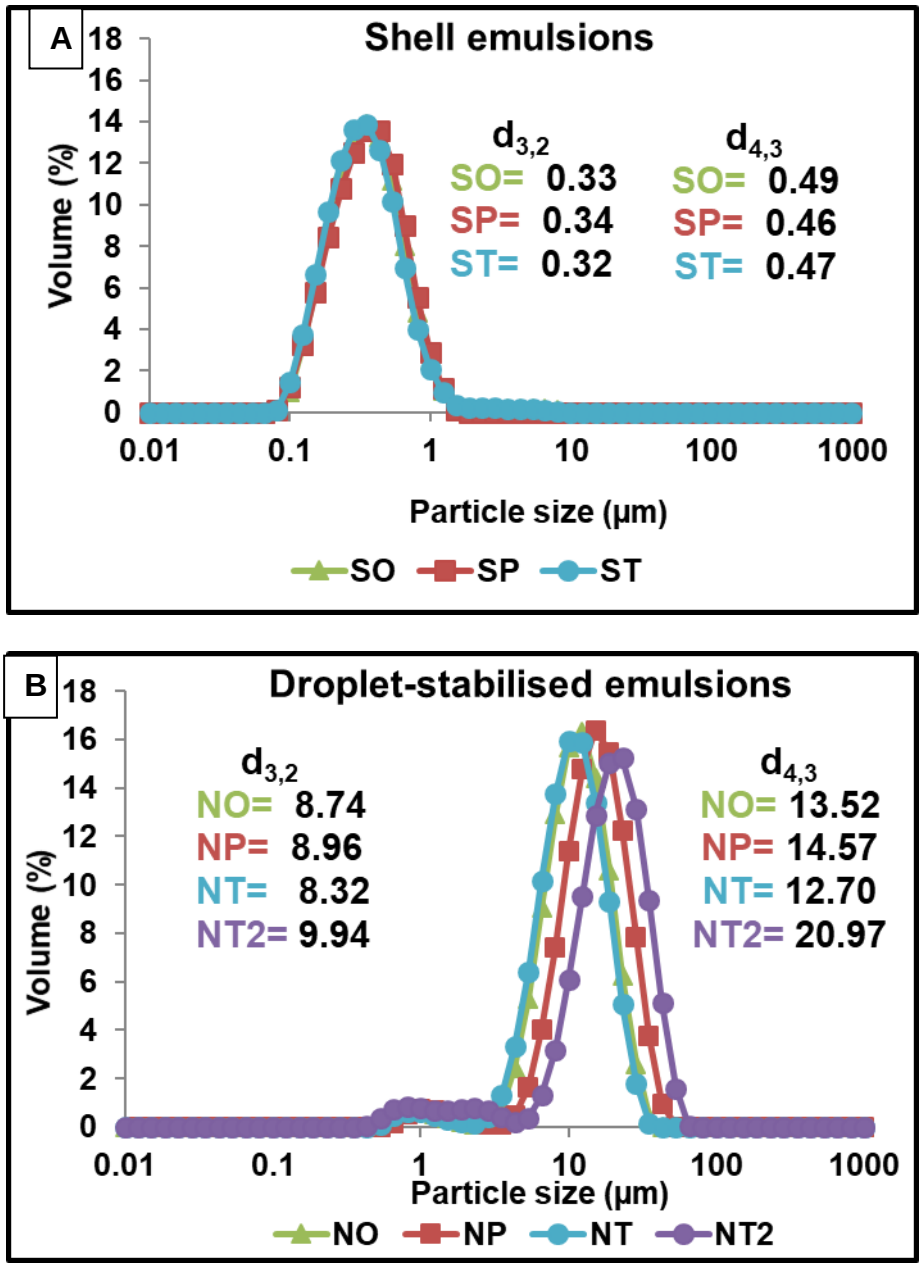

Figure 4.12 *Particle size distribution of shell (A) and droplet stabilised emulsions (B) comprising surface lipids of varying melting temperature*

SO, SP, ST, = shell emulsion olive, palmolein and trimyristin surface lipids respectively. NO = olive oil droplet-stabilised emulsion, NP = palmolein oil droplet-stabilised emulsion, NT = trimyristin droplet stabilised emulsion processed above 56°C & NT2 = trimyristin droplet-stabilised emulsion processed below 56°C

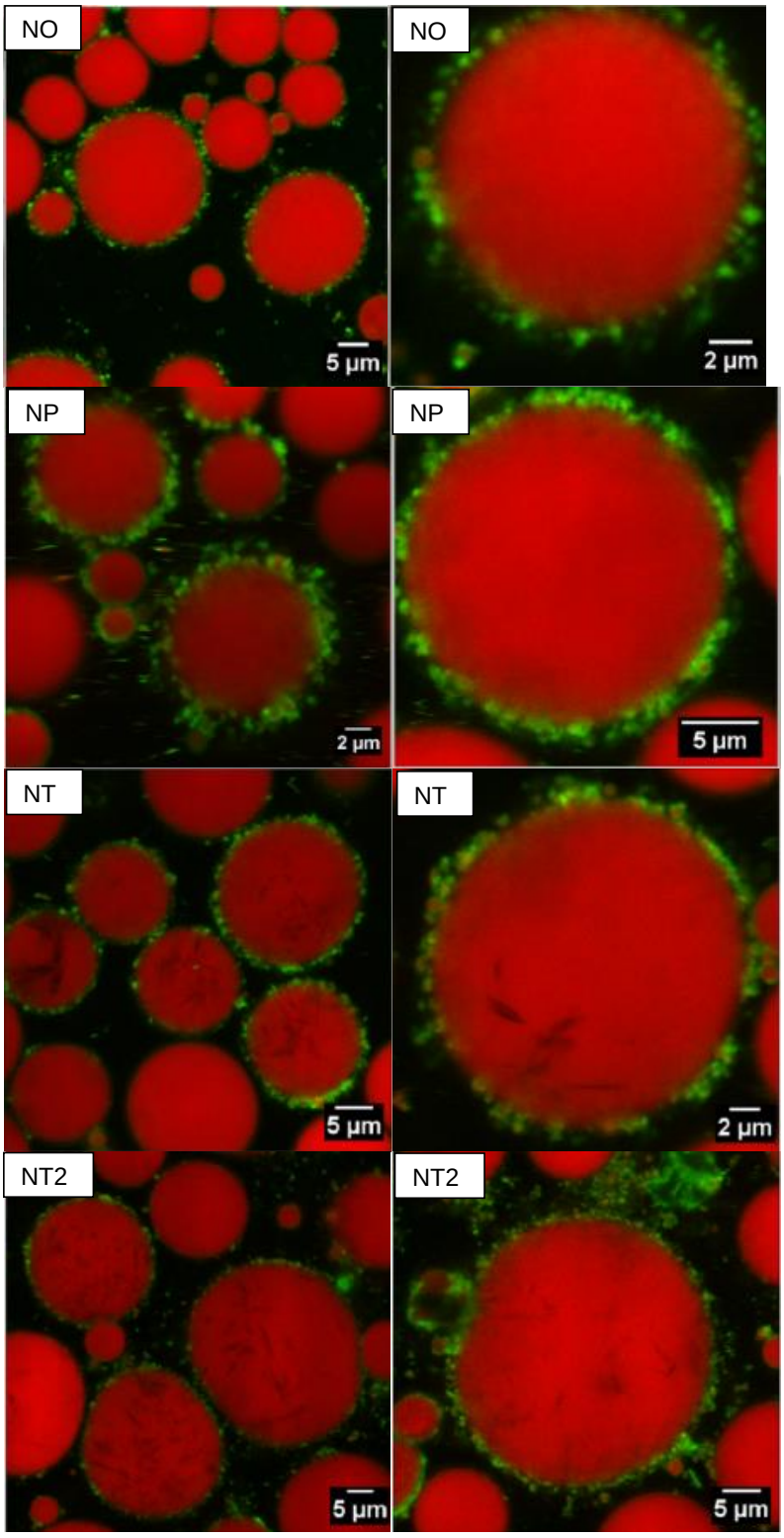

Figure 4.13 *Confocal microscopy images of droplet stabilised emulsions comprising surface lipids of varying melting temperature*

SO, SP, ST, = shell emulsion olive, palmolein and trimyristin surface lipids respectively. NO = olive oil droplet-stabilised emulsion, NP = palmolein oil droplet-stabilised emulsion, NT = trimyristin droplet stabilised emulsion processed above 56°C & NT2 = trimyristin droplet-stabilised emulsion processed below 56°C

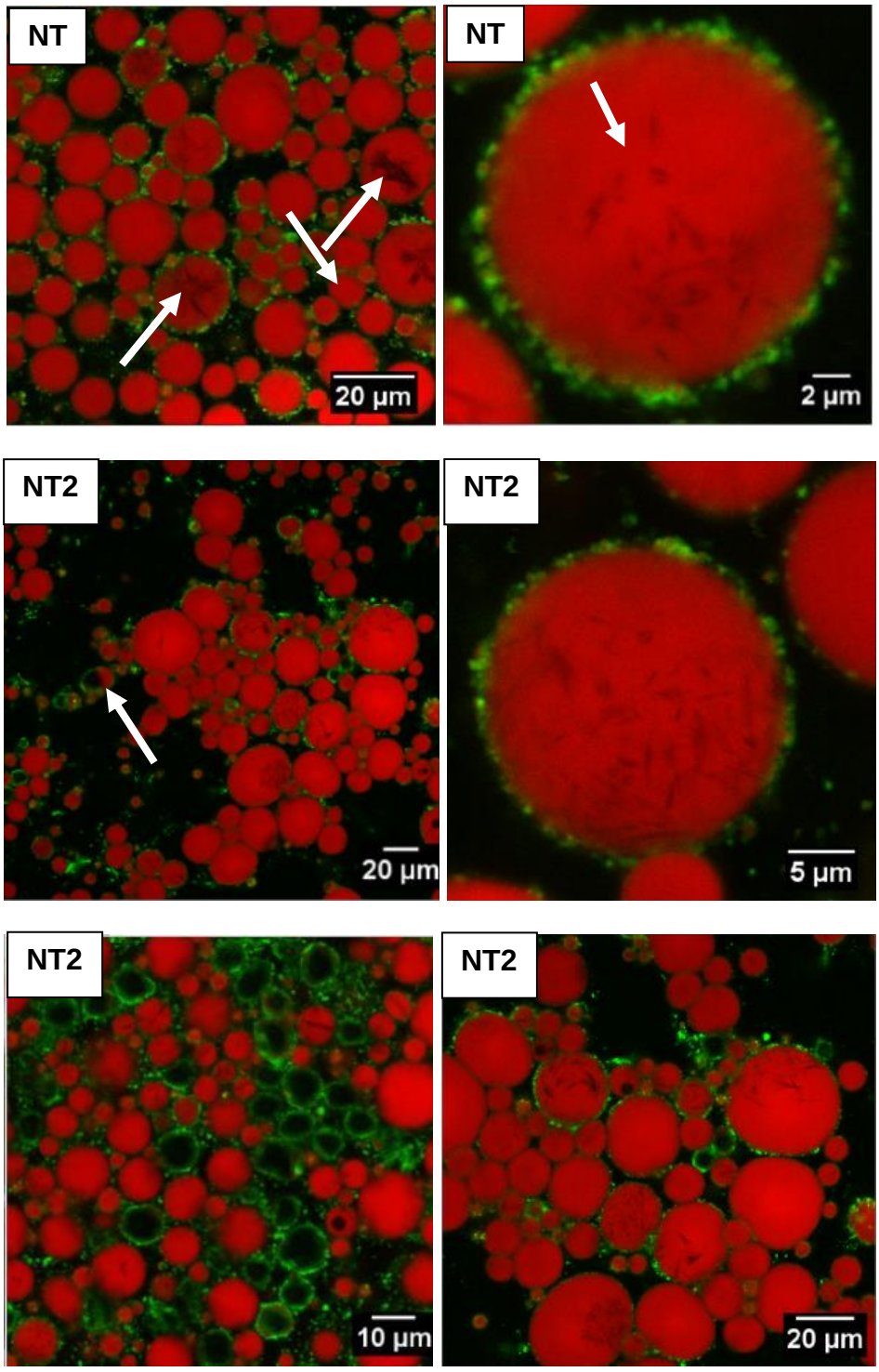

Figure 4.14 *Confocal microscopy Images of droplet stabilised emulsions with trimyristin surface lipid- NT= final homogenisation above 56°c and NT2 = final homogenisation below 56°C.*

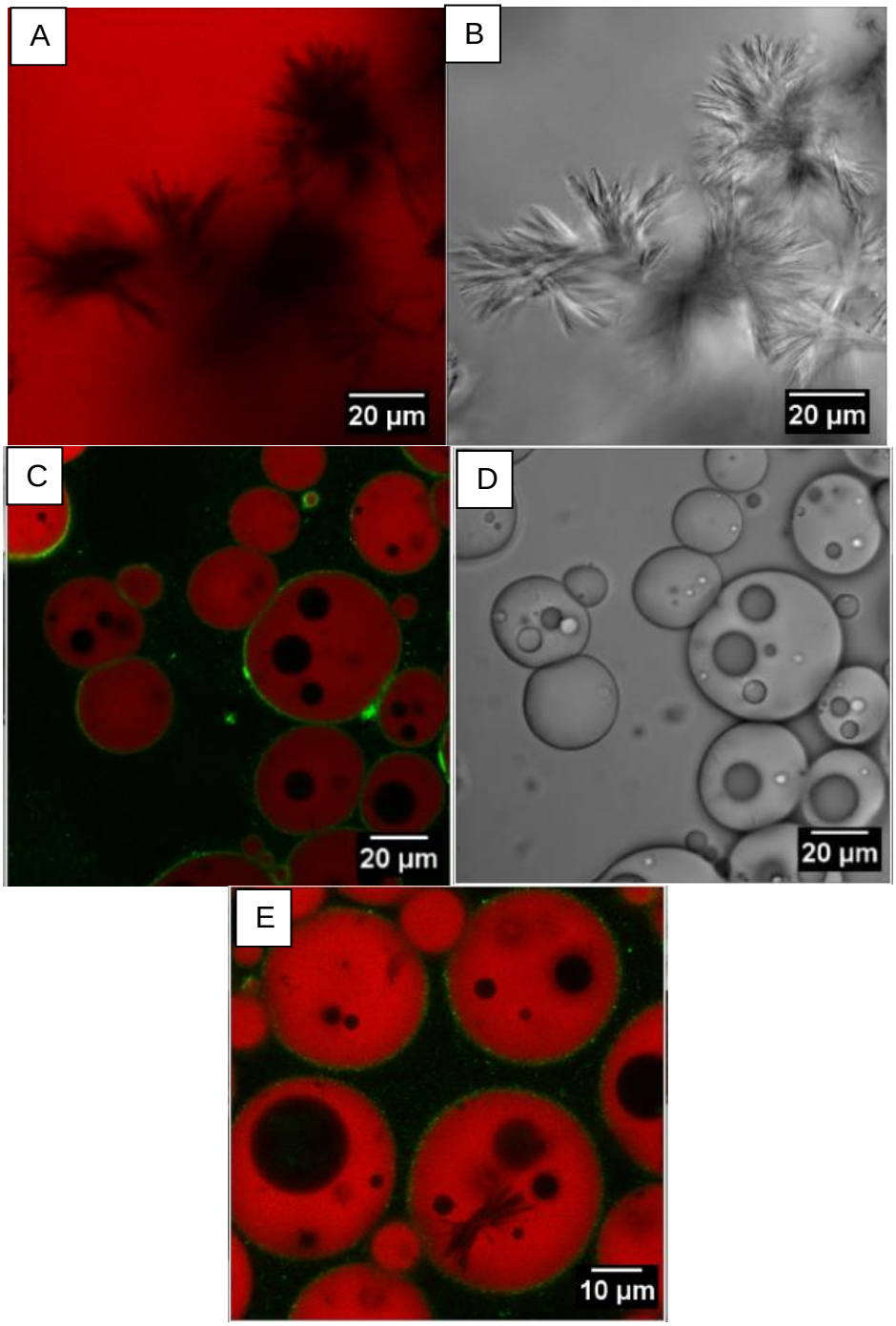

Figure 4.15 *Confocal microscopy images of mixed safflower oil and trimyristin- A & B (mixture heated to 65°C) and safflower oil/trimyristin coarse emulsion homogenised below melting temperature- C, D & E). Image B & D taken in DIC mode.*

4.5 Conclusions

The formation of droplet layers at the interface of food-grade oils was possible with MPC-stabilised shell droplets. Total interfacial coverage of core oil droplets by shell droplets processed with high protein and calcium MPCs (i.e. MPC 1 and 2) was obtained when the shell emulsions were processed via the two-stage homogeniser. On the other hand, excessive shell droplet aggregation prevented total interfacial coverage of core oil droplets when the shell droplets were processed through the microfluidizer at high pressures. Particle size of droplet-stabilised emulsion decreased with an increase in shell droplet concentration from 2 to 16% and the particle size distribution became bimodal at higher concentrations. Multi-droplet layers were formed at the interfaces of DSEs containing high shell emulsion concentrations (10% and 16%).

Total interfacial coverage of core oil droplets was also obtained with shell droplets processed with low protein MPC (MPC 3) containing similar calcium content as high protein MPC (MPC 1 & 2) and shell droplet stabilisation behaviour of MPC 3 shell emulsions was like that of MPC 1 and 2 shell emulsions.

Formation of droplet layers at the interface of food-grade oil droplets was not obtained with calcium-depleted MPC (MPC 4) containing similar protein content as MPC 1 and 2 both when the shell emulsions were processed through the microfluidizer and two-stage homogeniser, even though the shell droplet size was in the nano-scale.

Adsorption of MPC-coated shell droplets was more evident at the interface of soybean oil droplets than linoleic acid droplets. Droplet stabilisation was also

possible with surface lipids of low, medium and high melting points. Adsorption of high melting surface lipid droplets was possible either in liquid or solid state however, processing conditions or cooling rate influenced morphology and shape of crystals formed.

Calcium levels and aggregation state of milk protein concentrate are pertinent factors for droplet stabilisation with MPC. It can be hypothesised that modification of aggregated casein proteins in MPC influences their emulsifying capacity thus impacting their ability to form droplet layers at the oil-water interface. This study also shows that physicochemical properties of the core lipid also influences its ability to be stabilised by MPC-coated oil droplets.

This study provides critical information to ensure consistent successful production of droplet-stabilised food grade oil-in-water emulsions with milk protein concentrate and gives insightful knowledge about some structural properties of droplet-stabilised oil-in-water emulsions.

Chapter 5: Effect of droplet-stabilised oil-in-water emulsions on oxidative stability of unsaturated lipid incorporated within

Contents of this chapter have been published in a peer reviewed journal article and has been adapted with permission from:

Okubanjo, S. S., Loveday, S. M., Ye, A., Wilde, P. J., & Singh, H. (2019). Droplet-Stabilized Oil-in-Water Emulsions Protect Unsaturated Lipids from Oxidation. *Journal of Agricultural and Food Chemistry, 67*(9), 2626-2636.

5.1 Abstract

Droplet-stabilised emulsions use fine protein-coated lipid droplets - the shell - to emulsify larger droplets of a second lipid - the core. This study investigated the oxidation resistance of polyunsaturated fatty acid oil (PUFA oil) within droplet-stabilised emulsions, using shell lipids with a range of melting points: olive oil (low melting), trimyristin (high-melting) and palmolein oil (intermediate melting point). Oxidation of PUFA oil was accelerated with a fluorescent lamp in the presence of ferrous iron (100 μM) for nine days, and PUFA oxidation was monitored via conjugated dienes, lipid hydroperoxides and hexanal levels. Oxidation was slower in droplet-stabilised emulsions than in conventional emulsions or control emulsions of the same composition as droplet-stabilised emulsions but different structure, and trimyristin gave the greatest oxidation resistance. Results suggest the structured interface of droplet-stabilised emulsions limits contact between pro-oxidants and oxidation-sensitive bioactives encapsulated within, and this anti-oxidative effect is greatly enhanced with solid surface lipid.

Keywords: Droplet-stabilised emulsion; surface lipid; shell emulsion; core lipid; oxidation; long-chain polyunsaturated fatty acids

Graphical summary

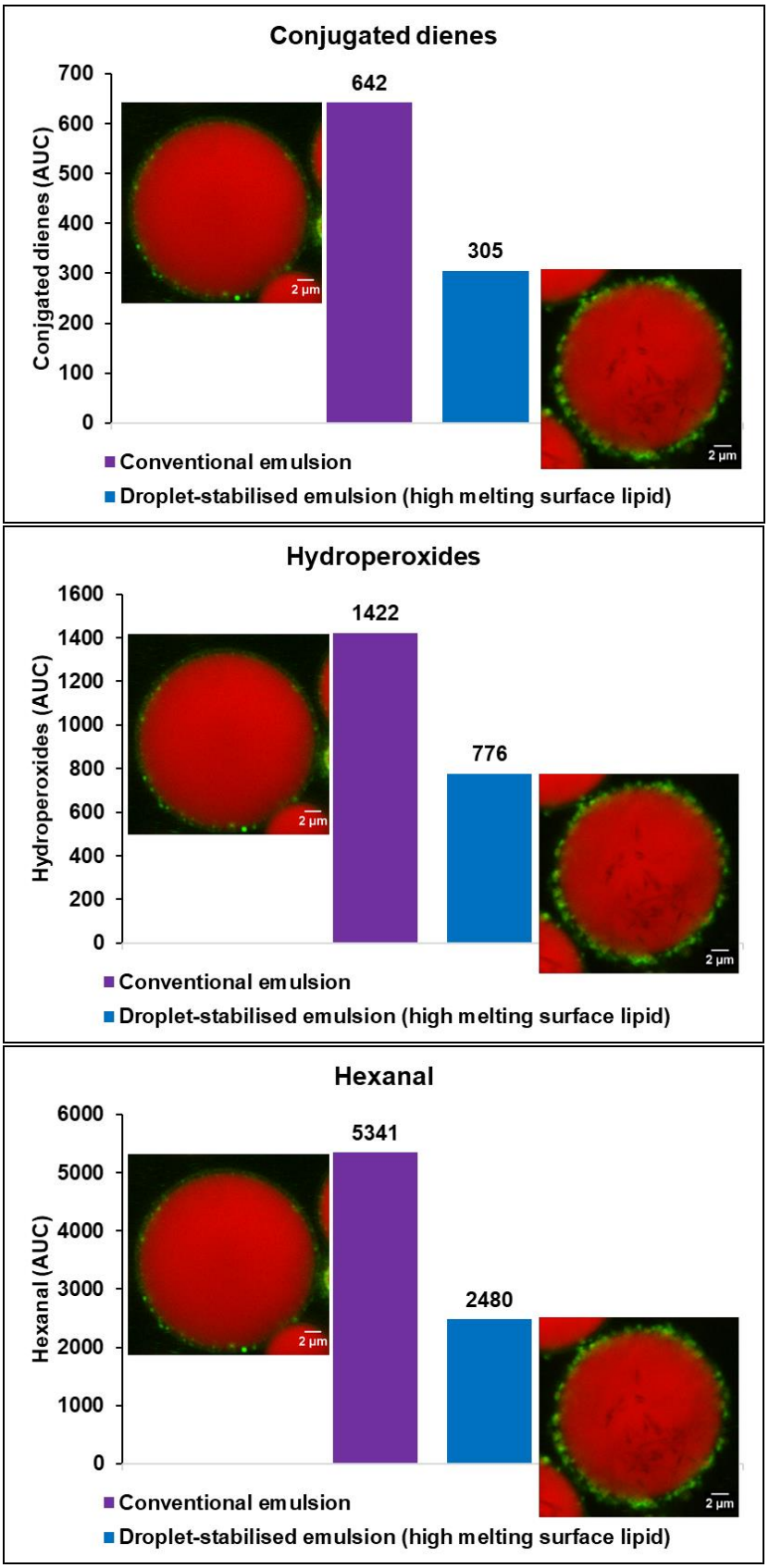

5.2 Introduction

As the spotlight on functional foods continues to grow, the challenges associated with incorporating bioactive compounds into food systems require practical and cost-effective solutions. Emulsions have become very important delivery vehicles for lipophilic bioactives, both to enhance their bioavailability and protect them from degradation.

Lipids rich in polyunsaturated fatty acids (PUFA) are beneficial for health (Mozaffarian & Wu, 2011; Yeong & So Bong, 2010) but they are highly susceptible to oxidation. Strategies such as the use of antioxidants and microencapsulation are currently employed to protect these lipids. Many studies have focused on incorporating these lipids in different emulsion systems to inhibit oxidation and thus maximize their benefits. Many of these studies have been carried out with oil-in-water emulsions (Djordjevic, McClements, & Decker, 2004; E. N. Frankel, Satue-Gracia, Meyer, & German, 2002; Katsuda et al., 2008).

Lipid oxidation is a complex process which leads to the breakdown of lipids into products that result in undesirable sensory properties of lipids. The mechanism of oxidation in bulk oils and emulsions differs (McClements & Decker, 2000). Oxidation in emulsions is mostly initiated by pro-oxidants located in the aqueous phase or at the interface (Mancuso, McClements, & Decker, 1999; Yoshida & Niki, 1992); therefore, the structure, characteristics and composition of the interface of an emulsion have significant impacts on its oxidative stability.

The oxidative stability of conventional emulsions is limited by physical instability under various processing conditions and characteristic porous thin interfacial

layer (Berton-Carabin, Sagis, & Schroën, 2018; Lesmes, Sandra, Decker, & McClements, 2010; McClements, 2010; Silvestre et al., 2000) which enables diffusion of pro-oxidants and subsequent reaction with the lipid phase. Interfacial engineering of emulsion systems can be explored to overcome the limitations of conventional emulsions because the interface is the gateway between pro-oxidants and the lipid phase, creating less permeable interfaces can limit oxidation by minimizing interactions between pro-oxidants and unsaturated lipids (Berton-Carabin, Ropers, & Genot, 2014; C. Berton et al., 2011).

Despite the many studies that seek to improve the oxidative stability of PUFA lipids by incorporating them into structured emulsions, several limitations such as porous structure, physical instability and high cost of production exist with various emulsion systems (Komaiko, Sastrosubroto, & McClements, 2016; McClements, Decker, & Weiss, 2007; Walker et al., 2015) . These limitations must be overcome to achieve the goal of efficient protection, delivery and enhanced bioavailability of PUFAs.

Ye et al. (2013) reported a patented (Singh, Ye, & Zhu, 2011) novel emulsion design whereby core oil droplets are stabilised by protein-coated nano-droplets. The reported structure has the potential to effectively protect bioactive compounds such as PUFA-rich lipids. Therefore, it could be of great benefit for the food industry if the potential of this novel emulsion to protect lipophilic bioactives such as PUFA-rich lipid from degradation is studied and established. Previous work by Ye et al. used only hexadecane in the lipid phases, whereas this study explores the formation of similar structures using several food-derived lipids and elucidates the effect of lipid type on oxidative stability. Making these

structures with food grade oils is more challenging as the interfacial tension in triacylglycerol oils is much lower than that of hexadecane used in the previous study, presenting a greater barrier for protein to adsorb and stabilise the droplets.

This study investigated the oxidation resistance of ‘droplet-stabilised’ emulsions by examining the impact of the interfacial structure and composition on the oxidative stability of PUFA-rich oil incorporated within.

5.3 Materials and methods

5.3.1 Materials

All materials, equipment and emulsion characterisation methods used in this chapter are detailed in Chapter 3. Only MPC 3 (470) was used in this study. Peroxide value of safflower oil and trimyristin as specified by supplier was 3 Meq O_2/kg. Initial conjugated dienes (CD), lipid hydroperoxides (LHP), and hexanal (hex) values of olive, palmolein and safflower oils as analyzed was less than 30 mM for CD and LHP and less than 2 µM for hexanal.

5.3.2 Droplet-stabilised emulsion preparation

Droplet-stabilised emulsions were prepared by a two-step process as shown in Figure 5.1. Firstly, solutions consisting of 5% (w/w) milk protein concentrate (MPC) were made by stirring MPC powder (5g) into Milli-Q water (95g) at room temperature for 1 h. The MPC solution was heated to 65 ºC and appropriate quantities of lipid (palmolein oil, olive oil, trimyristin) which is referred to as 'surface lipid' were added, i.e. 80% w/w MPC solution (consisting of 5% w/w MPC + 95% w/w water) and 20% w/w surface lipid. The mixtures were held at 65°C for 3-5 min and coarse emulsions made using a high-speed mixer (Labserv, D-130) at 6000 rpm for 3 min. The coarse emulsion was passed through a two-stage homogeniser (Homolab2, FBF Italia) at a first stage pressure of 400 bar and second stage pressure of 50 bar to produce a fine emulsion which is referred to as 'shell emulsion'. Hot water was passed through the homogeniser prior to passing the coarse emulsion to pre-heat it. In the second step the shell emulsion was added to appropriate quantities of PUFA-rich lipid (safflower oil), which is referred to as 'core lipid,' and potassium phosphate buffer (10mM K_2HPO_4 and

KH_2PO_4, pH 6.8-7.0), i.e. 10% w/w shell droplets, 20% w/w core lipid and 70% w/w buffer. To form droplet-stabilised emulsions, the mixture was heated to 65 °C and processed with a high-speed mixer (D-130, Labserv) at 6000 rpm for 5 min.

Droplet-stabilised emulsions comprising trimyristin surface lipid were processed at two different conditions to obtain shell droplet adsorption in liquid or solid state. To obtain droplet-stabilised emulsions with trimyristin in liquid or super-cooled state, shell emulsion, core and buffer mixture was heated to 65 °C prior to final homogenisation. To produce droplet-stabilised emulsion with trimyristin in the solid state, the shell emulsion was first cooled to 5 °C and then heated to 25°C prior to final homogenisation with core lipid and buffer.

Protein-stabilised safflower oil-in-water conventional control emulsions were processed by mixing appropriate quantities of 0.4% w/v MPC solution and safflower oil with a high-speed mixer as a reference emulsion (R). Control emulsions made up of the same composition as droplet-stabilised emulsions were processed by adding shell emulsions (10% w/w) to appropriate quantities of reference emulsion. The reference and control emulsions were processed at the same temperature as droplet-stabilised emulsions.

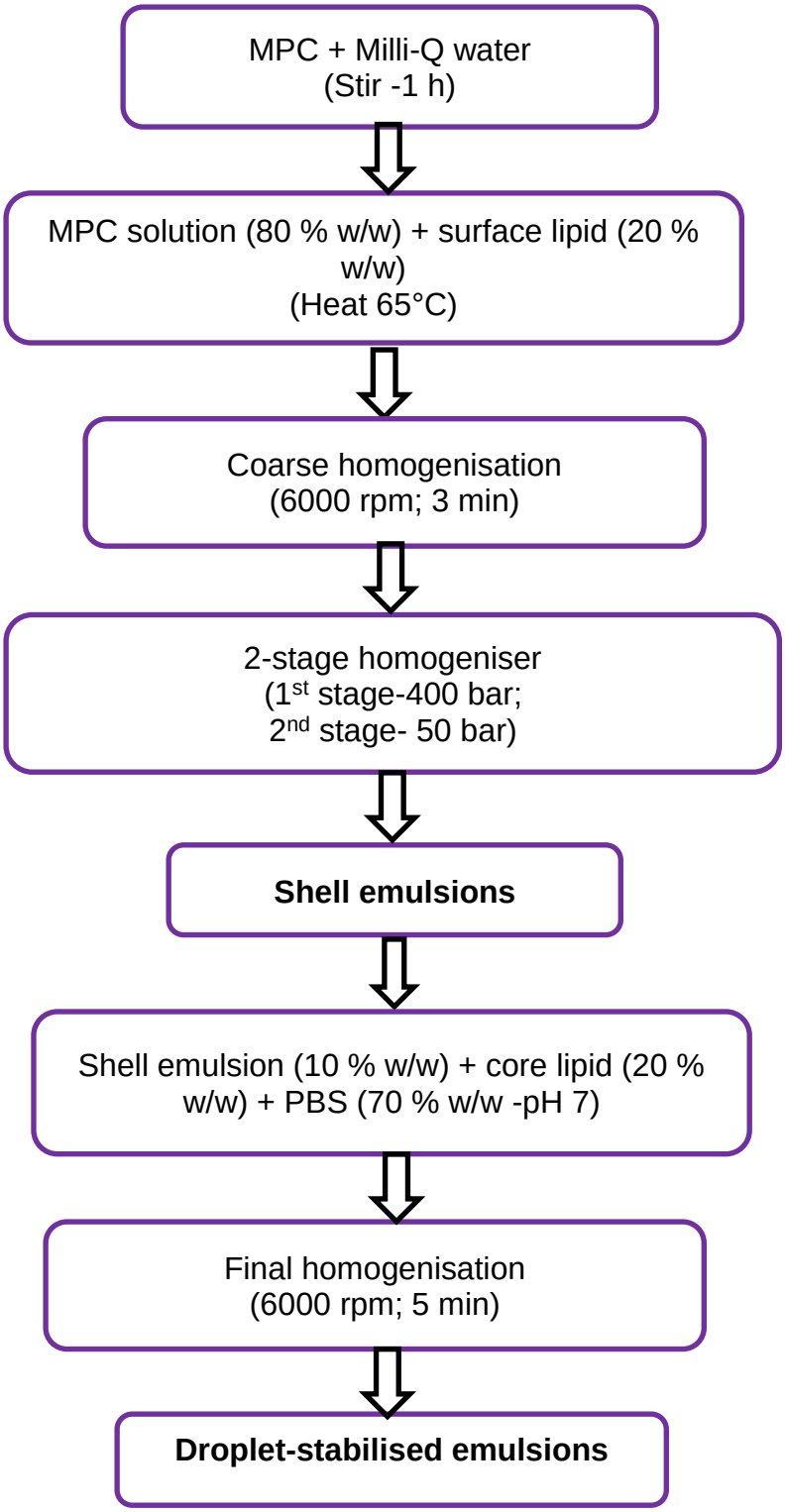

Figure 5.1 *Flow chart of droplet-stabilised oil-in-water emulsion production*

Table 5.1 summarizes and shows a description of the emulsion formulations. The reference control was a protein-stabilised conventional emulsion while the control emulsion was a conventional emulsion whose composition was matched with that of droplet-stabilised emulsions by addition of shell emulsion.

5.3.3 Accelerated Lipid Oxidation

Oxidation of safflower oil in droplet-stabilised and control emulsions was accelerated in sealed 12-well cell plates (1 mL emulsion per well) and 20 mL headspace glass vials (95% headspace) exposed to fluorescent lamp (8500-9000 lux) in the presence of ferrous iron (100 µM- $FeSO_4.7H_2O$ in HCl) for 9 days at 20°C. The distance from lamp to top of plates and vials was approximately 23 cm and 22 cm respectively. Sodium azide (0.02% w/v) was added to the emulsions to prevent microbial growth.

5.3.4 Lipid Oxidation Measurements

Samples were collected on days 1, 3, 5, 7 and 9, and stored at -20°C. Safflower oxidation was monitored via primary (conjugated dienes and lipid hydroperoxides) and secondary (hexanal) oxidation products. The emulsions were analysed within 1-2 weeks of freezing.

5.3.5 Lipid oxidation measurements

Conjugated dienes, lipid hydroperoxides and headspace hexanal were analysed according to the methods described in chapter 3, sections 3.3.10, 3.3.11 and 3.3.12 respectively.

5.3.6 Statistical Analysis

Oxidation data in this study was fitted using the following Gaussian equations.

$$\boldsymbol{CD = CD_0 + CD_{max} exp\left\{-\left(\frac{day-day_{max}}{w}\right)^2\right\}} \quad \textit{(Eq. 5-1)}$$

$$LHP = LHP_0 + LHP_{max} exp\left\{-\left(\frac{day-day_{max}}{w}\right)^2\right\} \quad \textit{(Eq. 5-2)}$$

$$Hex = Hex_0 + Hex_{max} exp\left\{-\left(\frac{day-day_{max}}{w}\right)^2\right\} \quad \textit{(Eq. 5-3)}$$

CD is the level of conjugated dienes (mM), CD_0 is the *CD* level at the start of oxidation trial, CD_{max} is the maximum *CD* level, *day* is the day number (independent variable), day_{max} is the day number at which CD_{max} occurs and *w* determines the width of the Gaussian curve (units are days). Corresponding parameters for Eq. 5.2 and 5.3 have the same meaning; units of LHP are mM and units of Hex are μM.

The areas under the curve (AUC) were derived by numerical integration between 0 and 9 days using Simpson's rule. Gaussian curves fitted the data well in most cases except for day 9 hexanal concentrations, which were higher than predicted by the fit line. To allow for this in AUC calculations for hexanal, Gaussian curves were integrated up to 7 days, and added to the area of the trapezoid described by drawing a straight line between the mean (measured) values at day 7 and day 9.

Normalisation of AUC involved dividing by the maximum AUC for each oxidation product then multiplying by 100.

5.4 Results

5.4.1 Formation of droplet-stabilised and control emulsions

Figure 5.2 shows confocal microscopic images of droplet-stabilised and control emulsions. Particle size of olive, palmolein and trimyristin shell emulsions was the same ($d_{3,2}$ = 0.4 µm and $d_{4,3}$ = 0.5 µm) and Table 5.1 shows the particle size data of droplet-stabilised and control emulsions. The particle sizes of shell emulsions with low-, intermediate- and high-melting surface lipids were not significantly different (p>0.05). Particle sizes of droplet-stabilised and control emulsions were also similar. Confocal microscopy and particle size analysis were used to validate the differences in interfacial structure between droplet-stabilised emulsions, control emulsions of same composition as droplet-stabilised emulsions, and conventional reference emulsion.

The interface of core safflower oil droplets in the reference emulsion (R) was coated by a thin protein layer (Figure 5.2-R). For the controls of same composition as droplet-stabilised emulsions (CO, CP and CT) the interfacial structure was the same as that of the reference emulsion but the shell droplets were dispersed in the surrounding phase (Figure 5.2-CO, CP & CT). In CO, CP and CT emulsions there was some spontaneous adsorption of shell droplets on to the core droplets, but much less than when shell emulsion and core lipid were mixed together at high speed and elevated temperature in the droplet-stabilised emulsion process.

Core safflower oil droplets in droplet-stabilised emulsions were stabilised by protein-coated shell oil droplets, which are evident in Figure 5.2-NO,NP, NT & NT2 at the interface of larger core safflower oil droplets, as the adsorption of small

shell oil droplets (red) coated with protein (green) is observed. This interfacial structure is similar to that reported by Ye et al. (2013) for hexadecane oil-in-water emulsions stabilised by micellar casein coated nanoemulsions.

***Table 5.1**: Average particle size of droplet-stabilised and control emulsions*

Emulsions	Description	Surface lipid	Surface-weighted mean diameter, $d_{3,2}$ (µm)	Volume weighted mean diameter, $d_{4,3}$ (µm)
R	protein stabilized safflower oil-in water emulsion (reference emulsion)	None	13.2 ± 2.5^{c}	15.3 ± 3.0^{c}
CO	R with added shell emulsion	Olive oil	7.1 ± 0.3^{a}	14.6 ± 1.1^{a}
CP	R with added shell emulsion	Palmolein oil	7.1 ± 0.1^{a}	14.0 ± 2.2^{a}
CT	R with added shell emulsion	Trimyristin	6.7 ± 0.2^{a}	15.0 ± 1.6^{a}
NO	droplet-stabilized emulsion	Olive oil	8.9 ± 0.6^{b}	15.2 ± 2.8^{b}
NP	droplet-stabilized emulsion	Palmolein oil	8.6 ± 0.3^{b}	13.3 ± 1.3^{b}
NT	droplet-stabilized emulsion processed at temperature above 56°C	Trimyristin	9.0 ± 1.0^{b}	15.8 ± 4.9^{b}
NT2	droplet-stabilized emulsion processed at temperature below 56°C	Trimyristin	9.5 ± 1.8^{b}	21.0 ± 2.6^{d}

Values are means of three measurements (3 runs per measurement) ± standard deviation. Different superscript letters ($^{a, b, c}$) represent different treatments. Means with same superscript are not significantly different (p>0.05)

- **R= protein-stabilised oil-in-water emulsion (reference emulsion); CO= R with added olive oil shell emulsion; CP= R with added palmolein oil shell emulsion; CT= R with added trimyristin shell emulsion; NO= droplet stabilised emulsion with olive oil shell droplets; NP= droplet stabilised emulsion with palmolein oil shell droplets; NT= droplet stabilised with trimyristin shell droplets processed above 56°C; NT2= droplet stabilised emulsion with trimyristin shell droplets processed below 56°C**

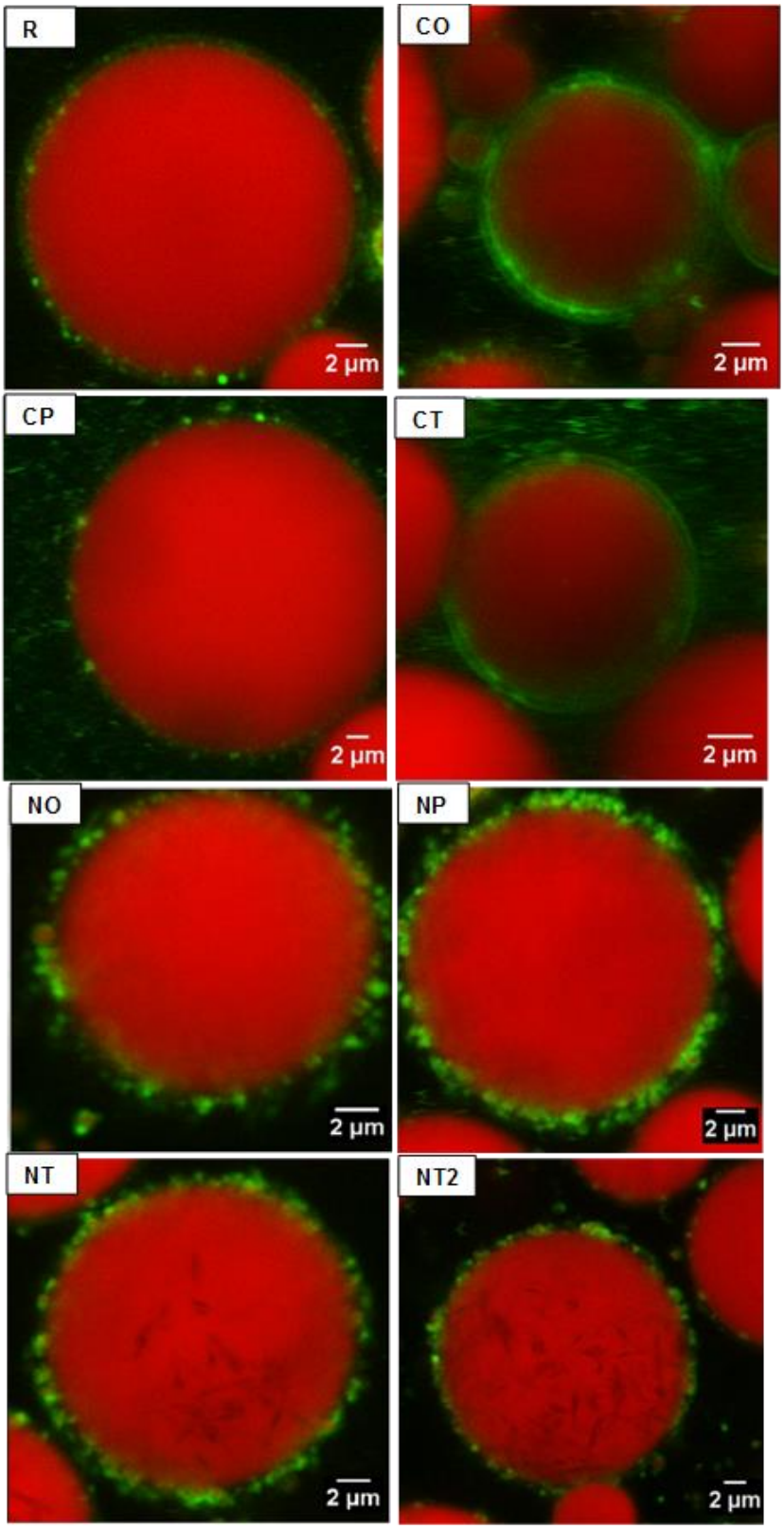

***Figure 5.2**: Confocal microscopy images of control and 'droplet-stabilised' emulsions*

R= protein-stabilised oil-in-water emulsion (reference emulsion); CO= R with added olive oil shell emulsion; CP= R with added palmolein oil shell emulsion; CT= R with added trimyristin shell emulsion; NO= droplet stabilised emulsion with olive oil shell droplets; NP= droplet stabilised emulsion with palmolein oil shell droplets; *NT= droplet stabilised with trimyristin shell droplets processed above 56°C; NT2= droplet stabilised emulsion with trimyristin shell droplets processed below 56°C*

5.4.2 Impact of droplet-stabilised emulsion structure on oxidative stability of core safflower oil

Figure 5.3 shows the evolution of conjugated dienes, hydroperoxides and hexanal in droplet-stabilised and control emulsions. Oxidation of core safflower oil steadily increased with >1 day of exposure to light. The highest conjugated dienes and hydroperoxide levels were observed after 5 days exposure, which was followed by a steady decrease, indicating decomposition of oxidation products. Primary oxidation products such as lipid hydroperoxides are usually stable at low temperatures and in the absence of metals but in the presence of metals they decompose very fast (Choe & Min, 2006) so it is not surprising that a rapid decrease in conjugated dienes and lipid hydroperoxides was observed, some studies on oxidative stability of emulsions have also shown similar trends (O' Dwyer, O' Beirne, Eidhin, & O' Kennedy, 2013; Ponginebbi, Nawar, & Chinachoti, 1999).

Hexanal increased due to the breakdown of primary oxidation products and then decreased, which was unexpected. Hexanal may have reacted or bound with other constituents (e.g. proteins), rendering it non-volatile, which would lead to decreased quantification on days 7 and 9 (F. Shahidi & Zhong, 2005). The fact that hexanal does not return to zero suggests that binding/reaction sites may have been saturated. A few published studies have shown a similar trend (Hu et al., 2003; Iglesias, Lois, & Medina, 2007) and the kinetics of secondary product development are known to differ for different oils (Choe & Min, 2006). Another probable explanation for the observed decrease in hexanal is competitive

adsorption of other volatiles produced during oxidation which may have limited hexanal adsorption on SPME fibre.

There were significant differences ($p < 0.05$) in core safflower oil oxidation between samples after 1, 3, 5, 7 and 9 days exposure. Oxidation of safflower oil in droplet-stabilised emulsions was slower and/or less extensive than in reference emulsion and composition-matched controls, for both the primary and secondary oxidation products.

Table 5.2 shows the parameters used to fit oxidation time courses in Figure 5.3, and the total amounts of oxidation products are expressed as area under the curve (AUC) values in Table 5.3. Table 5.2 shows the highest conjugated dienes (CD_{max}), lipid hydroperoxides (LHP_{max}) and hexanal (Hex_{max}) values for each emulsion. CD_{max}, LHP_{max} and Hex_{max} were highest in controls (R, CO, CP & CT) than droplet stabilised emulsions and lowest in droplet-stabilised emulsions of trimyristin surface lipid (NT & NT2) than olive and palmolein oil surface lipids (NO & NP).

According to AUC values, oxidation was reduced by up to 55% by the droplet-stabilised emulsion structure. All droplet-stabilised emulsions had lower values of all oxidation products compared with controls, which showed small differences among themselves. It was clear that trimyristin was the most effective surface lipid, followed by olive oil and palm oil. Formation of hexanal in controls of same composition as droplet-stabilised emulsion was slower than in reference emulsion (R) and this indicates that the addition of shell emulsion delayed

oxidation slightly, which may be due to spontaneous adsorption of protein-coated shell droplets to some core droplets (Figure 5.4D).

Figure 5.4 and Figure 5.5 show the structural changes in droplet-stabilised and control emulsions during oxidation. Aggregation was quantified by measuring the particle size distribution and microscopic structure was examined as oxidation products peaked (5 days) and decreased (7 days). For 5 days exposure, core droplet aggregation was observed in reference emulsion (Figure 5.4B). Shell droplets in control emulsions of same composition as droplet-stabilised emulsion flocculated and formed a network (Figure 5.4E) and core droplet aggregation was also observed. There were no observed structural changes in droplet-stabilised emulsions after 5 days exposure as the 'droplet-stabilised structure' was still evident at the interface of most core droplets (Figure 5.5). The changes observed at 7 days were same as observed at 5 days, but more aggregation was observed in each case. For droplet-stabilised emulsions, shell droplet aggregation appeared to have compromised interfacial structure integrity in some cases (Figure 5.5 I & L).

Figure 5.6 shows particle size changes for droplet-stabilised and control emulsions during oxidation. The observed particle size changes correspond to the changes in structure because particle size of control emulsions increased significantly during oxidation ($p < 0.05$). There were no significant changes in particle size of droplet-stabilised emulsions after 5 days, but after 7 days there was a significant increase in droplet size.

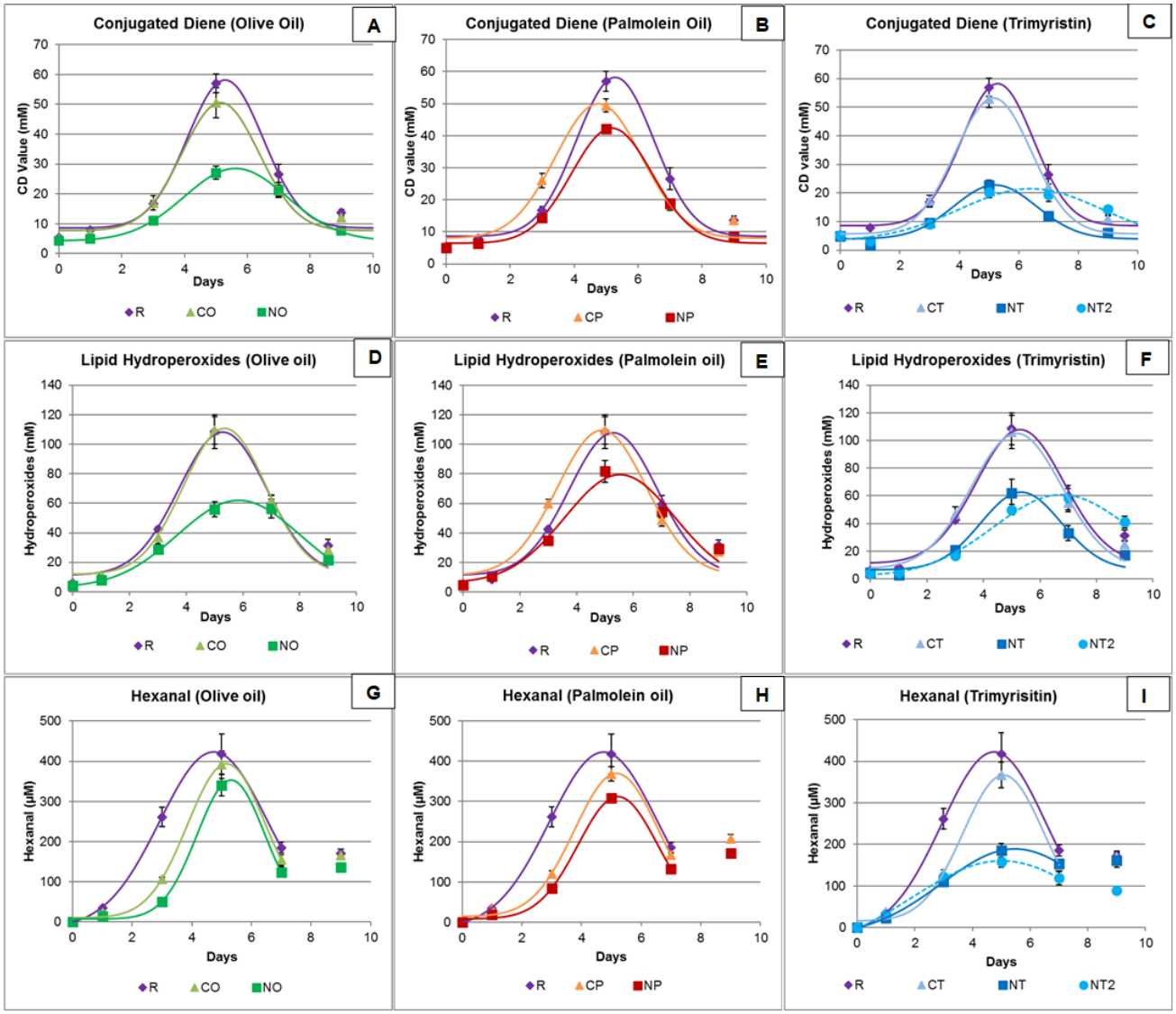

Figure 5.3 *Evolution of primary (conjugated diene-A, B & C and Hydroperoxides- D, E & F) and secondary (hexanal- G, H & I) oxidation products in core safflower oil in 'droplet-stabilised' and control emulsions exposed to fluorescent lamp in the presence of ferrous iron (100µM).*

Data points represent mean (n=2) ± standard error of mean and lines are fits with Eq. 2-4. Data points are average of two experiments with triplicate measurements. Some error bars fall within data points. R= protein-stabilised oil-in-water emulsion (reference emulsion); CO= R with added olive oil shell emulsion; CP= R with added palmolein oil shell emulsion; CT= R with added trimyristin shell emulsion; NO= droplet stabilised emulsion with olive oil shell droplets; NP= droplet stabilised emulsion with palmolein oil shell droplets; NT= droplet stabilised with trimyristin shell droplets processed above 56°C; NT2= droplet stabilised emulsion with trimyristin shell droplets processed below 56°C

***Table 5.2**: Oxidation parameters derived from fitting equations 2, 3 and 4 to oxidation data. Values in brackets are standard errors.*

Conjugated Dienes (CD)	CD_0 (mM)	CD_{max} (mM)	day_{max}	w
R	8.6 (1.3)^{a}	50.0 (2.7)^{a}	5.3 (0.1)^{bc}	1.7 (0.1)^{b}
CO	7.7 (1.5)^{a}	43.0 (2.9)^{ab}	5.2 (0.1)^{cd}	1.7 (0.1)^{b}
CP	8.1 (1.2)^{a}	42.0 (2.2)^{ab}	4.8 (0.1)^{d}	1.9 (0.1)^{b}
CT	5.7 (1.4)^{a}	47.5 (2.6)^{ab}	5.2 (0.1)^{c}	1.8 (0.1)^{b}
NO	4.4 (1.1)^{a}	24.2 (1.7)^{c}	5.7 (0.1)^{b}	2.3 (0.2)^{ab}
NP	6.4 (0.7)^{a}	36.0 (1.4)^{c}	5.2 (0.1)^{c}	1.8 (0.1)^{b}
NT	4.0 (0.7)^{a}	19.0 (1.3)^{c}	5.2 (0.1)^{b}	2.0 (0.2)^{b}
NT2	3.2 (1.6)^{a}	18.3 (1.7)^{c}	6.4 (0.2)^{a}	3.4 (0.5)^{a}

Superscript letters indicate significant differences (P<0.05) within columns.

Hydroperoxides (LHP)	LHP_0 (mM)	LHP_{max} (mM)	day_{max}	w
R	11.4 (4.4)^{a}	96.8 (7.1)^{a}	5.3 (0.1)^{bcd}	2.2 (0.2)^{a}
CO	12.0 (3.6)^{a}	99.0 (6.2)^{a}	5.4 (0.1^{bc}	2.1 (0.2)^{b}
CP	11.2 (3.8)^{a}	98.2 (6.0)^{a}	4.9 (0.1)^{d}	2.2 (0.2)^{a}
CT	7.5 (4.8)^{a}	97.8 (7.5)^{a}	5.2 (0.1)^{bcd}	2.3 (0.2)^{ab}
NO	2.9 (3.9)^{a}	59.3 (4.4)^{b}	5.9 (0.1)^{bc}	3.1 (0.3)^{a}
NP	6.4 (4.4)^{a}	73.2 (5.2)^{b}	5.5 (0.1)^{b}	2.8 (0.3)^{ab}
NT	6.6 (3.2)^{a}	56.1 (5.7)^{b}	5.3 (0.2)^{bcd}	2.0 (0.3)^{b}
NT2	1.8 (4.2)^{a}	59.3 (5.0)^{b}	6.8 (0.2)^{a}	3.4 (0.4)^{a}

Superscript letters indicate significant differences (P<0.05) within columns.

Hexanal (Hex)	Hex_0 (µM)	Hex_{max} (µM)	day_{max}	w
R	-15.0 (230.0)[a]	438.1 (33.9)[a]	4.7 (0.1)[b]	2.6 (0.3)[a]
CO	10.8 (12.1)[a]	383.6 (20.2)[a]	5.2 (0.1)[a]	1.9 (0.1)[ab]
CP	13.8 (7.7)[a]	356.7 (12.4)[a]	5.2 (0.1)[a]	2.0 (0.1)[ab]
CT	15.0 (12.3)[a]	351.5 (19.9)[ab]	5.1 (0.1)[ab]	2.0 (0.1)[ab]
NO	7.2 (9.7)[a]	346.8 (17.5)[ab]	5.3 (0.1)[a]	1.6 (0.1)[b]
NP	8.2 (6.1)[a]	303.5 (10.2)[b]	5.2 (0.1)[a]	2.0 (0.1)[b]
NT	-21.2 (17.5)[a]	210.2 (15.6)[c]	5.5 (0.1)[a]	3.6 (0.4)[a]
NT2	-62.9 (67.1)[a]	224.0 (62.6)[bc]	5.0 (0.2)[ab]	4.4 (1.2)[a]

Superscript letters indicate significant differences ($p<0.05$) within columns.

***Table 5.3**: Area under the curve (AUC) values for conjugated dienes (CD), lipid hydroperoxides (LHP) and hexanal, integrated over the whole oxidation time course.*

	R	CO	CP	CT	NO	NP	NT	NT2
			Raw AUC values					
CD	642	604	683	609	412	513	305	371
LHP	1422	1398	1456	1367	967	1198	776	928
hexanal	5341	4037	4146	4063	3198	3320	2743	2480
			Normalized AUC values					
CD	94	88	100	89	60	75	45	54
LHP	98	96	100	94	66	82	53	64
hexanal	100	76	78	76	60	62	51	46

Sample	Day-0	Day-5	Day-7
R	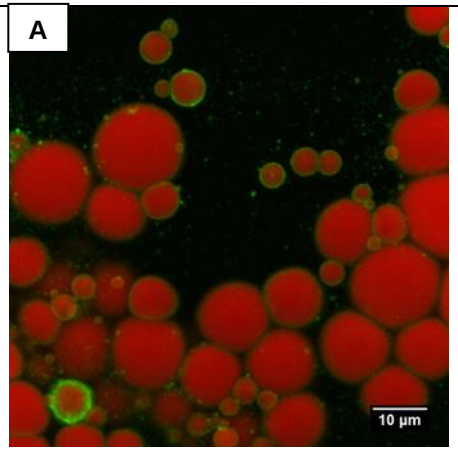	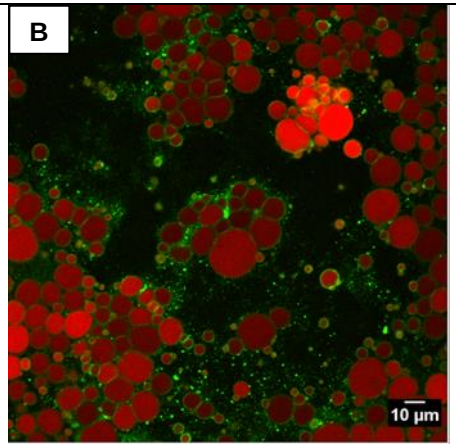	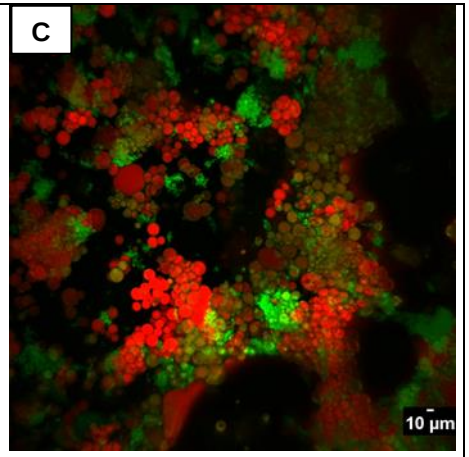
CO	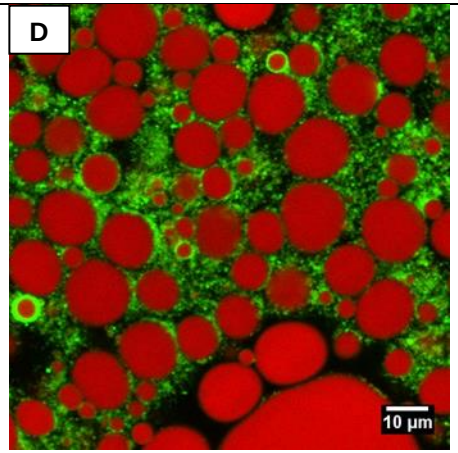	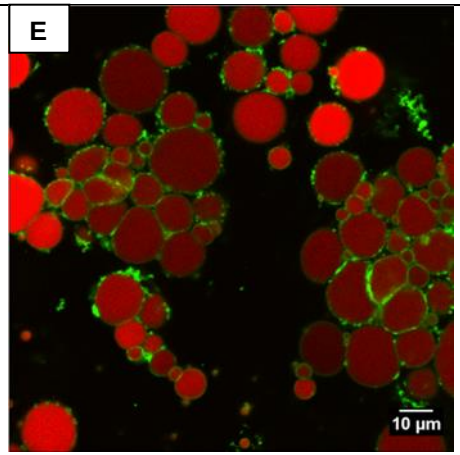	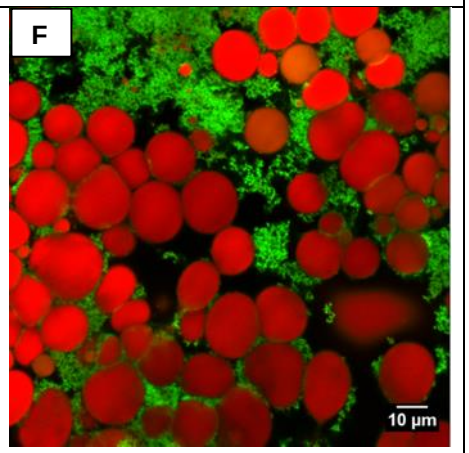

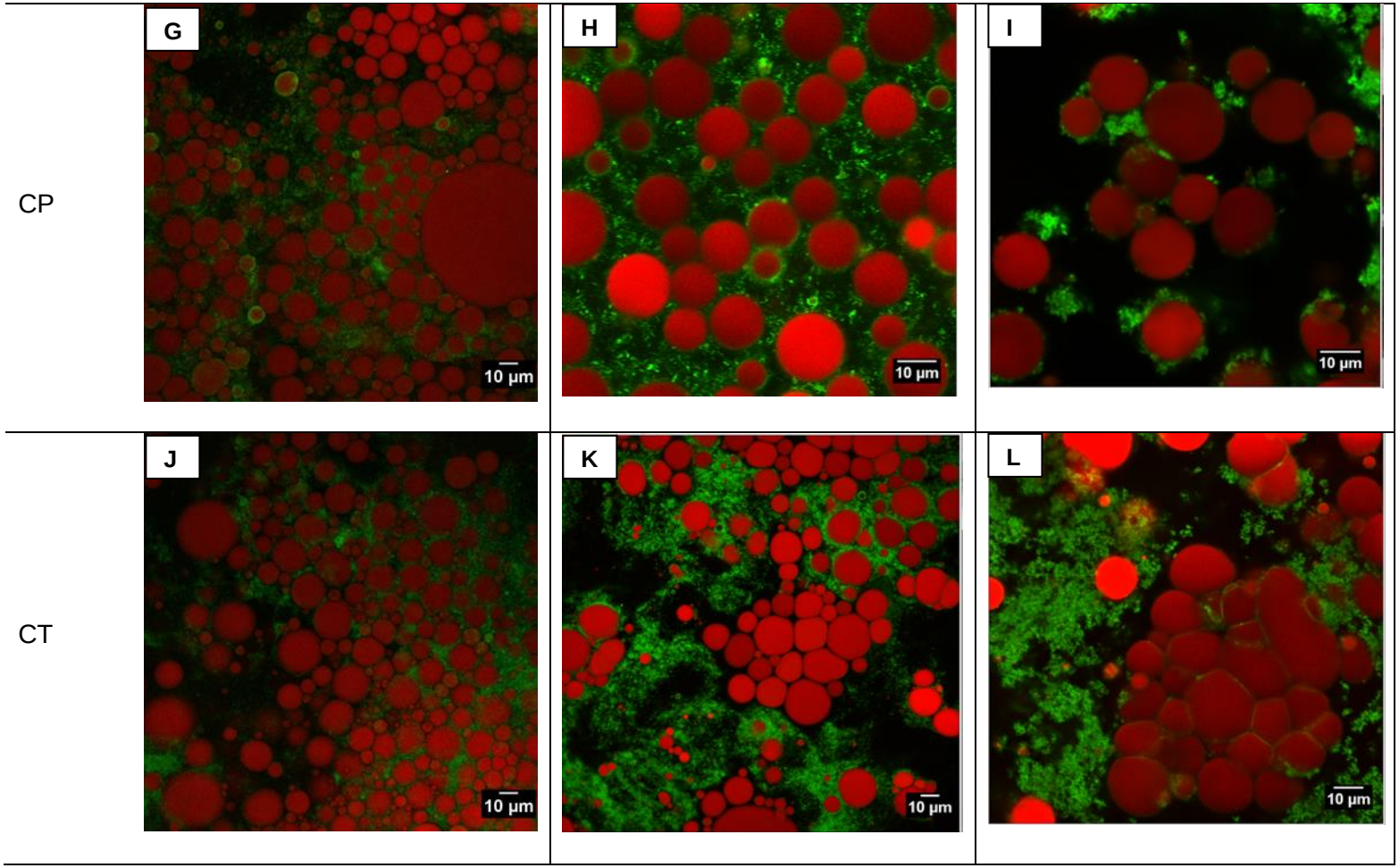

Figure 5.4 *Confocal Microscopy Images of control emulsions freshly prepared (Day 0) and after accelerated oxidation of core safflower oil (Day 5 and 7).*

R= protein-stabilised oil-in-water emulsion (reference emulsion); CO= R with added olive oil shell emulsion; CP= R with added palmolein oil shell emulsion; CT= R with added trimyristin shell emulsion

Sample	Day-0	Day-5	Day-7
NO	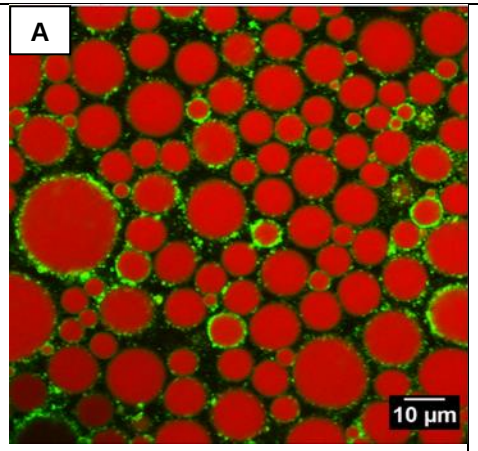	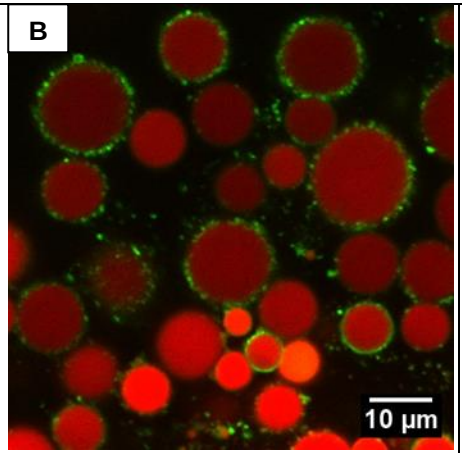	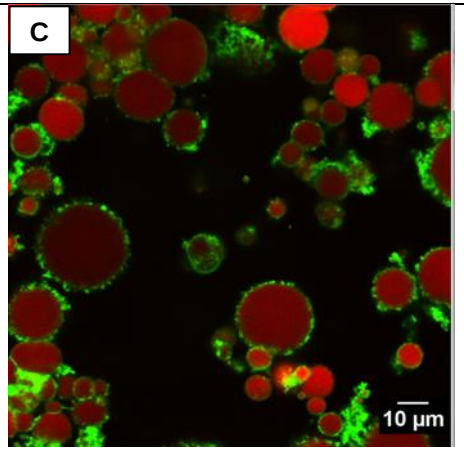
NP	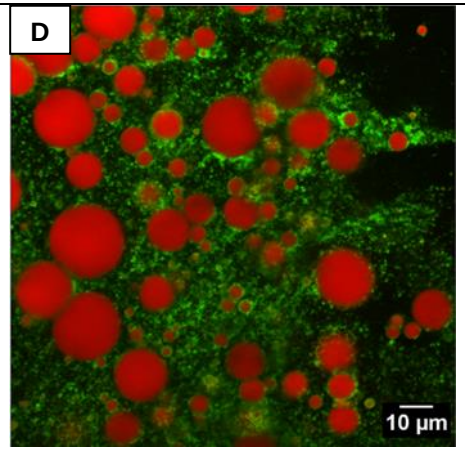	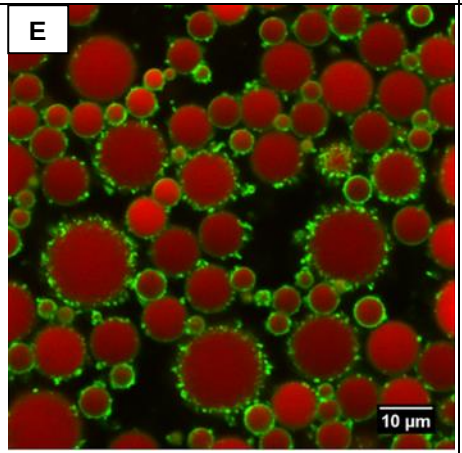	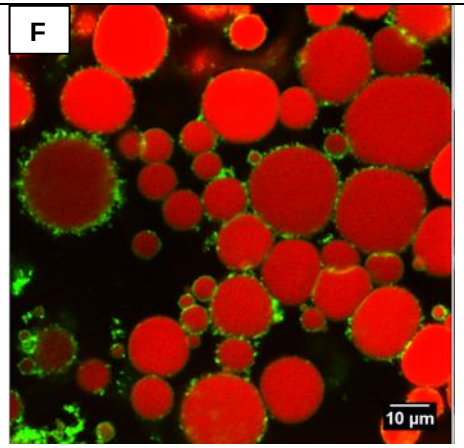

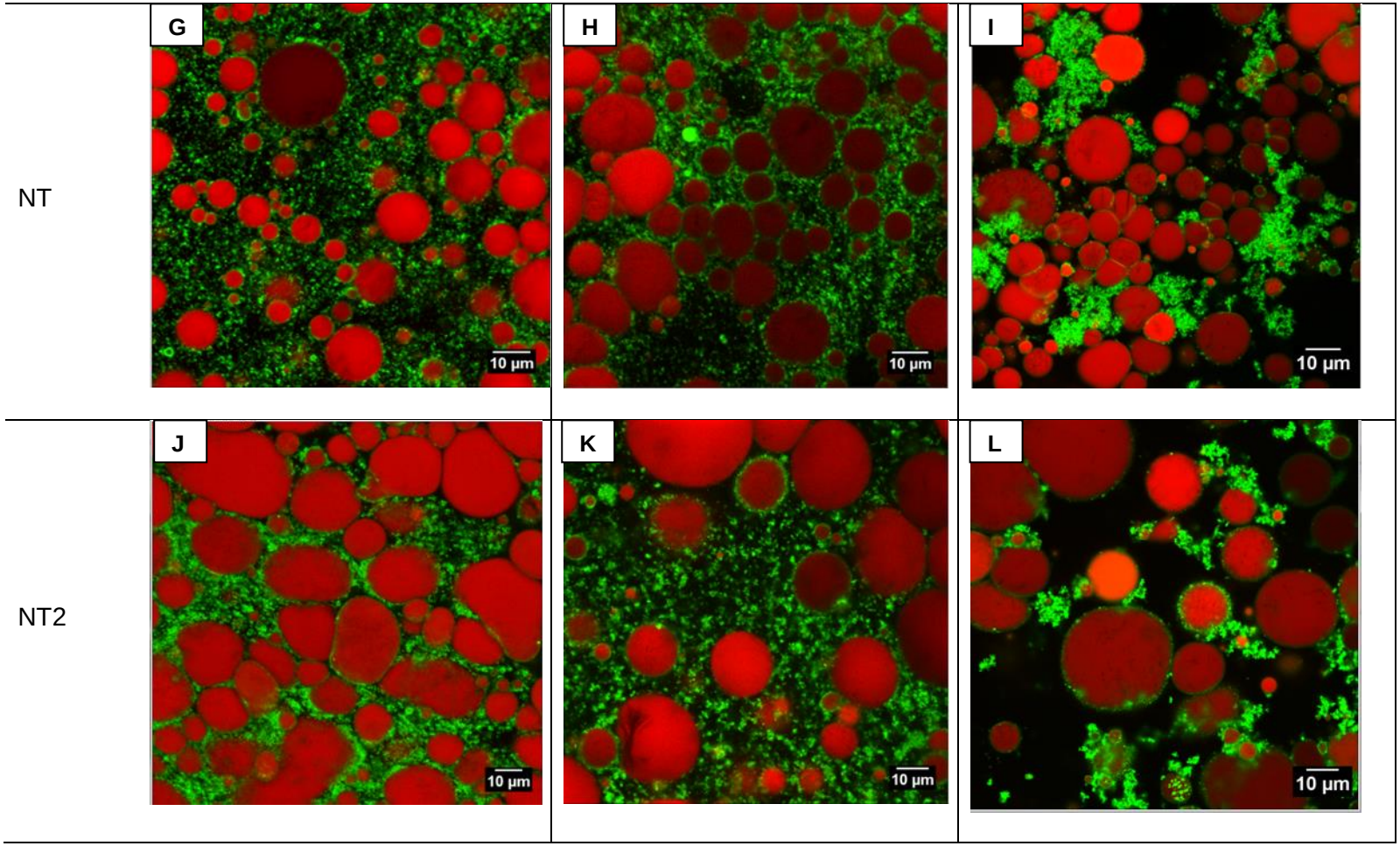

Figure 5.5 *Confocal Microscopy Images of droplet stabilised emulsions freshly prepared (Day 0) and after accelerated oxidation of core safflower oil (Day 5 and 7).*

NO= droplet stabilised emulsion with olive oil shell droplets; NP= droplet stabilised emulsion with palmolein oil shell droplets; NT= droplet stabilised emulsion with trimyristin shell droplets processed above 56°C; NT2= droplet stabilised emulsion with trimyristin shell droplets processed below 56°C

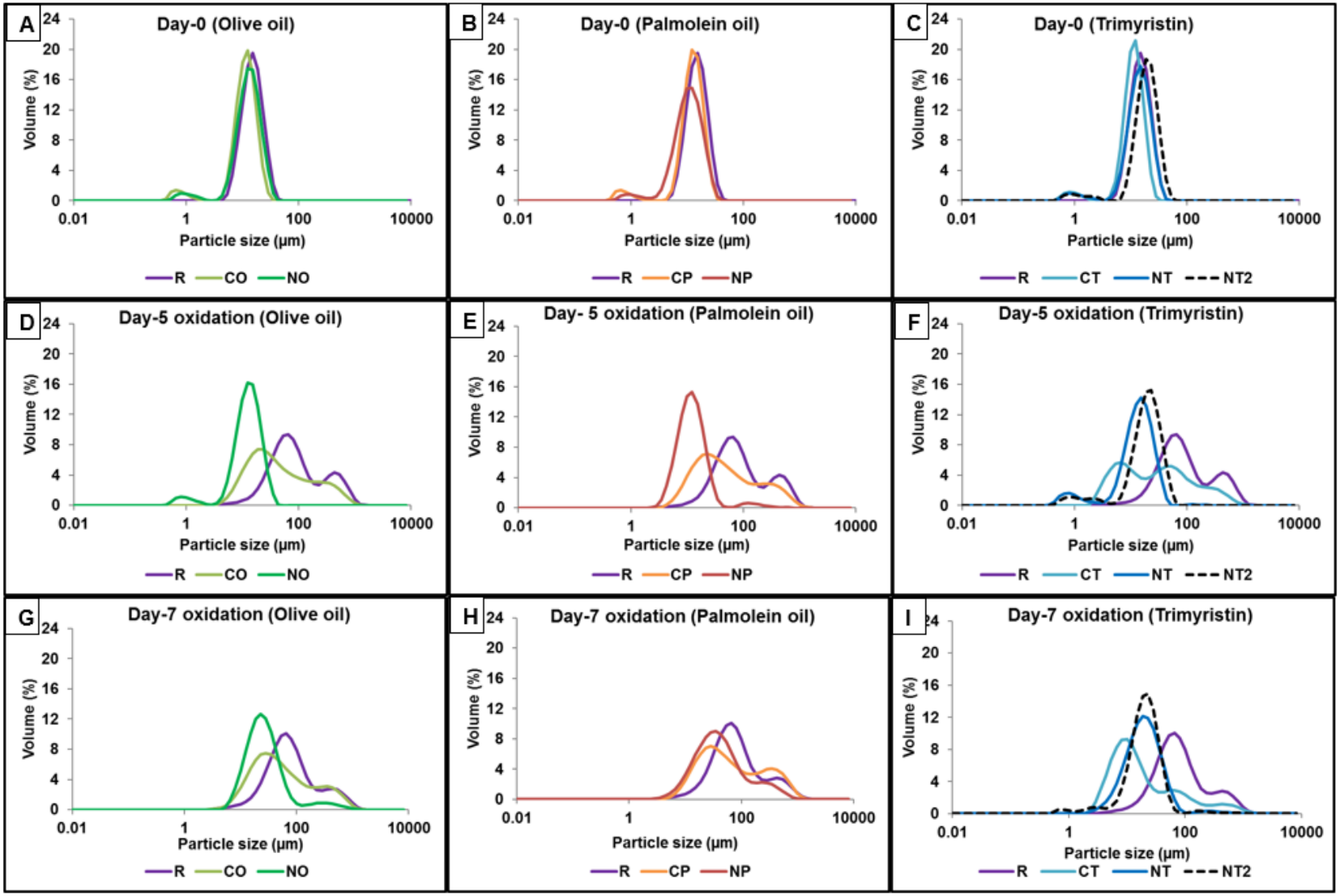

Figure 5.6 *Particle size distribution of 'droplet stabilised' emulsion and control emulsions freshly prepared (A, B & C) and during accelerated oxidation-day 5 (D, E & F) and day 7 (G, H & I).*

R= protein-stabilised oil-in-water emulsion (reference emulsion); CO= R with added olive oil shell emulsion; CP= R with added palmolein oil shell emulsion; CT= R with added trimyristin shell emulsion; NO= droplet stabilised emulsion with olive oil shell droplets; NP= droplet stabilised emulsion with palmolein oil shell droplets; NT= droplet stabilised with trimyristin shell droplets processed above 56°C; NT2= droplet stabilised emulsion with trimyristin shell droplets processed below 56°C

5.4.3 Effect of surface lipid type on oxidative stability of droplet-stabilised safflower oil emulsion

Safflower oil oxidation levels in droplet-stabilised emulsions of intermediate-melting (palmolein oil) surface lipid (NP) were higher than droplet-stabilised emulsions of low- (NO) and high-melting surface lipids (NT & NT2). Differences between NT and NT2 were subtle: for the NT emulsion AUC values were lower for CD and LHP and higher for hexanal, compared with NT2.

Higher levels of safflower oil oxidation in droplet-stabilised emulsion of medium-melting surface lipid (palmolein oil) were unexpected. However, structural changes observed during oxidation provide an explanation for these results. While droplet-stabilised emulsions made up of low- (NO) and high-melting surface lipids (NT and NT2) remained relatively stable during oxidation, that of medium melting surface lipid was less stable as observed with changes in structure (Figure 5.5) and droplet size (Figure 5.6). More uniform coating of core safflower oil droplets was observed with protein-coated olive and trimyristin shell droplets than with palmolein oil shell droplets (Figure 5.5). After five days' oxidation we observed a shift in the particle size distribution of palmolein oil droplet-stabilised emulsions to larger sizes (Figure 5.6 B & H).

5.4.4 Impact of surface lipid state on oxidative stability of droplet-stabilised emulsion

A significant difference ($p < 0.05$) in safflower oxidation levels between droplet stabilised emulsions of high melting surface lipid processed above its melting temperature (NT) and that processed below melting temperature (NT2) was only found after 9 days exposure for conjugated dienes, hydroperoxides and hexanal analysis.

The hypothesis was that for emulsions processed above trimyristin's melting temperature, trimyristin shell droplets adsorbed to safflower oil-water interface in a liquid state, while for those processed below trimyristin's melting temperature, shell droplets adsorbed in a solid state. Even though the emulsions processed above melting temperature subsequently cooled and remained in a supercooled state (Westesen & Bunjes, 1995) , the expectation was that droplet-stabilised emulsions processed below melting temperature (adsorption in solid state) would provide better oxidative stability than that processed above melting temperature (adsorption in liquid state). For NT2 it was expected that the solid matrix would entrap the core lipid immediately after processing and delay oxidation, but there was no significant difference ($p > 0.05$) in oxidation levels between these formulations except after 7 days exposure. The emulsion processed above melting temperature (NT) appeared to inhibit oxidation better than that processed below melting temperature (NT2) (Table 5.2) but oxidation peak time for NT2 was longer than NT for formation of primary oxidation products (CD and LHP) and shorter for secondary oxidation product (hexanal). This suggests a distinct delay in oxidation with NT2 emulsions **(**Table 5.3).

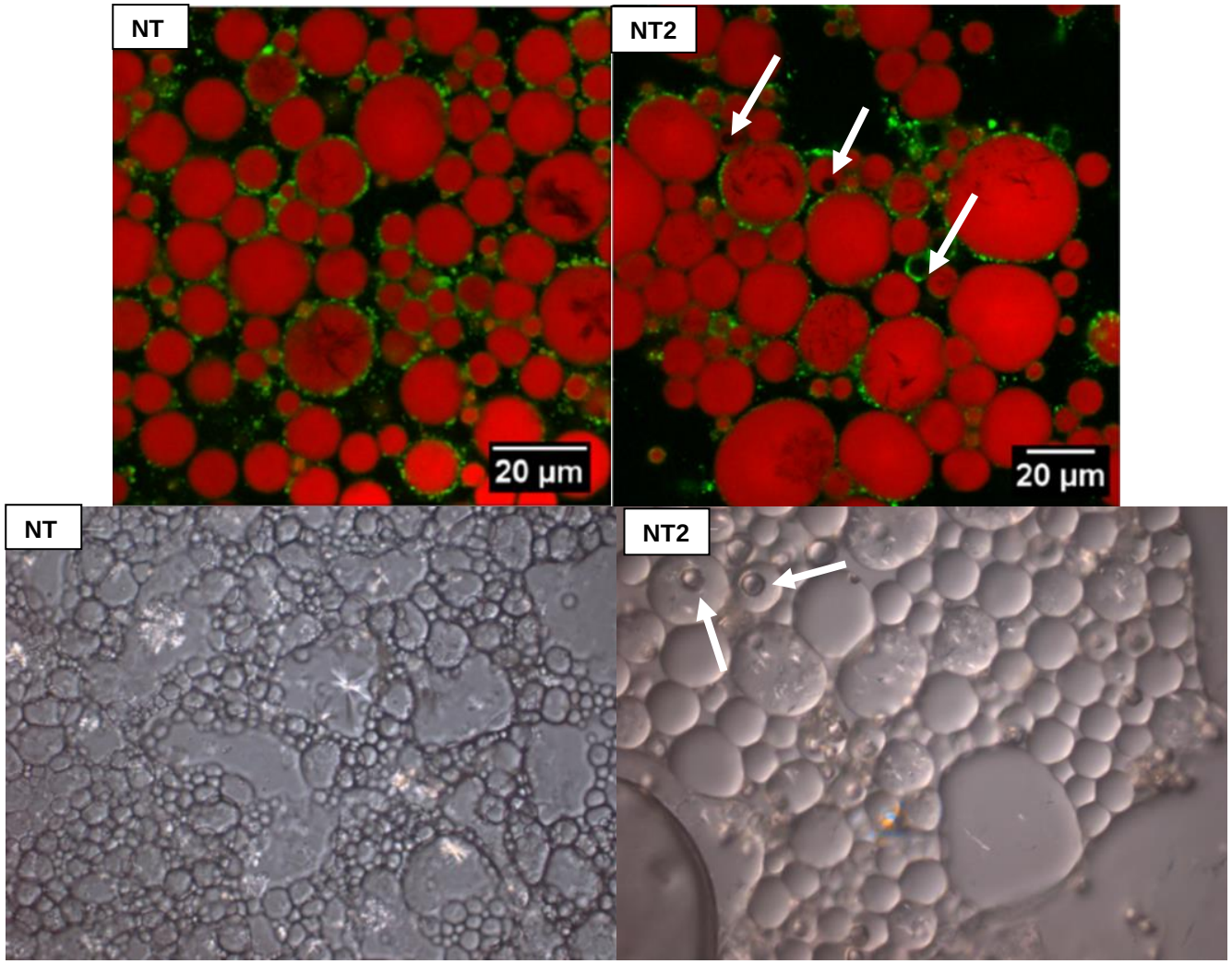

Figure 5.7 *Confocal (top) and differential interference contrast (bottom) microscopy images of droplets stabilised emulsions with trimyristin surface lipid; NT-processed above melting temperature; NT2-processed below melting temperature - Arrows show different crystal morphology for NT2*

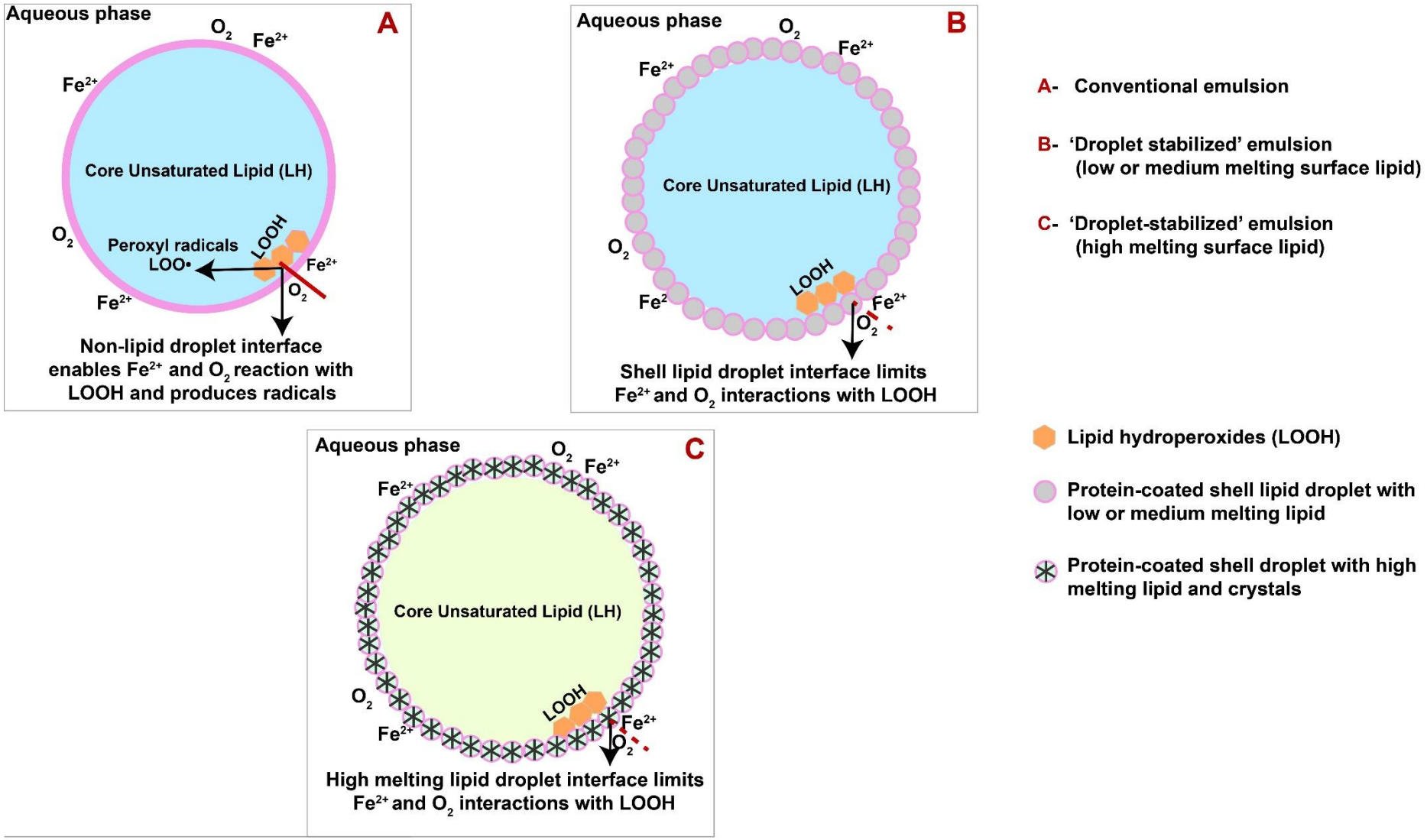

Figure 5.8 *Schematic diagram of oxidation in conventional and droplet-stabilised emulsions. A)- Conventional emulsion; B)- Droplet-stabilised emulsion with low or medium melting surface lipid; C)- Droplet-stabilised emulsion droplet with high melting surface lipid.*

5.5 Discussion

Lipid oxidation in emulsions is influenced by catalysts such as singlet oxygen, metal ions, light, temperature and enzymes. Oxidation by light follows two possible pathways or mechanisms. In type 1 mechanism, an excited sensitizer such as chlorophyll or riboflavin directly abstracts hydrogen from a fatty acid and produces a free-radical, this mechanism is most likely to occur under low oxygen concentrations. While in type 2 mechanism when oxygen is readily available, an excited sensitizer emits or transfers energy absorbed to triplet oxygen ($^3O_2$) generating singlet oxygen ($^1O_2$). Singlet oxygen directly reacts with the double bonds of unsaturated fatty acids (Kanofsky, 2016). In this study, the most probable mechanism of accelerated oxidation is the type 2 mechanism. As emulsions were exposed to light in the presence of ferrous ions, accelerated oxidation by oxygen and ferrous ions is envisaged. Singlet oxygen ($^1O_2$) reacts with core safflower oil to yield lipid hydroperoxides (LHP) and then ferrous ions catalyse decomposition of hydroperoxides.

Droplet surface area, droplet charge, interfacial permeability, interfacial thickness and interfacial composition are some of the factors that can impact lipid oxidation in oil-in-water emulsions (Waraho, McClements, & Decker, 2011). While many studies on the oxidative stability of protein-stabilised emulsions have reported about the impact of droplet surface area and charge on oxidation, it is important to emphasise that oxidation is not only influenced by these factors.

Reports on the effect of droplet size on oxidative stability are contradictory: some studies report decreased oxidative stability with increased surface area (S. J. Lee

et al., 2011) but other studies show the reverse trend (Nakaya et al., 2005). In this study, the particle size of droplet-stabilised and control emulsions was not so different. Even though the particle size of reference emulsion (R) was slightly higher than droplet stabilised emulsions (Table 5.1), it is unlikely that increased oxidative stability of droplet stabilised emulsions was due to droplet surface area, because if this was the predominant factor, the oxidative stability of R should have been better than other controls (CO, CP & CT) and droplet-stabilised emulsions or vice versa.

The pH of emulsions was measured after 5 and 7 days under accelerated oxidation conditions. All emulsions had pH values in the range 6 to 7 (where milk proteins would carry a net negative charge), except R in which pH decreased to 5.5 after five days under accelerated oxidation conditions. Haahr and Jacobsen (2008) reported faster formation of peroxides and volatiles at pH 3 than pH 7 in omega-3 enriched emulsions irrespective of iron addition, a similar trend was also reported for mayonnaise enriched with fish oil (Charlotte Jacobsen, Timm, & Meyer, 2001). Another study reported slower formation of peroxides and volatiles at pH 3 than pH 7 in salmon oil-in-water emulsions without addition of iron (Mancuso et al., 1999) and attributed the increased oxidation rates at pH 7 to low solubility of iron in the continuous phase at pH 7. In this study, the pH of emulsions after homogenisation was the same therefore differences in oxidative stability between emulsions could not have been influenced by differences in pH. The observed pH decrease in R on day 5 can be attributed to the production of short chain aliphatic acids during the formation of secondary oxidation products (Dimakou, Kiokias, Tsaprouni, & Oreopoulou, 2007).

The ability of proteins to bind or chelate metals has been reported to limit lipid oxidation by partitioning metal ions away from the droplet interface and reducing their reactivity (Caetano-Silva, Mariutti, Bragagnolo, Bertoldo-Pacheco, & Netto, 2018; Guzun-Cojocaru et al., 2011; Sugiarto, Ye, Taylor, & Singh, 2010) . The presence of unadsorbed proteins in emulsions has also been shown to limit oxidation (Faraji, McClements, & Decker, 2004). The amount of unadsorbed proteins in this study was not quantified and so it is difficult to evaluate the effect, but the amounts of protein used in droplet-stabilised emulsions and composition-matched controls were similar therefore it is unlikely that the presence of unadsorbed proteins in the continuous phase favoured oxidative stability of droplet-stabilised emulsions over composition-matched controls. Composition-matched controls (CO, CP & CT) consisted of two types of droplets: shell droplets and the core emulsion droplets, both stabilised by the adsorption of MPC proteins. The actual structure of MPC proteins on the droplet surface is not clearly known but likely to contain casein micelle and its fragments and some whey proteins. The interfacial structures of MPC proteins in shell droplets and the core emulsion droplets are likely to be similar, although it is possible that casein micelles adsorbed onto the shell droplets may be more dissociated due to high homogenisation pressure used in their preparation. Assuming there are no interactions between shell droplets and the core emulsion droplets upon gentle mixing, the proportions of shell droplets in composition-matched controls and droplet-stabilised emulsions would be the same. The only expected difference would be the location of the droplets. In droplet stabilised emulsions, the shell droplets stabilised by MPC protein act as an emulsifying agent for the core oil, because the outer regions of adsorbed casein micelles are able to adsorb and

stabilise the core oil droplets as the shell droplets connect with each other and form a layer along the core droplet interface as reported by Ye et al. (2013). The actual structure and conformation of protein that stabilise the core droplets is not known and being investigated in other studies.

The physicochemical properties of lipids can influence the physical stability of an emulsion and consequently impact oxidative stability (McClements, 2015b). This study also examined the impact of surface lipids of varying physical properties and it is possible that due to the physical instability (interface thinning and partial coalescence) of palmolein oil droplet-stabilised emulsions during oxidation, the droplet-stabilised interface became more accessible to ferrous ions and oxygen thus promoting interactions between ferrous ions or oxygen and core safflower oil which resulted in higher levels of conjugated dienes, lipid hydroperoxides and hexanal recorded.

The presence of naturally-occurring antioxidants such as tocopherols or carotenoids in oils can also inhibit oxidation in emulsions (Berton-Carabin et al., 2014), as can naturally-occurring oxidation products and pro-oxidants such as chlorophyll. The olive oil used here was a highly-refined low-acidity product without added antioxidants. Similarly, trimyristin was free from added antioxidants and as a fully saturated lipid, it is unlikely to contain oxidation products at significant levels. Palmolein oil did not contain added antioxidants but may have contained low levels of oxidation products and/or naturally-occurring pro- and antioxidants. It is clear from Figure 5.3 that the initial levels of oxidation products in emulsions varied very little with surface lipid. Palmolein droplet-stabilised emulsions generally oxidised faster than comparable emulsions with other

surface lipids, and a contribution from naturally-occurring pro-oxidants in palmolein cannot be ruled out.

Another factor that may have contributed to the differences in oxidative stability between surface lipids is their differences in hydrophobicity (low levels of polar groups) which could have influenced the partitioning of ferrous ion and oxygen. Lipid hydrophobicity was not characterised in this study, so it is difficult to evaluate.

The physical state of lipids in emulsions can influence oxidation because it affects the distribution of lipid-soluble components between the phases, diffusion rate of molecules through the lipid droplets (Okuda, McClements, & Decker, 2005) and may trap the lipid within a crystalline matrix making it less accessible to aqueous pro-oxidants and oxygen (McClements et al., 2007). Increased oxidative stability with NT and NT2 emulsions relative to other surface lipids was observed (Figure 5.3, Table 5.2 & Table 5.3), which may be attributable to the protective effect of droplet stabilisation and the solid lipid matrix formed at the interface upon trimyristin crystallization.

Looking at the structural changes of NT and NT2 during oxidation, there appear to be no marked differences in structure between these two emulsions that could have given rise to the observed differences in oxidation rates; however, one possible explanation can be drawn from the observed differences in structure when the emulsions are freshly formed. In both emulsions, crystalline structures were observed but the crystalline morphology (Figure 5.7) in the emulsions processed below melting temperature (NT2) was different from that processed

above melting temperature (NT) and this morphology may have resulted in a different distribution or location of trimyristin shell droplets which impacted oxidative stability of core unsaturated safflower oil.

Overall, both emulsions (NT and NT2) showed significantly increased oxidative stability over control emulsions (R & CT) and droplet-stabilised emulsions of low (NO) and medium (NP) melting surface lipids (Table 5.2 & Table 5.3). These results show that the oxidation resistance of droplet-stabilised emulsions can be greatly enhanced with the use of high melting surface lipids.

The ability of pro-oxidant metal ions or oxygen to diffuse into the lipid phase of an emulsion can be limited by making the interface less accessible and so carefully structuring the interface of emulsions may be a good strategy that can inhibit oxidation in emulsions (McClements & Decker, 2000). The interfacial layer of an oil-in-water emulsion plays a significant role in the oxidative stability of the oil phase because it is the gateway between aqueous pro-oxidant metals, oxygen and the oil phase. Once metal ions and oxygen cross the interface they can interact with the core-unsaturated lipid (Kargar et al., 2011; Silvestre et al., 2000)

The formation of cohesive protein layers by cross-linking protein with transglutaminase to increase oxidative stability has been reported but, these layers were still porous and did not inhibit lipid oxidation (Kellerby, Gu, McClements, & Decker, 2006). Alternatively, structural design of emulsion interface to make it thicker and less permeable as seen with multi-layered and Pickering emulsions have been reported to increase oxidative stability (Gudipati et al., 2010; Kargar et al., 2011; Klinkesorn, Sophanodora, Chinachoti,

McClements, & Decker, 2005; Ogawa, Decker, & McClements, 2003). The mechanism by which multi-layered emulsions inhibit oxidation by metal ions differs with that of Pickering emulsions while the former depends greatly on electrostatic repulsions between the charged outer layer and metal ions, the latter tends to form a rigid barrier which prevents metal ions from reacting with the lipid phase.

This study shows that the structured interface of droplet-stabilised emulsions provides a barrier to pro-oxidant metal ions and oxygen, which can almost halve oxidation compared with conventional protein-stabilised emulsions (Figure 5.3 & Table 5.3).

Proteins are reported to stabilise emulsions by forming thick interfaces which can retard oxidation (Fang & Dalgleish, 1993; Hu et al., 2003). In droplet-stabilised emulsions, the interface is covered by protein-coated lipid droplets in a somewhat aggregated network and this appears to form a protective interface that may be responsible for the increased oxidative stability observed. It is also possible that this protective effect was further enhanced by the adsorption of any free non-adsorbed proteins to the interfaces of core oil droplets not fully covered or coated by shell droplets.

According to Mancuso et al. (1999) increased pH implies a decrease in iron solubility in the continuous phase, causing it to precipitate at the droplet interface and promote oxidation. If ferrous ion partitioned at the interface of emulsions and promoted oxidation in controls but oxidation was less extensive in droplet-stabilised emulsions, it can be hypothesise that the lipid droplet interface (shell

droplets) in droplet-stabilised emulsions limited the proximity between ferrous ion and lipid hydroperoxides, as illustrated in Figure 5.8. It can also be hypothesised that the lipid droplet interface in droplet-stabilised emulsions may have influenced partitioning of pro-oxidant metal ions away from the droplet interface and limited interactions that promote oxidation.

In conclusion, safflower oil oxidation in droplet-stabilised emulsion was significantly slower and/or less extensive than in composition-matched conventional protein-stabilised emulsions. These results indicate that the structured interface of droplet-stabilised emulsion limits contact between pro-oxidant metals, oxygen and lipid substrate. Addition of shell droplets to conventional emulsions delayed formation of secondary oxidation products which also shows the impact of protein-coated shell droplet stabilisation. These results confirm the oxidation resistance of droplet-stabilised emulsions. Oxidative stability of safflower oil in droplet-stabilised emulsions was greatly enhanced with protein-coated high-melting surface lipid, both when the emulsions were processed above and below the surface lipid's melting temperature. These results show that oxidation resistance of droplet-stabilised emulsions can also be improved by changing the interfacial composition.

This study provides critical knowledge for the functional food industry about plausible applications and functional properties of droplet-stabilised emulsions.

Chapter 6: Impact of antioxidant location in droplet-stabilised oil-in-water emulsions on oxidative stability of unsaturated lipid incorporated within

6.1 Abstract

This study investigated and compared performance of antioxidant (butylated hydroxyanisole- BHA) when incorporated in shell droplets or in the core lipid of droplet-stabilised emulsions. Emulsions consisted of a core of polyunsaturated fatty acid (PUFA) oil emulsified with shell emulsions of low (olive oil), or high (trimyristin) melting point lipids. Oxidation of emulsions was accelerated with a fluorescent lamp in the presence of ferrous iron (500 μM) for eleven days, and PUFA oxidation was monitored via the formation of conjugated dienes, lipid hydroperoxides and hexanal. At 500 ppm, oxidation was slower in droplet-stabilised emulsions with BHA-in-shell droplets than emulsions with BHA-in-core PUFA oil, but the reverse trend was observed at 50 ppm. Trimyristin DSEs processed below the melting temperature gave the greatest oxidation resistance at both BHA levels. Results suggest that incorporating BHA-in-shell droplets of DSEs can be more effective than incorporating in core PUFA oil, and BHA performance in DSEs may be dependent on its concentration, transfer mechanism and time to reaction sites. The combined effect of BHA and the structured interface of high melting lipid provides superior anti-oxidative effect.

Keywords: Droplet-stabilised emulsion; surface lipid; shell emulsion; core lipid; oxidation; polyunsaturated fatty acid oil; butylated hydroxyanisole

Graphical summary

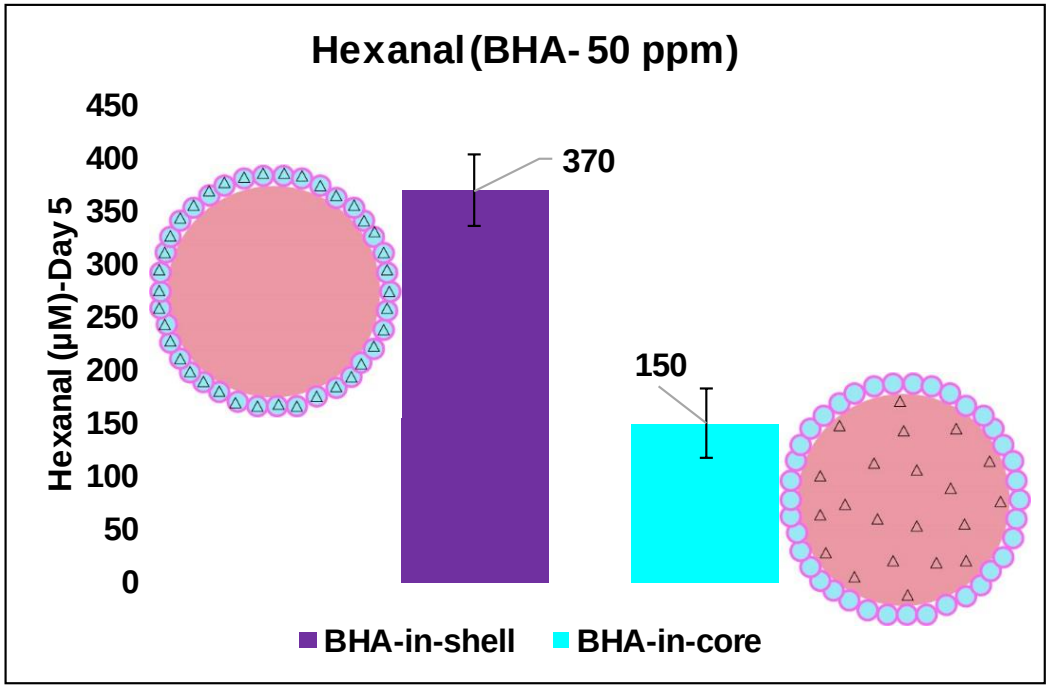

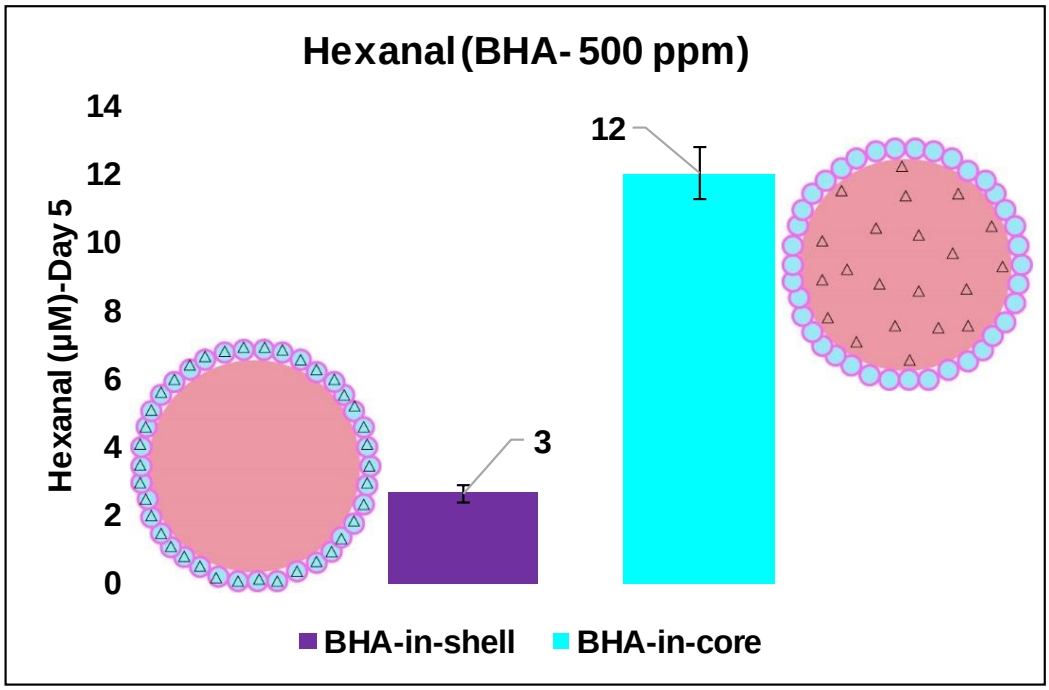

6.2 Introduction

Over the years, effective performance of antioxidants was predicted by their polarity and partitioning behaviour according to the polar paradox hypothesis (Fereidoon Shahidi & Zhong, 2011). The polar paradox theory proposes that polar antioxidants are more effective in bulk oil, while non-polar antioxidants are most effective in oil-in-water emulsions (Porter et al., 1989). Studies supporting this theory propose effective performance of non-polar antioxidants in oil-in-water emulsions because they partition at the oil-water interface where lipid oxidation is thought to be initiated (Huang et al., 1994; Huang, Frankel, Schwarz, Aeschbach, & German, 1996).

Controversies have arisen with regards to the polar paradox theory because other studies (Chaiyasit et al., 2005; Yuji et al., 2007) have shown that non-polar antioxidants can also be effective in bulk oil and vice versa. This implies that antioxidant polarity should not be the sole determinant in evaluating antioxidant performance and other factors such as antioxidant concentration, mobility, size, interfacial structure and composition must also be considered. The questions arising are not about the occurrence of lipid oxidation at the interface of emulsions, as many studies have supported this hypothesis, but rather about other possible factors that influence antioxidant partitioning apart from polarity.

Laguerre et al. (2009) studied the relationship between antioxidants and hydrophobicity and found a non-linear behaviour whereby antioxidant capacity increased as antioxidant hydrophobicity increased to a certain level, after which further increase led to a decrease in antioxidant capacity. This study supports the

general cut-off effect in biological systems reported by Balgavý and Devínsky (1996). The cut-off theory implies that at a certain critical hydrophobicity, antioxidants are located at the oil-water interface and above this critical hydrophobicity level, antioxidants are not located at the interface.

Studies on the effect of antioxidant concentration on the polar paradox theory are scarce. Zhong and Shahidi (2012) were the first to evaluate if the polar paradox applies only over a certain antioxidant concentration range and they showed that antioxidant capacity of polar and non-polar antioxidants in bulk oils was greatly dependent on their concentration.

The interface of droplet-stabilised emulsion consists of protein-stabilised oil droplets (the shell) and this presents the possibility of incorporating antioxidants at the interface, close to where oxidation is promoted. The primary objective of this study was to test whether oxidation resistance of droplet-stabilised PUFA emulsions is influenced by the location of a hydrophobic antioxidant, i.e. at the interface (in the shell lipid) or in the PUFA-rich oil (the core).

6.3 Materials and methods

Materials, equipment and emulsion structure characterization methods used in this study are detailed in Chapter 3. A summary of the experimental set-up in this study is also shown in Figure 3.1.

The peroxide value of safflower oil and trimyristin as specified by supplier was 3 Meq O_2/kg. Initial conjugated dienes (CD), lipid hydroperoxides (LHP) and hexanal (hex) values of olive and safflower oils as analysed was less than 30 mM for CD and LHP and less than 2 µM for hexanal.

6.3.1 Antioxidant-loaded droplet-stabilised emulsions

Antioxidant-loaded droplet-stabilised emulsions used in this study were prepared according to the process shown in Figure 6.1 and Figure 6.2**.**

Lipid phases were prepared by magnetic stirring and heating butylated hydroxyanisole (BHA) into the surface or core lipid for 15 min at 70°C. The total amount of BHA was the same for emulsions with BHA in the core lipid (core-loaded BHA DSE) and emulsions with BHA in the surface lipid (surface-loaded BHA DSE). The concentrations and final amounts of BHA in emulsions used in this study are shown in Table 6.1 and Table 6.2.

Droplet-stabilised emulsions (DSEs) comprising trimyristin surface lipid were processed under two different conditions as detailed in Chapter 5 (see section 5.3.2) to obtain shell droplet adsorption in liquid or solid state.

Table 6.3 and Table 6.4 summarise and shows a description of the emulsions processed for the study. Table 6.3 shows the emulsions processed at final BHA amounts of 50 ppm [0.005% (w/w of droplet-stabilised emulsion)] and Table 6.4 Shows emulsions processed at final BHA amounts of 500 ppm [0.05% (w/w of droplet-stabilised emulsion)].

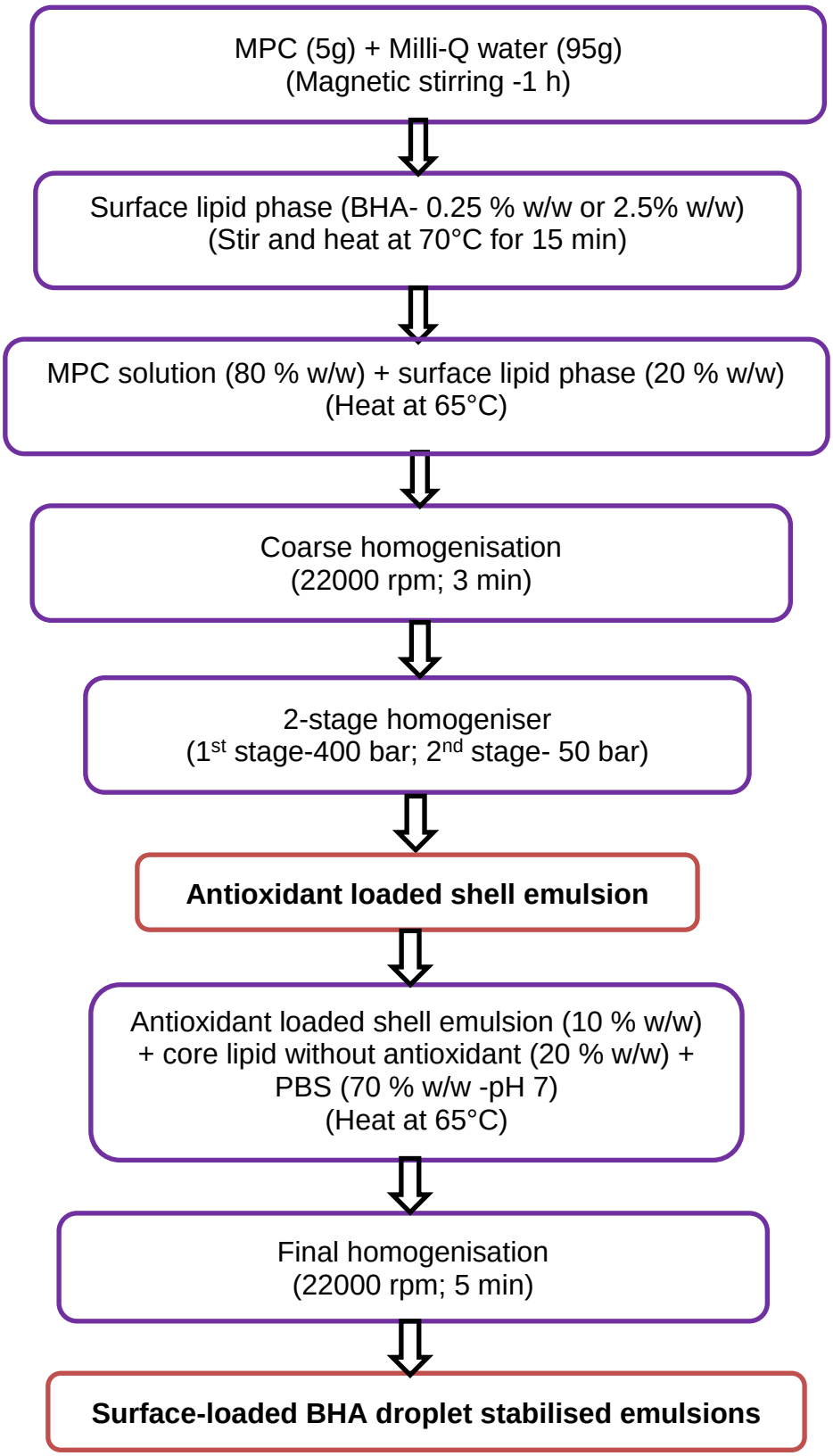

Figure 6.1 *Flow chart of surface-loaded BHA droplet-stabilised emulsion formation*

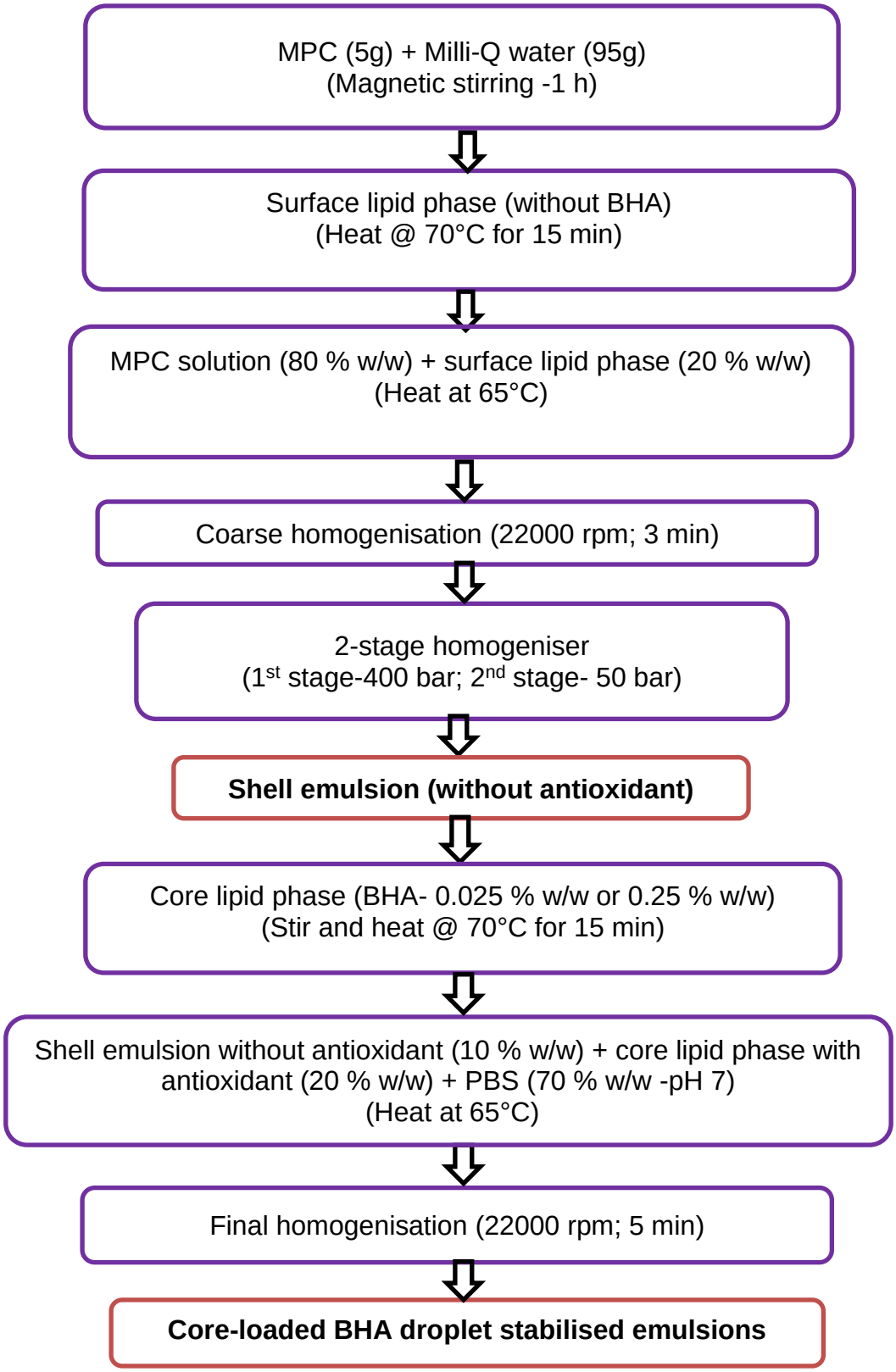

Figure 6.2 *Flow chart of core-loaded BHA droplet-stabilised emulsion formation*

6.3.2 Accelerated Lipid Oxidation

Oxidation of safflower oil in droplet-stabilised and control emulsions was accelerated in sealed 12-well cell plates (1 mL emulsion per well) and 20 mL headspace glass vials (90% headspace) exposed to fluorescent lamp (8500-9000 lux) in the presence of ferrous iron (500 µM- $FeSO_4.7H_2O$ in HCl) for 11 days at 20°C. The distance from lamp to top of plates and vials was approximately 23 cm and 22 cm respectively. Sodium azide (0.02% w/v) was added to the emulsions to prevent microbial growth.

6.3.3 Lipid Oxidation Measurements

Samples were collected on days 3, 5, 7, 9 and 11, and stored at -20°C. Safflower oxidation was monitored via primary (conjugated dienes and lipid hydroperoxides) and secondary (hexanal) oxidation products. The emulsions were analysed within 1-4 weeks of freezing.

Conjugated dienes, lipid hydroperoxides and headspace hexanal were analysed according to the methods described in chapter 3, sections 10, 11 and 12 respectively.

Table 6.1 *Formulation of antioxidant (BHA) loaded droplet-stabilised emulsions with low BHA level (50 ppm) in shell and core droplets used for oxidation study*

Emulsions	MPC solution (% w/w)	Surface lipid (% w/w)	Antioxidant in surface lipid (%w/w of surface lipid phase)	Antioxidant in surface lipid (%w/w of shell emulsion)	
Shell emulsion	80	20	0.25	0.05	
	Shell emulsion (% w/w)	**Core lipid (% w/w)**	**Phosphate Buffer solution (%w/w)**	**Antioxidant (% w/w of surface lipid phase)**	**Antioxidant (% w/w of final emulsion)**
surface-loaded BHA DSE	10	20	70	0.25	0.005
	Shell emulsion (% w/w)	**Core lipid (% w/w)**	**Phosphate Buffer solution (%w/w)**	**Antioxidant (% w/w of core lipid phase)**	**Antioxidant (% w/w of final emulsion)**
core-loaded BHA DSE	10	20	70	0.025	0.005

Table 6.2 *Formulation of antioxidant (BHA) loaded droplet-stabilised emulsions with high BHA level (500 ppm) in shell and core droplets used for oxidation study*

Emulsions	MPC solution (% w/w)	Surface lipid (% w/w)	Antioxidant in surface lipid (%w/w of surface lipid phase)	Antioxidant in surface lipid (%w/w of shell emulsion)	
Shell emulsion	80	20	2.5	0.5	
	Shell emulsion (% w/w)	**Core lipid (% w/w)**	**Phosphate Buffer solution (%w/w)**	**Antioxidant (% w/w of surface lipid phase)**	**Antioxidant (% w/w of final emulsion)**
surface-loaded BHA DSE	10	20	70	2.5	0.05
	Shell emulsion (% w/w)	**Core lipid (% w/w)**	**Phosphate Buffer solution (%w/w)**	**Antioxidant (% w/w of core lipid phase)**	**Antioxidant (% w/w of final emulsion)**
core-loaded BHA DSE	10	20	70	0.25	0.05

Table 6.3: *Emulsion formulations for low BHA level (50 ppm).*

Sample codes	Description	Surface lipid	Core Lipid	BHA Location	BHA amounts in final emulsion (%w/w)
NO	Droplet-stabilised emulsion no BHA	Olive oil	Safflower oil	None	0
NOS-50	Droplet-stabilised emulsion with BHA-in-shell	Olive oil	Safflower oil	shell	0.005
NOC-50	Droplet-stabilised emulsion with BHA-in-core- **BHA amount matched with NOS-50**	Olive oil	Safflower oil	Core	0.005
NT	Droplet-stabilised emulsion no BHA and processed at temperature above 56°C	Trimyristin	Safflower oil	None	0
NTS-50	Droplet-stabilised emulsion with BHA-in-shell and processed at temperature above 56°C	Trimyristin	Safflower oil	shell	0.005

NTC-50	Droplet-stabilised emulsion with BHA-in-core and processed at temperature above 56°C- **BHA amount matched with NTS-50**	Trimyristin	Safflower oil	Core	0.005
NT2	Droplet-stabilised emulsion no BHA and processed at temperature below 56°C	Trimyristin	Safflower oil	None	0
NT2-S50	Droplet-stabilised emulsion with BHA-in-shell and processed at temperature below 56°C	Trimyristin	Safflower oil	shell	0.005
NT2-C50	Droplet-stabilised emulsion with BHA-in-core and processed at temperature below 56°C- **BHA amount matched with NT2-S50**	Trimyristin	Safflower oil	Core	0.005

***Table 6.4**: Emulsion formulations for high BHA level (500 ppm).*

Sample codes	Description	Surface lipid	Core Lipid	BHA Location	BHA amount in final emulsion
NO	Droplet-stabilised emulsion no BHA	Olive oil	Safflower oil	None	0
NOS-500	Droplet-stabilised emulsion with BHA-in-shell	Olive oil	Safflower oil	Interface	0.05
NOC-500	Droplet-stabilised emulsion with BHA-in-core--**BHA amount matched with NOS-500**	Olive oil	Safflower oil	Core	0.05
NT	Droplet-stabilised emulsion no BHA and processed at temperature above 56°C	Trimyristin	Safflower oil	None	0
NTS-500	Droplet-stabilised emulsion with BHA-in-shell and processed at temperature above 56°C	Trimyristin	Safflower oil	Interface	0.05

NTC-500	Droplet-stabilised emulsion with BHA-in-core and processed at temperature above 56°C- **BHA amount matched with NTS-500**	Trimyristin	Safflower oil	Core	0.05
NT2	Droplet-stabilised emulsion no BHA and processed at temperature below 56°C	Trimyristin	Safflower oil	None	0
NT2-S500	Droplet-stabilised emulsion with BHA-in-shell and processed at temperature below 56°C	Trimyristin	Safflower oil	Interface	0.05
NT2-C500	Droplet-stabilised emulsion with BHA-in-core and processed at temperature below 56°C- **BHA amount matched with NT2-S500**	Trimyristin	Safflower oil	Core	0.05

6.4 Results

6.4.1 Particle size and microscopic structure of droplet-stabilised oil-in-water emulsions

Figure 6.3 and Figure 6.4 show confocal microscopic images of droplet-stabilised emulsions without BHA (NO, NT & NT2) and with BHA incorporated either in the shell (NOS-50, NOS-500, NTS-50, NTS-500, NT2-S-50 & NT2-S-500) or core droplets (NOC-50, NOC-500, NTC-50, NTC-500, NT2-C-50 & NT2-C-500) at 50 and 500 ppm respectively. There were no observed differences in interfacial structure of emulsions without BHA and with BHA either in the shell or core.

Particle size of shell emulsions without and with BHA were not significantly different (p>0.05). The average surface-weighted mean diameter ($d_{3,2}$) of olive oil and trimyristin shell emulsions with and without BHA was 0.4 µm ± 0.1 and the average volume weighted mean diameter ($d_{4,3}$) was 0.5 µm ± 0.2. Table 6.5 shows the particle size data of droplet-stabilised emulsions without BHA and with BHA incorporated in the shell or core droplets. Particle size of droplet-stabilised emulsions without BHA and with BHA-in-shell or core droplets were also similar for emulsions of same surface lipid and treatment. Particle size of NT2 DSEs were significantly different (p<0.05) from NO and NT DSEs.

Sample	Control	BHA-in-shell	BHA-in-core
Olive	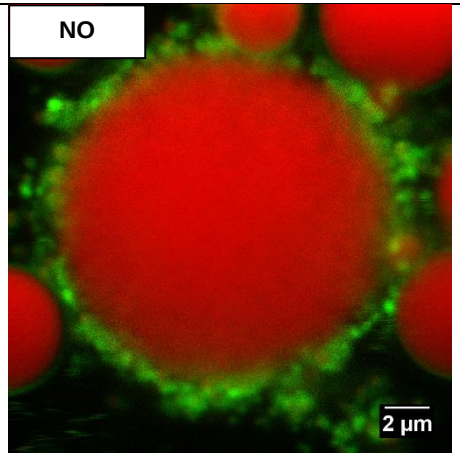	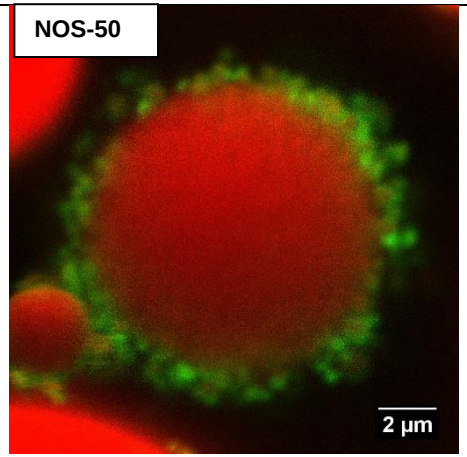	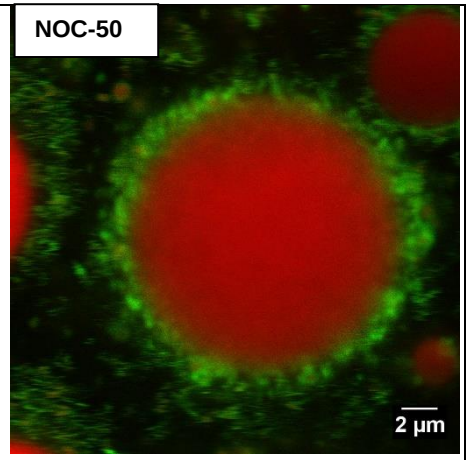
Trimyristin (processed above 56 °C)	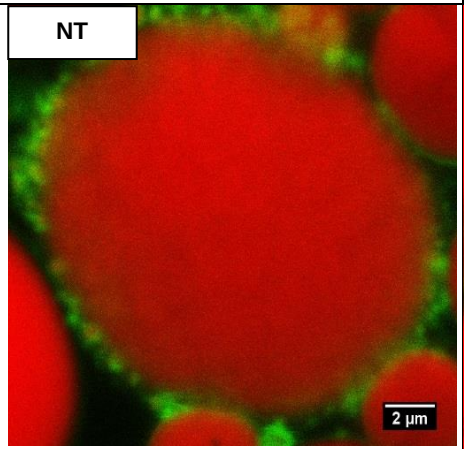	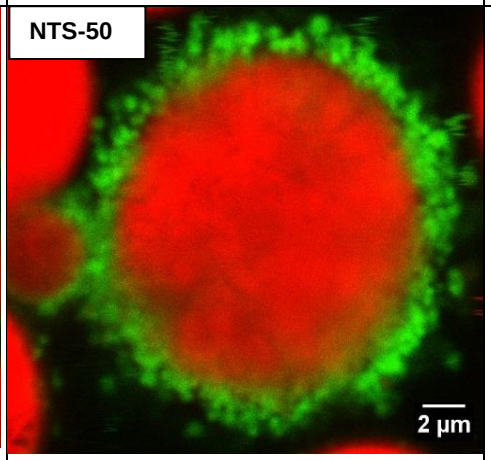	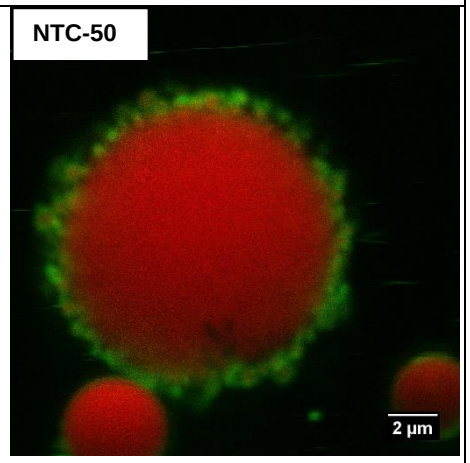

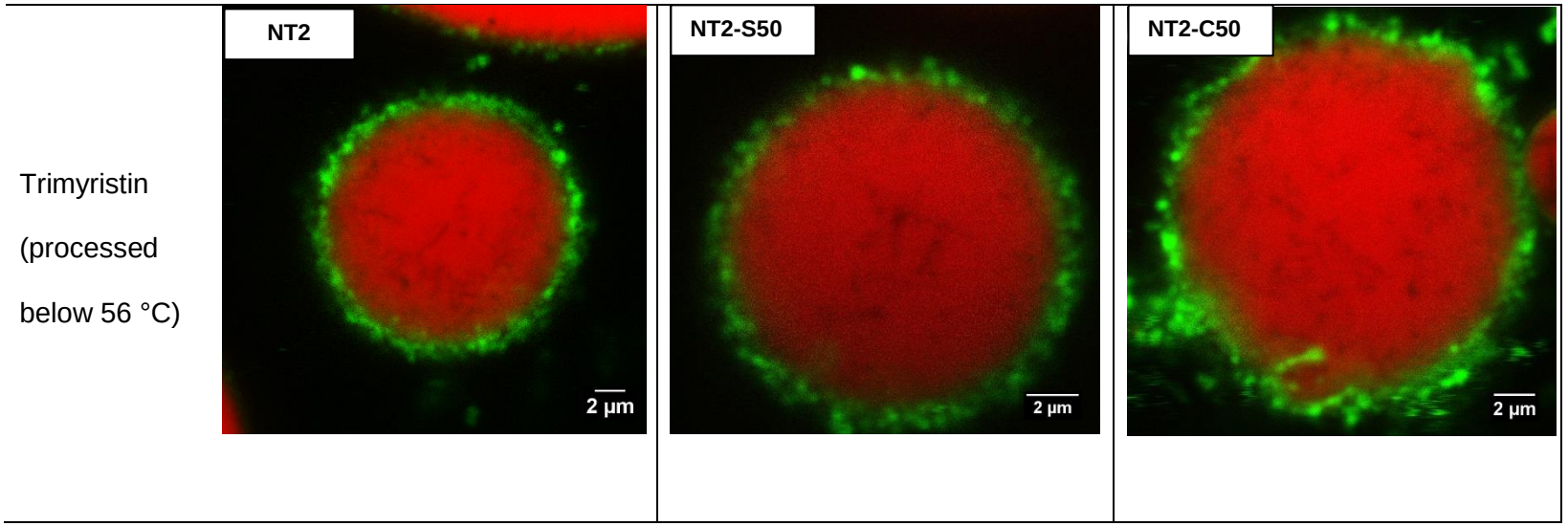

Figure 6.3 *Confocal microscopy images of droplet-stabilised emulsions without BHA and with BHA (50 ppm) in shell droplets or core droplets*

NO= droplet-stabilised emulsion (DSE) with olive oil shell; NOS-50= DSE with olive shell & BHA-in-shell; NOC-50=DSE with olive shell & BHA-in-core safflower; NT-=DSE with trimyristin shell processed above 56 °C; NTS-50= DSE with trimyristin shell processed above 56 °C & BHA-in-shell; NTC-50=- DSE with trimyristin shell processed above 56 °C & BHA-in-core safflower; NT2= DSE with trimyristin shell processed below 56 °C; NT2-S50= DSE with trimyristin shell processed below 56 °C & BHA-in-shell; NT2-C50= DSE with trimyristin shell processed below 56 °C & BHA-in-core safflower.

Sample	Control	BHA-in-shell	BHA-in-core
Olive	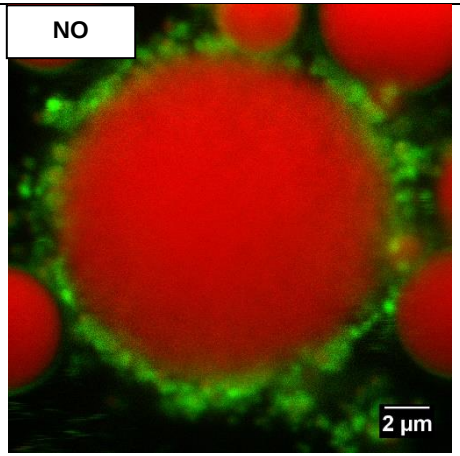	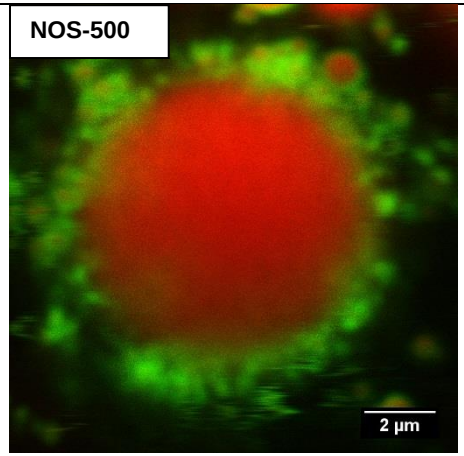	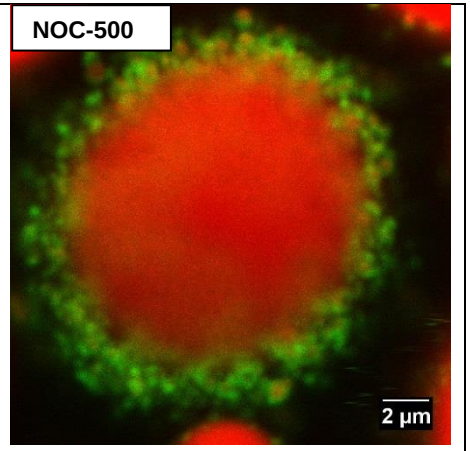
Trimyristin (processed above 56 °C)	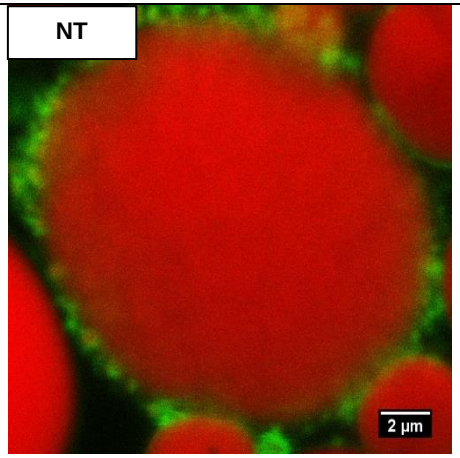	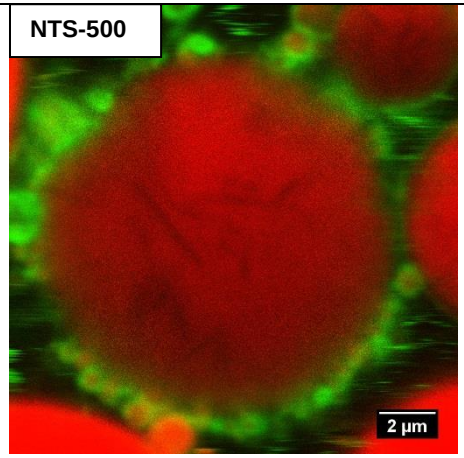	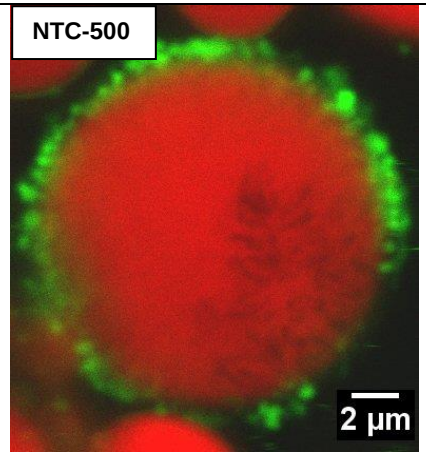

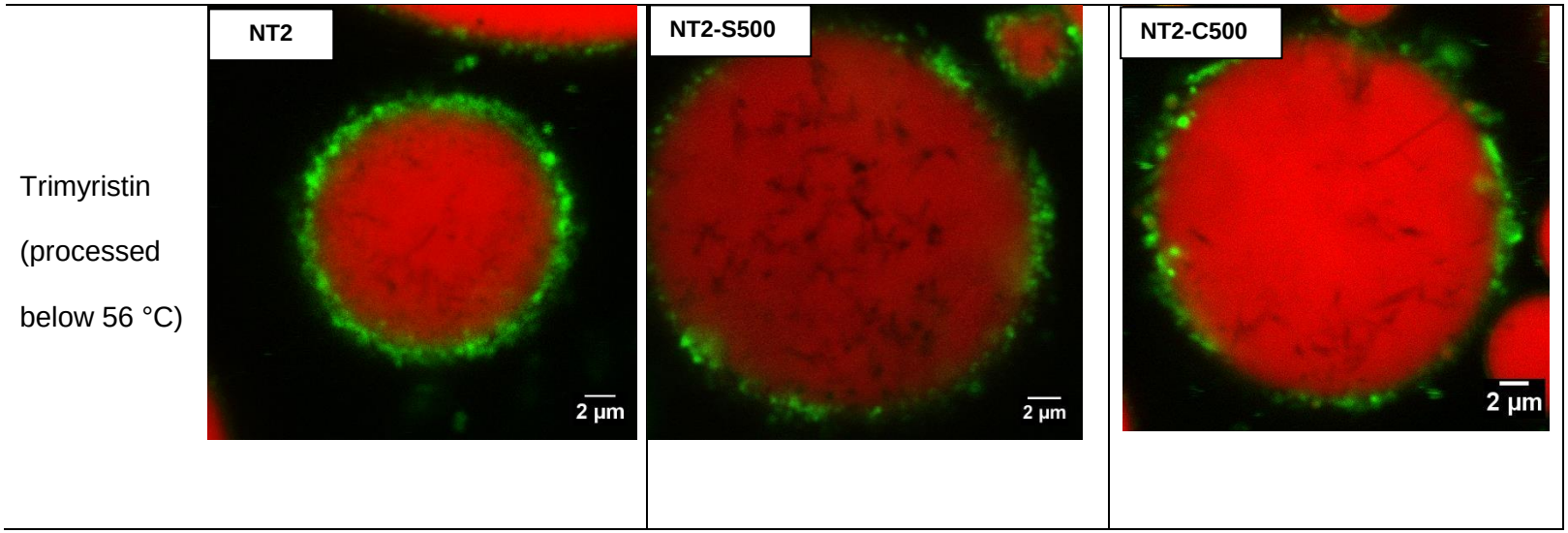

Figure 6.4 *Confocal microscopy images of droplet-stabilised emulsions without BHA and with BHA (500 ppm) in shell droplets or core droplets*

NO= droplet-stabilised emulsions (DSE) with olive oil shell; NOS-500= DSE with olive shell & BHA-in-shell; NOC-500=DSE with olive shell & BHA-in-core safflower; NT= DSE with trimyristin shell processed above 56 °C; NTS-500= DSE with trimyristin shell processed above 56 °C & BHA-in-shell; NTC-500= DSE with trimyristin shell processed above 56 °C & BHA-in-core safflower; NT2- DSE with trimyristin shell processed below 56 °C; NT2-S500= DSE with trimyristin shell processed below 56 °C & BHA-in-shell; NT2-C500= DSE with trimyristin shell processed below 56 °C & BHA-in-core safflower.

Table 6.5 *Average particle size of droplet-stabilised emulsions with and without BHA*

Sample codes	Surface lipid	BHA Location & amount (ppm)	Surface-weighted mean diameter, $d_{3,2}$ (μm)	Volume weighted mean diameter, $d_{4,3}$ (μm)
NO	Olive oil	None	8.0 ± 1[a]	12.5 ± 2.7[a]
NOS-50	Olive oil	shell (50 ppm)	8.0 ± 1[a]	12.6 ± 3.2[a]
NOC-50	Olive oil	Core (50 ppm)	8.1 ± 0.9[a]	14.6 ± 1.1[a]
NOS-500	Olive oil	Shell (500 ppm)	8.1 ± 0.1[a]	14.7 ± 0.5[a]
NOC-500	Olive oil	Core (500 ppm)	8.2 ± 1.2[a]	12.9 ± 3[a]
NT	Trimyristin	None	8.0 ± 0.8[a]	12.9 ± 3.4[a]
NTS-50	Trimyristin	Shell (50 ppm)	7.7 ± 0.6[a]	13 ± 3.8[a]
NTC-50	Trimyristin	Core (50 ppm)	7.5 ± 0.3[a]	14.5 ± 1.2[a]
NTS-500	Trimyristin	Shell (500 ppm)	8.0 ± 0.2[a]	14 ± 0.4[a]
NTC-500	Trimyristin	Core (500 ppm)	8.1 ± 0.3[a]	13.8 ± 3.5[a]
NT2	Trimyristin	None	10.4 ± 0.6[b]	22.6 ± 2.8[b]
NT2-S50	Trimyristin	Shell (50 ppm)	10.3 ± 0.4[b]	23.4 ± 3.1[b]
NT2-C50	Trimyristin	Core (50 ppm)	10.5 ± 0.2[b]	25.9 ± 1.2[b]
NT2-S500	Trimyristin	Shell (500 ppm)	11.6 ± 1.9[b]	24.6 ± 2.4[b]
NT2-C500	Trimyristin	Core (500 ppm)	10.7 ± 0.9[b]	24.4 ± 5.1[b]

6.4.2 Impact of incorporating BHA (50 ppm) in shell droplets versus core droplets of droplet-stabilised emulsions on oxidative stability

Figure 6.5 shows the formation of conjugated dienes, hydroperoxides and hexanal in droplet-stabilised emulsions without BHA and with BHA incorporated in the shell droplets or the core droplets at low amounts (50 ppm). The formation of CD and LHP in emulsions with BHA was slower than in controls, as expected. CD and LHP formation in emulsions with BHA was delayed for 3 days after which, CD and LHP gradually increased and peaked on day 5 (Figure 6.5 A, B, D, E & F), except for NT2 where the onset of CD formation for BHA-in-shell was faster than BHA-in-core droplets (Figure 6.5C), and for NT where the onset of hydroperoxide formation appeared to be similar for control and BHA emulsions (Figure 6.5E).

Breakdown of CD in control emulsions began after day 5 while breakdown of CD in BHA emulsions was delayed and began after day 7 (Figure 6.5 A, B & C). The same trend was observed for LHP breakdown but only for olive oil emulsions. For trimyristin BHA emulsions, breakdown of LHP was similar to controls (Figure 6.5 E & F). Breakdown of CD & LHP in emulsions with BHA-in-shell droplets appeared to be faster than emulsions with BHA-in-core droplets for all surface lipid types (Figure 6.5 A, B, C, D, E & F).

Hexanal formation in controls was faster than emulsions with BHA. Formation of hexanal was faster in emulsions with BHA-in-shell than BHA-in-core for all surface lipid types (Figure 6.5 G, H & I). Hexanal formation in emulsions with BHA-in-shell was slower for trimyristin emulsions processed below 56 °C than trimyristin emulsions processed above 56 °C and olive oil.

In summary, BHA introduced a lag phase for CD and LHP, and appeared to slow down their decomposition, but its location in the shell or the core made little difference. Differences were larger for hexanal: BHA in the core consistently reduced hexanal formation more than BHA in the shell.

Figure 6.6 shows changes in particle size distribution of emulsions during oxidation. There were no marked differences between emulsions with BHA-in-shell and BHA-in-core except for trimyristin emulsions processed below 56 °C, where the particle size distribution on day 5 in emulsion with BHA-in-shell was similar to the control emulsion.

Looking at the changes in $d_{3,2}$ and $d_{4,3}$ shown in Table 6.6, the $d_{3,2}$ values between BHA-in-shell and BHA-in-core DSEs were significantly different ($p<0.05$) after day 5 for only NT2 emulsions while the $d_{4,3}$ values were different for all surface lipid types. After day 7, there were significant differences in $d_{3,2}$ and $d_{4,3}$ values between BHA-in-shell and core DSEs for only NT and NT2 emulsions respectively. Generally, particle size of BHA-in-shell DSEs appeared to increase over BHA-in-core DSEs but this trend was not consistent.

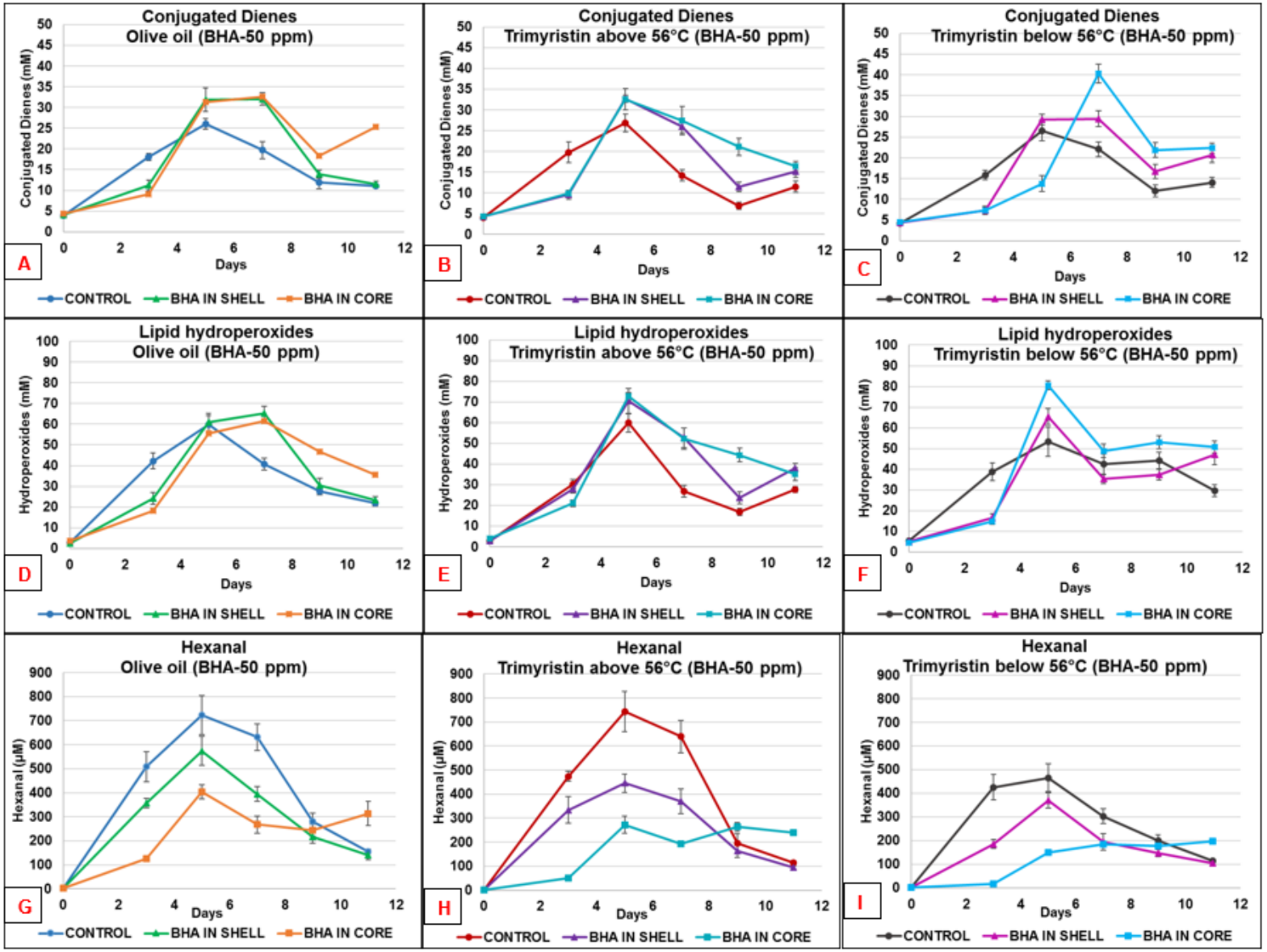

Figure 6.5 *Evolution of conjugated dienes, lipid hydroperoxides and hexanal in droplet-stabilised safflower oil-in-water emulsions without BHA and with BHA (50 ppm).*

A=CD olive DSEs; B= CD trimyristin DSEs processed above 56 °C; C= CD trimyristin DSEs processed below 56 °C; D= LHP olive DSEs; E= LHP trimyristin DSEs processed above 56 °C; F= LHP trimyristin DSEs processed below 56 °C; G= Hexanal olive DSEs; H= Hexanal trimyristin DSEs processed above 56 °C; I= Hexanal trimyristin DSEs processed below 56 °C

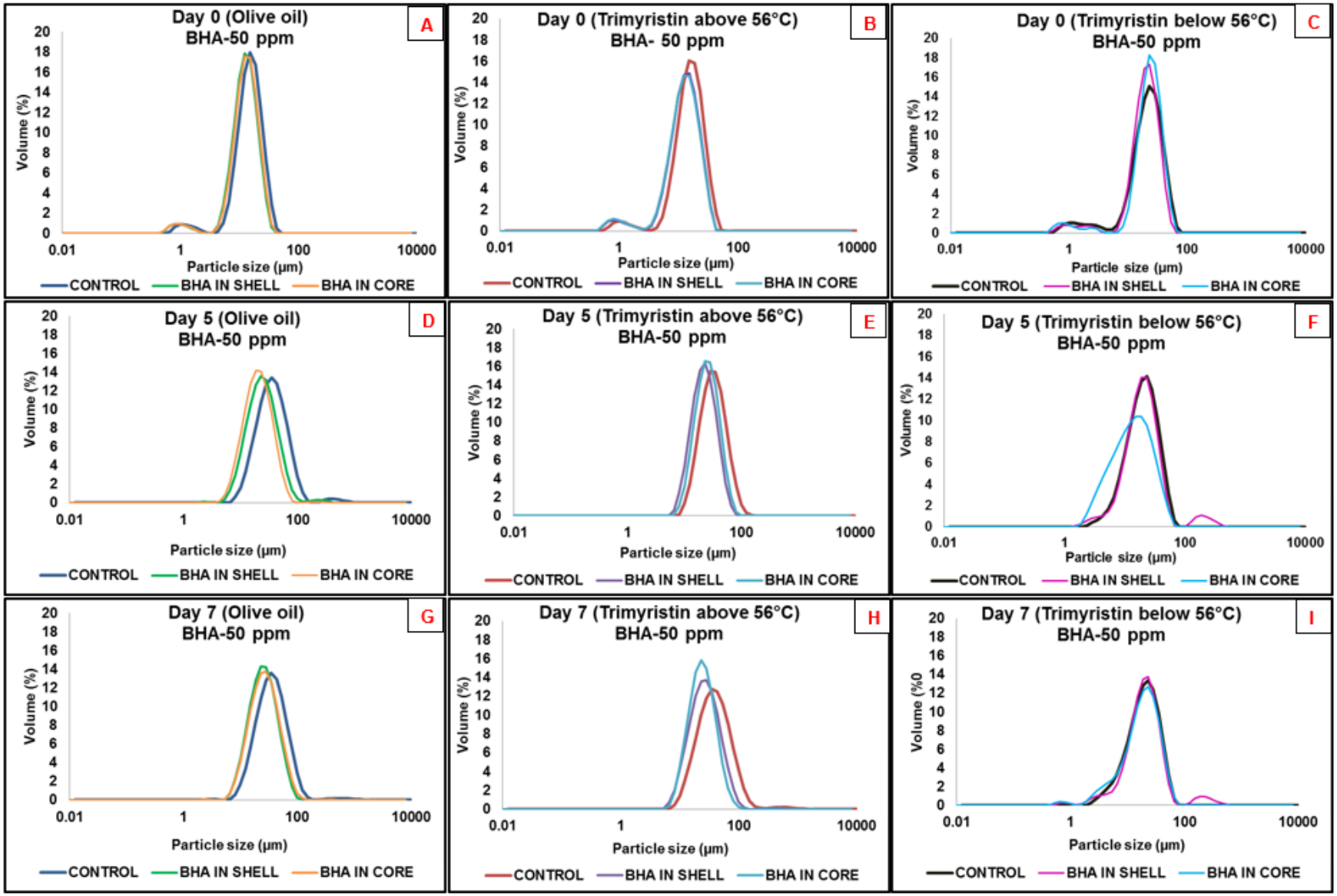

Figure 6.6 *Particle size distribution of droplet-stabilised safflower oil-in-water emulsions without BHA and with BHA (50 ppm) freshly prepared and during accelerated oxidation (day 5 and 7)*

A= fresh olive DSEs; B= fresh trimyristin DSEs processed above 56 °C; C= fresh trimyristin DSEs processed below 56 °C; D= day 5 olive DSEs; E= day 5 trimyristin DSEs processed above 56 °C; F= day 5 trimyristin DSEs processed below 56 °C; G= day 7 olive DSEs; H= day 7 trimyristin DSEs processed above 56 °C; I= day 7 trimyristin DSEs processed below 56 °C.

Table 6.6: *Particle size changes of droplet-stabilised safflower oil-in-water emulsions without BHA and with BHA (50 ppm) freshly prepared and during accelerated oxidation (day 5 and 7)*

DSEs- (BHA-50 ppm)						
	Average Surface-weighted mean diameter, $d_{3,2}$ (µm)			**Average Volume weighted mean diameter, $d_{4,3}$ (µm)**		
	Olive DSEs			**Olive DSEs**		
Sample	**Day-0**	**Day-5**	**Day-7**	**Day-0**	**Day-5**	**Day-7**
Control	8 ± 1^{a}	28 ± 2^{a}	26 ± 3^{b}	13 ± 3^{a}	49 ± 6^{a}	43 ± 7^{b}
BHA-in-shell	8 ± 1^{a}	23 ± 2^{bc}	24 ± 2^{b}	13 ± 4^{a}	35 ± 3^{b}	32 ± 3^{c}
BHA-in-core	9 ± 1^{a}	21 ± 2^{c}	25 ± 2b	15 ± 2^{a}	29 ± 3^{cd}	36 ± 4^{bc}
	Trimyristin (above 56°C) DSEs			**Trimyristin (above 56°C) DSEs**		
Sample	**Day-0**	**Day-5**	**Day-7**	**Day-0**	**Day-5**	**Day-7**
Control	8 ± 1^{a}	25 ± 3^{b}	29 ± 3^{a}	13 ± 4^{a}	32 ± 5^{bc}	53 ± 11^{a}
BHA-in-shell	8 ± 1^{a}	22 ± 2^{c}	26 ± 2^{b}	13 ± 4^{a}	31 ± 5^{bc}	36 ± 7^{bc}
BHA-in-core	8 ± 1^{a}	21 ± 6^{c}	21 ± 4^{c}	15 ± 2^{a}	26 ± 7^{d}	38 ± 12^{bc}
	Trimyristin (below 56°C) DSEs			**Trimyristin (below 56°C) DSEs**		
Sample	**Day-0**	**Day-5**	**Day-7**	**Day-0**	**Day-5**	**Day-7**
Control	11 ± 1^{b}	$14 \pm 1d^{e}$	14 ± 2^{d}	23 ± 3^{b}	19 ± 2^{e}	21 ± 2^{d}
BHA-in-shell	11 ± 1^{b}	17 ± 2^{d}	15 ± 2^{d}	24 ± 4^{b}	34 ± 1^{bc}	35 ± 2^{c}
BHA-in-core	11 ± 1^{b}	12 ± 1^{e}	13 ± 2^{d}	26 ± 2^{b}	19 ± 1^{e}	24 ± 1^{d}

Values are means of two measurements (3 runs per measurement) ± standard deviation. Superscript letters indicate significant differences within same column. Means with same superscript are not significantly different (p>0.05).

6.4.3 Impact of incorporating BHA (500 ppm) in shell droplets versus core droplets of droplet-stabilised emulsions on oxidative stability

Figure 6.7 shows the formation of CD, LHP and hexanal in droplet-stabilised emulsions without BHA and with BHA incorporated in the shell droplets or the core droplets at higher amounts (500 ppm). Plots without control are shown in appendix C for easy comparison between BHA-in-shell and BHA-in-core emulsions. Formation of CD and LHP for emulsions without BHA was faster than emulsions with BHA-in-shell and core droplets.

The formation of CD and LHP in emulsions with BHA-in-shell droplets and BHA-in-core droplets was similar for olive and trimyristin below 56 °C emulsions (Figure 6.7 A,C, D & F) while for trimyristin above 56 °C emulsions, the formation of CD and LHP in emulsions with BHA-in-core droplets was slightly faster than emulsions with BHA-in-shell droplets (Figure 6.7 B & E).

It was expected that the differences in CD and LHP formation between emulsions with BHA-in-shell and core droplets for trimyristin emulsions processed below 56 °C would be more pronounced but there were no significant differences ($p < 0.05$). It is possible that BHA migration from solid shell particles to the interface coincided with BHA migration from core droplets to interface thus reaction rates in both emulsions were similar.

As expected, the formation of hexanal was faster in controls than emulsions with BHA. Hexanal formation in emulsions with BHA-in-shell and core was mostly similar but faster in emulsions with BHA-in-core than BHA-in-shell (Figure 6.7 G, H & I). On day

5, hexanal in olive, trimyristin above 56 °C, and trimyristin below 56 °C emulsions with BHA-in-core was 12 µM ± 1, 14 µM ± 2, and 12 µM ± 1 respectively while for the emulsions with BHA-in-shell hexanal was 5 µM ± 0.2, 2 µM ± 0.1, and 3 µM ± 0.3 respectively.

In summary, BHA location in the shell or the core made little difference for CD and LHP formation. Differences were larger for hexanal: BHA in the shell reduced hexanal more than BHA in the core.

Figure 6.8 shows the particle size distribution of emulsions during oxidation. There were no marked differences in particle size distribution between emulsions with BHA-in-shell and BHA-in-core for olive and trimyristin above 56 °C emulsions. For trimyristin below 56 °C emulsions, the particle size distribution in emulsions with BHA-in-shell was similar to the control emulsion (Figure 6.8F).

Looking at changes in $d_{3,2}$ and $d_{4,3}$ shown in Table 6.7, average $d_{3,2}$ and $d_{4,3}$ between BHA-in-shell and BHA-in-core DSEs were significantly different ($p<0.05$) after day 5 for only olive and NT2 emulsions. After day 7, there were significant differences in $d_{3,2}$ between BHA-in-shell and core DSEs for all surface lipid types while $d_{4,3}$ was significantly different for only Olive and NT2 emulsions. Generally, particle size of BHA-in-shell olive and NT2 DSEs appeared to increase over BHA-in-core DSEs while particle size of BHA-in-shell and core NT DSEs were similar.

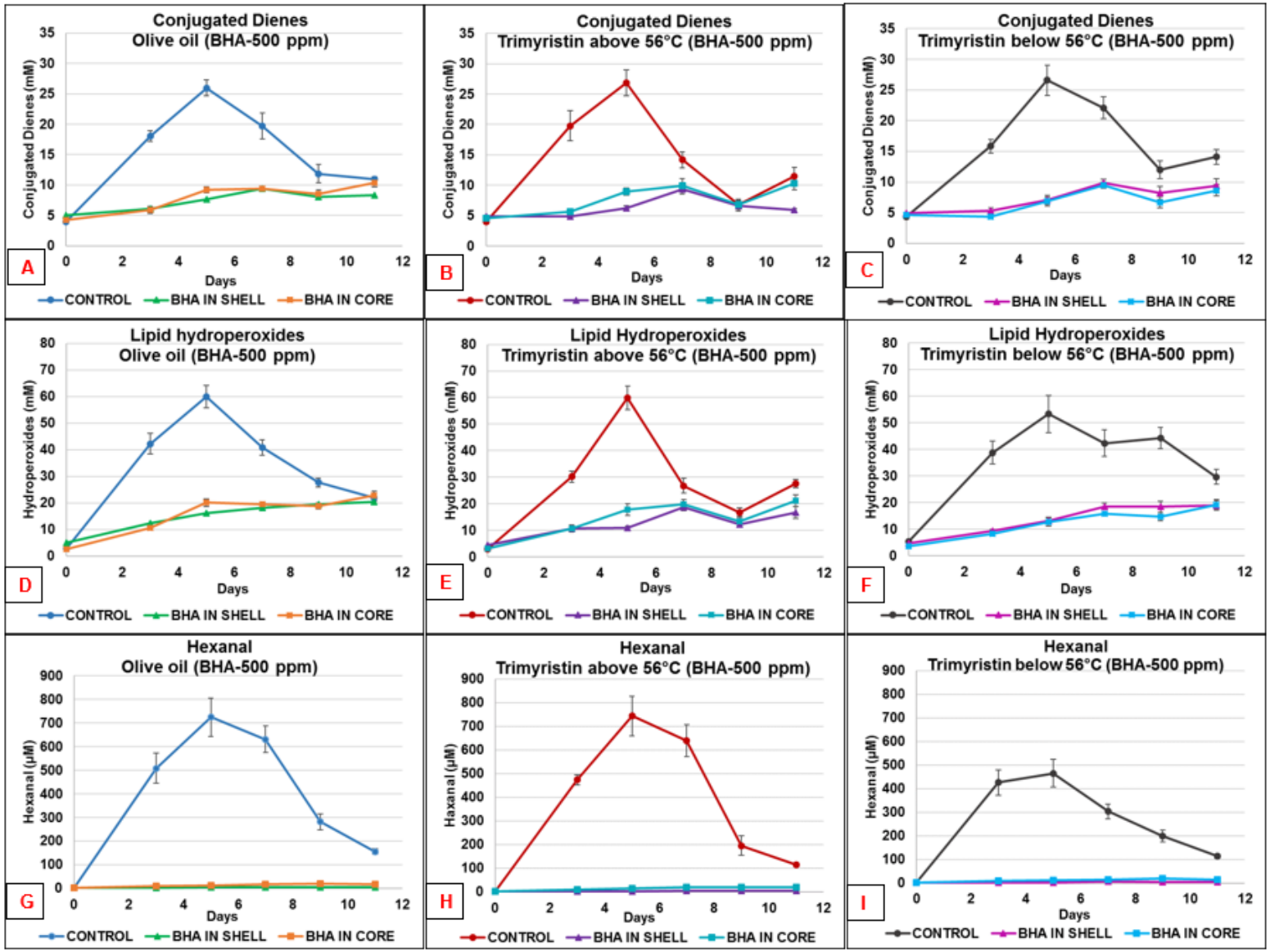

Figure 6.7 *Evolution of conjugated dienes, lipid hydroperoxides and hexanal in droplet-stabilised safflower oil-in-water emulsions without BHA and with BHA (500 ppm)-*

A=CD olive DSEs; B= CD trimyristin DSEs processed above 56 °C; C= CD trimyristin DSEs processed below 56 °C; D= LHP olive DSEs; E= LHP trimyristin DSEs processed above 56 °C; F= LHP trimyristin DSEs processed below 56 °C; G= Hexanal olive DSEs; H= Hexanal trimyristin DSEs processed above 56 °C; I= Hexanal trimyristin DSEs processed below 56 °C- **Plots without control are shown in appendix C for easy comparison between BHA-in-shell and BHA-in-core emulsions**

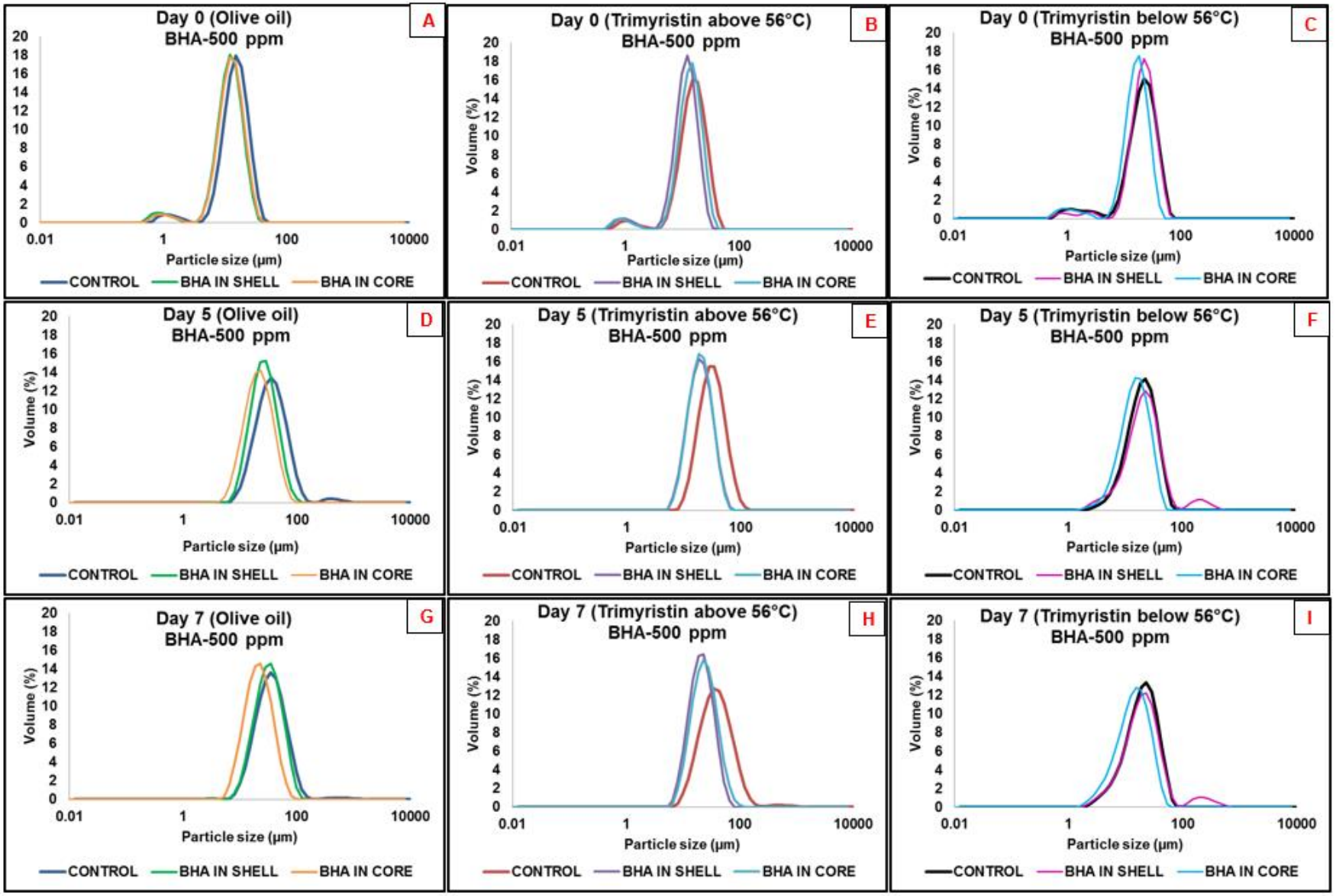

Figure 6.8 *Particle size distribution of droplet-stabilised safflower oil-in-water emulsions without BHA and with BHA (500 ppm) freshly prepared and during accelerated oxidation (day 5 and 7)*

A= fresh olive DSEs; B= fresh trimyristin DSEs processed above 56 °C; C= fresh trimyristin DSEs processed below 56 °C; D= day 5 olive DSEs; E= day 5 trimyristin DSEs processed above 56 °C; F= day 5 trimyristin DSEs processed below 56 °C; G= day 7 olive DSEs; H= day 7 trimyristin DSEs processed above 56 °C; I= day 7 trimyristin DSEs processed below 56 °C

Table 6.7: *Particle size changes of droplet-stabilised safflower oil-in-water emulsions without BHA and with BHA (500 ppm) freshly prepared and during accelerated oxidation (day 5 and 7)*

DSEs (BHA-500 ppm)						
	Average Surface-weighted mean diameter, $d_{3,2}$ (µm)			**Average Volume weighted mean diameter, $d_{4,3}$ (µm)**		
	Olive oil DSEs			**Olive oil DSEs**		
Sample	**Day-0**	**Day-5**	**Day-7**	**Day-0**	**Day-5**	**Day-7**
Control	8 ± 1^{a}	28 ± 2^{a}	26 ± 3^{b}	13 ± 3^{a}	49 ± 6^{a}	43 ± 7^{b}
BHA-in-shell	8 ± 1^{a}	26 ± 2^{ab}	30 ± 2^{a}	15 ± 1^{a}	34 ± 4^{c}	40 ± 4^{b}
BHA-in-core	9 ± 1^{a}	21 ± 2^{c}	21 ± 2^{c}	13 ± 3^{a}	29 ± 3^{de}	27 ± 3^{c}
	Trimyristin (above 56°C) DSEs			**Trimyristin (above 56°C) DSEs**		
Sample	**Day-0**	**Day-5**	**Day-7**	**Day-0**	**Day-5**	**Day-7**
Control	8 ± 1^{a}	25 ± 3^{b}	29 ± 3^{a}	13 ± 4^{a}	32 ± 5^{cd}	53 ± 11^{a}
BHA-in-shell	8 ± 1^{a}	20 ± 1^{c}	22 ± 2^{c}	14 ± 1^{a}	25 ± 2^{ef}	26 ± 2^{cd}
BHA-in-core	8 ± 1^{a}	20 ± 2^{c}	18 ± 2^{d}	14 ± 4^{a}	25 ± 4^{f}	21 ± 2^{de}
	Trimyristin (below 56°C) DSEs			**Trimyristin (below 56°C) DSEs**		
Sample	**Day-0**	**Day-5**	**Day-7**	**Day-0**	**Day-5**	**Day-7**
Control	11 ± 1^{b}	14 ± 1^{e}	14 ± 2^{e}	23 ± 3^{b}	19 ± 2^{g}	21 ± 2^{de}
BHA-in-shell	11 ± 1^{b}	17 ± 1^{d}	15 ± 2^{e}	25 ± 3^{b}	38 ± 2^{b}	40 ± 3^{b}
BHA-in-core	11 ± 1^{b}	14 ± 1^{e}	12 ± 1^{f}	25 ± 6^{b}	19 ± 1^{g}	19 ± 1^{e}

Values are means of two measurements (3 runs per measurement) ± standard deviation. Superscript letters indicate significant differences within same column. Means with same superscript are not significantly different (p>0.05).

6.5 Discussion

Emulsions were exposed to light in the presence of ferrous ion therefore two possible pathways of lipid oxidation initiation are envisaged, as illustrated in Figure 6.9. In the first instance (Figure 6.9A), singlet oxygen ($^1O_2$) reacts with core safflower oil (LH) to yield lipid hydroperoxides (LOOH) and then ferrous ions catalyse the decomposition of hydroperoxides to peroxyl radicals ($LOO^{\bullet)}$ which are unstable. In the second instance (Figure 6.9B), ferrous ions react directly with core safflower oil (LH) to yield free lipid radicals ($L^{\bullet}$) and singlet oxygen reacts with the lipid radical to yield peroxyl radicals ($LOO^{\bullet}$). BHA (AH) reacts with formed radicals ($LOO^{\bullet}$) to produce more stable lipid products (LOOH) and antioxidant radicals ($A^{\bullet}$) thus terminating the free radical chain reaction (*Eq. 6-1, 6-2 & 6-3*). Therefore, BHA delays hydroperoxide decomposition.

$$LOO^{\bullet} + AH \longrightarrow LOOH + A^{\bullet} \qquad \textit{(Eq. 6-1)}$$

$$LO^{\bullet} + AH \longrightarrow LOH + A^{\bullet} \qquad \textit{(Eq. 6-2)}$$

$$L^{\bullet} + AH \longrightarrow LH + A^{\bullet} \qquad \textit{(Eq. 6-3)}$$

As expected oxidative stability of emulsions with high amounts of BHA-in-shell and core were better than emulsions with low amounts of BHA-in-shell and core.

Based on the polar paradox theory, it is expected that BHA as a non-polar antioxidant would be very effective in the emulsion systems studied particularly when incorporated in the shell droplets located at the oil-water interface of DSEs, because hydroperoxides formed during oxidation are surface active and accumulate at the interface (Nuchi, Hernandez, McClements, & Decker, 2002).

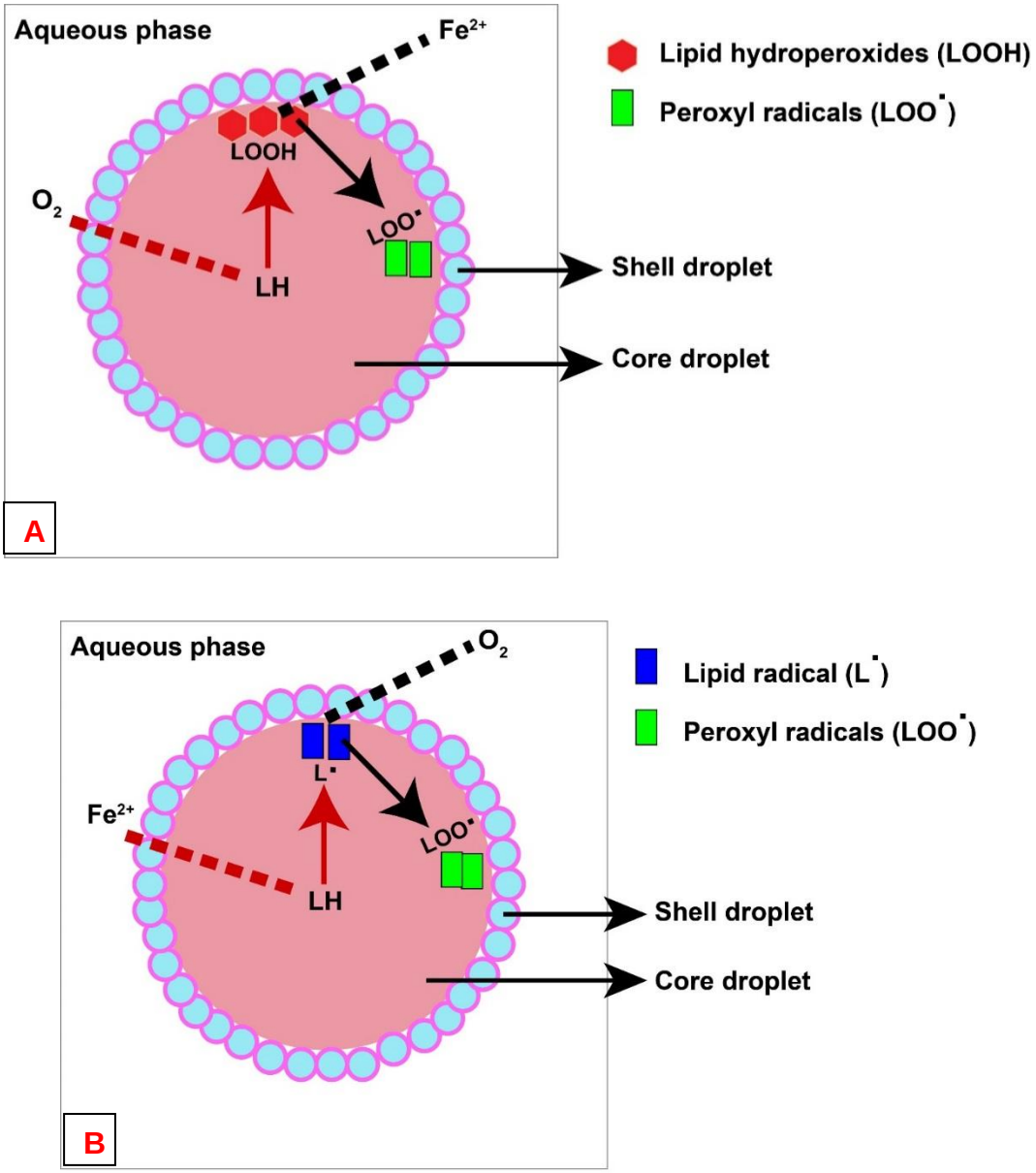

Figure 6.9 *Possible pathways of lipid oxidation in droplet-stabilised emulsions exposed to light in the presence of ferrous ions (500 µm)*

It is not clear why hexanal formation in emulsions with BHA-in-shell was slower than BHA-in-core at 500 ppm, but this was not the case at 50 ppm. Considering that the emulsions were treated under the same conditions, it is possible that observed differences in BHA performance at 50 and 500 ppm was mostly dependent on BHA's reaction with singlet oxygen, mobility and distribution.

BHA is most popular for inhibiting oxidation by scavenging radicals but, there are also reports of BHA's ability to quench singlet oxygen. Two singlet oxygen quenching mechanisms have been reported: physical and chemical mechanism. High chemical quenching rate of an antioxidant results in its rapid consumption along with singlet oxygen thus limiting the antioxidant's activity. BHA is reported to quench singlet oxygen mainly by physical mechanism (J. H. Lee & Jung, 2010) but the possibility of chemical quenching has also been reported (Chacón, Gaggini, Sinclair, & Smith, 2000; J. H. Lee & Jung, 2010). Yasaei, Yang, Warner, Daniels, and Ku (1996) reported that BHA reacted with singlet oxygen faster than methyl lineolate in the presence of photo-sensitizers yielding BHA hydroperoxides.

It is possible that at 50 ppm, BHA-in-shell droplets reacted with singlet oxygen (chemical quenching mechanism) and was rapidly consumed; hence its antioxidant activity did not last very long. BHA-in-shell droplets was located at the interface, so it could have reacted faster with singlet oxygen than BHA-in-core droplets which was in the interior of the core. Possible production of singlet oxygen, chemical quenching rate, and consumption rates of BHA were not determined in this study so it is difficult to conclude.

Laguerre, Bily, Roller, and Birtić (2017) suggests three possible transportation pathways for oxidants and antioxidants in emulsions: diffusion, collision-exchange-separate transfer and micelle-assisted transfer. Raudsepp, Brüggemann, and Andersen (2014) showed the possibility of free radical transfer from one droplet to another which was responsible for spreading oxidation between droplets and other studies have shown the transportation of antioxidants from oil phase to aqueous phase

or interface (Kiralan, Doğu-Baykut, Kittipongpittaya, McClements, & Decker, 2014; Panya et al., 2012).

Highly reactive antioxidants require mobility to the site of action (Laguerre et al., 2013) and the chemical reactivity of antioxidants is dependent on their concentration and rate constant of reaction in each phase of the emulsion. Pastoriza-Gallego et al. (2009) showed that temperature increase (15°C – 30°C) and surfactant volume fraction promoted spontaneous transfer of tocopherol from oil to interfacial region of emulsions which was entropy driven. This provided some insights into the possible driving force for spontaneous transfer of phenolic antioxidants from oil to interface.

If the mass-transfer or dynamic approach of oxidation in emulsions indicated by Raudsepp et al. (2014) is considered then it can be assumed that oxidation in emulsion droplets does not occur all at once but progresses gradually as reactants transfer and spread across the droplets. Based on this assumption, it is possible that oxidation did not occur simultaneously in DSEs or the oxidation rate between droplets differed due to droplet size heterogeneity and variation in layers of shell droplet interface formed [see Chapter 4 and (Ye et al., 2013)]. Therefore, the concept of mass transfer phenomena in lipid oxidation and anti-oxidation reported by Laguerre et al. (2017) may also provide an explanation for the observed differences in BHA performance.

1) **Diffusion via aqueous phase**: BHA transfer from one droplet to another by diffusion through the aqueous phase is unlikely given BHA's very poor solubility in aqueous media (Schillaci, Nepravishta, & Bellomaria, 2014).
2) **Micelle-assisted transfer:** DSEs were not stabilised by surfactants but through the adsorption of casein micelles from MPC (Dybowska, 2008; Ye,

2011). However, particle size distribution of DSEs processed with 10% shell droplets indicate the presence of some unadsorbed shell droplets (see Chapter 4, Figure 6.6 and Figure 6.8). These unadsorbed shell droplets are likely to play a role in the transfer of BHA. Therefore, in DSEs, the most probable mechanisms of BHA transfer may be via unadsorbed protein or shell droplets. BHA binding to milk proteins where the phenol groups reversibly interact with the carboxyl group of proteins has been reported (Cornell, De Vilbiss, & Pallansch, 1971).

Unadsorbed shell droplets in BHA-in-shell DSEs contained BHA. If oxidation rates are faster in smaller DSE droplets than larger DSE droplets, then BHA activity will also be faster in smaller DSE droplets requiring faster BHA replenishment. If unadsorbed shell droplets in these emulsions spontaneously connected or interacted with adsorbed shell droplets (see Chapter 5) of smaller DS droplets with faster oxidation rates as illustrated in Figure 6.10, then BHA transfer is likely to occur resulting in faster transport or replenishment of BHA at the interface and increased anti-oxidant activity. This mechanism of transfer is unlikely in emulsions with BHA-in-core because the unadsorbed shell droplets do not contain any BHA therefore, inhibition of oxidation by BHA will be solely reliant on BHA dispersed in the core lipid. At 50 ppm, because it is possible that BHA-in-shell reacted with singlet oxygen faster than BHA-in-core, the amount of BHA was not sufficient to replenish BHA and retard hydroperoxide decomposition. While at 500 ppm, BHA amount was sufficient for replenishment and retarded hydroperoxide decomposition better than BHA-in-core because it was located at the interface.

Another important factor to consider is the fact that shell droplets stabilise the core droplet with some level of aggregation (see Chapter 4) therefore it is also possible that BHA transfer between shell droplets themselves will be rapid. Looking at the particle size changes in these emulsions during oxidation, it is observed that unadsorbed shell droplets visible at day 0 disappear at day 5 and 7 (Figure 6.6 and Figure 6.8) indicating possible shell droplet interaction with DSE droplets over time and subsequent BHA transfer through Ostwald ripening.

3) **Collision-exchange separation transfer:** Considering the phenomena of Brownian movement in emulsions and DSEs tendency to cream due to their characteristic large droplet sizes (> 7µm), this mechanism of transfer can also be considered. It is possible that due to droplet interactions or collision, transfer of BHA from shell droplets of one 'DSE droplet' to shell droplets of another 'DSE droplet' during collision was faster than BHA transfer from the core droplet of one 'DSE droplet' to shell droplets of another 'DSE droplet', If the distance between one droplet and another is denoted by 'TD', then it implies that when the droplets collide, 'TD' in emulsions with BHA-in-shell will be less than 'TD' in emulsions with BHA-in-core droplets as illustrated in Figure 6.11. Therefore, it is possible that at 50 ppm, because BHA-in-shell was consumed faster than BHA-in-core, when DSE droplets collided or creamed, there was no BHA exchange between colliding droplets. Therefore, hexanal formation was faster at 50 ppm while at 500 ppm, BHA amounts were sufficient for exchange between colliding droplets.

Overall, oxidative stability of BHA-in-shell emulsions was better than BHA-in-core emulsions at 500 ppm and vice versa at 50 ppm. Oxidative stability of emulsions with BHA-in-shell and core was superior to controls for all surface lipid types at both 500 and 50 ppm.

In Trimyristin DSEs, it is assumed that solid lipid entraps all the BHA and BHA migration or transfer will be slower or non-existent but, considering that crystal morphology influences distribution of shell droplets (see Chapter 4 & 5), then it is possible that crystal morphology influenced BHA's location such that not all BHA was entrapped within the solid matrix. This may account for the similar oxidation rates between olive and trimyristin DSEs. Therefore, It can be hypothesised that at low amounts (50 ppm), BHA-in-shell gets consumed faster than BHA-in-core and there is not enough BHA to replenish BHA while at higher amounts (500 ppm), although BHA-in-shell and core are consumed, BHA replenishment is governed by factors or mechanisms that promote BHA transfer to the interface or reaction sites and these mechanisms favour faster BHA replenishment in BHA-in-shell DSEs over BHA-in-core DSEs.

For trimyristin emulsions processed below 56 °C, the breakdown of CD and LHP was similar for both BHA-in-shell and core emulsion at both amounts of 50 and 500 ppm; this could be because BHA migration from solid shell particles to the reaction site was usually slower and so coincided with BHA migration from core droplets to the reaction site. Therefore, the reaction rates in both emulsions were similar, or the presence of solid shell droplets interface in both emulsions slowed oxidation in both systems.

It can thus be hypothesised that the observed slower hydroperoxide decomposition in trimyristin DSEs (processed below 56°C) over olive and trimyristin (processed above 56°C) DSEs was a combined effect of BHA's anti-oxidation activity and interfacial structure of high melting shell droplets limiting reactions between oxygen, ferrous ions and formed lipid hydroperoxides.

In this study, particle size of BHA-in-shell and BHA-in-core DSEs were similar for all surface lipid types so differences in CD, LHP and hexanal were possibly not due to particle size differences of final DSE. Particle size of BHA-in-shell DSEs increased over BHA-in-core DSEs in some cases (Table 6.6 & Table 6.7). However, the effect of particle size changes on CD, LHP, and hexanal levels appeared to be subtle because the oxidation trends at 50 ppm and 500 ppm differed regardless of similar trends in particle size changes between BHA-in-shell and core DSEs. Moreover, the oxidation trends were also similar (Figure 6.5 & Figure 6.7) in cases where particle size changes were not different (Table 6.6 & Table 6.7).

Interfacial structure of droplet-stabilised emulsions provides better protection of safflower oil than conventional emulsion (see Chapter 5) and this protective effect is greatly enhanced with the use of high melting surface lipid at the interface. Results from this study agree with results presented in Chapter 5.

In conclusion, BHA-in-shell droplets of DSEs counteracts oxidation of core safflower oil through the same mechanism as BHA-in-core oil. Location-based performance of BHA in DSEs was concentration-dependent: at 500ppm it was more effective in the shell; at 50ppm it was more effective in the core. BHA's ability to increase the oxidative

stability of DSEs was greatly enhanced with high-melting shell droplets either when incorporated in shell droplets or core droplets.

This study provides crucial information on antioxidant behaviour in droplet-stabilised emulsions and sets the foundation for plausible functional food applications of droplet-stabilised emulsions.

A very important aspect of this study requiring investigation is the question of possible migration or diffusion of BHA incorporated in shell droplets of DSE to core droplets. The efforts made to investigate this aspect is shown and discussed in Chapter 7.

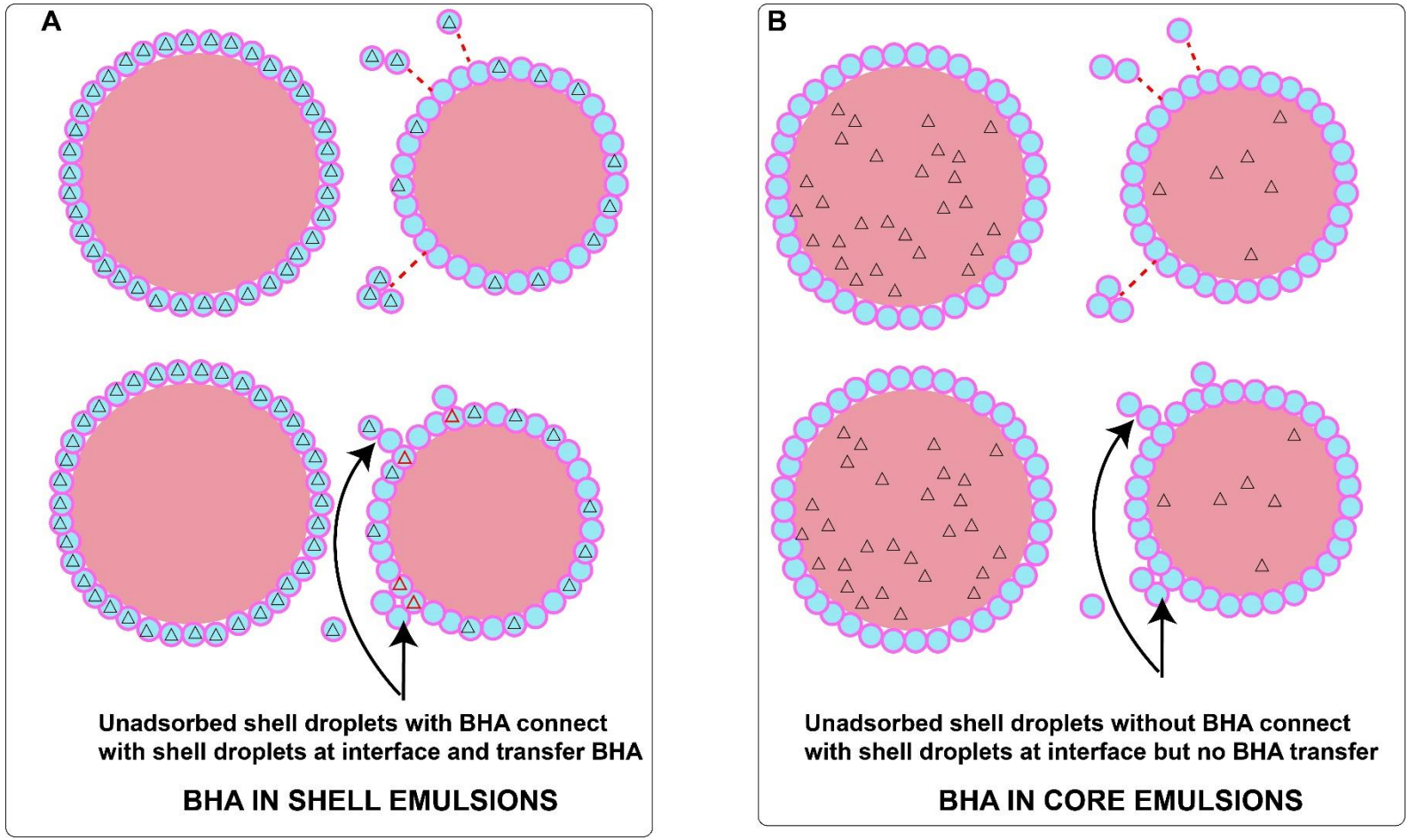

Figure 6.10 *Schematic illustration of possible BHA transfer pathway in droplet-stabilised emulsions- A= BHA-in-shell droplets; B = BHA-in-core droplets. Red arrows indicate shell droplet spontaneous adsorption and black arrows indicate BHA transfer after shell droplet adsorption.*

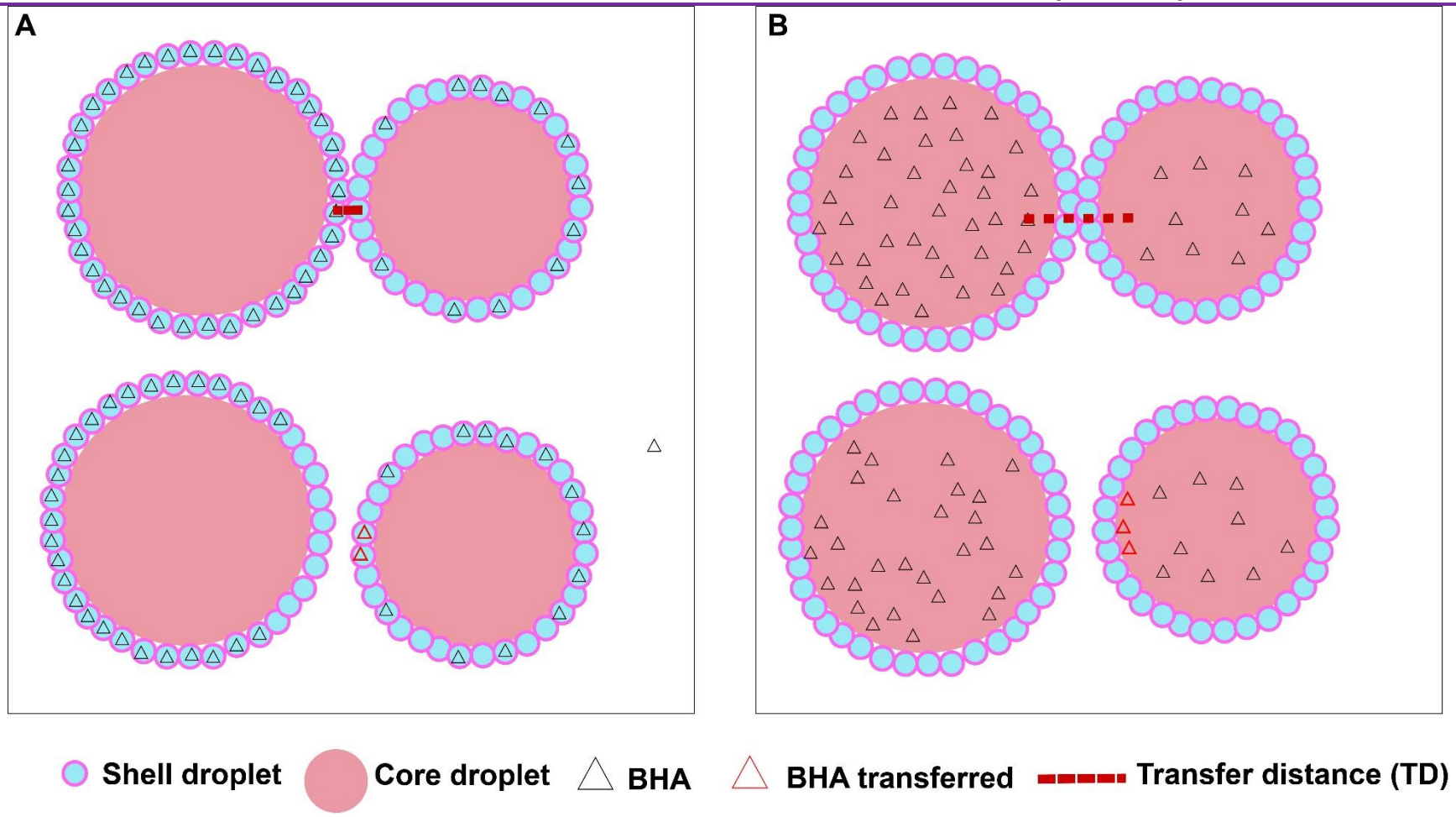

Figure 6.11 *Schematic illustration of possible BHA transfer pathway in droplet-stabilised emulsions- A= BHA-in-shell droplets; B = BHA-in-core droplets*

Chapter 7: Probing the location of antioxidants incorporated in droplet-stabilised oil-in-water emulsions

7.1 Abstract

This study sought to probe the location and mobility of antioxidants incorporated at the interface of droplet-stabilised emulsions (DSEs), using saturated transfer difference (STD)-nuclear magnetic resonance (NMR) and confocal Raman microscopy. Butylated hydroxyanisole was used for the STD study while beta-carotene was used for the Raman study.

The results obtained from STD experiments were not conclusive but indicated that STD could be successfully employed to study the diffusion of antioxidants in DSEs. Results from confocal Raman spectroscopy indicated that the migration of beta-carotene incorporated in shell droplets of olive oil and trimyristin DSEs to core droplets was minimal and beta-carotene remained mostly localised at the interface even after 3 days of production.

This study revealed that the migration of beta-carotene between shell and core was minimal and hence it may be possible to concurrently deliver two incompatible compounds by spatially segregating them between shell and core compartments. This work demonstrates new methods of studying antioxidant location and mobility in emulsions without separating the emulsion phases.

Keywords: Droplet-stabilized emulsion; surface lipid; shell emulsion; core lipid; oxidation; long-chain polyunsaturated fatty acids

Graphical Summary

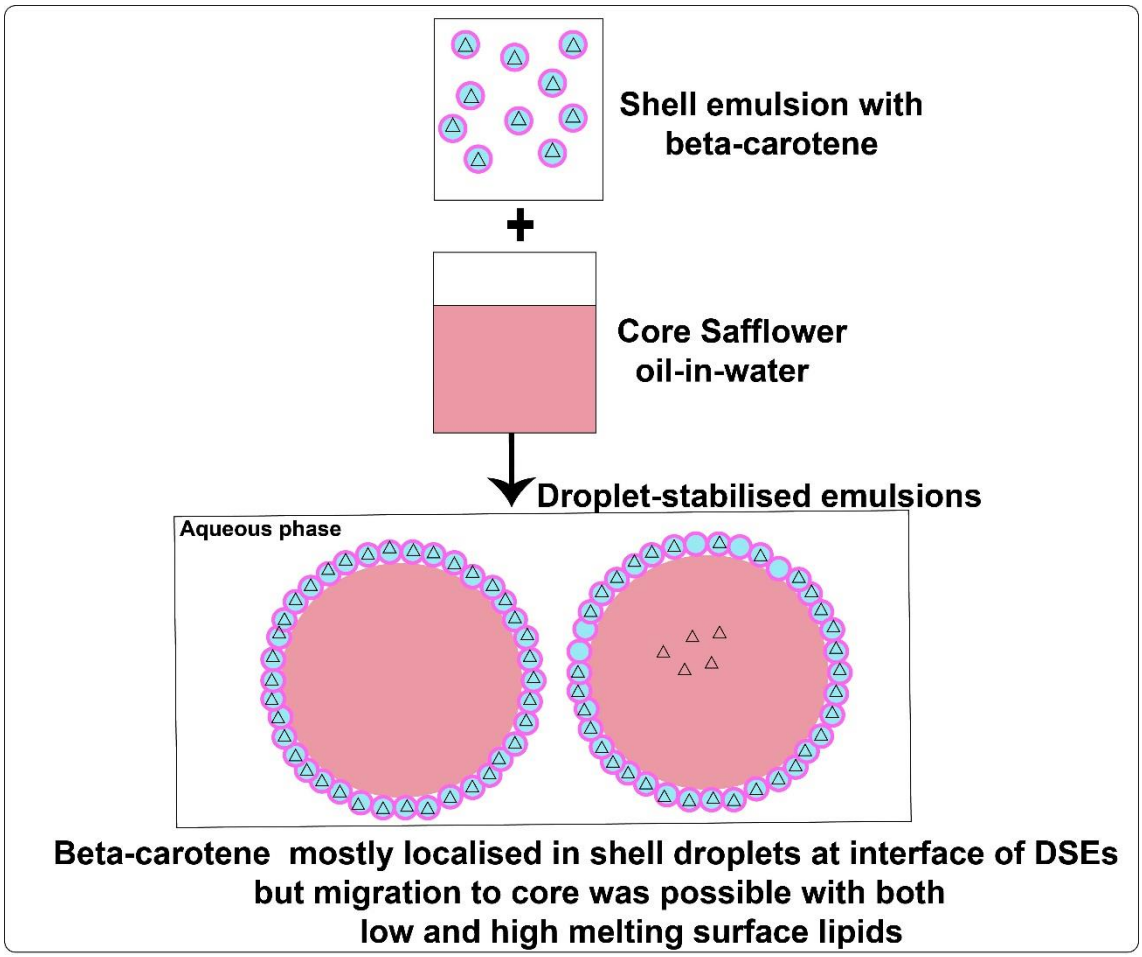

7.2 Introduction

The partitioning behaviour or pattern of an antioxidant incorporated within delivery systems such as emulsions, influences the antioxidant's functional performance. Most partitioning studies to determine the distribution or precise location of antioxidants incorporated in emulsions involve separation of the phases and quantification of the antioxidant within each phase (Charlotte Jacobsen, Schwarz, Stöckmann, Meyer, & Adler-Nissen, 1999; Pekkarinen, Stöckmann, Schwarz, Heinonen, & Hopia, 1999; Stöckmann & Schwarz, 1999). The ability of antioxidants incorporated in oil-in-water emulsions to limit oxidation depends on their ability to counteract factors that promote oxidation and so location and mobility of antioxidants in oil-in-water emulsions are key factors influencing their antioxidant activity.

The unique structure of droplet-stabilised emulsions (DSEs) presents the possibility of incorporating antioxidants in shell droplets located at the interface rather than in the interior of the core lipid. In Chapter 6, butylated hydroxyanisole (BHA) incorporated in olive and trimyristin shell droplets of DSEs limited oxidation of core safflower oil to a similar extent to when they were dispersed directly in core safflower oil of DSEs. DSEs also have the potential to be used as a delivery system to concurrently deliver two different bioactives by incorporating one in shell droplets and another in the core droplets.

This study addresses the question of possible migration of BHA or any other bioactive from shell droplets to core droplets of DSEs by testing whether antioxidants incorporated at the interface of droplet-stabilised emulsions (in shell

droplets) remain localised at the interface or migrate over time into core droplets. This cannot be achieved using the conventional approach of separating the oil and water phases, and requires a more advanced method to determine the partitioning in situ between two different oil phases. Here the use of two techniques: - saturated transfer difference (STD)-nuclear magnetic resonance and confocal Raman microscopy was investigated.

7.3 Materials and methods

Materials used in this study are detailed in Chapter 3. Two antioxidants were used in this study: butylated hydroxyanisole (BHA) and beta-carotene. Beta-carotene was chosen for the study because of its ability to exhibit very strong Raman scattering.

Antioxidant loaded shell and droplet-stabilised emulsions in this chapter were prepared according to the flow charts shown in Figure 7.1 and Figure 7.2. The lipid phases were prepared by stirring the antioxidant in the surface or core lipid for 15 min at 70°C. The total antioxidant concentration in the final DSE was the same whether the antioxidant was in the core lipid or incorporated in the surface lipid. The concentrations and final amounts of antioxidant in emulsions used in this study are shown in Table 7.1 and Table 7.2. A summary of the experimental set-up is also shown in Figure 3.1.

Table 7.3 and Table 7.4 summarizes and shows a description of the emulsions processed for the study. Table 7.3 shows the emulsions processed with BHA for the saturation transfer difference study and Table 7.4 shows emulsions processed with beta-carotene for the confocal Raman microscopy study.

7.3.1 Saturation Transfer Nuclear Magnetic Resonance

The ^{1}H saturation transfer experiment works by applying a weak radiofrequency pulse at the frequency of a particular signal in the NMR spectrum. This weak, frequency-selective pulse causes the proton spin populations to become “saturated” and the peak subsequently disappears. However, it is possible for some of spin population to be transferred to nearby ^{1}H nuclei, causing a reduction

in their signal intensity. Therefore, this method can be used to test for proximity of different molecules.

In this study, coconut and safflower oil were used as the surface and core lipid respectively. Coconut oil was chosen for this study to overcome the challenge of fatty acid profile overlaps between surface and core lipids which was encountered when olive or palmolein oil were used as surface lipids.

^{1}H NMR spectra of BHA dissolved in the surface lipid (coconut oil) and core lipid (safflower oil) were recorded using a Bruker Avance 700 MHz spectrometer to identify a unique peak present in one of the lipids but absent in the other. A peak at approximately 3 ppm was observed in the core lipid (safflower oil) which was almost completely absent in the surface lipid (coconut oil). This peak was used for subsequent saturation transfer experiments which, in principle, could reveal proximity of BHA to safflower oil. This peak was saturated in the droplet-stabilised emulsions made up of BHA dissolved either in the surface lipid (NC-BHA) or core lipid (NC-C-BHA). The saturation transfer was performed by alternating the frequency of the 2 s saturation pulse from 3 ppm (coinciding with the peak unique to the safflower oil) to a control where the frequency of the saturation peak was set to ~ 11 ppm (outside the spectral range). The latter spectrum served as a control. The difference spectrum was examined for a change in intensity of the BHA signals. A reduction in intensity of the BHA signals in the spectrum saturated at 3 ppm could indicate proximity of BHA to safflower oil.

The detection limit for this technique is dependent on BHA concentration and minimum useable signal to noise ratio.

7.3.2 Confocal Raman Spectroscopy

Two confocal Raman experiments were carried out. In the first experiment, DSEs were deposited on microscope slides and fixed with agarose as detailed in Chapter 3, section 3.3.4 and Raman data collected, while in the second experiment, a microfluidic channel chip as detailed in this section (7.3.2) was used for analysis. A schematic diagram of the microfluidic channel chip used is shown in Figure 7.3.

The location and mobility of antioxidant incorporated in droplet-stabilised emulsion was probed using a confocal WITec alpha300 RA Raman microscope. Raman data was collected on the same microscope with a 532 nm source between 3 mW and 15 mW at the sample. 50 µL of emulsion was loaded into a 15 µm deep microfluidic channel chip (Figure 7.3). The loaded microfluidic channel chip was mounted to a fixed point on the electronic XYZ three-axis stage, where the microfluidic channel position and focal depth were recorded for ease of alignment between samples. The emulsions were brought into focus and then 1D, 2D or 3D scans in this region were performed. For beam-sensitive 1D scans, lower power was used, and the laser was blocked immediately before and after scans to minimize laser-induced antioxidant degradation during alignment on the droplets. The location of antioxidant was probed after 3 days production of DSEs.

The detection limit for this technique is dependent on the scattering activity of each molecule in the sample, wavelength and experimental setup.

7.3.3 Raman Data Analysis

Raman data was exported from WITec project 2.10 software via CytoSpec (version 2.00.05) hyperspectral imaging software. The data was exported from CytoSpec into a compatible format and Raman spectra plots obtained using Python 3.0 software. To plot Raman spectra corresponding to selected emulsion droplets, image maps were plotted, and a line drawn or scanned across droplets using x, y coordinates from the mapped image. Raman spectra corresponding to the points along the drawn lines were obtained and Raman intensities of components of interest along the scanned area (line scan) plotted.

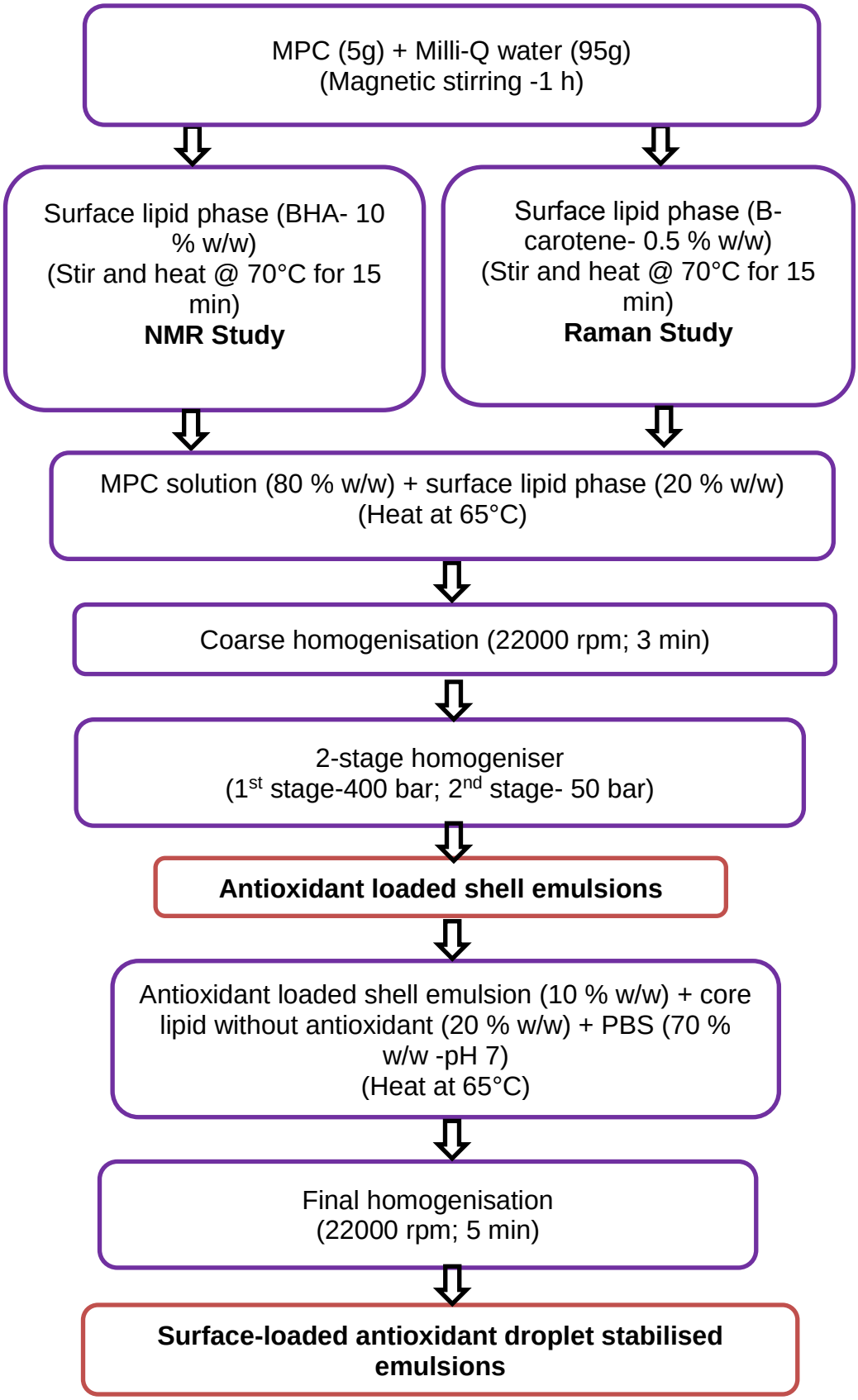

Figure 7.1 *Flow chart of surface-loaded antioxidant droplet-stabilised emulsion production*

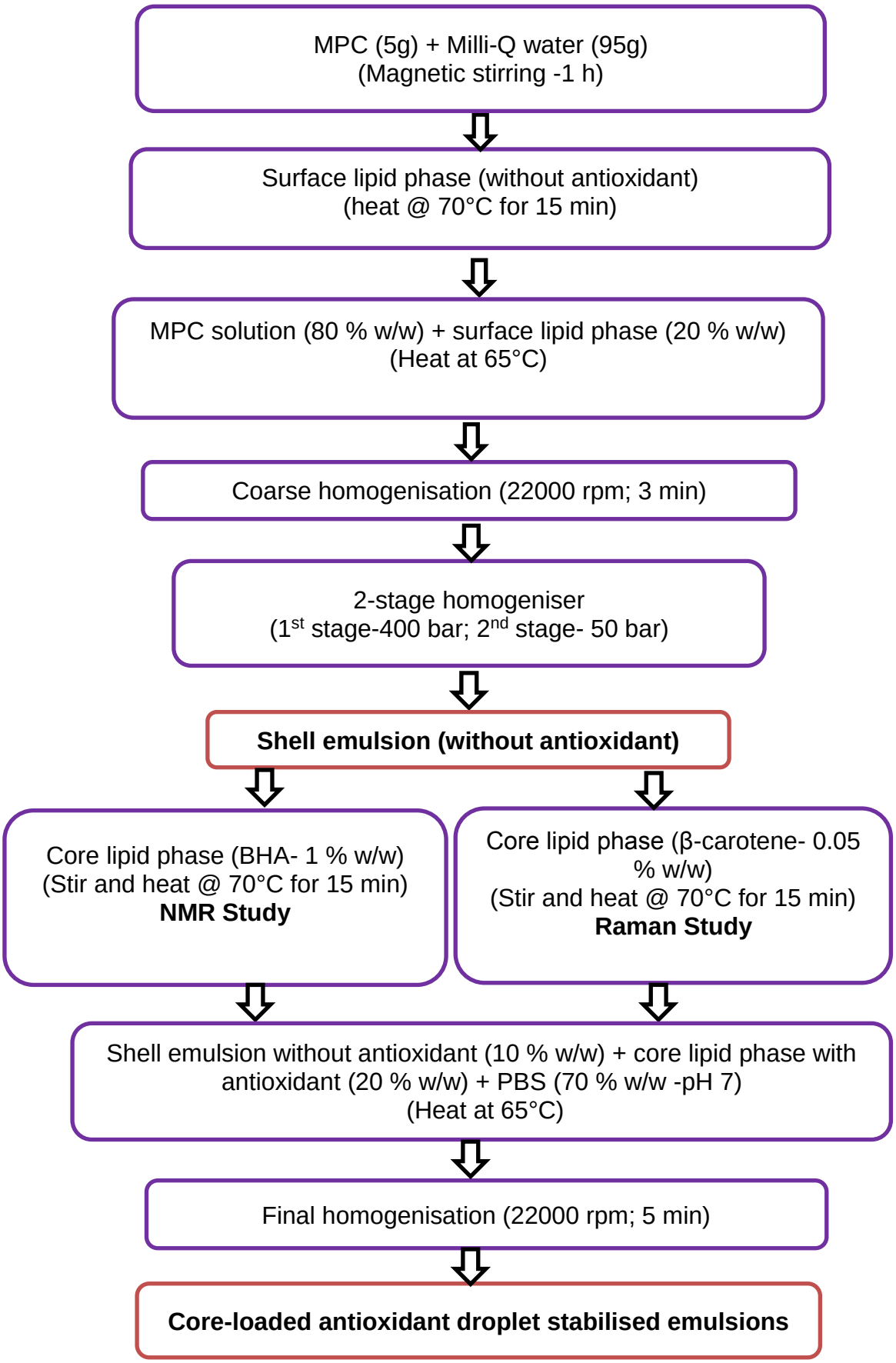

Figure 7.2 *Flow chart of core-loaded antioxidant droplet-stabilised emulsion production*

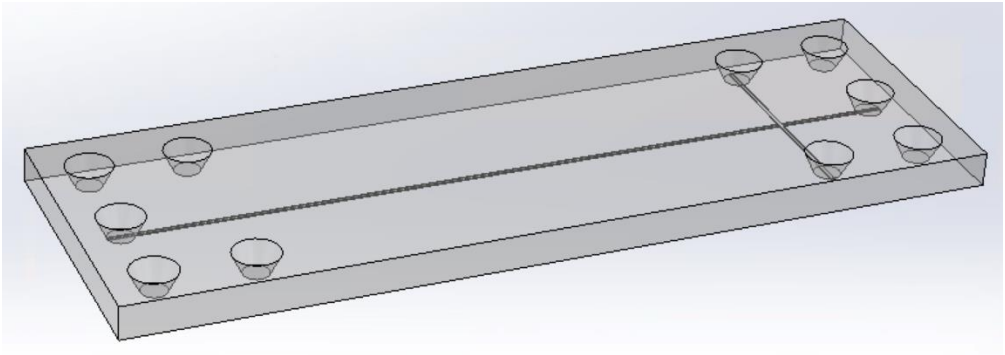

Figure 7.3: *Schematic diagram of microfluidic channel chip used to isolate DSE droplets for confocal Raman microscopy*

Table 7.1 *Formulation of antioxidant (BHA) loaded droplet-stabilised emulsions with BHA in shell and core droplets used for NMR saturated transfer difference study*

Emulsions	MPC solution (% w/w)	Surface lipid (% w/w)	Antioxidant in surface lipid (%w/w of surface lipid phase)	Antioxidant in surface lipid (%w/w of shell emulsion)	
Shell emulsion	80	20	10	2	
	Shell emulsion (% w/w)	**Core lipid (% w/w)**	**Phosphate Buffer solution (%w/w)**	**Antioxidant (% w/w of surface lipid phase)**	**Antioxidant (% w/w of final emulsion)**
Surface-loaded BHA DSE	10	20	70	10	0.2
	Shell emulsion (% w/w)	**Core lipid (% w/w)**	**Phosphate Buffer solution (%w/w)**	**Antioxidant (% w/w of core lipid phase)**	**Antioxidant (% w/w of final emulsion)**
Core-loaded BHA DSE	10	20	70	1	0.2

Table 7.2 *Formulation of antioxidant (Beta-carotene) loaded droplet-stabilised emulsions with beta-carotene-in-shell and core droplets used for confocal Raman microscopy study*

Emulsions	MPC solution (% w/w)	Surface lipid (% w/w)	Antioxidant in surface lipid (%w/w of surface lipid phase)	Antioxidant in surface lipid (%w/w of shell emulsion)	
Shell emulsion	80	20	0.5	0.1	
	Shell emulsion (% w/w)	**Core lipid (% w/w)**	**Phosphate Buffer solution (%w/w)**	**Antioxidant (% w/w of surface lipid phase)**	**Antioxidant (% w/w of final emulsion)**
Surface-loaded beta-carotene DSE	10	20	70	0.5	0.01
	Shell emulsion (% w/w)	**Core lipid (% w/w)**	**Phosphate Buffer solution (%w/w)**	**Antioxidant (% w/w of core lipid phase)**	**Antioxidant (% w/w of final emulsion)**
Core-loaded beta-carotene DSE	10	20	70	0.05	0.01

Table 7.3: *BHA loaded droplet-stabilised emulsions (DSE)*

Samples	Description	Surface lipid	Core Lipid	BHA Location	BHA amounts in final emulsion (%w/w)
NC-BHA	Droplet-stabilized emulsion with BHA in shell	Coconut oil	Safflower oil	Interface	0.2
NC-C-BHA	Droplet-stabilized emulsion with BHA in core- **BHA amount matched with NC-BHA**	Coconut oil	Safflower oil	Core	0.2

Table 7.4: *Beta-carotene loaded droplet-stabilised emulsions (DSE)*

Samples	Description	Surface lipid	Core Lipid	Beta-carotene location	Beta-carotene amounts in final emulsion
NO	Droplet-stabilized emulsion (DSE) no beta-carotene	Olive oil	Safflower oil	None	
NO-β	DSE with beta-carotene-in-shell- beta-carotene	Olive oil	Safflower oil	Interface	0.01
NO-C-β	DSE with BHA in core **beta-carotene amount matched with NO- β**	Olive oil	Safflower oil	Core	0.01
NT	DSE no beta-carotene and processed at temperature above 56°C	Trimyristin	Safflower oil	None	
NT-β	DSE with beta-carotene-in-shell and processed at temperature above 56°C-	Trimyristin	Safflower oil	Interface	0.01
NT- C-β	DSE with beta-carotene-in-core and processed at temperature above 56°C- **beta-carotene amount matched with NT- β**	Trimyristin	Safflower oil	Core	0.01

7.4 Results

7.4.1 Particle size of antioxidant loaded droplet-stabilised emulsions

Figure 7.4 shows the particle size data of droplet-stabilised emulsions with BHA incorporated in coconut oil shell and safflower oil core droplets used for the saturated transfer difference study. The average particle sizes of droplet-stabilised emulsions with BHA in shell and BHA in core droplets were similar.

Figure 7.5 shows the particle size data of DSEs with beta-carotene incorporated in shell or core droplets and composition-matched control emulsions (discussed in Chapter 5) with beta-carotene-in-shell droplets gently stirred-in to a conventional protein-stabilised safflower oil emulsion. The average ($d_{3,2}$) and volume ($d_{4,3}$) weighted mean diameters of DSE with beta-carotene-in-shell and in core were similar.

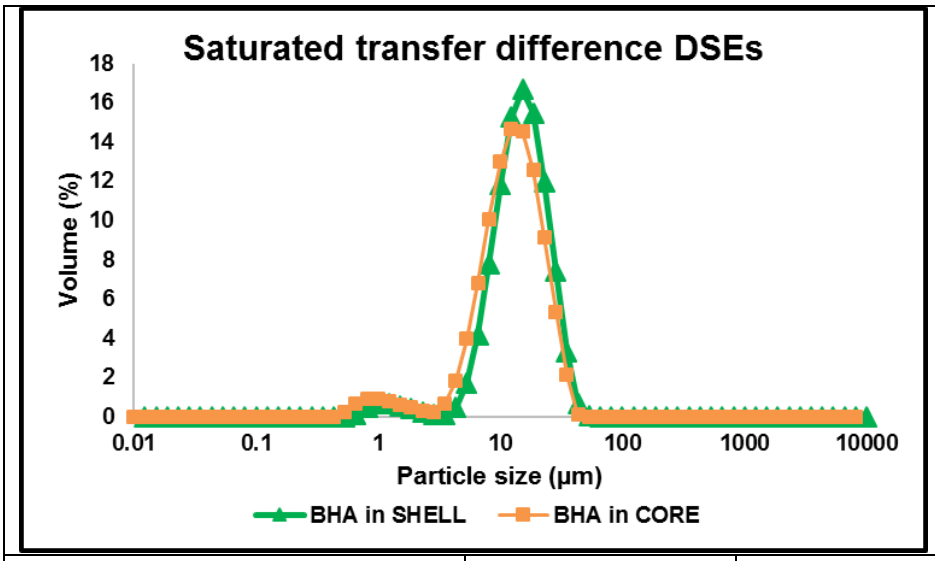

Coconut oil DSEs	$d_{3,2}$	$d_{4,3}$
BHA-in-shell	9.14	14.30
BHA-in-core	8.33	15.26

Figure 7.4: *Particle size distribution of coconut oil DSEs with BHA in shell and core used for saturated transfer difference experiment*

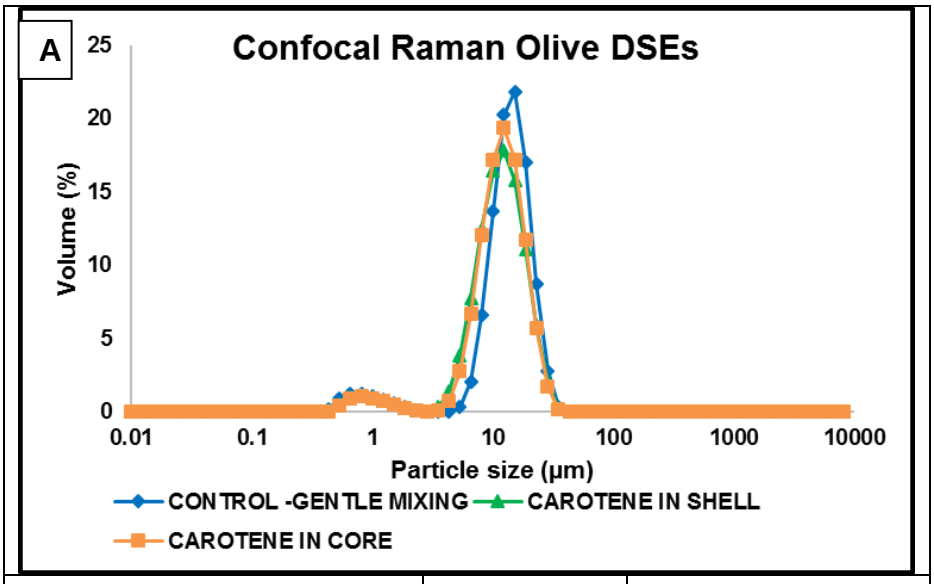

Olive DSEs	$d_{3,2}$ (µm)	$d_{4,3}$ (µm)
Control-gentle mixing	7.50	15.59
beta-carotene-in-shell	7.52	13.48
beta-carotene-in-core	8.00	13.76

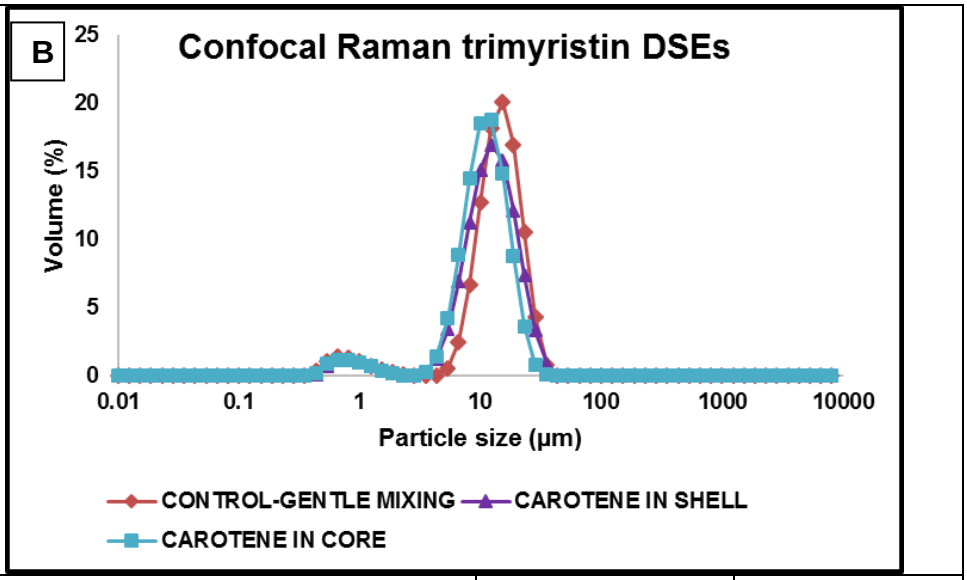

Trimyristin DSEs	$d_{3,2}$ (µm)	$d_{4,3}$ (µm)
Control-gentle mixing	7.11	13.17
beta-carotene-in-shell	7.33	14.31
beta-carotene-in-core	6.77	12.47

Figure 7.5: *Particle size distribution of olive (A) and trimyristin (B) DSEs with beta-carotene incorporated in shell and core*

7.4.2 Saturated transfer difference (STD)

Figure 7.6 shows the full spectral width of BHA dissolved in coconut oil (a), safflower oil (b) and DS emulsions with BHA in shell (c) and core (d). The STD spectra are at the top in red and blue. The unique peak saturated in the safflower oil is at 2.7 ppm. This is irradiated in the red spectra. There were small decreases in intensity of the nearby oil peaks, probably due to saturation transfer. The bottom two spectra (a & b) are the coconut oil and safflower oil respectively. The coconut oil has BHA dissolved in it. The aromatic BHA peaks are labelled (BHA) and the $–OCH_3$ and t-Bu groups are marked with asterisks.

Figure 7.7 shows an expansion of the aromatic BHA peaks in the STD spectra. The top spectra (c) is DSE with BHA in core, middle spectra (b) is DSE with BHA in shell and bottom spectra (a) is coconut oil with BHA. The reference STD spectra (blue) were recorded first in each case followed by the STD spectrum (with the peak at 2.7 ppm irradiated). There were some tiny changes in both STD spectra. However, due to the large DSE particle size, the droplets tended to cream and induce some phase separation during analysis, therefore it is possible that the observed changes were simply due to changes in the sample composition over time rather than changes specific to the migration of BHA from shell to core or vice versa.

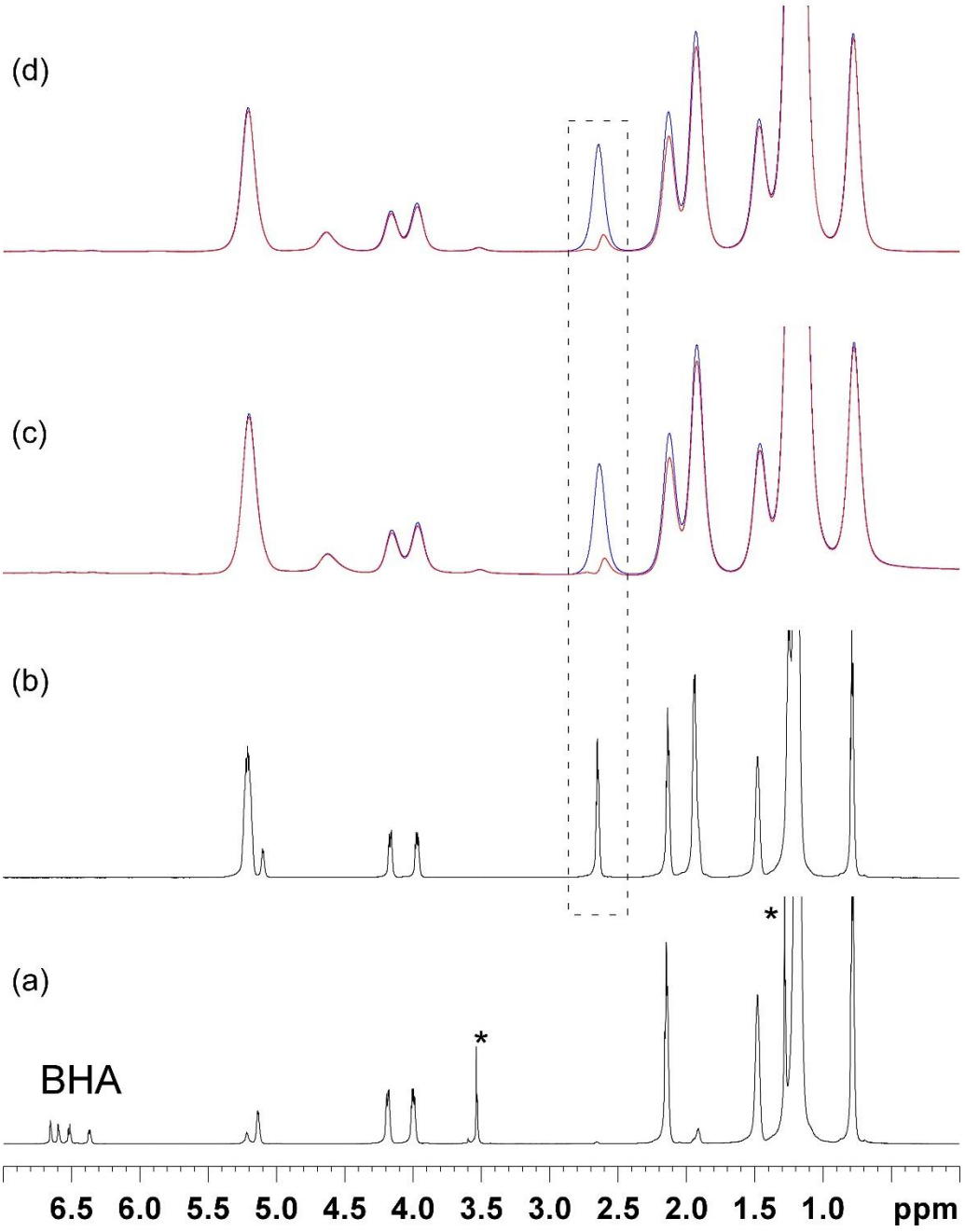

Figure 7.6: *STD full spectral width of coconut oil with BHA; safflower oil; and droplet-stabilised emulsions with BHA incorporated in shell; & in core.*

a)- Coconut oil with BHA; b) Safflower oil; c) Droplet-stabilised emulsions with BHA-in-shell; d) Droplet-stabilised emulsion with BHA-in-core; * BHA- OCH_3 and tert-butyl groups. Blue spectra = reference STD spectra recorded first; red spectra = STD spectra with irradiated safflower oil peak

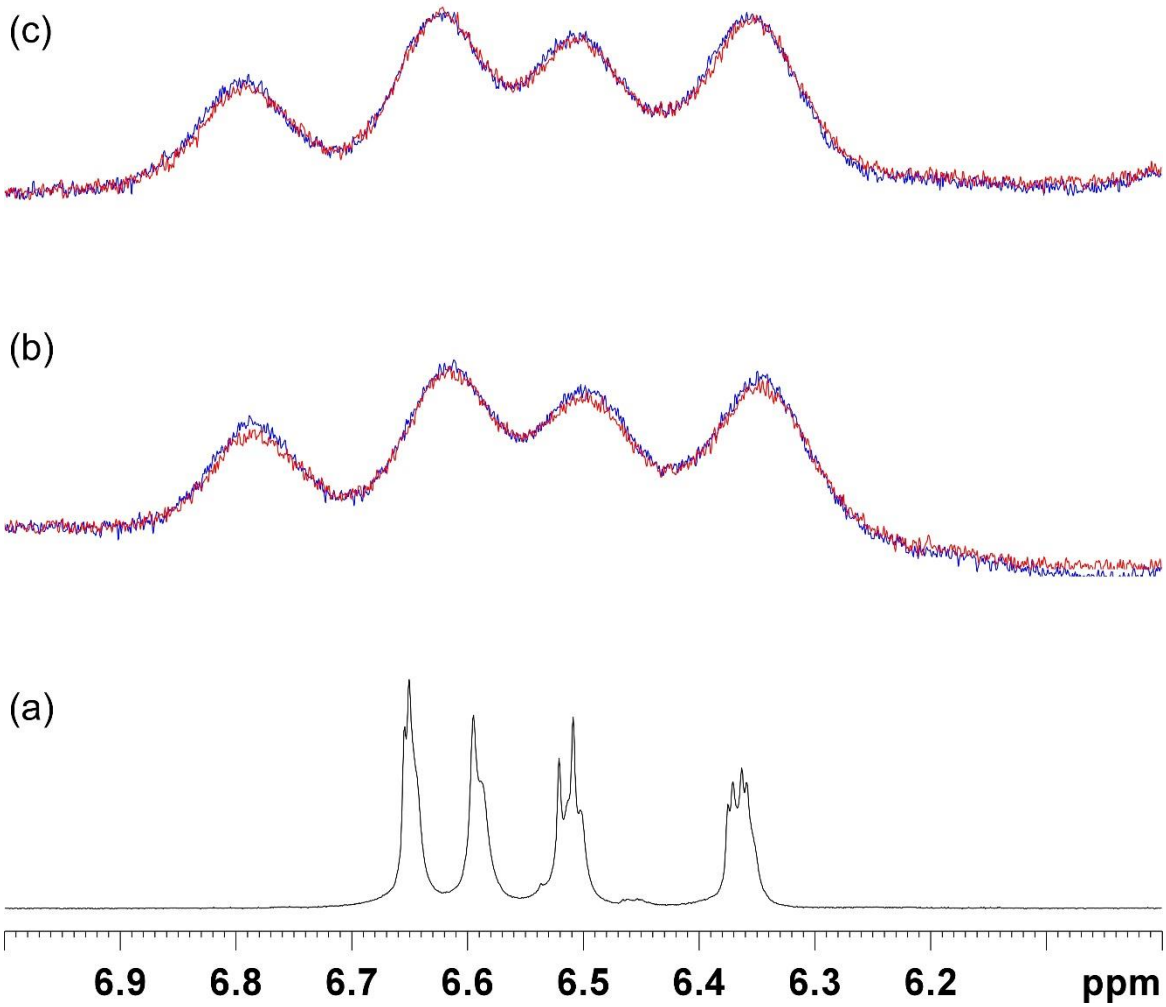

Figure 7.7: *STD expanded aromatic BHA peaks in coconut oil; DSE with BHA in shell and DSE with BHA in core. Blue spectra = reference STD spectra recorded first; red spectra = STD spectra with irradiated safflower oil peak*

(a) Coconut oil with BHA; (b) Droplet-stabilised emulsion with BHA-in-shell; (c) Droplet-stabilised emulsion with BHA-in-core. Blue spectra = reference STD spectra recorded first; red spectra = STD spectra with irradiated safflower oil peak

7.4.3 Confocal Raman Microscopy (microscope slides)

Figure 7.8 shows Raman spectra of beta-carotene loaded DSEs. The red trace shows the intensity profile of the carotene band from the Raman spectrum (shaded red) along the line (also shown in red) in the optical image. A unique olive oil band was identified at ~ 1650 cm^{-1}. The band at ~ 2900 cm^{-1} is due to overlapping contributions from various C-H vibrational modes of the emulsion components. The green and blue traces show the intensity profile of olive oil and CH bands respectively. The intensity profile correlates to the red line scan in the optical images shown in Figure 7.9, Figure 7.10, and Figure 7.11.

Figure 7.9 shows bright field reflectance optical images and Raman spectra corresponding to the line scanned region of DSE without beta-carotene droplets in the optical image. Figure 7.10 and Figure 7.11 also shows the optical images and Raman spectra corresponding to the line scanned regions of DSEs with beta-carotene incorporated in shell droplets and beta-carotene incorporated in core droplets respectively.

As expected, there were no spikes in Raman intensity of beta-carotene as DSE droplets without beta-carotene were scanned because there was no beta-carotene incorporated but changes in intensities of the CH band was observed (Figure 7.9b & d).

As DSE droplets with beta-carotene-in-shell droplets were scanned (Figure 7.10a), increases or spikes in Raman intensity of beta-carotene at the interfaces of DSE droplets were recorded and gradual decreases recorded as the scan continued across the core droplets (Figure 7.10 b & d). The reverse case was

observed with DSE droplets with beta-carotene-in-core droplets whereby spikes in Raman intensity of beta-carotene (Figure 7.11 b & d) were recorded while scanning through the core droplets (Figure 7.11a).

However, fixing the emulsions in agarose made it very difficult to isolate single droplets. The problem was compounded by the thickness of the sample as well, therefore it is likely that Raman scattering was being collected from more than one droplet at once. To overcome this challenge, the possibility of isolating a single droplet was explored with the use of a microfluidic channel as detailed in section 7.3.2.

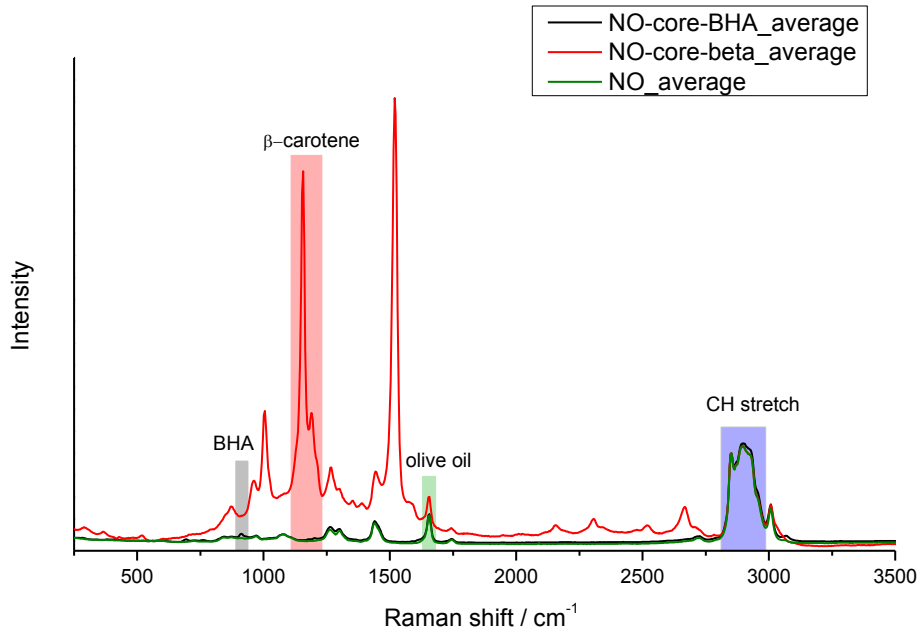

Figure 7.8: *Raman spectra of DSEs with and without antioxidants (BHA & beta-carotene)*

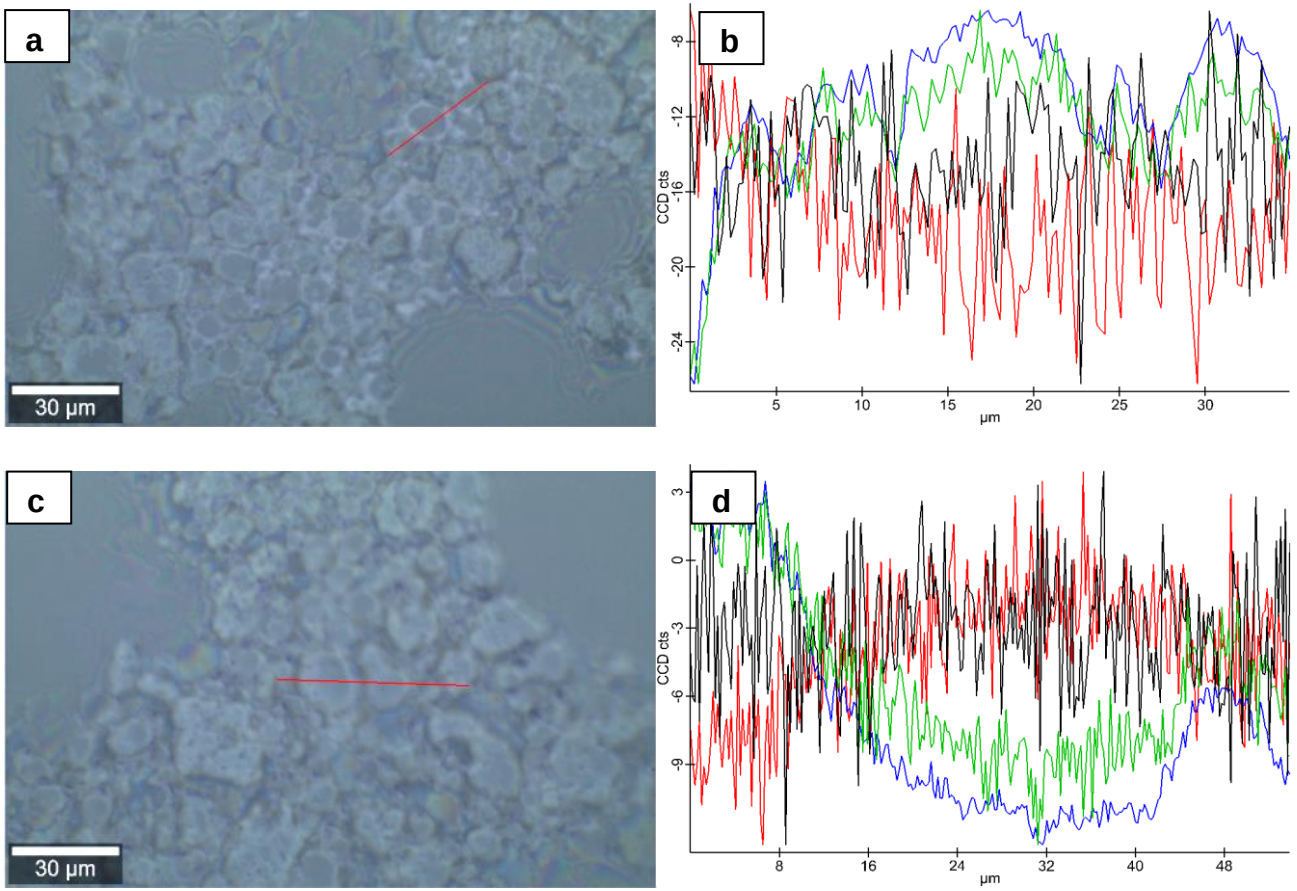

Figure 7.9 *Olive oil DSE (without Beta-carotene) with 150 points (top) & 265 points (bottom) (a & c) bright field reflectance mode images, (b & d) peak integral distribution (red trace= beta-carotene; blue trace= CH band; green trace= olive oil).*

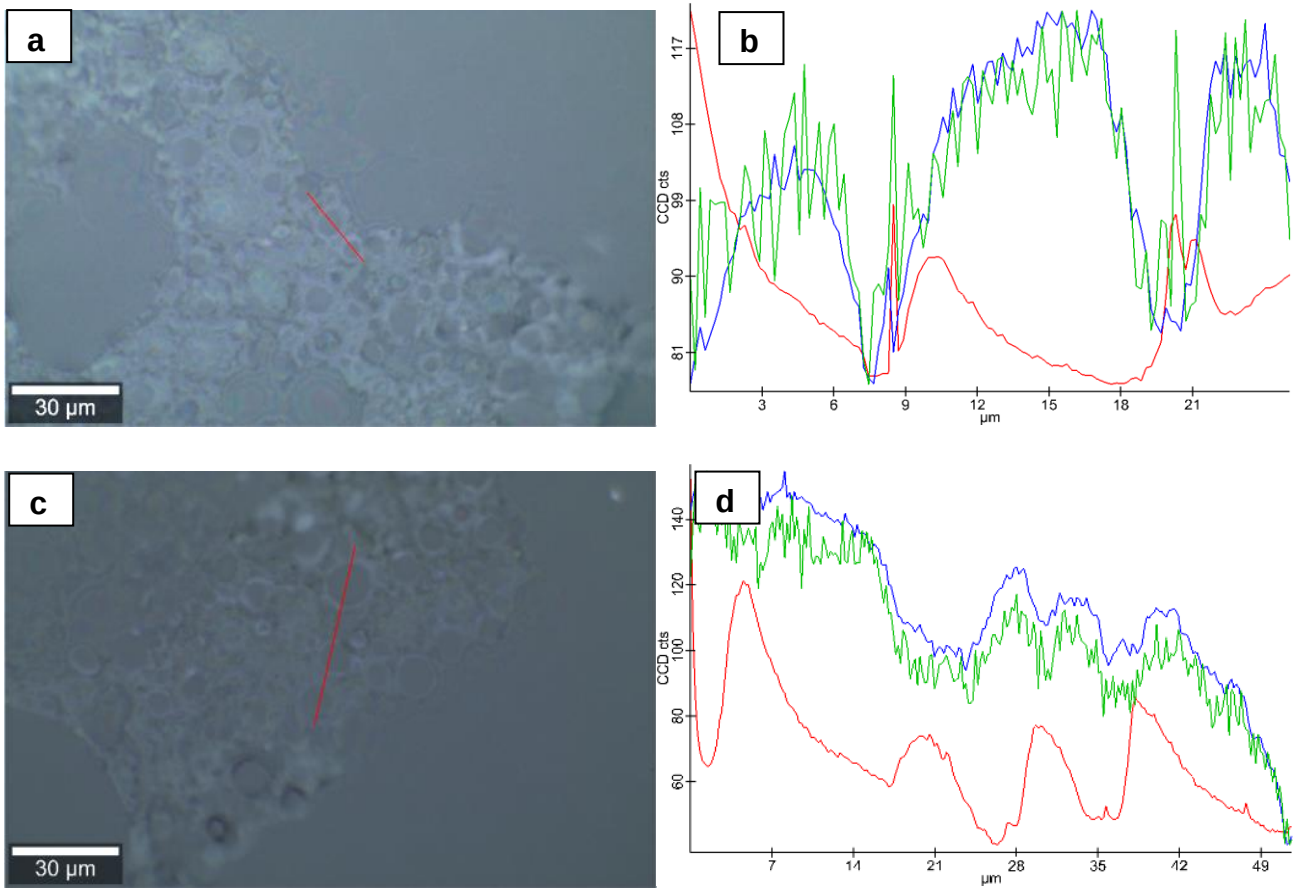

Figure 7.10 *Olive DSE (beta-in-shell) with 122 points (top); & 250 points (bottom). (a & c) bright field reflectance mode image, (b & d) peak integral distribution (red trace= beta-carotene; blue trace= CH band; green trace= olive oil).*

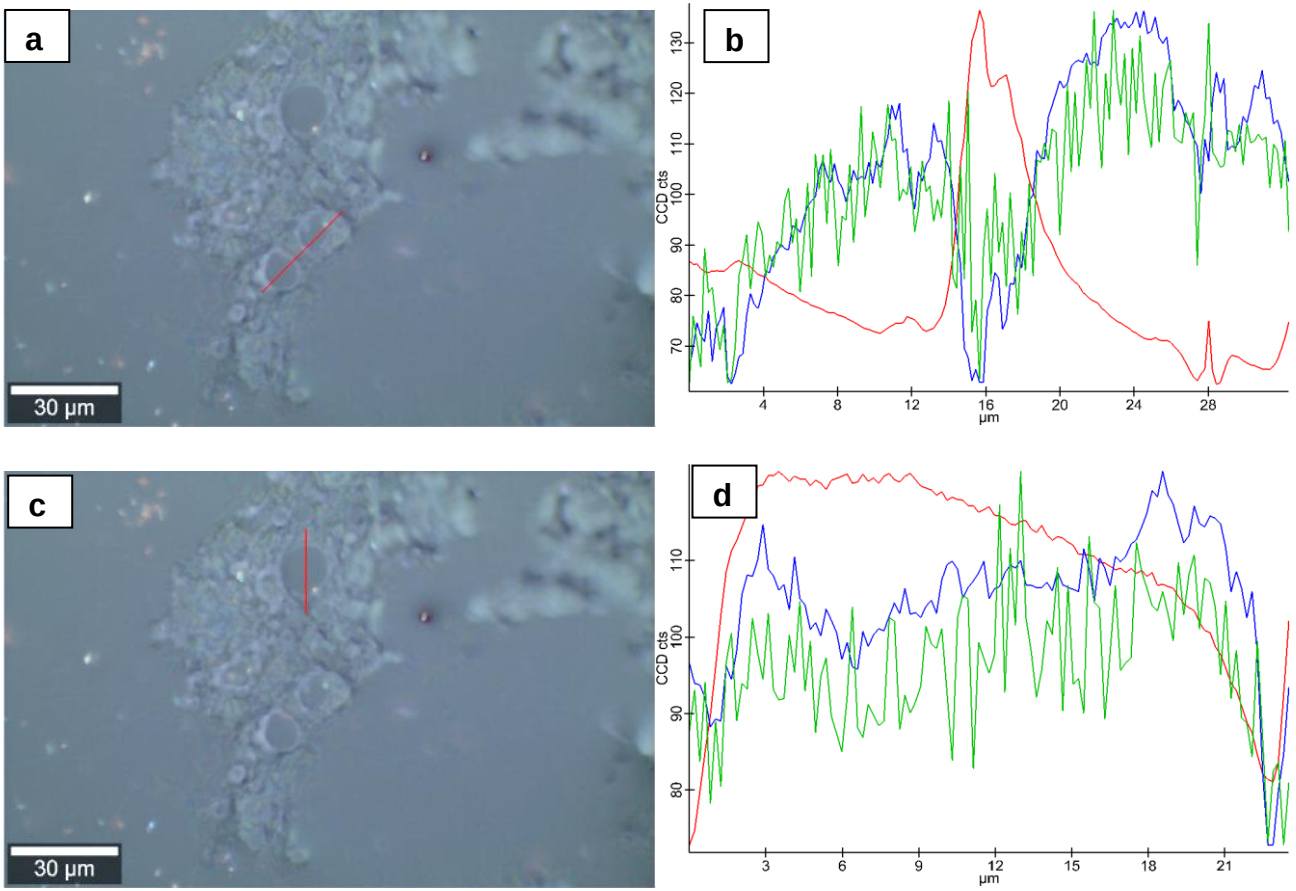

Figure 7.11 *Olive DSE (beta-in-core) with 158 points (top) & 115 points (bottom). (a & c) bright field reflectance mode image, (b & d) peak integral distribution (red trace= beta-carotene; blue trace= CH band; green trace= olive oil).*

7.4.4 Confocal Raman Microscopy (Microfluidic channel)

Figure 7.12 shows Raman spectra of olive oil, safflower oil, trimyristin and beta-carotene. Beta-carotene has two intense Raman bands at 1156 cm^{-1} and 1514 cm^{-1}. Olive oil, safflower oil and trimyristin have intense bands from their C-H groups at about 2886-2899 cm^{-1}. Olive oil and safflower oil have slightly intense bands at 1654 cm^{-1}. Figure 7.13, Figure 7.14 and Figure 7.15 show confocal Raman images and Raman spectral plots of olive oil control emulsions, DSEs with beta-carotene-in-shell and DSEs with beta-carotene-in-core respectively while Figure 7.16, Figure 7.17, and Figure 7.18 shows that of trimyristin (processed above 56°C) control emulsions, DSEs with beta-carotene-in-shell and DSEs with beta-carotene-in-core droplets. For each sample, three confocal Raman 'channels' (channels refers to a specific frequency or band of frequencies) are shown: beta-carotene, safflower oil and CH band channels. These channels show Raman signals corresponding to beta-carotene, safflower oil and the CH vibrations.

Control emulsions consisted of beta-carotene loaded shell droplets gently stirred into protein-stabilised safflower oil droplets, shell droplets were dispersed in the surrounding phase with some spontaneous adsorption as explained in Chapter 5. Scanning from shell droplets surrounding the interface of core droplet and across the droplet (Figure 7.13D & Figure 7.16D) showed changes in the Raman intensity of beta-carotene (Figure 7.13E & Figure 7.16E).

Raman intensity profile of olive control emulsions (Figure 7.13E) showed high intensities of beta-carotene at line scan positions (~ 0-5, 20-30 & 40-50) corresponding to interfacial regions with olive oil shell droplets containing beta-

carotene while very low beta-carotene intensities were obtained at line scan positions (10-20, 30-40) corresponding to core safflower oil droplets. The same trend was observed with trimyristin control emulsions (Figure 7.16E) which showed high intensities of beta-carotene at line scan positions (~ 0-3, 17-21 & 36-40) corresponding to interfacial regions with trimyristin shell droplets containing beta-carotene while very low beta-carotene intensities were obtained at line scan positions (~ 3-16 & 23-35) corresponding to core safflower oil droplets.

Raman intensity profile across olive DSEs droplets with beta-carotene-in-shell droplets (Figure 7.14E) showed high beta-carotene intensities and low CH band intensities at line scan positions (~ 0.-3 & 23-25) corresponding to the interfaces of safflower oil droplets while, low beta-carotene intensities and high CH band intensities were observed at line scan positions (4-23) corresponding to core safflower oil droplets. The reverse trend was observed with intensity profiles of olive DSEs droplets with beta-carotene-in-core safflower oil droplets (Figure 7.15E) whereby, high beta-carotene and high CH band intensities were obtained at line scan positions (~ 2-14) corresponding to core safflower oil droplets. Low beta-carotene and low CH band intensities were also observed at line scan positions (~ 0-1) correspondng to the interfaces of core safflower oil droplets composed of shell droplets without beta-carotene.

Raman intensity profile of trimyristin DSEs with beta-carotene-in-shell droplets (Figure 7.17E) showed high beta-carotene and low CH band intensities at line scan positions (~ 0-5 & 48-50) corresponding to the interfaces of safflower oil droplets while, low beta-carotene and high CH band intensities were observed at line scan positions (~ 12-45) corresponding to core safflower oil droplets. A

reverse trend was observed with Raman intensity profile of trimyristin DSEs droplets with beta-carotene-in-core safflower oil droplets (Figure 7.18E) whereby, high beta-carotene and high CH band intensities were obtained at line scan positions (~ 3-11 & 15-20) corresponding to core safflower oil droplets, and low beta-carotene intensities were observed at line scan positions (~ 10-12) correspondng to the interfaces of core safflower oil droplets composed of shell droplets without beta-carotene

Figure 7.19 shows confocal Raman images and intensity profile plots of olive DSEs with beta-carotene incorporated in shell droplets. Raman intensity profile shows high beta-carotene intensities at line scan positions (~ 7-10) corresponding to core safflower oil droplets. Raman intensity profile of trimyristin DSEs with beta-carotene-in-shell are shown in Figure 7.20 and high beta-carotene intensities at line scan positions (~ 1-12) corresponding to core safflower oil droplets was also observed. These results indicate some beta-carotene migration to core safflower oil droplets.

Figure 7.21 shows confocal Raman images of DSEs with beta-carotene-in-core safflower oil droplets analysed at high power exposure (15 mW). The beta-carotene channels indicate some photo-bleaching occured while scanning at high power. Photo-bleaching of beta-carotene provides an expalanation for why some beta-carotene-in-core droplets did not appear to have beta-carotene (Figure 7.15A & D).

Beta-carotene was chosen for this study because it exhibits very strong intrinsic Raman scattering, characterised by the Raman scattering cross-section. Raman intensities of beta-carotene and other analysed components (safflower oil, CH

band) differ, therefore, it may appear from the intensities of the safflower oil and CH bands that there are very low levels of these components in the emulsion regions scanned but this is not the case, it is rather a case of these components having much lower Raman cross-section compared to beta-carotene. Theoretically, it is possible to obtain the concentrations of components, if the Raman cross-sections are known but technically it is very challenging because there are several experimental factors that also determine the Raman intensity.

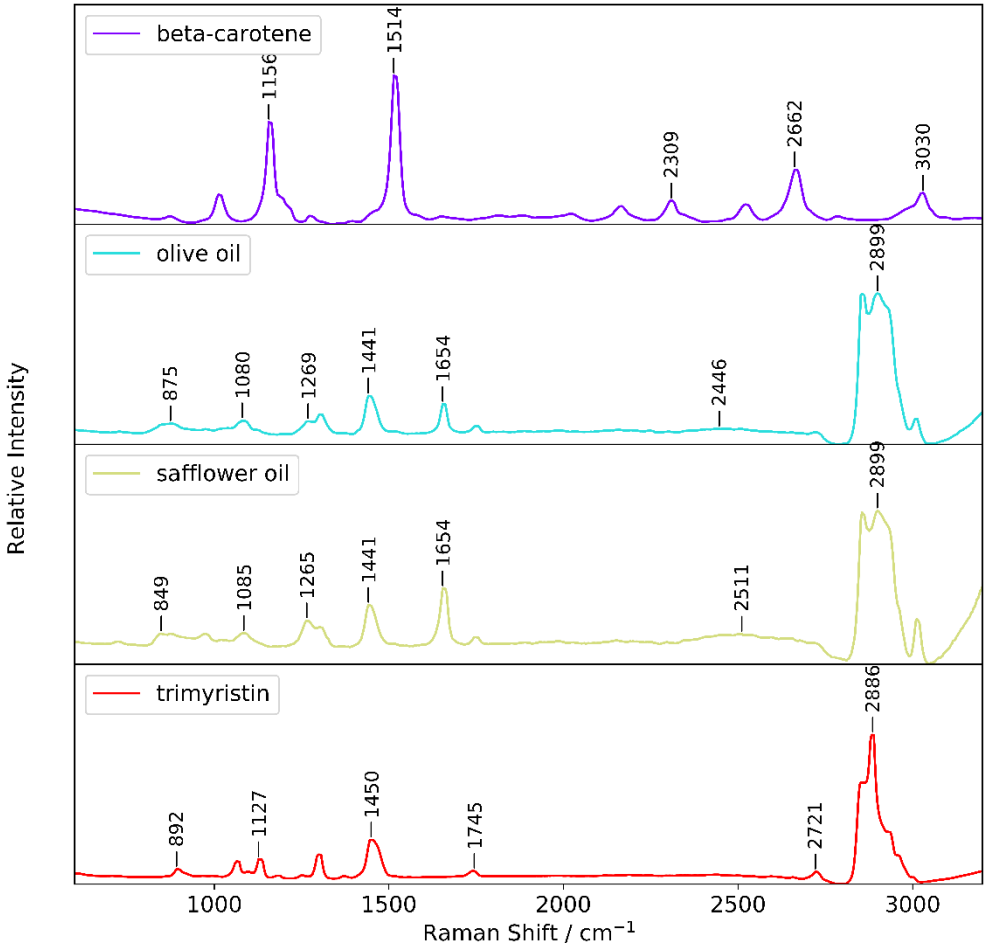

Figure 7.12 *Raman spectra of beta-carotene, olive oil, safflower oil, and trimyristin*

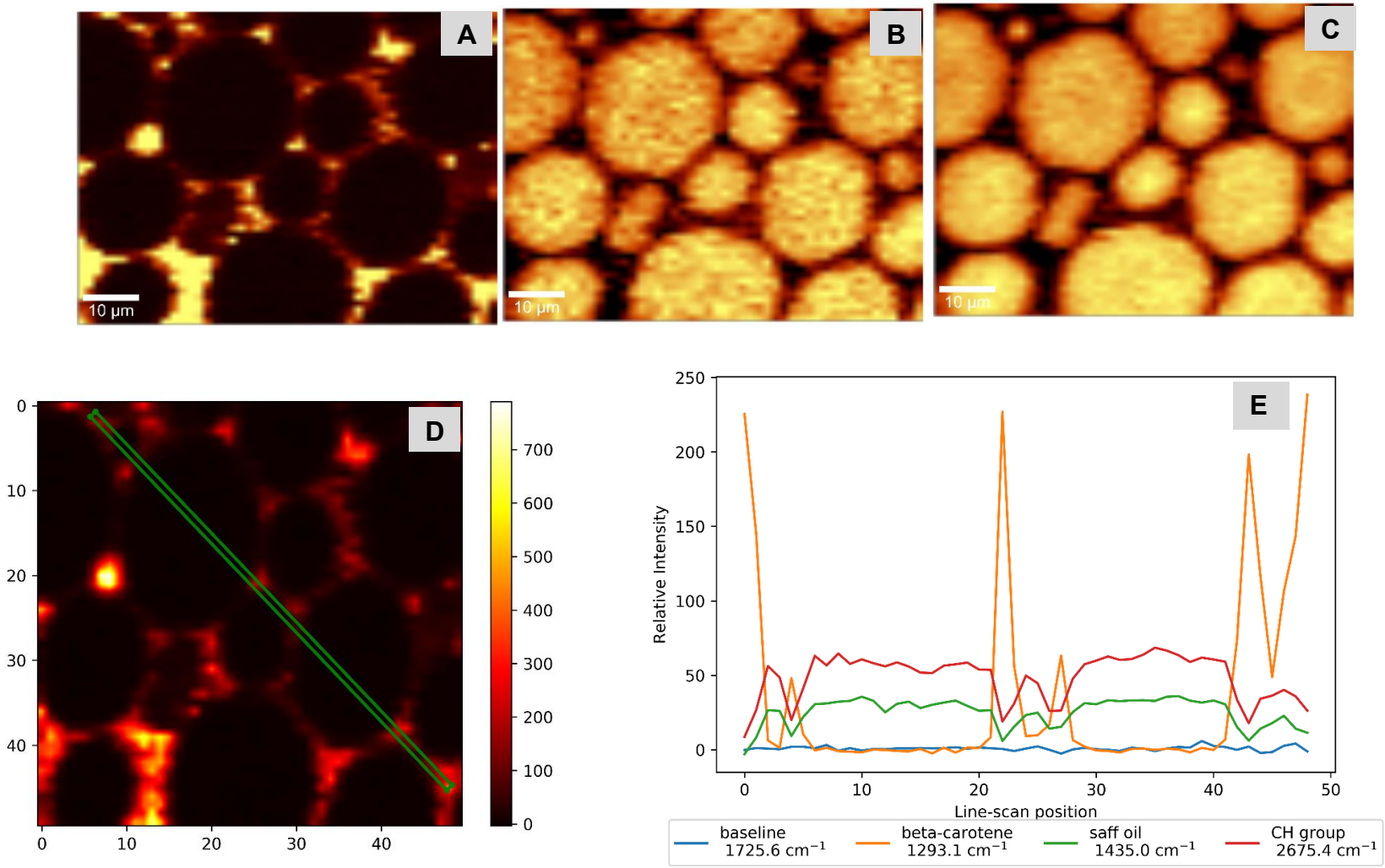

Figure 7.13 *Confocal Raman microscopy images and intensity profile of Olive oil control emulsions (shell gently stirred-in) - A, B, & C= beta-carotene, safflower oil and CH band Raman channels respectively; D= Line scan location across droplets; E= Intensity profiles for selected Raman channels across line scan shown in D*

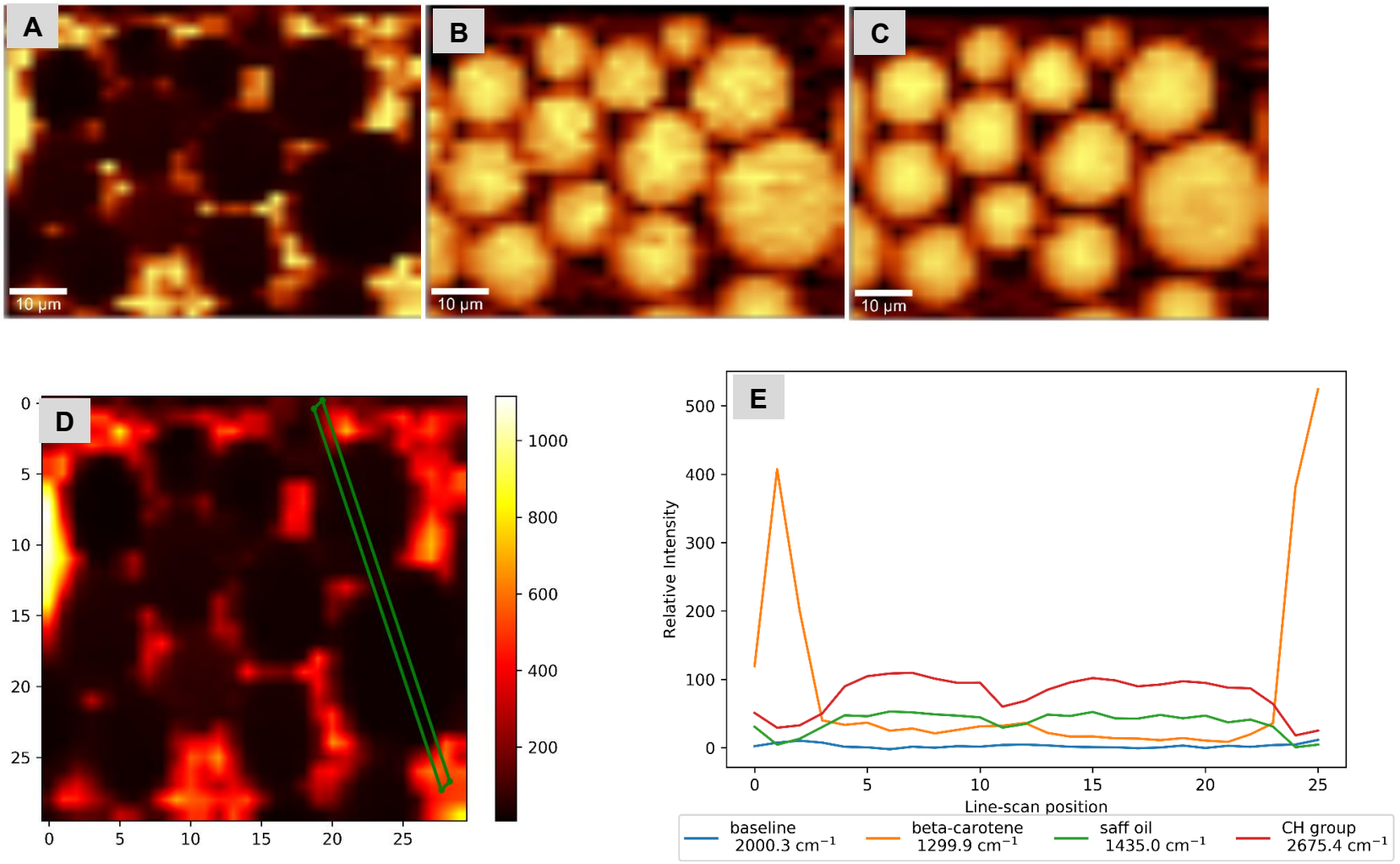

Figure 7.14 *Confocal Raman microscopy images and intensity profile of Olive oil DSEs with beta-carotene-in-shell droplets- A, B, & C= beta-carotene, safflower oil and CH band Raman channels respectively; D= Line scan location across droplets; E= Intensity profiles for selected Raman channels across line scan shown in D*

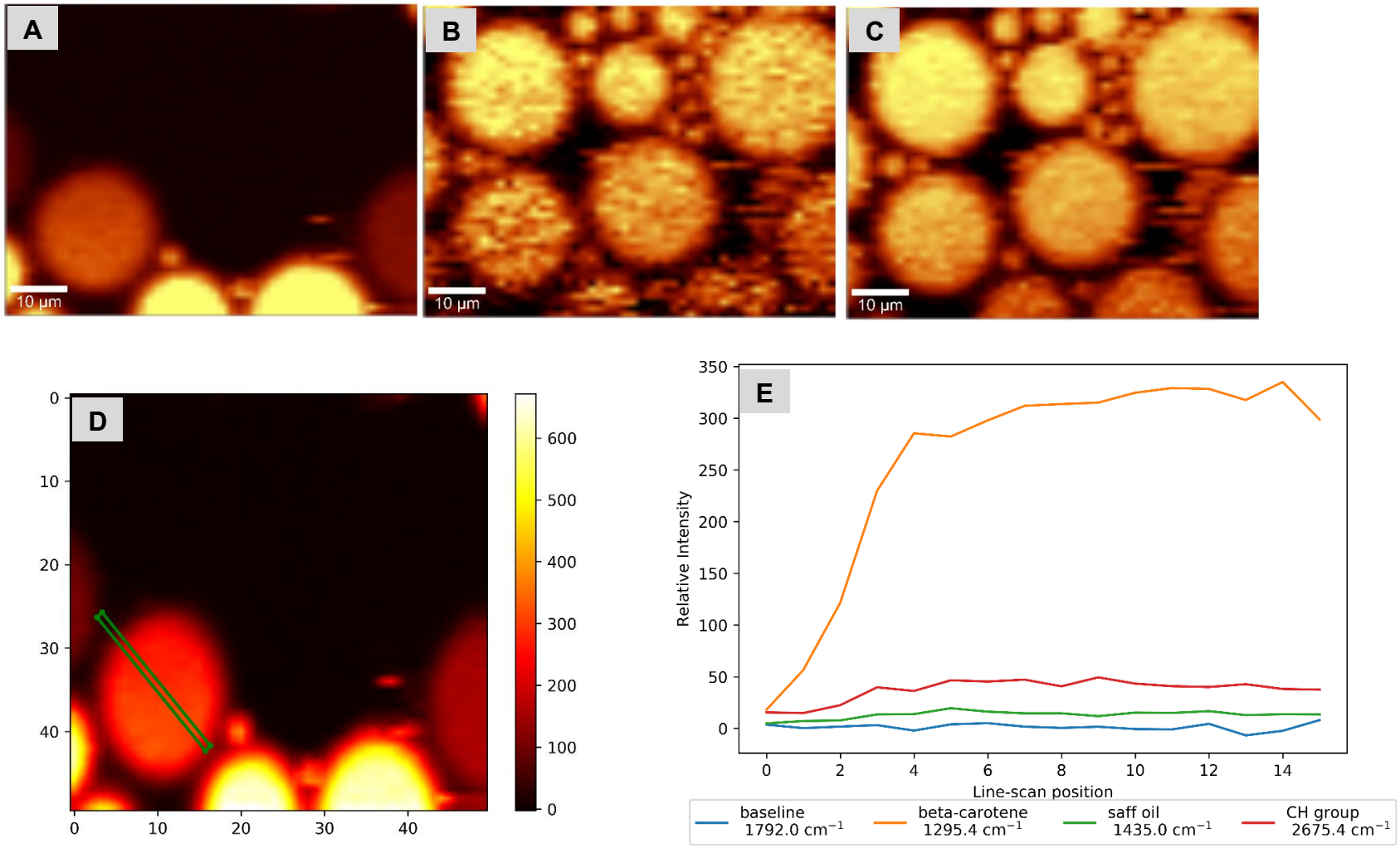

Figure 7.15 *Confocal Raman microscopy images and intensity profile of olive oil DSEs with beta-carotene-in-core droplets- A, B, & C= beta-carotene, safflower oil and CH band Raman channels respectively; D= Line scan location across droplets; E= Intensity profiles for selected Raman channels across line scan shown in D*

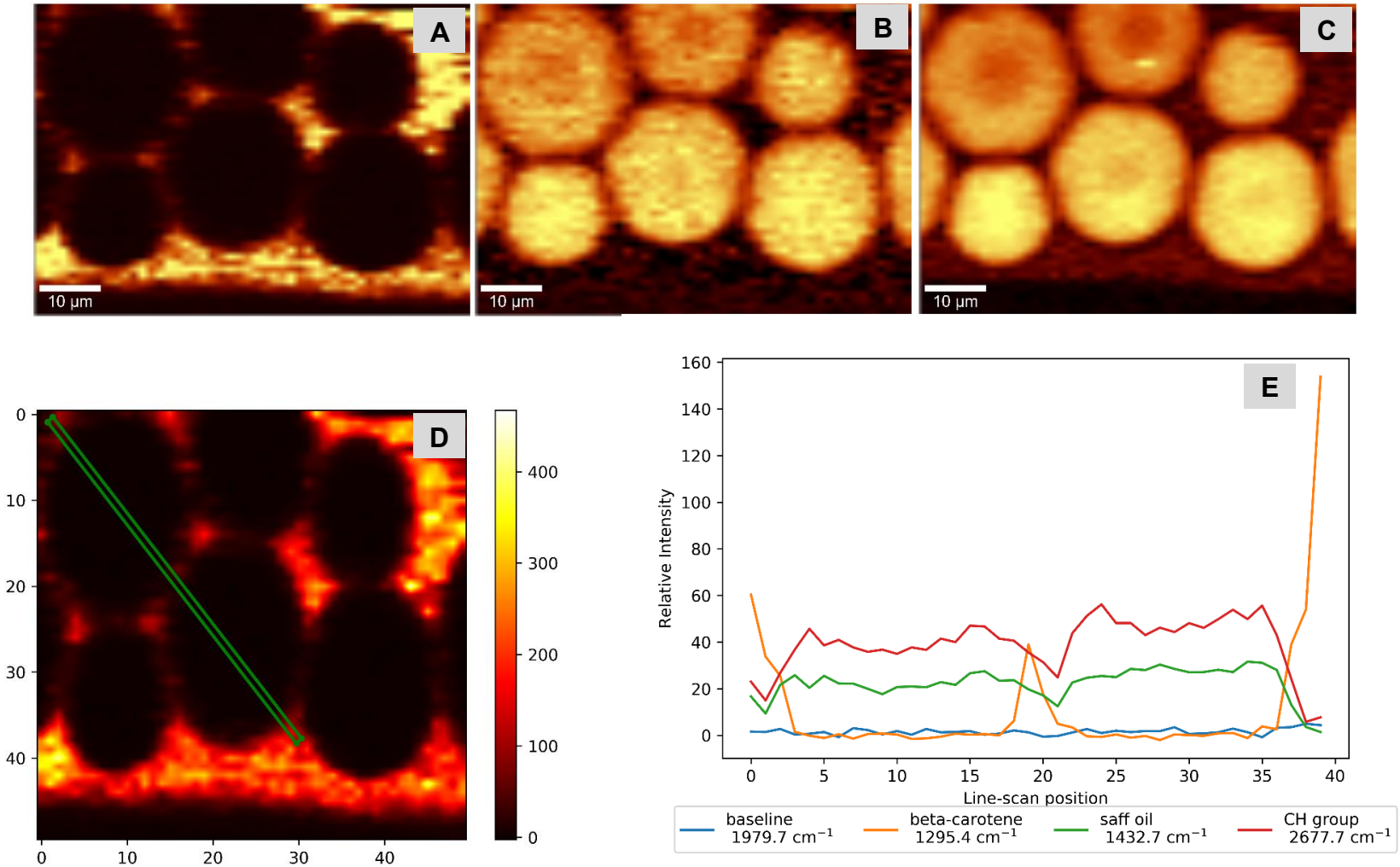

Figure 7.16 *Confocal Raman microscopy images and intensity profile of trimyristin control emulsion (shell gently stirred-in) - A, B, & C= beta-carotene, safflower oil and CH band Raman channels respectively; D= Line scan location across droplets; E= Intensity profiles for selected Raman channels across line scan shown in D*

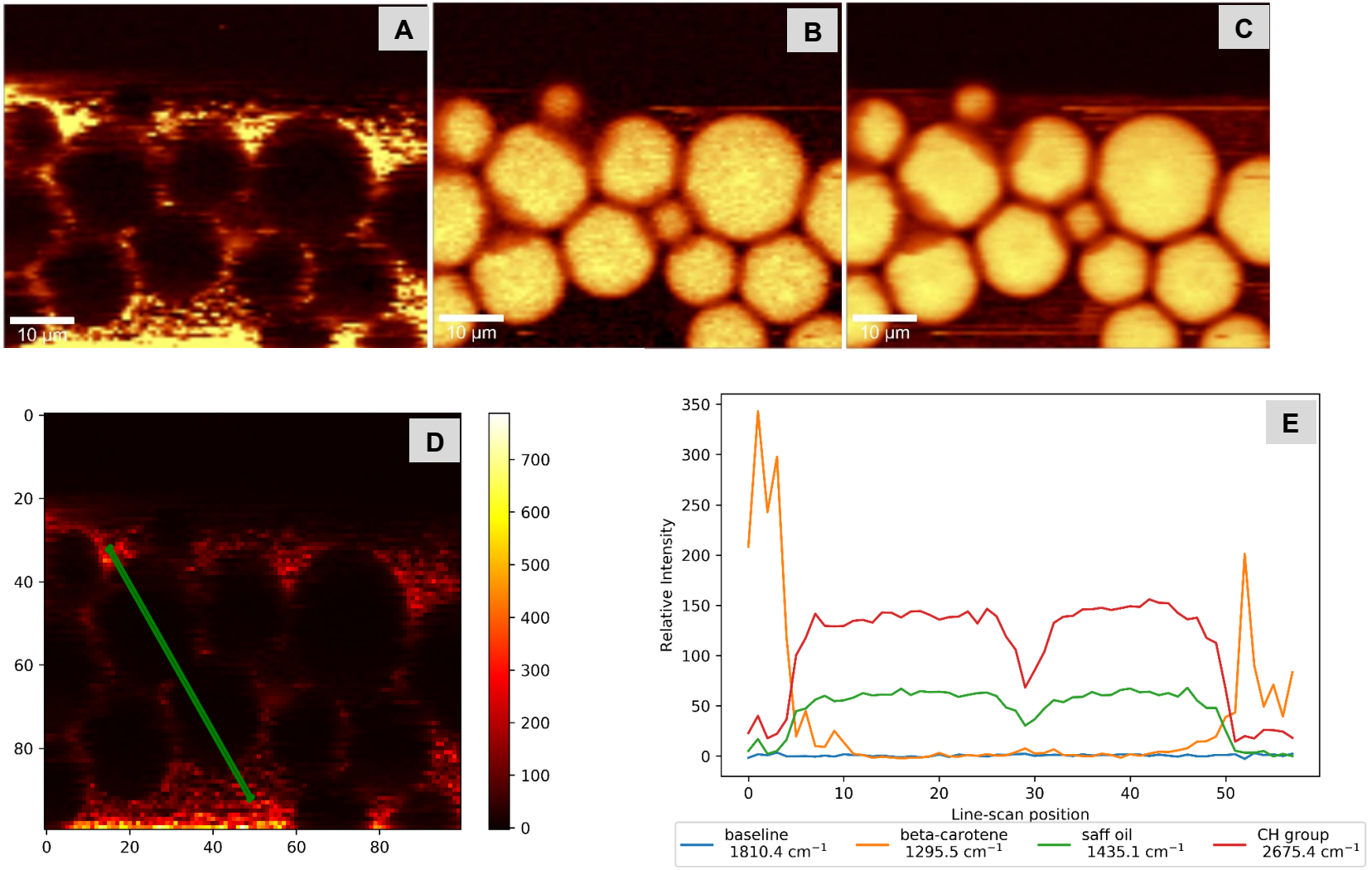

Figure 7.17 *Confocal Raman microscopy images and intensity profile of trimyristin DSEs with beta-carotene-in-shell droplets- A, B, & C= beta-carotene, safflower oil and CH band Raman channels respectively; D= Line scan location across droplets; E= Intensity profiles for selected Raman channels across line scan shown in D*

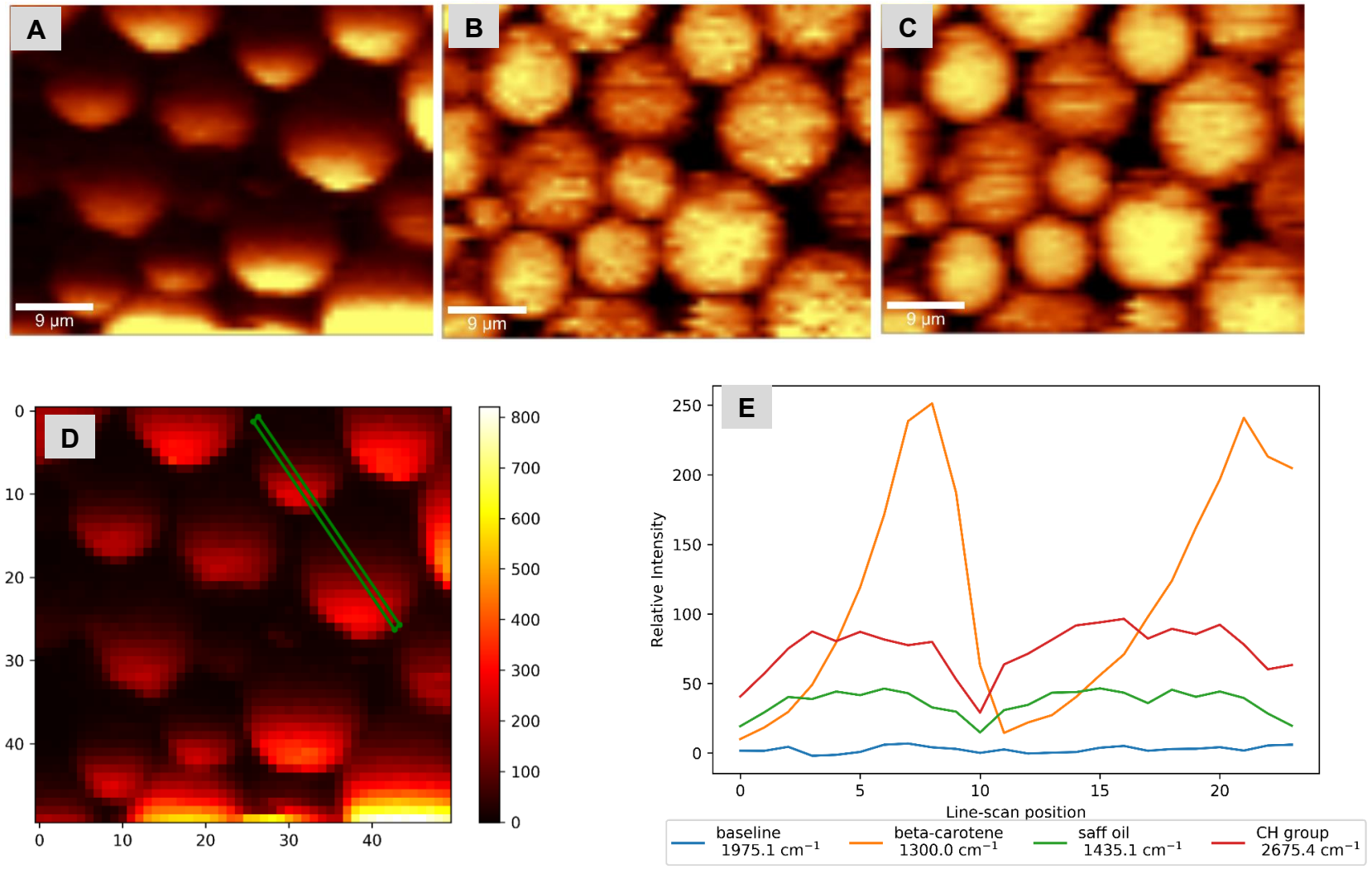

Figure 7.18 *Confocal Raman microscopy images and intensity profile of trimyristin DSEs with beta-carotene-in-core droplets- A, B, & C= beta-carotene, safflower oil and CH band Raman channels respectively; D= Line scan location across droplets; E= Intensity profiles for selected Raman channels across line scan shown in D*

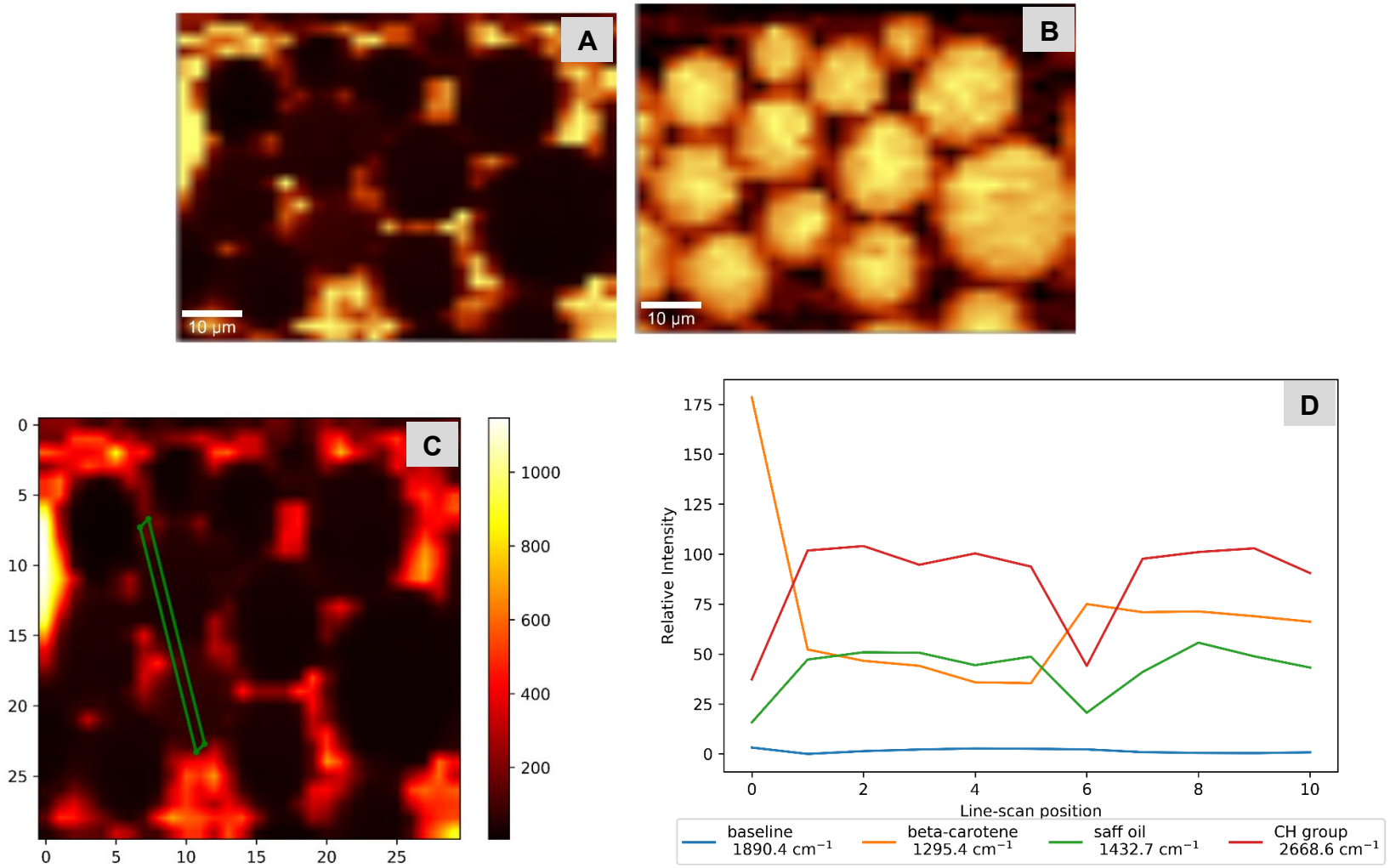

Figure 7.19: *Confocal Raman microscopy images and intensity profile of olive DSEs with beta-carotene-in-shell droplets showing evidence of possible migration to core – A & B= beta-carotene and safflower oil Raman channels respectively; C= Line scan location across droplets; D= Intensity profiles for selected Raman channels across line scan shown in C*

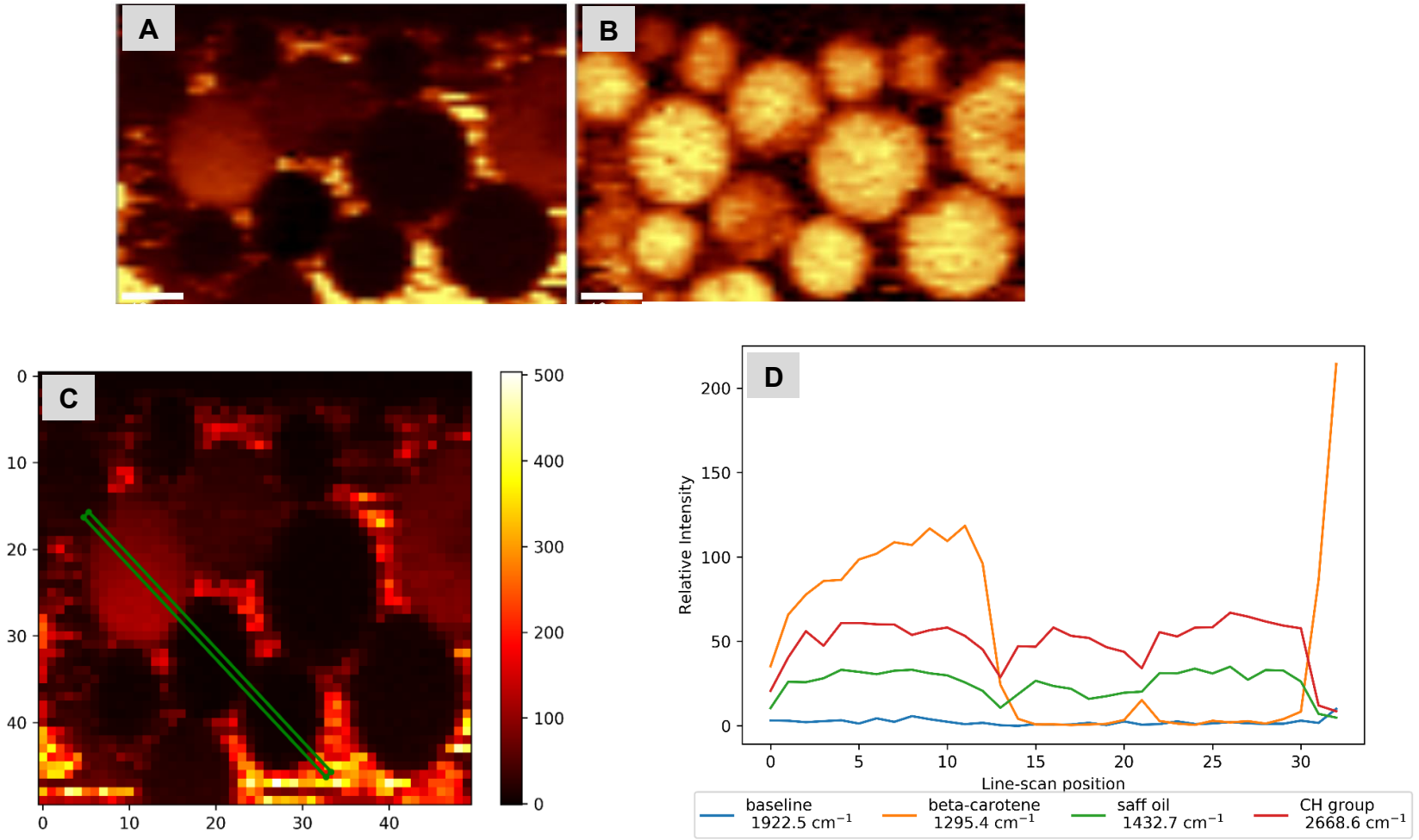

Figure 7.20 *Confocal Raman microscopy images and intensity profile of trimyristin DSEs with beta-carotene-in-shell droplets showing evidence of possible migration to core- A & B= beta-carotene and safflower oil Raman channels respectively; C= Line scan location across droplets; D= Intensity profiles for selected Raman channels across line scan shown in C.*

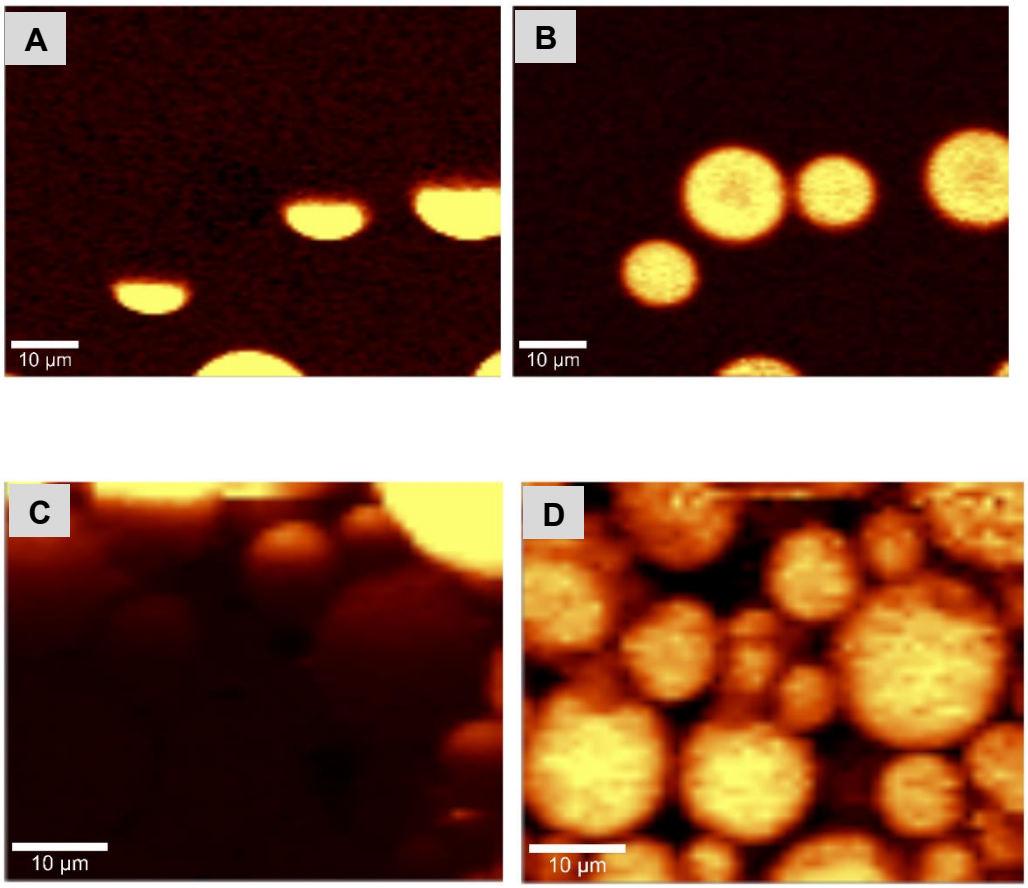

Figure 7.21: *Confocal Raman microscopy images of DSEs scanned at high power (15 mW) showing evidence of possible photo-bleaching of beta-carotene. A & C= beta-carotene Raman channels, B & D= safflower oil Raman channels.*

7.5 Discussion

The similarities or overlaps in fatty acid profiles of the surface and core lipids used in DSEs makes investigating possible exchange of shell droplets to core droplets very challenging particularly with the STD method. However, selecting lipids with minimal overlapping fatty acid profiles such as coconut and safflower oil used in this study provided a good solution because the unique peak in safflower oil used for saturation was almost totally absent in coconut oil. Particle size of DSEs are quite large and so they tend to cream very quickly posing another challenge with the STD method. The expectation was that changes to BHA peaks will be due to saturation transfer from the saturated safflower oil peak indicating BHA migration to safflower oil. However, changes in BHA peak were observed in both DSEs with BHA incorporated in the shell and core, making it difficult to evaluate if the changes were due to BHA migration. It is possible that the changes may have been due to a change in the emulsion's stability arising from the large particles moving upwards (i.e. creaming) and not BHA migration. It is also possible that magnetization relaxed very quickly before any saturation could have taken place. Based on these results, the STD method was inconclusive but could prove very promising if the highlighted challenges of DSEs rapid creaming and fatty acid profile overlaps of surface and core lipids are addressed.

Confocal Raman microsocpy results from the DSEs fixed in agarose indicated that beta-carotene incorporated in shell droplets of DSEs remained localised within the droplets but looking at the Raman spectra there appeared to be strong beta-carotene signals in scanned areas corresponding to core safflower oil droplets and the inablity to isolate droplets made it difficult to evaluate possible beta-carotene migration.

Using the microfluidic channel to isolate a single layer of droplets made it possible to overcome the challenge experienced with collecting Raman data when DSEs were fixed in agarose. Looking at the results obtained with the microfluidic channel, beta-carotene incorporated in shell droplets of DSEs remained mostly localised within the shell droplets but, appreciable beta-carotene signals obtained within the core of some safflower oil droplets confirm limited migration of beta-carotene from shell to core.

The emulsions were analysed after 3 days of production and all samples were analysed within 3-5 days of production, so it is difficult to evaluate at what point the observed beta-carotene shell to core exchange occurred. However, looking at the Raman data of the control emulsions where no high speed mixing was done but rather the shell droplets containing beta-carotene was gently stirred in, there were no beta-carotene signals in the core safflower oil indicating there was no migration or diffusion from the gently stirred-in shell to core. This suggests that migration occurred during high-speed mixing.

The absence of beta-carotene signals in core safflower oil droplets of control emulsions indicate that beta-carotene exchange from shell to core in DSEs may have occured during adsorption of shell droplets to core droplets in the final mixing step of DSE formation. However, considering the time scale required for shell droplets to adsorb to the interface of core droplets is short, it is unlikely that beta-carotene transfer occurred by diffusion across the interface. Beta-carotene transfer from shell to core may have occurred through occasional coalescence between shell and core droplets. Beta-carotene transfer from shell to core was minimal so it implies that the emulsions are relatively stable to coalescence or the

level of coalescence is so low that beta-carotene concentrations are small in core droplets.

In the confocal Raman method, only a small amount of emulsion was introduced into the microfluidic channel for analysis so results may not be fully representative of the whole sample, but consistency between different emulsions suggests that small field of view did not compromise representativeness. The emulsions were analysed 3 days after production due to logistical limitations so it is quite difficult to conclude that the beta-carotene exchange in DSEs occured during shell droplet adsorption in the final mixing step.

Overlaps in Raman signals of the lipids (olive, safflower and trimyristin-Figure 7.12) and inability to identify unique intense signals from trimyristin and olive oil made it difficult to evaluate if beta-carotene exchange from shell to core was due to shell droplet or surface lipid exchange to core droplets, or due to beta-carotene diffusion from shell droplets across the protein interface to the core.

Results from this study do not provide a quantitiative measure to enable comparative analysis between low (olive) and high (trimyristin) melting DSEs in terms of levels of beta-carotene exchange from shell to core, and if the exchange was slower with high melting shell droplets. Another challenge observed with the confocal Raman study was that at high power exposure, beta-carotene was susceptible to photo-bleaching and so it was difficult to determine the extent of beta-carotene exhange. Overall, observation of most DSEs droplets at low power exposure showed that beta-carotene remained localised within shell droplets.

In conclusion, results from this study reveal that STD method can be used to probe the location or study mobility of antioxidants or other compounds incorporated in DSEs provided some of the challenges identified in this study could be overcome. Results from confocal Raman study shows that microfluidic channels can be used to isolate DSE droplets to enable efficient location probing and diffusion or mobility studies of antioxidants or other components incorporated within. The results also indicate that antioxidants or bioactives incorporated in shell droplets of DSEs may remain mostly localised within the shell droplets, but limited migration may occur either due to high speed mixing of shell droplets and core droplets or overtime.

This study demonstrated new methods that can be used to study antioxidant location and mobility in emulsion systems without separating emulsion phases and has also provided critical information about the possible fate of antioxidants incorporated in shell droplets of DSEs.

Chapter 8: Final Perspectives and Recommendations

8.1 Summary

The hydrophobic nature of many bioactive compounds remains a challenge for the food industry. Despite extensive research into many compounds with potential health benefits that can be incorporated in foods, effective protection of these bioactives from degradation during food processing, storage, and gastro-intestinal processing are key priorities that must be continuously addressed to ensure successful development of functional foods. Amongst the current encapsulation strategies for bioactive oils and compounds is the use of interface-structured oil-in-water emulsion systems to slow down or retard oxidation in these lipids.

In this study, a novel structured food-grade oil-in-water emulsion system stabilised by protein-coated oil droplets (droplet-stabilised emulsion) has been examined to understand the effect of interfacial structure and composition on oxidative stability of unsaturated lipid and plausible applications of such an interface-structured emulsion delivery system.

8.2 Formation of food-grade droplet-stabilised oil-in-water emulsions

In the study carried out by Ye et al. (2013) nano-droplets ($d_{3,2}$ = 0.15 µm) were produced with micellar casein-stabilised hexadecane-in-water droplets and used to stabilise DSEs. In the current study, droplet-stabilised interfacial structure was successfully reproduced with a food-grade emulsifier and lipids. Food-grade DSEs were produced with milk protein concentrate (MPC) under varying conditions. MPC-stabilised emulsions produced were not in the nano-scale size range but bigger, and the size varied depending on the emulsification equipment and homogenisation conditions used. In the current study, the stabilising emulsion is referred to as 'shell' emulsion.

MPC-stabilised emulsions processed via a two-stage homogeniser resulted in different droplet sizes depending on the pressure conditions. At 1st and 2nd stage pressures of 200 and 40 bar respectively, $d_{3,2}$ ranged from 0.6 µm to 1.4 µm depending on the calcium level of MPC used (Chapter 4), while at 1st and 2nd stage pressures of 400 and 50 bar respectively $d_{3,2}$ ranged from 0.3 µm to 0.4 µm dependent on the type of surface lipid used (Chapter 5 and 6).

The type of emulsification equipment greatly influenced the structure and particle size of MPC shell emulsions, however, the extent of structure modification was dependent on the type of MPC used. Calcium-depleted (~ 1260 mg/100g) MPC produced fine shell emulsions with $d_{3,2}$ less than 1 µm, irrespective of the emulsification equipment, while $d_{3,2}$ of shell emulsions produced with higher calcium level (> 2000 mg/100g) MPC was dependent on the emulsification equipment used. Ye (2011) also reported smaller droplet size emulsions produced with calcium-depleted MPC.

When MPC shell emulsions were processed with a microfluidizer, smaller particle sizes (<1 μm) were only achieved with calcium-depleted or non-aggregated MPC (MPC 4). For the aggregated or higher calcium level MPCs (MPC 1, 2 & 3), particle sizes of shell emulsions were bigger possibly due to over-processing (Chapter 4).

Non-aggregated milk proteins have better emulsifying capability than their aggregated counterparts. However, aggregated milk proteins can modify droplet flocculation in such a manner that is desirable in some dairy products, as droplet aggregation is responsible for structure formation (Euston & Hirst, 1999; Singh, 2011; Singh & Ye, 2008; Ye, 2011; Ye, Srinivasan, & Singh, 2000). Results from the current study showed that for structure formation in MPC-based DSEs, an optimal level of protein aggregation was required, implying that for MPC-stabilised shell droplets to sufficiently stabilise core oil-in-water droplets, an optimal level of calcium content is required for casein proteins to retain their aggregated structure. Any changes in calcium content of MPC below optimal levels results in modification of their aggregated structure and droplet-stabilisation can be affected.

The differences in particle size of MPC shell emulsions found in this study showed that particle size of protein-stabilised emulsions was dependent on protein structure, protein concentration, homogenisation pressure, homogenisation equipment and oil type. It also showed that the mechanism of droplet disruption used for emulsion formation influenced final structural properties and stability.

Shell emulsion concentration influenced the final particle size and interfacial coating of DSEs. Particle size of DSEs decreased as shell emulsion

concentration (2%, 10% & 16% shell emulsion) increased just as increasing the concentration of nano-droplets in the study of Ye et al. (2013) resulted in a decrease in the final particle size of droplet stabilised hexadecane oil droplets. The observed results showed that at low shell emulsion concentrations (2% shell emulsion), there were insufficient shell droplets to cover the interface of core droplets resulting in bigger particle sizes. Conversely, at higher concentrations, there were sufficient shell droplets available to cover the interface of core droplets. The relationship between shell emulsion concentration and DSE particle size is reflected in the particle size distribution of DSEs which was mono-modal at low shell droplet concentration and bimodal as shell droplet concentration increases (chapter 4).

Varying the interfacial composition of DSEs by changing the shell droplets from low melting point shell droplets to medium and high melting point shell droplets provides the same interfacial structure as obtained with low melting point shell droplets. However, there are indications of some shell droplet transfer to core droplets (Chapter 4 & 5), evidenced by the presence of crystalline-like structures within core droplets. The morphology of these crystal structures was dependent on the cooling rate, suggesting that some of the high melting point lipids had been transferred to the core droplets.

A good understanding of the processing and compositional conditions required to form stable, food-grade DSEs as detailed in this study is very important because it provides a framework for consistent DSE formation for future food applications. This also defines some structural characteristics of food-grade DSEs thus, providing insight into the possible impact on texture if incorporated in real food systems. To the author’s knowledge, this is the first study that defines

the relationship between calcium content of MPCs and their ability to form DSEs and highlights the emulsification conditions required for optimal droplet formation and stabilisation.

8.3 Lipid oxidation in oil-in-water emulsions

Reaction mechanisms governing the oxidation of bulk oils are generally applicable in oil-in-water emulsions, but several factors contribute significantly to the mechanism of oxidation in oil-in-water emulsions because of the various phases formed in oil-in-water emulsions.

Interfacial structure and composition of oil-in-water emulsions play a vital role in their chemical stability (Qian & McClements, 2011; Surh, Decker, & McClements, 2006; Wooster & Augustin, 2006) and other factors associated with the aqueous and lipid phases also contribute to oxidative stability of emulsions. The degree of unsaturation, presence of trace lipophilic components, droplet surface area and physical state of the lipid phase are some properties that also impact oxidative reactions in emulsions.

Interfacial permeability of emulsion droplets is an important consideration when designing emulsion systems for effective protection against lipid oxidation because it controls the ability of oxidation reactants to diffuse into lipid droplets. In the current study, the ability of the hydrophobic interfacial structure in DSEs to retard lipid oxidation of unsaturated lipids in the core droplets was confirmed. Oxidation of high linoleic acid safflower oil was delayed when incorporated in DSEs, as compared with a simple conventional protein-stabilised emulsion system. The protective effect against safflower oil oxidation in DSEs was further improved by changing the interfacial composition i.e. shell droplets from low

(olive) and medium (palmolein oil) melting point shell droplets to high (trimyristin) melting point shell droplets.

In this study, lipid oxidation was accelerated by exposing DSEs to light (fluorescent lamps) in the presence of ferrous ions (Fe^{2+}). The oxidation pathway or mechanism considered under these conditions involved a possible type II photosensitisation mechanism (Chapter 5 and 6). Based on the envisaged oxidation pathway in this study, it implied that oxygen and ferrous ions have to permeate across the emulsion interface to gain access to core safflower oil and surface-active oxidation products. The study (chapter 5) showed that oxygen and ferrous ions crossed the interface of an MPC protein layer of a conventional emulsion and accelerated safflower oil oxidation faster than for a droplet interface of droplet-stabilised emulsions.

DSEs comprising high melting point lipid shell droplets provided a superior protective effect against safflower oil oxidation, proving that a combination of a hydrophobic interfacial structure with the solid phase state of the interfacial lipid provided a less permeable interface than conventional emulsions and DSEs with low and medium melting point interfacial lipid. In selecting the interfacial lipid for DSEs, it is imperative that lipids with very low susceptibility to oxidation are chosen to minimise or eliminate oxidation reactions between oxygen, metals and other pro-oxidants with the surface lipid.

This study emphasized the significant role an emulsion's interfacial structure and composition plays in providing good chemical stability, thus reiterating the need to pay attention to the interfacial structure when selecting emulsions for delivery of bioactives in foods.

This study has observed protective effects of DSEs as shown by their ability to delay and limit degradation of oxidation-sensitive lipids incorporated within. High linoleic acid safflower oil was used as the bioactive lipid, but the outcomes and mechanisms observed in this study should be applicable to other degradation-prone lipophilic bioactives. Health beneficial bioactive lipids such as omega-3 rich oils can also be used in place of safflower oil. Alternatively, beneficial lipid-soluble bioactives can also be dissolved in other common lipids used for solubilisation of bioactives such as soybean oil, sunflower oil etc. which in turn can be incorporated in DSEs for effective protection of the lipid-soluble bioactive.

Outcomes of this study have paved the way for functional food application of DSEs. To the authors' knowledge, this is the first study establishing the ability of DSEs to limit oxidation of safflower oil over conventional emulsions and reporting superior anti-oxidative effects of DSEs with high melting point lipid droplets at the interface over low and medium melting point lipid droplet interfaces.

8.4 Location-based antioxidant performance in emulsions

Antioxidant positioning at the oil-water interface has the potential to be very effective in protecting droplets against oxidation (Cui et al., 2014; Feng et al., 2018; Gu et al., 2017; Wan et al., 2014). However, merely locating an antioxidant at the oil-water interface does not necessarily imply effective performance as shown in the current study (Chapter 6). The location-based approach of boosting antioxidant performance in oil-in-water emulsions cannot be effective if other factors influencing antioxidant location or distribution between the various phases of oil-in-water emulsions is not understood. The mechanism of action, concentration and mobility of the antioxidant must always be considered.

In the current study, butylated hydroxyanisole (BHA) a common chain-breaking antioxidant was used. BHA works by counteracting oxidation by donating hydrogen and converting highly unstable free radicals into more stable products. This study aimed to show the impact of locating antioxidants at the interface of oil-in-water emulsions and the influence of antioxidant concentration on location-based antioxidant performance.

The roles of antioxidant hydrophobicity or chain length and emulsifier type on antioxidant performance in emulsions has been shown (Laguerre et al., 2010; Losada Barreiro, Bravo-Díaz, Paiva-Martins, & Romsted, 2013; Panya et al., 2012; Stöckmann et al., 2000).

The roles of antioxidant concentration and transport mechanisms on performance of antioxidants are very critical phenomena which are beginning to gain more research attention.

In this study, the impact of antioxidant location in DSEs was evaluated at two concentrations of BHA (50 and 500 ppm) and results showed that BHA performance, when located at the interface varied with the amount of BHA. At 50 ppm, hexanal formation was faster in BHA-in-shell DSEs (interface location) than BHA-in-core DSEs. At 500 ppm, BHA behaved contrarily to its behaviour at 50 ppm, hexanal formation was faster in BHA-in-core DSEs than BHA-in-shell DSEs. However, at 500 ppm both BHA-in-shell and BHA-in-core DSEs retarded oxidation effectively compared to oxidative stability for either locations at 50 ppm. Hexanal formation was always faster with low melting point lipid droplet emulsifiers than high melting point shell droplet emulsifiers, irrespective of the BHA location indicating a combined effect of BHA activity and use of high melting point shell droplet emulsifiers (Chapter 5 & 6).

These results reveal that locating antioxidants at the interface of DSEs will not always guarantee effective performance and so it is extremely important to understand and consider all the factors that could influence effective performance of antioxidants in emulsions prior to selecting antioxidants and locating them at the interface. It is important to pay attention to oxidation pathways and consider possible reactions that could occur between pro-oxidants or reactants and antioxidants which could jeopardise antioxidant activity.

Based on this study, a deeper understanding of other factors apart from polarity or hydrophobicity that can drive performance of antioxidants is required. This means that antioxidation studies in emulsions based mostly on proving or disproving the polar paradox and cut-off theory cannot provide a complete picture of requirements that should be fulfilled to ensure antioxidants perform effectively. Studies must begin to look further than the location-based and hydrophobicity

approach and begin to consider the role of concentration and the concept of mobility or transport mechanisms of antioxidants in emulsions. The work of Laguerre et al. (2017) provided a very good review of transport mechanisms in lipid oxidation and antioxidation but, more work is required to fully understand the correlation between concentration, mobility, distribution of antioxidants and antioxidant performance in oil-in-water emulsions.

This study has established that the unique structure of DSEs provides an opportunity to locate hydrophobic antioxidants at the interface where it effectively counteracts lipid oxidation just as it would if located in the core unsaturated lipid or even better (depending on antioxidant concentration). By incorporating BHA in shell droplets of DSEs made up of core unsaturated lipid, the study also confirms that it is possible to concurrently encapsulate two hydrophobic bioactives in DSEs by loading one bioactive in shell droplets and the other in core droplets.

To the authors' knowledge, only the study carried out by Zhong and Shahidi (2012) has attempted to investigate the relationship between antioxidant concentration and the polar paradox and this study was done on bulk oils. If the author's assertion is correct, then the current study is the first work to investigate the influence of antioxidant concentration on location-based antioxidant performance in an emulsion system.

8.5 Mobility of antioxidants incorporated in emulsions

Current practice of incorporating antioxidants in emulsions usually require dissolution of the antioxidant in the phase in which it is most soluble. Determining the location or distribution of antioxidants incorporated in oil-in-water emulsions involves separation of the oil and aqueous phases with subsequent quantification of the antioxidant within the individual phases (Edwin N. Frankel et al., 1996; Freiría-Gándara, Losada-Barreiro, Paiva-Martins, & Bravo-Díaz, 2018; Keller, Locquet, & Cuvelier, 2016). This approach is a good predictor of antioxidant behaviour or mobility in oil-in-water emulsions.

In this study, BHA or beta-carotene was dissolved in the surface lipid of DSEs and the surface-loaded shell droplet used to stabilise safflower oil-in-water droplets. To confirm if BHA or beta-carotene incorporated in shell droplets of DSEs remained localised within shell droplets or diffused into core droplets over time. A different approach from the usual phase separation approach was explored in this study because DSEs consist of two lipid phases and so the conventional phase separation approach will not segregate the core and shell emulsion droplets. Therefore, new methods that are non-destructive to DSEs' structure are required.

The saturation transfer difference method did not provide any conclusive results in terms of the location or mobility of BHA. An alternative to ^{1}H-NMR used in this study would be to use the ^{13}C spectrum, which is easy to get for the surface and core lipids but not for BHA. To obtain a ^{13}C spectrum for BHA, ^{13}C-labelled BHA is required; this is an option for future consideration.

Beta-carotene's strong Raman scattering ability makes it a good antioxidant choice for the confocal Raman method but, it is susceptible to photo-bleaching at high power exposures. Therefore, to determine if it remains localised in the primary phase in which it is incorporated, low power exposure is required for this method.

Beta-carotene migration from shell droplets of DSEs to core droplets is subtle and the absence of beta-carotene in core droplets of composition-matched controls (gentle stirring-in of beta-carotene loaded shell droplets) indicates a very high probability that beta-carotene migration from shell droplets to core droplets can be controlled during processing (Chapter 7). Slow diffusion of beta-carotene, high shear-induced droplet coalescence and lipid-exchange assisted migration are possible transport mechanisms by which beta-carotene migration from shell droplets to core droplets could occur. Beta-carotene migration depends on its affinity toward the different phases and its ability to access or move to the reaction site. It is possible that the antioxidation mechanism of antioxidants incorporated in shell droplets of DSEs will greatly influence its mobility.

Droplet-stabilised oil-in-water emulsion offers unique functional applications because of its structural characteristics. Unlike Pickering and multi-layered emulsions, DSEs consists of two lipid phases providing opportunities to load more bioactives and incorporate antioxidants in shell droplets located at the interface without having to crosslink the antioxidant with the emulsifier, make conjugates or complexes or directly incorporate in core lipid as is currently done with other structured emulsion systems such as multi-layered and Pickering emulsions.

8.6 Outcomes and Applications

Formation of food-grade droplet-stabilised emulsions (DSEs) requires careful selection of emulsifier and interfacial lipid. DSE processing can be easily scaled-up and does not require sophisticated equipment. DSEs can effectively protect encapsulated hydrophobic bioactives from chemical degradation and has the capacity for efficient loading of bioactives due to the presence of two lipid phases. It can also be used as a dual delivery system by encapsulating one bioactive in shell droplets and another in the core. However, bioactive migration from shell to core may need to be controlled to prevent any detrimental reactions between bioactives in shell and core. In cases where synergistic effects between bioactives in shell and core is envisaged, bioactive migration from shell to core may be desirable.

The characteristic large droplet size of DSEs makes it prone to creaming during storage but, changes in droplet size after 7 days shows it remains stable to droplet coalescence. Development of methods to further reduce droplet size and use of thickeners are plausible solutions to prevent creaming of DSEs in real food systems. The exact mechanism of shell droplet adsorption at the interface of DSEs is still unknown but currently under investigation. It is also unknown if the gastro-intestinal fate of DSEs will differ from that of other emulsion systems previously studied; interfacial structure and composition of DSEs may influence digestion rates.

This study provides vital and useful information about droplet-stabilised emulsions, and communicates knowledge about the following:

- ✓ Broader and better understanding of processing parameters and factors required for formation of stable, functional DSEs.
- ✓ Composition changes capable of influencing DSE formation.
- ✓ Practical formation of DSEs involving readily available food ingredients.
- ✓ Chemical stability of DSEs and factors responsible for changes in chemical stability.
- ✓ Practical and plausible functional use of DSEs involving readily available antioxidants.
- ✓ Mobility of bioactives incorporated at the interface of DSEs.
- ✓ New and practical approach or techniques for examining precise location of bioactives incorporated in DSEs.

The highlighted outcomes could lead to the following potential applications:

- ✓ Production of food-grade droplet-stabilised beverage emulsions or development of other suitable food products.
- ✓ Efficient encapsulation of health-promoting, hydrophobic bioactives in DSEs and development of functional foods.
- ✓ Preferential utilisation of DSEs over other structured emulsion systems for easy interfacial localisation of antioxidants without formation of conjugates or complexes.
- ✓ Concurrent encapsulation of two different hydrophobic bioactives in DSEs by incorporating one in the shell and the other in the core.
- ✓ Efficient loading of bioactives by incorporation in both shell and core.

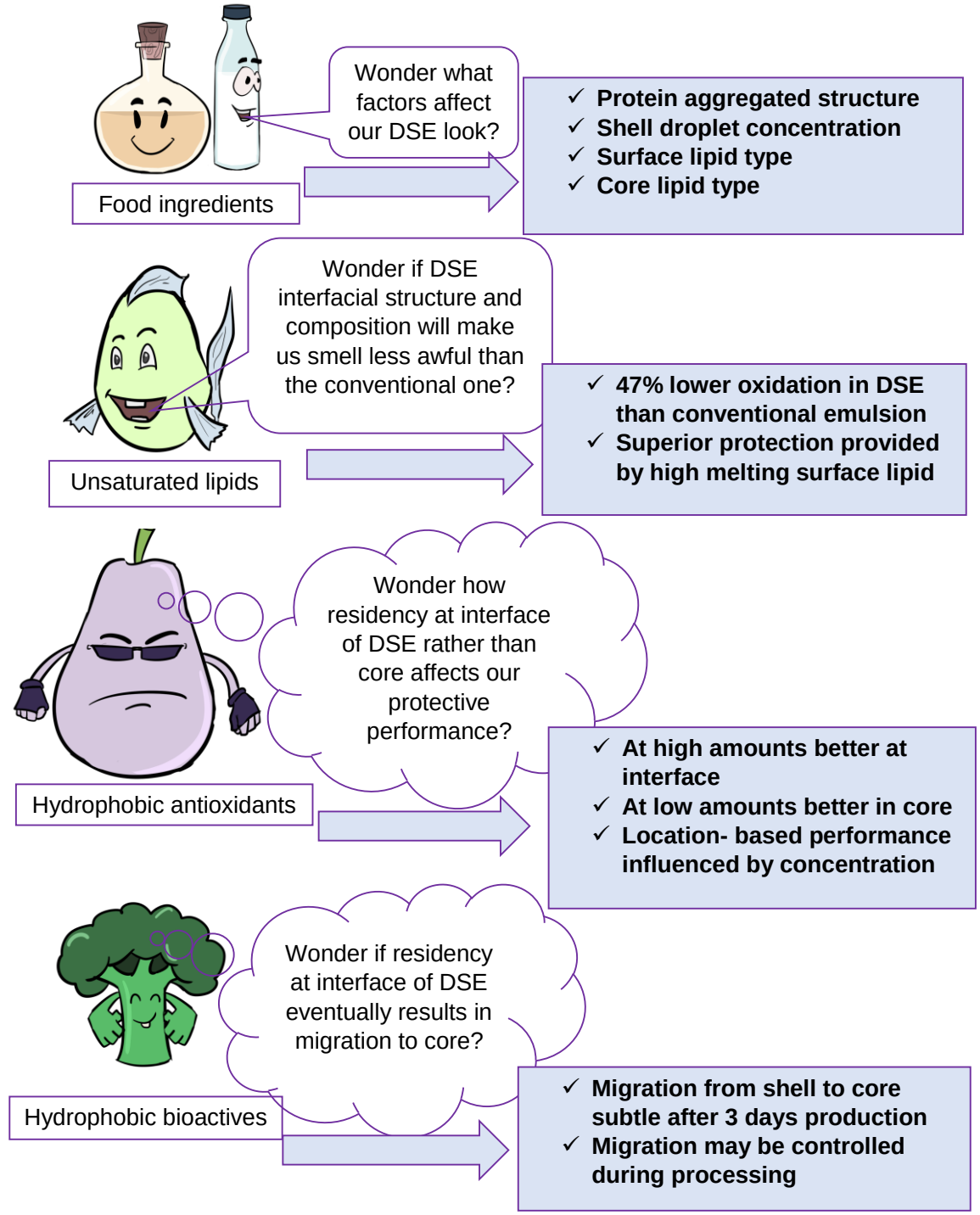

Figure 8.1: *Summary of study outcomes*

8.7 Recommendations for future research

- The exact protein aggregation levels required for formation of MPC DSEs is unknown. Further research is required to determine and define optimal levels of protein aggregation required to form stable DSEs with MPCs or other aggregate biopolymers. It will be interesting to investigate the possibility of altering the ability of MPC with calcium levels (1260 mg/100 g) similar to MPC 4 (calcium-depleted MPC) used in the current study (Chapter 4) to form droplet-stabilised emulsions by adding calcium in quantities equivalent to MPC 1, 2 and 3. The minimum amounts of calcium required in milk protein concentrate for successful formation of droplet-stabilised emulsions will provide useful information.

- The emulsifier and shell emulsion concentration in the current study were fixed. In future, it will be important to examine and compare oxidative stability of unsaturated lipids incorporated in DSEs of varying shell emulsion concentrations. In Chapter 4, DSEs were successfully formed at 2%, 10% and 16% concentrations and the shell emulsion concentration influenced the final particle size of DSEs and the amounts of un-adsorbed shell droplets. Further studies to examine the effect of varying the shell emulsion concentration and the particle size of DSEs on oxidative stability of DSEs will provide a robust understanding of factors that can influence the oxidative stability of DSEs.

- The emulsifier (MPC) used in the current study was also fixed. It is unknown if the type of protein emulsifier will influence oxidation rates in DSEs like reported for other emulsion systems. It will be important to

compare oxidative stability of DSEs formed with other protein emulsifiers with that of MPC using the same shell and core lipid systems used in the current study.

- In this study, oxidative stability of safflower oil in DSEs was compared with stability in conventional emulsion. It is not known if oxidative stability of DSEs will be better than similar structured emulsion systems or not. In future it will be interesting to compare oxidative stability of safflower oil or any other oxidation prone lipid in DSEs with stability in other similar structured emulsion systems such as multi-layered and Pickering emulsions.

- Accelerated oxidation conditions in the current study included light and ferrous iron. Further research to fully understand the kinetics of oxidation in DSEs will deepen the understanding of oxidation mechanisms in DSEs. It will be interesting to study the oxidative stability of DSEs exposed to other accelerated oxidation conditions commonly used in other oxidation studies such as in the dark at higher temperatures, exposure to light without addition of ferrous iron, addition of a radical generator etc.

- Only one hydrophobic antioxidant was used in the current study. Future research to investigate and compare antioxidant capacity of other hydrophobic antioxidants (e.g. tocopherols, BHT, TBHQ, etc.) in DSEs will be necessary to fully understand antioxidation mechanisms in DSEs. Comparing the ability of different hydrophobic antioxidants to counteract oxidation in DSEs when the antioxidant is incorporated in shell lipid versus

the core lipid will also provide a broad understanding of location-based antioxidation mechanisms in DSEs.

- In the current study, only two amounts of BHA (50 ppm and 500 ppm) in DSE were explored, it may be necessary to expand the range of BHA amounts or any other hydrophobic antioxidant (for example 100-400 ppm) in DSEs to provide a better understanding on the relationship between the amounts of antioxidant and location-based antioxidant capacity in DSEs.

- Future studies to examine synergistic effect of antioxidants incorporated in DSEs will also be an important area to explore. BHA and BHT (butylated hydroxytoluene) for example are reported to provide excellent synergistic anti-oxidative effects. Studying and comparing the antioxidant capacity of a mixture of BHA and BHT in DSEs with that of the antioxidants alone will be interesting. Another interesting synergistic antioxidant effect study would be concurrent incorporation of a hydrophilic and lipophilic antioxidant. For example, ascorbic acid and tocopherols have been reported to provide superior anti-oxidative effects. Therefore, future studies investigating oxidative stability of DSEs with a hydrophilic antioxidant incorporated in the aqueous phase and a lipophilic antioxidant incorporated either in the shell or core droplets will deepen the understanding of antioxidation mechanisms in DSEs.

- Future investigation of transportation mechanisms of antioxidants in DSEs and the driving force for migration of antioxidants from shell to core is essential. Possible exchange of oil droplets in DSEs needs to be

investigated. If the highlighted challenges associated with the saturated transfer difference and confocal Raman techniques are resolved, they can be used to determine shell lipid exchange to core.

- DSEs ability to effectively deliver bioactives incorporated within at targeted sites is unknown. Future studies comparing targeted delivery and release of bioactives incorporated in DSEs made up of surface lipids of varying melting points and the gastro-intestinal fate of DSE structure will also be interesting.

References

Acosta, E. (2009). Bioavailability of nanoparticles in nutrient and nutraceutical delivery. *Current Opinion in Colloid & Interface Science, 14*(1), 3-15.

Aditya, N. P., Aditya, S., Yang, H. J., Kim, H. W., Park, S. O., Lee, J., & Ko, S. (2015). Curcumin and catechin co-loaded water-in-oil-in-water emulsion and its beverage application. *Journal of Functional Foods, 15*, 35-43.

Ahmed, K., Li, Y., McClements, D. J., & Xiao, H. (2012). Nanoemulsion- and emulsion-based delivery systems for curcumin: Encapsulation and release properties. *Food Chemistry, 132*(2), 799-807.

Akhtar, M., & Dickinson, E. (2007). Whey protein–maltodextrin conjugates as emulsifying agents: An alternative to gum arabic. *Food Hydrocolloids, 21*(4), 607-616.

Anton, N., & Vandamme, T. (2011). Nano-emulsions and Micro-emulsions: Clarifications of the Critical Differences. *Pharmaceutical Research, 28*(5), 978-985.

Aoki, T., Decker, E. A., & McClements, D. J. (2005). Influence of environmental stresses on stability of O/W emulsions containing droplets stabilized by multilayered membranes produced by a layer-by-layer electrostatic deposition technique. *Food Hydrocolloids, 19*(2), 209-220.

Aust, S. D., Morehouse, L. A., & Thomas, C. E. (1985). Role of metals in oxygen radical reactions. *Journal of Free Radicals in Biology & Medicine, 1*(1), 3-25.

Aveyard, R., Binks, B. P., & Clint, J. H. (2003). Emulsions stabilised solely by colloidal particles. *Advances in Colloid and Interface Science, 100–102*, 503-546.

Balgavý, P., & Devínsky, F. (1996). Cut-off effects in biological activities of surfactants. *Advances in Colloid and Interface Science, 66*, 23-63.

Beicht, J., Zeeb, B., Gibis, M., Fischer, L., & Weiss, J. (2013). Influence of layer thickness and composition of cross-linked multilayered oil-in-water emulsions on the release behavior of lutein. *Food & Function, 4*(10), 1457-1467.

Berton-Carabin, C. C., Ropers, M.-H., & Genot, C. (2014). Lipid Oxidation in Oil-in-Water Emulsions: Involvement of the Interfacial Layer. *Comprehensive Reviews in Food Science and Food Safety, 13*(5), 945-977.

Berton-Carabin, C. C., Sagis, L., & Schroën, K. (2018). Formation, Structure, and Functionality of Interfacial Layers in Food Emulsions. *Annual Review of Food Science and Technology, 9*(1), null.

Berton-Carabin, C. C., & Schroën, K. (2015). Pickering emulsions for food applications: Background, trends, and challenges. *Annual Review of Food Science and Technology, 6*, 263-297.

Berton, C., Ropers, M.-H., Viau, M., & Genot, C. (2011). Contribution of the interfacial layer to the protection of emulsified lipids against oxidation. *Journal of Agricultural and Food Chemistry, 59*(9), 5052-5061.

Berton, C., Ropers, M. H., Bertrand, D., Viau, M., & Genot, C. (2012). Oxidative stability of oil-in-water emulsions stabilised with protein or surfactant emulsifiers in various oxidation conditions. *Food Chemistry, 131*(4), 1360-1369.

Bibette, J., Leal-Calderon, F., & Schmitt, V. (2007). *Emulsion Science: Basic Principles* (2nd ed.). New York: Springer.

Biesalski, H.-K., Dragsted, L. O., Elmadfa, I., Grossklaus, R., Müller, M., Schrenk, D., . . . Weber, P. (2009). Bioactive compounds: Definition and assessment of activity. *Nutrition, 25*(11–12), 1202-1205.

Buck, D. F. (1991). Antioxidants. In J. Smith (Ed.), *Food Additive User's Handbook* (pp. 1-46): Springer US.

Butnariu, M., & Grozea, I. (2012). Antioxidant (Antiradical) Compounds. *Bioequiv Availab, 4*(6), xvii-xix.

Caetano-Silva, M. E., Mariutti, L. R. B., Bragagnolo, N., Bertoldo-Pacheco, M. T., & Netto, F. M. (2018). Whey Peptide-Iron Complexes Increase the Oxidative Stability of Oil-in-Water Emulsions in Comparison to Iron Salts. *Journal of Agricultural and Food Chemistry, 66*(8), 1981-1989.

Chacón, J. N., Gaggini, P., Sinclair, R. S., & Smith, F. J. (2000). Photo- and thermal-oxidation studies on methyl and phenyl linoleate: anti-oxidant behaviour and rates of reaction. *Chemistry and Physics of Lipids, 107*(1), 107-120.

Chaiyasit, W., McClements, D. J., & Decker, E. A. (2005). The Relationship between the Physicochemical Properties of Antioxidants and Their Ability to Inhibit Lipid Oxidation in Bulk Oil and Oil-in-Water Emulsions. *Journal of Agricultural and Food Chemistry, 53*(12), 4982-4988.

Chevalier, Y., & Bolzinger, M.-A. (2013). Emulsions stabilized with solid nanoparticles: Pickering emulsions. *Colloids and Surfaces A: Physicochemical and Engineering Aspects, 439*, 23-34.

Choe, E., & Min, D. B. (2006). Mechanisms and Factors for Edible Oil Oxidation. *Comprehensive Reviews in Food Science and Food Safety, 5*(4), 169-186.

Chung, C., & McClements, D. J. (2015). 7 - Structure and texture development of food-emulsion products A2 - Chen, Jianshe. In A. Rosenthal (Ed.), *Modifying Food Texture* (pp. 133-155): Woodhead Publishing.

Cornacchia, L., & Roos, Y. H. (2011). Stability of β-Carotene in Protein-Stabilized Oil-in-Water Delivery Systems. *Journal of Agricultural and Food Chemistry, 59*(13), 7013-7020.

Cornell, D. G., De Vilbiss, E. D., & Pallansch, M. J. (1971). Binding of Antioxidants by Milk Proteins. *Journal of Dairy Science, 54*(5), 634-637.

Corongiu, F. P., & Banni, S. (1994). [30] Detection of conjugated dienes by second derivative ultraviolet spectrophotometry. In *Methods in Enzymology* (Vol. 233, pp. 303-310): Academic Press.

Cui, Z., Kong, X., Chen, Y., Zhang, C., & Hua, Y. (2014). Effects of rutin incorporation on the physical and oxidative stability of soy protein-stabilized emulsions. *Food Hydrocolloids, 41*, 1-9.

Das, K. P., & Kinsella, J. E. (1990). Stability Of Food Emulsions: Physicochemical Role Of Protein And Nonprotein Emulsifiers. *Advances in Food and Nutrition Research, 34*, 81-201.

Davidson, R. S. (1979). Mechanisms of photo-oxidation reactions. *Pesticide Science, 10*(2), 158-170.

de Folter, J. W. J., van Ruijven, M. W. M., & Velikov, K. P. (2012). Oil-in-water Pickering emulsions stabilized by colloidal particles from the water-insoluble protein zein. *Soft Matter, 8*(25), 6807-6815.

Demetriades, K., Coupland, J. N., & McClements, D. J. (1997). Physical properties of whey protein stabilized emulsions as related to pH and NaCl. *Journal of Food Science, 62*(2), 342-347.

Desai, M. P., Labhasetwar, V., Amidon, G. L., & Levy, R. J. (1996). Gastrointestinal uptake of biodegradable microparticles: Effect of particle size. *Pharmaceutical Research, 13*(12), 1838-1845.

Deshpande, S. S., Deshpande, U. S., & Salunkhe, D. K. (1996). Nutritional and health aspects of food antioxidants. In D. L. Madhavi, S. S. Deshpande, & D. K. Salunkhe (Eds.), *Food Antioxidants: Technological, Toxicological & Health Perspectives* (pp. 361-470). New York: Dekker.

Desrumaux, A., & Marcand, J. (2002). Formation of sunflower oil emulsions stabilized by whey proteins with high-pressure homogenisation (up to 350 MPa): effect of pressure on emulsion characteristics. *International Journal of Food Science & Technology, 37*(3), 263-269.

Dickinson, E. (1992). Faraday research article. Structure and composition of adsorbed protein layers and the relationship to emulsion stability. *Journal of the Chemical Society, Faraday Transactions, 88*(20), 2973-2983.

Dickinson, E. (1997). Properties of Emulsions Stabilized with Milk Proteins: Overview of Some Recent Developments. *Journal of Dairy Science, 80*(10), 2607-2619.

Dickinson, E. (2003). Hydrocolloids at interfaces and the influence on the properties of dispersed systems. *Food Hydrocolloids, 17*(1), 25-39.

Dickinson, E., & Galazka, V. B. (1991). Emulsion stabilization by ionic and covalent complexes of β-lactoglobulin with polysaccharides. *Food Hydrocolloids, 5*(3), 281-296.

Dimakou, C. P., Kiokias, S. N., Tsaprouni, I. V., & Oreopoulou, V. (2007). Effect of Processing and Storage Parameters on the Oxidative Deterioration of Oil-in-Water Emulsions. *Food Biophysics, 2*(1), 38.

Djordjevic, D., McClements, D. J., & Decker, E. A. (2004). Oxidative Stability of Whey Protein-stabilized Oil-in-water Emulsions at pH 3: Potential ω-3 Fatty Acid Delivery Systems (Part B). *Journal of Food Science, 69*(5), C356-C362.

Dybowska, B. E. (2008). Properties of milk protein concentrate stabilized oil-in-water emulsions. *Journal of Food Engineering, 88*(4), 507-513.

Einhorn-Stoll, U., Ulbrich, M., Sever, S., & Kunzek, H. (2005). Formation of milk protein–pectin conjugates with improved emulsifying properties by controlled dry heating. *Food Hydrocolloids, 19*(2), 329-340.

Erickson, M. C. (2002). Lipid oxidation of muscle foods. In M. D. B. Akoh Casimir C. (Ed.), *Food lipids* (2nd ed., pp. 383-430). New York: Marcel Dekker Inc.

Erickson, M. C., & Sista, R. V. (1996). Influence of microenvironment on oxidative susceptibility of lipids. *Abstracts of Papers of the American Chemical Society, 212*, 76-AGFD.

Estévez, M., Kylli, P., Puolanne, E., Kivikari, R., & Heinonen, M. (2008). Fluorescence spectroscopy as a novel approach for the assessment of myofibrillar protein oxidation in oil-in-water emulsions. *Meat Science, 80*(4), 1290-1296.

Euston, S. R., & Hirst, R. L. (1999). Comparison of the concentration-dependent emulsifying properties of protein products containing aggregated and non-aggregated milk protein. *International Dairy Journal, 9*(10), 693-701.

Fang, Y., & Dalgleish, D. G. (1993). Dimensions of the Adsorbed Layers in Oil-in-Water Emulsions Stabilized by Caseins. *Journal of Colloid and Interface Science, 156*(2), 329-334.

Faraji, H., McClements, D. J., & Decker, E. A. (2004). Role of Continuous Phase Protein on the Oxidative Stability of Fish Oil-in-Water Emulsions. *Journal of Agricultural and Food Chemistry, 52*(14), 4558-4564.

Feng, J., Cai, H., Wang, H., Li, C., & Liu, S. (2018). Improved oxidative stability of fish oil emulsion by grafted ovalbumin-catechin conjugates. *Food Chemistry, 241*, 60-69.

Frankel, E. N. (2012). *Lipid Oxidation* (2nd ed.). Cambridge, UK: Woodhead Publishing.

Frankel, E. N., Huang, S.-W., Aeschbach, R., & Prior, E. (1996). Antioxidant Activity of a Rosemary Extract and Its Constituents, Carnosic Acid, Carnosol, and Rosmarinic

Acid, in Bulk Oil and Oil-in-Water Emulsion. *Journal of Agricultural and Food Chemistry, 44*(1), 131-135.

Frankel, E. N., Satue-Gracia, T., Meyer, A. S., & German, J. B. (2002). Oxidative stability of fish and algae oils containing long-chain polyunsaturated fatty acids in bulk and in oil-in-water emulsions. *Journal of Agricultural and Food Chemistry, 50*(7), 2094-2099.

Freiría-Gándara, J., Losada-Barreiro, S., Paiva-Martins, F., & Bravo-Díaz, C. (2018). Enhancement of the antioxidant efficiency of gallic acid derivatives in intact fish oil-in-water emulsions through optimization of their interfacial concentrations. *Food & Function, 9*(8), 4429-4442.

Gallier, S., Gragson, D., Jimenez-Flores, R., & Everett, D. (2010). Using Confocal Laser Scanning Microscopy To Probe the Milk Fat Globule Membrane and Associated Proteins. *Journal of Agricultural and Food Chemistry, 58*(7), 4250-4257.

Gao, Z.-M., Yang, X.-Q., Wu, N.-N., Wang, L.-J., Wang, J.-M., Guo, J., & Yin, S.-W. (2014). Protein-Based Pickering Emulsion and Oil Gel Prepared by Complexes of Zein Colloidal Particles and Stearate. *Journal of Agricultural and Food Chemistry, 62*(12), 2672-2678.

Gaonkar, A. G., & Borwankar, R. P. (1991). Adsorption behavior of monoglycerides at the vegetable oil/water interface. *Journal of Colloid and Interface Science, 146*(2), 525-532.

Gaziano, J. M., & Hennekens, C. H. (1993). The Role of Beta-Carotene in the Prevention of Cardiovascular Disease. *Annals of the New York Academy of Sciences, 691*(1), 148-155.

Goff, H. D. (1997). Instability and Partial Coalescence in Whippable Dairy Emulsions. *Journal of Dairy Science, 80*(10), 2620-2630.

Golding, M., & Wooster, T. J. (2010). The influence of emulsion structure and stability on lipid digestion. *Current Opinion in Colloid & Interface Science, 15*(1), 90-101.

Gordon, M. H. (1990). The Mechanism of Antioxidant Action in Vitro. In B. J. F. Hudson (Ed.), *Food Antioxidants* (pp. 1-18): Springer Netherlands.

Gould, J., Vieira, J., & Wolf, B. (2013). Cocoa particles for food emulsion stabilisation. *Food & Function, 4*(9), 1369-1375.

Griffin, W. C. (1949). Classification of Surface-active Agents by 'HLB'. *Cosmetic Chemists*(1), 311.

Gu, L., Su, Y., Zhang, M., Chang, C., Li, J., McClements, D. J., & Yang, Y. (2017). Protection of β-carotene from chemical degradation in emulsion-based delivery systems using antioxidant interfacial complexes: Catechin-egg white protein conjugates. *Food Research International, 96*, 84-93.

Gudipati, V., Sandra, S., McClements, D. J., & Decker, E. A. (2010). Oxidative Stability and in Vitro Digestibility of Fish Oil-in-Water Emulsions Containing Multilayered Membranes. *Journal of Agricultural and Food Chemistry, 58*(13), 8093-8099.

Guezey, D., & McClements, D. J. (2006). Influence of environmental stresses on OAV emulsions stabilized by beta-lactoglobulin-pectin and beta-lactoglobulin-pectin-chitosan membranes produced by the electrostatic layer-by-layer deposition technique. *Food Biophysics, 1*(1), 30-40.

Gurkov, T. D., Dimitrova, D. T., Marinova, K. G., Bilke-Crause, C., Gerber, C., & Ivanov, I. B. (2005). Ionic surfactants on fluid interfaces: determination of the adsorption; role of the salt and the type of the hydrophobic phase. *Colloids and Surfaces A: Physicochemical and Engineering Aspects, 261*(1), 29-38.

Gutiérrez, J. M., González, C., Maestro, A., Solè, I., Pey, C. M., & Nolla, J. (2008). Nano-emulsions: New applications and optimization of their preparation. *Current Opinion in Colloid & Interface Science, 13*(4), 245-251.

Guzey, D., & McClements, D. J. (2006). Formation, stability and properties of multilayer emulsions for application in the food industry. *Advances in Colloid and Interface Science, 128-130*, 227-248.

Guzun-Cojocaru, T., Koev, C., Yordanov, M., Karbowiak, T., Cases, E., & Cayot, P. (2011). Oxidative stability of oil-in-water emulsions containing iron chelates: Transfer of iron from chelates to milk proteins at interface. *Food Chemistry, 125*(2), 326-333.

Haahr, A. M., & Jacobsen, C. (2008). Emulsifier type, metal chelation and pH affect oxidative stability of n-3-enriched emulsions. *European Journal of Lipid Science and Technology, 110*(10), 949-961.

Hategekirnana, J., Masamba, K. G., Ma, J., & Zhong, F. (2015). Encapsulation of vitamin E: Effect of physicochemical properties of wall material on retention and stability. *Carbohydrate Polymers, 124*, 172-179.

Hemar, Y., Cheng, L. J., Oliver, C. M., Sanguansri, L., & Augustin, M. (2010). Encapsulation of Resveratrol Using Water-in-Oil-in-Water Double Emulsions. *Food Biophysics, 5*(2), 120-127.

Hsieh, R. J., & Kinsella, J. E. (1989). Oxidation of Polyunsaturated Fatty Acids: Mechanisms, Products, and Inhibition with Emphasis on Fish. In E. K. John (Ed.), *Advances in Food and Nutrition Research* (Vol. 33, pp. 233-341): Academic Press.

Hu, M., McClements, D. J., & Decker, E. A. (2003). Lipid oxidation in corn oil-in-water emulsions stabilized by casein, whey protein isolate, and soy protein isolate. *Journal of Agricultural and Food Chemistry, 51*(6), 1696-1700.

Huang, S.-W., Frankel, E. N., & German, J. B. (1994). Antioxidant activity of .alpha.- and .gamma.-tocopherols in bulk oils and in oil-in-water emulsions. *Journal of Agricultural and Food Chemistry, 42*(10), 2108-2114.

Huang, S.-W., Frankel, E. N., Schwarz, K., Aeschbach, R., & German, J. B. (1996). Antioxidant Activity of Carnosic Acid and Methyl Carnosate in Bulk Oils and Oil-in-Water Emulsions. *Journal of Agricultural and Food Chemistry, 44*(10), 2951-2956.

Iglesias, J., Lois, S., & Medina, I. (2007). Development of a solid-phase microextraction method for determination of volatile oxidation compounds in fish oil emulsions. *Journal of Chromatography A, 1163*(1), 277-287.

Ingold, K. U. (1968). Inhibition of Autoxidation. In *Oxidation of Organic Compounds* (Vol. 75, pp. 296-305): AMERICAN CHEMICAL SOCIETY.

Innis, S. M., & Friesen, R. W. (2008). Essential n-3 fatty acids in pregnant women and early visual acuity maturation in term infants. *American Journal of Clinical Nutrition, 87*(3), 548-557.

Jackson, H. W. (1981). Techniques for flavor and odor evaluation of soy oil. *Journal of the American Oil Chemists' Society, 58*(3), 227-231.

Jacobsen, C., Hartvigsen, K., Lund, P., Thomsen, M. K., Skibsted, L. H., Adler-Nissen, J., . . . Meyer, A. S. (2000). Oxidation in fish oil-enriched mayonnaise3. Assessment of the influence of the emulsion structure on oxidation by discriminant partial least squares regression analysis. *European Food Research and Technology, 211*(2), 86-98.

Jacobsen, C., Schwarz, K., Stöckmann, H., Meyer, A. S., & Adler-Nissen, J. (1999). Partitioning of Selected Antioxidants in Mayonnaise. *Journal of Agricultural and Food Chemistry, 47*(9), 3601-3610.

Jacobsen, C., Timm, M., & Meyer, A. S. (2001). Oxidation in Fish Oil Enriched Mayonnaise: Ascorbic Acid and Low pH Increase Oxidative Deterioration. *Journal of Agricultural and Food Chemistry, 49*(8), 3947-3956.

Jadhav, S., Nimbalkar, S., Kulkarni, A., & Madhavi, D. (1996). Lipid oxidation in biological and food systems. In D. L. Madhavi, D. S.S, & S. D.K (Eds.), *Food Antioxidants: Technological, Toxicolgical & Health Perspectives* (pp. 5-64). Dekker, New York.

Jafari, S. M., Assadpoor, E., He, Y., & Bhandari, B. (2008). Re-coalescence of emulsion droplets during high-energy emulsification. *Food Hydrocolloids, 22*(7), 1191-1202.

Jafari, S. M., He, Y., & Bhandari, B. (2007). Optimization of nano-emulsions production by microfluidization. *European Food Research and Technology, 225*(5), 733-741.

Jo, Y.-J., Chun, J.-Y., Kwon, Y.-J., Min, S.-G., & Choi, M.-J. (2015). Formulation Development of Multilayered Fish Oil Emulsion by using Electrostatic Deposition of Charged Biopolymers. *International Journal of Food Engineering, 11*(1), 31-39.

Johnson, D. R., & Decker, E. A. (2015). The Role of Oxygen in Lipid Oxidation Reactions: A Review. *Annual Review of Food Science and Technology, 6*(1), 171-190.

Johnson, L. E. (1995). Food technology of the antioxidant nutrients. *Critical Reviews in Food Science and Nutrition, 35*(1-2), 149-159.

Kabalnov, A. (2001). Ostwald Ripening and Related Phenomena. *Journal of Dispersion Science and Technology, 22*(1), 1-12.

Kanner, J., German, J. B., Kinsella, J. E., & Hultin, H. O. (1987). Initiation of lipid peroxidation in biological systems. *C R C Critical Reviews in Food Science and Nutrition, 25*(4), 317-364.

Kanofsky, R. J. (2016). Photosensitization. In S. Nonell & C. Flors (Eds.), *Singlet Oxygen: Applications in Biosciences and Nanosciences* (pp. 93-103). Cambridge, UK: Royal Society of Chemistry.

Kargar, M., Spyropoulos, F., & Norton, I. T. (2011). The effect of interfacial microstructure on the lipid oxidation stability of oil-in-water emulsions. *Journal of Colloid and Interface Science, 357*(2), 527-533.

Kartal, C., Unal, M. K., & Otles, S. (2016). Flaxseed Oil-In-Water Emulsions Stabilized by Multilayer Membranes: Oxidative Stability and the Effects of pH. *Journal of Dispersion Science and Technology, 37*(12), 1683-1691.

Katsuda, M. S., McClements, D. J., Miglioranza, L. H. S., & Decker, E. A. (2008). Physical and Oxidative Stability of Fish Oil-in-Water Emulsions Stabilized with β-Lactoglobulin and Pectin. *Journal of Agricultural and Food Chemistry, 56*(14), 5926-5931.

Keller, S., Locquet, N., & Cuvelier, M.-E. (2016). Partitioning of vanillic acid in oil-in-water emulsions: Impact of the Tween®40 emulsifier. *Food Research International, 88*, 61-69.

Kellerby, S. S., Gu, Y. S., McClements, D. J., & Decker, E. A. (2006). Lipid Oxidation in a Menhaden Oil-in-Water Emulsion Stabilized by Sodium Caseinate Cross-Linked with Transglutaminase. *Journal of Agricultural and Food Chemistry, 54*(26), 10222-10227.

Kiralan, S. S., Doğu-Baykut, E., Kittipongpittaya, K., McClements, D. J., & Decker, E. A. (2014). Increased Antioxidant Efficacy of Tocopherols by Surfactant Solubilization in Oil-in-Water Emulsions. *Journal of Agricultural and Food Chemistry, 62*(43), 10561-10566.

Klinkesorn, U., Sophanodora, P., Chinachoti, P., McClements, D. J., & Decker, E. A. (2005). Increasing the Oxidative Stability of Liquid and Dried Tuna Oil-in-Water Emulsions with Electrostatic Layer-by-Layer Deposition Technology. *Journal of Agricultural and Food Chemistry, 53*(11), 4561-4566.

Kolb, G., Viardot, K., Wagner, G., & Ulrich, J. (2001). Evaluation of a New High-Pressure Dispersion Unit (HPN) for Emulsification. *Chemical Engineering & Technology, 24*(3), 293-296.

Komaiko, J., Sastrosubroto, A., & McClements, D. J. (2016). Encapsulation of ω-3 fatty acids in nanoemulsion-based delivery systems fabricated from natural emulsifiers: Sunflower phospholipids. *Food Chemistry, 203*, 331-339.

Laguerre, M., Bayrasy, C., Lecomte, J., Chabi, B., Decker, E. A., Wrutniak-Cabello, C., . . . Villeneuve, P. (2013). How to boost antioxidants by lipophilization? *Biochimie, 95*(1), 20-26.

Laguerre, M., Bily, A., Roller, M., & Birtić, S. (2017). Mass Transport Phenomena in Lipid Oxidation and Antioxidation. *Annual Review of Food Science and Technology, 8*(1), 391-411.

Laguerre, M., Chen, B., Lecomte, J., Villeneuve, P., McClements, D. J., & Decker, E. A. (2011). Antioxidant Properties of Chlorogenic Acid and Its Alkyl Esters in Stripped Corn Oil in Combination with Phospholipids and/or Water. *Journal of Agricultural and Food Chemistry, 59*(18), 10361-10366.

Laguerre, M., López Giraldo, L. J., Lecomte, J., Figueroa-Espinoza, M.-C., Baréa, B., Weiss, J., . . . Villeneuve, P. (2009). Chain Length Affects Antioxidant Properties of Chlorogenate Esters in Emulsion: The Cutoff Theory Behind the Polar Paradox. *Journal of Agricultural and Food Chemistry, 57*(23), 11335-11342.

Laguerre, M., López Giraldo, L. J., Lecomte, J., Figueroa-Espinoza, M.-C., Baréa, B., Weiss, J., . . . Villeneuve, P. (2010). Relationship between Hydrophobicity and Antioxidant Ability of “Phenolipids” in Emulsion: A Parabolic Effect of the Chain Length of Rosmarinate Esters. *Journal of Agricultural and Food Chemistry, 58*(5), 2869-2876.

Lee, J. H., & Jung, M. Y. (2010). Direct Spectroscopic Observation of Singlet Oxygen Quenching and Kinetic Studies of Physical and Chemical Singlet Oxygen Quenching Rate Constants of Synthetic Antioxidants (BHA, BHT, and TBHQ) in Methanol. *Journal of Food Science, 75*(6), C506-C513.

Lee, S. H., Yamaguchi, K., Kim, J. S., Eling, T. E., Safe, S., Park, Y., & Baek, S. J. (2006). Conjugated linoleic acid stimulates an anti-tumorigenic protein NAG-1 in an isomer specific manner. *Carcinogenesis, 27*(5), 972-981.

Lee, S. J., Choi, S. J., Li, Y., Decker, E. A., & McClements, D. J. (2011). Protein-Stabilized Nanoemulsions and Emulsions: Comparison of Physicochemical Stability, Lipid Oxidation, and Lipase Digestibility. *Journal of Agricultural and Food Chemistry, 59*(1), 415-427.

Lesmes, U., Sandra, S., Decker, E. A., & McClements, D. J. (2010). Impact of surface deposition of lactoferrin on physical and chemical stability of omega-3 rich lipid droplets stabilised by caseinate. *Food Chemistry, 123*(1), 99-106.

Lethuaut, L., Métro, F., & Genot, C. (2002). Effect of droplet size on lipid oxidation rates of oil-in-water emulsions stabilized by protein. *Journal of the American Oil Chemists' Society, 79*(5), 425-430.

Li, Y., Kong, B., Liu, Q., Xia, X., & Chen, H. (2017). Improvement of the emulsifying and oxidative stability of myofibrillar protein prepared oil-in-water emulsions by addition of zein hydrolysates. *Process Biochemistry, 53*, 116-124.

Liu, F., Wang, D., Sun, C., McClements, D. J., & Gao, Y. (2016). Utilization of interfacial engineering to improve physicochemical stability of β-carotene emulsions: Multilayer coatings formed using protein and protein–polyphenol conjugates. *Food Chemistry, 205*, 129-139.

Logan, A., Nienaber, U., & Pan, X. (2013). *Lipid oxidation : challenges in food systems*: Urbana, Illinois : AOCS Press, [2013].

López-Montilla, J. C., Herrera-Morales, P. E., Pandey, S., & Shah, D. O. (2002). Spontaneous Emulsification: Mechanisms, Physicochemical Aspects, Modeling, and Applications. *Journal of Dispersion Science and Technology, 23*(1-3), 219-268.

Losada Barreiro, S., Bravo-Díaz, C., Paiva-Martins, F., & Romsted, L. S. (2013). Maxima in Antioxidant Distributions and Efficiencies with Increasing Hydrophobicity of Gallic Acid and Its Alkyl Esters. The Pseudophase Model Interpretation of the “Cutoff Effect”. *Journal of Agricultural and Food Chemistry, 61*(26), 6533-6543.

Lu, W., Kelly, A. L., Maguire, P., Zhang, H., Stanton, C., & Miao, S. (2016). Correlation of Emulsion Structure with Cellular Uptake Behavior of Encapsulated Bioactive Nutrients: Influence of Droplet Size and Interfacial Structure. *Journal of Agricultural and Food Chemistry, 64*(45), 8659-8666.

Mahdi Jafari, S., He, Y., & Bhandari, B. (2006). Nano-Emulsion Production by Sonication and Microfluidization—A Comparison. *International Journal of Food Properties, 9*(3), 475-485.

Mancuso, J. R., McClements, D. J., & Decker, E. A. (1999). The Effects of Surfactant Type, pH, and Chelators on the Oxidation of Salmon Oil-in-Water Emulsions. *Journal of Agricultural and Food Chemistry, 47*(10), 4112-4116.

Marciani, L., Wickham, M., Singh, G., Bush, D., Pick, B., Cox, E., . . . Spiller, R. C. (2007). Enhancement of intragastric acid stability of a fat emulsion meal delays gastric emptying and increases cholecystokinin release and gallbladder contraction. *American Journal of Physiology-Gastrointestinal and Liver Physiology, 292*(6), G1607-G1613.

Marie, P., Perrier-Cornet, J. M., & Gervais, P. (2002). Influence of major parameters in emulsification mechanisms using a high-pressure jet. *Journal of Food Engineering, 53*(1), 43-51.

Martínez-Palou, R., Mosqueira, M. d. L., Zapata-Rendón, B., Mar-Juárez, E., Bernal-Huicochea, C., de la Cruz Clavel-López, J., & Aburto, J. (2011). Transportation of heavy and extra-heavy crude oil by pipeline: A review. *Journal of Petroleum Science and Engineering, 75*(3), 274-282.

Martirosyan, D. M., & Singh, J. (2015). A new definition of functional food by FFC: what makes a new definition unique? *Functional Foods in Health and Disease, 5*(6), 209-223.

Matos, M., Gutiérrez, G., Coca, J., & Pazos, C. (2014). Preparation of water-in-oil-in-water (W1/O/W2) double emulsions containing trans-resveratrol. *Colloids and Surfaces A: Physicochemical and Engineering Aspects, 442*, 69-79.

Matsumoto, S. (1983). Development of W/O/W-type dispersion during phase inversion of concentrated w/o emulsions. *Journal of Colloid and Interface Science, 94*(2), 362-368.

Matsumoto, S. (1985). Formation and stability of water-in-oil-in-water emulsions. *Acs Symposium Series, 272*, 415-436.

Matsumoto, S. (1986). W/O/W-type multiple emulsions with a view to possible food applications1. *Journal of Texture Studies, 17*(2), 141-159.

Matsumoto, S., Koh, Y., & Michiura, A. (1985). Preparation of w/o/w emulsions in an edible form on the basis of phase inversion technique. *Journal of Dispersion Science and Technology, 6*(5), 507-521.

McClements, D. J. (2004). Protein-stabilized emulsions. *Current Opinion in Colloid & Interface Science, 9*(5), 305-313.

McClements, D. J. (2005). *Food emulsions: Principles, practices and techniques* (2nd ed.). Boca Raton: CRC press, (Chapter 6).

McClements, D. J. (2010). Emulsion Design to Improve the Delivery of Functional Lipophilic Components. *Annual Review of Food Science and Technology, 1*(1), 241-269.

McClements, D. J. (2012). Nanoemulsions versus microemulsions: terminology, differences, and similarities. *Soft Matter, 8*(6), 1719-1729.

McClements, D. J. (2015a). *Food Emulsions*. Boca Raton, UNITED STATES: CRC Press.

McClements, D. J. (2015b). *Food Emulsions : Principles, Practices, and Techniques, Third Edition*. Boca Raton, UNITED KINGDOM: Chapman and Hall/CRC.

McClements, D. J., & Decker, E. A. (2000). Lipid Oxidation in Oil-in-Water Emulsions: Impact of Molecular Environment on Chemical Reactions in Heterogeneous Food Systems. *Journal of Food Science, 65*(8), 1270-1282.

McClements, D. J., Decker, E. A., & Weiss, J. (2007). Emulsion-Based Delivery Systems for Lipophilic Bioactive Components. *Journal of Food Science, 72*(8), R109-R124.

McClements, D. J., & Li, Y. (2010). Structured emulsion-based delivery systems: Controlling the digestion and release of lipophilic food components. *Advances in Colloid and Interface Science, 159*(2), 213-228.

McClements, D. J., & Weiss, J. (2005). Lipid Emulsions. In *Bailey's Industrial Oil and Fat Products*: John Wiley & Sons, Inc.

Mezdour, S., Lepine, A., Erazo-Majewicz, P., Ducept, F., & Michon, C. (2008). Oil/water surface rheological properties of hydroxypropyl cellulose (HPC) alone and mixed with lecithin: Contribution to emulsion stability. *Colloids and Surfaces A: Physicochemical and Engineering Aspects, 331*(1-2), 76-83.

Min, D. B., & Boff, J. M. (2002a). Chemistry and Reaction of Singlet Oxygen in Foods. *Comprehensive Reviews in Food Science and Food Safety, 1*(2), 58-72.

Min, D. B., & Boff, J. M. (2002b). Lipid oxidation of edible oil. In M. D. B. Akoh Casimir C. (Ed.), *Food Lipids* (2nd ed., pp. 353- 381). New York: Marcel Dekker Inc.

Mozaffarian, D., & Wu, J. H. Y. (2011). Omega-3 Fatty Acids and Cardiovascular Disease: Effects on Risk Factors, Molecular Pathways, and Clinical Events. *Journal of the American College of Cardiology, 58*(20), 2047-2067.

Mulvihill, D. M., & Murphy, P. C. (1991). Surface active and emulsifying properties of caseins/caseinates as influenced by state of aggregation. *International Dairy Journal, 1*(1), 13-37.

Muschiolik, G. (2007). Multiple emulsions for food use. *Current Opinion in Colloid & Interface Science, 12*(4–5), 213-220.

Nadin, M., Rousseau, D., & Ghosh, S. (2014). Fat crystal-stabilized water-in-oil emulsions as controlled release systems. *LWT - Food Science and Technology, 56*(2), 248-255.

Nakaya, K., Ushio, H., Matsukawa, S., Shimizu, M., & Ohshima, T. (2005). Effects of droplet size on the oxidative stability of oil-in-water emulsions. *Lipids, 40*(5), 501-507.

Naz, S., Siddiqi, R., Sheikh, H., & Sayeed, S. A. (2005). Deterioration of olive, corn and soybean oils due to air, light, heat and deep-frying. *Food Research International, 38*(2), 127-134.

Norn, V. (2014). Introduction to Food Emulsifiers and Colloidal System. In *Emulsifiers in Food Technology* (pp. 1-20): John Wiley & Sons, Ltd.

Nuchi, C. D., Hernandez, P., McClements, D. J., & Decker, E. A. (2002). Ability of Lipid Hydroperoxides To Partition into Surfactant Micelles and Alter Lipid Oxidation Rates in Emulsions. *Journal of Agricultural and Food Chemistry, 50*(19), 5445-5449.

O' Dwyer, S. P., O' Beirne, D., Eidhin, D. N., & O' Kennedy, B. T. (2013). Effects of sodium caseinate concentration and storage conditions on the oxidative stability of oil-in-water emulsions. *Food Chemistry, 138*(2), 1145-1152.

Ogawa, S., Decker, E. A., & McClements, D. J. (2003). Influence of Environmental Conditions on the Stability of Oil in Water Emulsions Containing Droplets Stabilized by Lecithin−Chitosan Membranes. *Journal of Agricultural and Food Chemistry, 51*(18), 5522-5527.

Okuda, S., McClements, D. J., & Decker, E. A. (2005). Impact of Lipid Physical State on the Oxidation of Methyl Linolenate in Oil-in-Water Emulsions. *Journal of Agricultural and Food Chemistry, 53*(24), 9624-9628.

Olson, D. W., White, C. H., & Richter, R. L. (2004). Effect of Pressure and Fat Content on Particle Sizes in Microfluidized Milk*. *Journal of Dairy Science, 87*(10), 3217-3223.

Osborn, H. T., & Akoh, C. C. (2004). Effect of emulsifier type, droplet size, and oil concentration on lipid oxidation in structured lipid-based oil-in-water emulsions. *Food Chemistry, 84*(3), 451-456.

Panya, A., Laguerre, M., Bayrasy, C., Lecomte, J., Villeneuve, P., McClements, D. J., & Decker, E. A. (2012). An Investigation of the Versatile Antioxidant Mechanisms of Action of Rosmarinate Alkyl Esters in Oil-in-Water Emulsions. *Journal of Agricultural and Food Chemistry, 60*(10), 2692-2700.

Pastoriza-Gallego, M. J., Sánchez-Paz, V., Losada-Barreiro, S., Bravo-Díaz, C., Gunaseelan, K., & Romsted, L. S. (2009). Effects of Temperature and Emulsifier Concentration on α-Tocopherol Distribution in a Stirred, Fluid, Emulsion. Thermodynamics of α-Tocopherol Transfer between the Oil and Interfacial Regions. *Langmuir, 25*(5), 2646-2653.

Patel, H., Patel, S., & Agarwal, S. (2014). Milk protein concentrates: Manufacturing and applications. *US Dairy Export Council*, 3-4.

Pekkarinen, S. S., Stöckmann, H., Schwarz, K., Heinonen, I. M., & Hopia, A. I. (1999). Antioxidant Activity and Partitioning of Phenolic Acids in Bulk and Emulsified Methyl Linoleate. *Journal of Agricultural and Food Chemistry, 47*(8), 3036-3043.

Phan, T. T. Q., Le, T. T., Van de Walle, D., Van der Meeren, P., & Dewettinck, K. (2016). Combined effects of milk fat globule membrane polar lipids and protein concentrate on the stability of oil-in-water emulsions. *International Dairy Journal, 52*, 42-49.

Pickering, S. U. (1907). CXCVI.-Emulsions. *Journal of the Chemical Society, Transactions, 91*(0), 2001-2021.

Pinheiro, A. C., Coimbra, M. A., & Vicente, A. A. (2016). In vitro behaviour of curcumin nanoemulsions stabilized by biopolymer emulsifiers – Effect of interfacial composition. *Food Hydrocolloids, 52*, 460-467.

Piorkowski, D. T., & McClements, D. J. (2013). Beverage emulsions: Recent developments in formulation, production, and applications. *Food Hydrocolloids*.

Ponginebbi, L., Nawar, W. W., & Chinachoti, P. (1999). Oxidation of linoleic acid in emulsions: Effect of substrate, emulsifier, and sugar concentration. *Journal of the American Oil Chemists' Society, 76*(1), 131.

Porter, W. L., Black, E. D., & Drolet, A. M. (1989). Use of polyamide oxidative fluorescence test on lipid emulsions: contrast in relative effectiveness of antioxidants in bulk versus dispersed systems. *Journal of Agricultural and Food Chemistry, 37*(3), 615-624.

Qian, C., Decker, E. A., Xiao, H., & McClements, D. J. (2012). Nanoemulsion delivery systems: Influence of carrier oil on β-carotene bioaccessibility. *Food Chemistry, 135*(3), 1440-1447.

Qian, C., & McClements, D. J. (2011). Formation of nanoemulsions stabilized by model food-grade emulsifiers using high-pressure homogenisation: Factors affecting particle size. *Food Hydrocolloids, 25*(5), 1000-1008.

Rajalakshmi, D., & Narasimhan, S. (1995). Food antioxidants: Sources and Methods of Evaluation. In D. L. Madhavi, S. S. Deshpande, & D. K. Salunkhe (Eds.), *Food Antioxidants: Technological, Toxicological and Health Perspectives* (pp. 65-157). New York: Marcel Dekker Inc.

Rao, J., & McClements, D. J. (2011). Food-grade microemulsions, nanoemulsions and emulsions: Fabrication from sucrose monopalmitate & lemon oil. *Food Hydrocolloids, 25*(6), 1413-1423.

Rao, V., & Agarwal, S. (2000). Role of Antioxidant Lycopene in Cancer and Heart Disease. *Journal of the American College of Nutrition, 19*(5), 563-569.

Raudsepp, P., Brüggemann, D. A., & Andersen, M. L. (2014). Evidence for Transfer of Radicals between Oil-in-Water Emulsion Droplets as Detected by the Probe (E,E)-3,5-Bis(4-phenyl-1,3-butadienyl)-4,4-difluoro-4-bora-3a,4a-diaza-s-indacene, BODIPY665/676. *Journal of Agricultural and Food Chemistry, 62*(51), 12428-12435.

Rayner, M., Sjöö, M., Timgren, A., & Dejmek, P. (2012). Quinoa starch granules as stabilizing particles for production of Pickering emulsions. *Faraday Discussions, 158*(0), 139-155.

Reische, D. W., Lillard, D. A., & Eitenmiller, R. R. (2002). Antioxidants. In A. C. Casimir & D. B. Min (Eds.), *Food Lipids: Chemistry, Nutrition, and Biotechnology* (second ed., pp. 507-534). New York: Marcel dekker.

Repetto, M., Boveris, A., & Semprine, J. (2012). *Lipid peroxidation: chemical mechanism, biological implications and analytical determination*: INTECH Open Access Publisher.

Ribaya-Mercado, J. D., & Blumberg, J. B. (2004). Lutein and Zeaxanthin and Their Potential Roles in Disease Prevention. *Journal of the American College of Nutrition, 23*(sup6), 567S-587S.

Robin, O., Blanchot, V., Vuillemard, J., C., & Paquin, P. (1992). Microfluidization of dairy model emulsions. I. Preparation of emulsions and influence of processing and formulation on the size distribution of milk fat globules. *Lait, 72*(6), 511-531.

Rosen, M. J., & Kunjappu, J. T. (2012). Characteristic Features of Surfactants. In *Surfactants and Interfacial Phenomena* (pp. 1-38): John Wiley & Sons, Inc.

Salvia-Trujillo, L., Qian, C., Martín-Belloso, O., & McClements, D. J. (2013). Influence of particle size on lipid digestion and β-carotene bioaccessibility in emulsions and nanoemulsions. *Food Chemistry, 141*(2), 1472-1480.

Sarkar, A., Goh, K. K. T., Singh, R. P., & Singh, H. (2009). Behaviour of an oil-in-water emulsion stabilized by β-lactoglobulin in an in vitro gastric model. *Food Hydrocolloids, 23*(6), 1563-1569.

Sasaki, K., Alamed, J., Weiss, J., Villeneuve, P., López Giraldo, L. J., Lecomte, J., . . . Decker, E. A. (2010). Relationship between the physical properties of chlorogenic acid esters and their ability to inhibit lipid oxidation in oil-in-water emulsions. *Food Chemistry, 118*(3), 830-835.

Schillaci, C., Nepravishta, R., & Bellomaria, A. (2014). Antioxidants in food and pharmaceutical research. *Albanian Journal of Pharmaceutical Sciences, 1*(1), 9-15.

Shah, B. R., Zhang, C., Li, Y., & Li, B. (2016). Bioaccessibility and antioxidant activity of curcumin after encapsulated by nano and Pickering emulsion based on chitosan-tripolyphosphate nanoparticles. *Food Research International, 89*, 399-407.

Shahidi, F., & Wanasundara, U. (2008). Methods for measuring oxidative rancidity in fats and oils. In M. D. B. Akoh Casimir C. (Ed.), *Food lipids: Chemistry, Nutrition and Biotechnology* (3rd ed.): CRC press.

Shahidi, F., Wanasundara, U., & Brunet, N. (1994). Oxidative stability of oil from blubber of harp seal (Phoca groenlandica) as assessed by NMR and standard procedures. *Food Research International, 27*(6), 555-562.

Shahidi, F., & Zhong, Y. (2005). Lipid Oxidation: Measurement Methods. In *Bailey's Industrial Oil and Fat Products*: John Wiley & Sons, Inc.

Shahidi, F., & Zhong, Y. (2011). Revisiting the Polar Paradox Theory: A Critical Overview. *Journal of Agricultural and Food Chemistry, 59*(8), 3499-3504.

Shi, Y., Liang, B., & Hartel, R. W. (2005). Crystal morphology, microstructure, and textural properties of model lipid systems. *Journal of the American Oil Chemists' Society, 82*(6), 399-408.

Silvestre, M. P. C., Chaiyasit, W., Brannan, R. G., McClements, D. J., & Decker, E. A. (2000). Ability of Surfactant Headgroup Size To Alter Lipid and Antioxidant Oxidation in Oil-in-Water Emulsions. *Journal of Agricultural and Food Chemistry, 48*(6), 2057-2061.

Singh, H. (2011). Aspects of milk-protein-stabilised emulsions. *Food Hydrocolloids, 25*(8), 1938-1944.

Singh, H., & Sarkar, A. (2011). Behaviour of protein-stabilised emulsions under various physiological conditions. *Advances in Colloid and Interface Science, 165*(1), 47-57.

Singh, H., Tamehana, M., Hemar, Y., & Munro, P. A. (2003). Interfacial compositions, microstructure and stability of oil-in-water emulsions formed with mixtures of milk proteins and κ-carrageenan: 2. Whey protein isolate (WPI). *Food Hydrocolloids, 17*(4), 549-561.

Singh, H., & Ye, A. (2008). Interactions and Functionality of Milk Proteins in Food Emulsions. In *Milk Proteins* (pp. 321-345).

Singh, H.; Ye, A.; Zhu, X. Q. (2011) Emulsion. *U.S. patent PCT/WO2011/136662*.

Solans, C., Izquierdo, P., Nolla, J., Azemar, N., & Garcia-Celma, M. J. (2005). Nano-emulsions. *Current Opinion in Colloid & Interface Science, 10*(3–4), 102-110.

Sørensen, A.-D. M., Nielsen, N. S., Decker, E. A., Let, M. B., Xu, X., & Jacobsen, C. (2011). The Efficacy of Compounds with Different Polarities as Antioxidants in

Emulsions with Omega-3 Lipids. *Journal of the American Oil Chemists' Society, 88*(4), 489-502.

Spicer, P. T., & Hartel, R. W. (2005). Crystal Comets: Dewetting During Emulsion Droplet Crystallization. *Australian Journal of Chemistry, 58*(9), 655-659.

Stöckmann, H., & Schwarz, K. (1999). Partitioning of Low Molecular Weight Compounds in Oil-in-Water Emulsions. *Langmuir, 15*(19), 6142-6149.

Stöckmann, H., Schwarz, K., & Huynh-Ba, T. (2000). The influence of various emulsifiers on the partitioning and antioxidant activity of hydroxybenzoic acids and their derivatives in oil-in-water emulsions. *Journal of the American Oil Chemists' Society, 77*(5), 535-542.

Sugiarto, M., Ye, A., Taylor, M. W., & Singh, H. (2010). Milk protein-iron complexes: Inhibition of lipid oxidation in an emulsion. *Dairy Sci. Technol., 90*(1), 87-98.

Surh, J., Decker, E. A., & McClements, D. J. (2006). Influence of pH and pectin type on properties and stability of sodium-caseinate stabilized oil-in-water emulsions. *Food Hydrocolloids, 20*(5), 607-618.

Tadros, T. (2013). Food Surfactants. In T. Tadros (Ed.), *Encyclopedia of Colloid and Interface Science* (pp. 555-556): Springer Berlin Heidelberg.

Tadros, T., Izquierdo, P., Esquena, J., & Solans, C. (2004). Formation and stability of nano-emulsions. *Advances in Colloid and Interface Science, 108–109*, 303-318.

Tadros, T. F. (2014). *An Introduction to Surfactants*. Berlin: De Gruyter.

Tan, & Nakajima, M. (2005). β-Carotene nanodispersions: preparation, characterization and stability evaluation. *Food Chemistry, 92*(4), 661-671.

Tan, Xu, K., Niu, C., Liu, C., Li, Y., Wang, P., & Binks, B. P. (2014). Triglyceride–water emulsions stabilised by starch-based nanoparticles. *Food Hydrocolloids, 36*, 70-75.

Taylor, P. (1998). Ostwald ripening in emulsions. *Advances in Colloid and Interface Science, 75*(2), 107-163.

Thanasukarn, P., Pongsawatmanit, R., & McClements, D. J. (2006). Utilization of layer-by-layer interfacial deposition technique to improve freeze-thaw stability of oil-in-water emulsions. *Food Research International, 39*(6), 721-729.

Tokle, T., Mao, Y., & McClements, D. J. (2013). Potential Biological Fate of Emulsion-Based Delivery Systems: Lipid Particles Nanolaminated with Lactoferrin and beta-lactoglobulin Coatings. *Pharmaceutical Research, 30*(12), 3200-3213.

Tornberg, E. (1980). Functional characteristics of protein stabilized emulsions: emulsifying behavior of proteins in a sonifier. *Journal of Food Science, 45*(6), 1662-1668.

Tschirner, N., Schenderlein, M., Brose, K., Schlodder, E., Mroginski, M. A., Hildebrandt, P., & Thomsen, C. (2008). Raman excitation profiles of β -carotene – novel insights into the nature of the v1-band. *physica status solidi (b), 245*(10), 2225-2228.

Tucker, J. M., & Townsend, D. M. (2005). Alpha-tocopherol: roles in prevention and therapy of human disease. *Biomedicine & Pharmacotherapy, 59*(7), 380-387.

Uauy, R., Hoffman, D. R., Peirano, P., Birch, D. G., & Birch, E. E. (2001). Essential fatty acids in visual and brain development. *Lipids, 36*(9), 885-895.

Vauzour, D., Rodriguez-Mateos, A., Corona, G., Oruna-Concha, M. J., & Spencer, J. P. E. (2010). Polyphenols and Human Health: Prevention of Disease and Mechanisms of Action. *Nutrients, 2*(11), 1106.

von Staszewski, M., Pizones Ruiz-Henestrosa, V. M., & Pilosof, A. M. R. (2014). Green tea polyphenols-β-lactoglobulin nanocomplexes: Interfacial behavior, emulsification and oxidation stability of fish oil. *Food Hydrocolloids, 35*, 505-511.

Walker, R., Decker, E. A., & McClements, D. J. (2015). Development of food-grade nanoemulsions and emulsions for delivery of omega-3 fatty acids: opportunities and obstacles in the food industry. *Food & Function, 6*(1), 41-54.

Walstra, P. (1993). Principles of emulsion formation. *Chemical Engineering Science, 48*(2), 333-349.

Walstra, P. (2003). *Physical Chemistry of Foods*. New york: Marcel Dekker.

Wan, Z.-L., Wang, J.-M., Wang, L.-Y., Yuan, Y., & Yang, X.-Q. (2014). Complexation of resveratrol with soy protein and its improvement on oxidative stability of corn oil/water emulsions. *Food Chemistry, 161*, 324-331.

Wanasundara, U. N., Shahidi, F., & Jablonski, C. R. (1995). Comparison of standard and NMR methodologies for assessment of oxidative stability of canola and soybean oils. *Food Chemistry, 52*(3), 249-253.

Wang, L.-J., Hu, Y.-Q., Yin, S.-W., Yang, X.-Q., Lai, F.-R., & Wang, S.-Q. (2015). Fabrication and Characterization of Antioxidant Pickering Emulsions Stabilized by Zein/Chitosan Complex Particles (ZCPs). *Journal of Agricultural and Food Chemistry, 63*(9), 2514-2524.

Wang, L., Gao, Y., Li, J., Subirade, M., Song, Y., & Liang, L. (2016). Effect of resveratrol or ascorbic acid on the stability of alpha-tocopherol in O/W emulsions stabilized by whey protein isolate: Simultaneous encapsulation of the vitamin and the protective antioxidant. *Food Chemistry, 196*, 466-474.

Waraho, T., McClements, D. J., & Decker, E. A. (2011). Mechanisms of lipid oxidation in food dispersions. *Trends in Food Science & Technology, 22*(1), 3-13.

Weers, J. (1998). Molecular diffusion in emulsions and emulsion mixtures. In *Modern aspects of emulsion science* (pp. 292-327). Cambridge, Uk: The Royal Society of Chemistry.

Westesen, K., & Bunjes, H. (1995). Do nanoparticles prepared from lipids solid at room temperature always possess a solid lipid matrix? *International Journal of Pharmaceutics, 115*(1), 129-131.

Wheatley, R. A. (2000). Some recent trends in the analytical chemistry of lipid peroxidation. *TrAC Trends in Analytical Chemistry, 19*(10), 617-628.

White, P. (1995). Conjugated diene, anisidine value, and carbonyl value analyses. *Methods to assess quality and stability of oils and fat-containing foods*, 159-178.

Wooster, T. J., & Augustin, M. A. (2006). β-Lactoglobulin–dextran Maillard conjugates: Their effect on interfacial thickness and emulsion stability. *Journal of Colloid and Interface Science, 303*(2), 564-572.

Wooster, T. J., Golding, M., & Sanguansri, P. (2008). Impact of Oil Type on Nanoemulsion Formation and Ostwald Ripening Stability. *Langmuir, 24*(22), 12758-12765.

Wrolstad, E. R., Acree, E. T., Decker, E. A., Penner, M. H., Reid, D. S., Schwartz, J. S., . . . Sporns, P. (Eds.). (2005). *Handbook of Food Analytical chemistry*. New Jersey: John wiley & sons Inc.

Yang, Y., & McClements, D. J. (2013). Encapsulation of vitamin E in edible emulsions fabricated using a natural surfactant. *Food Hydrocolloids, 30*(2), 712-720.

Yao, M., Xiao, H., & McClements, D. J. (2014). Delivery of Lipophilic Bioactives: Assembly, Disassembly, and Reassembly of Lipid Nanoparticles. *Annual Review of Food Science and Technology, 5*(1), 53-81.

Yasaei, P. M., Yang, G. C., Warner, C. R., Daniels, D. H., & Ku, Y. (1996). Singlet oxygen oxidation of lipids resulting from photochemical sensitizers in the presence of antioxidants. *Journal of the American Oil Chemists' Society, 73*(9), 1177-1181.

Ye, A. (2011). Functional properties of milk protein concentrates: Emulsifying properties, adsorption and stability of emulsions. *International Dairy Journal, 21*(1), 14-20.

Ye, A., Srinivasan, M., & Singh, H. (2000). Influence of NaCl addition on the properties of emulsions formed with commercial calcium caseinate. *Food Chemistry, 69*(3), 237-244.

Ye, A., Zhu, X., & Singh, H. (2013). Oil-in-Water Emulsion System Stabilized by Protein-Coated Nanoemulsion Droplets. *Langmuir, 29*(47), 14403-14410.

Yeong, L. H., & So Bong, J. (2010). Effects of conjugated linoleic acid on body fat reduction and physical exercise enhancement of obese male middle school students. *Korean Journal of Life Science, 20*(12), 1844-1850.

Yi, J., Li, Y., Zhong, F., & Yokoyama, W. (2014). The physicochemical stability and in vitro bioaccessibility of beta-carotene in oil-in-water sodium caseinate emulsions. *Food Hydrocolloids, 35*, 19-27.

Yi, J., Li, Y., Zhong, F., & Yokoyama, W. (2015). The physicochemical stability and in vitro bioaccessibility of beta- carotene in oil- in-water sodium caseinate emulsions (vol 35, pg 19, 2014). *Food Hydrocolloids, 51*, 519-519.

Yoshida, Y., & Niki, E. (1992). Oxidation of methyl linoleate in aqueous dispersions induced by copper and iron. *Archives of Biochemistry and Biophysics, 295*(1), 107-114.

Yuji, H., Weiss, J., Villeneuve, P., López Giraldo, L. J., Figueroa-Espinoza, M.-C., & Decker, E. A. (2007). Ability of Surface-Active Antioxidants To Inhibit Lipid Oxidation in Oil-in-Water Emulsion. *Journal of Agricultural and Food Chemistry, 55*(26), 11052-11056.

Yusoff, A., & Murray, B. S. (2011). Modified starch granules as particle-stabilizers of oil-in-water emulsions. *Food Hydrocolloids, 25*(1), 42-55.

Zhong, Y., & Shahidi, F. (2012). Antioxidant Behavior in Bulk Oil: Limitations of Polar Paradox Theory. *Journal of Agricultural and Food Chemistry, 60*(1), 4-6.

Appendix A (chapter 4)

A.1 Exploring uniform interfacial droplet stabilisation with MPC shell emulsions processed via the microfluidizer

The role of MPC concentration and pre-heating MPC solution prior to emulsification of shell emulsions with the microfluidizer on excessive aggregation experienced with high calcium MPCs was investigated. The effect of applying low and high pressures during emulsification was also observed. Particle size distribution and confocal microscopy images of shell and droplet-stabilised emulsions (DSEs) produced with MPC concentrations of 2%, 4% and 6% (w/w) either pre-heated or not pre-heated and passed via the microfluidizer either at 300 or 1700 bar are shown in below.

When MPC solution (4% w/w) was not pre-heated and processed at 1700 bar, droplet stabilisation improved but there was still excessive shell droplet aggregation which prevented uniform droplet stabilisation (Figure A-2). The same effect was observed when MPC solution of 2% w/w was pre-heated prior to emulsification at the same pressure (Figure A-3). Shell emulsions processed with pre-heated MPC solution (6% w/w) at 300 bar gave the most promising results but excessive aggregation still prevented uniform droplet stabilisation (Figure A-4).

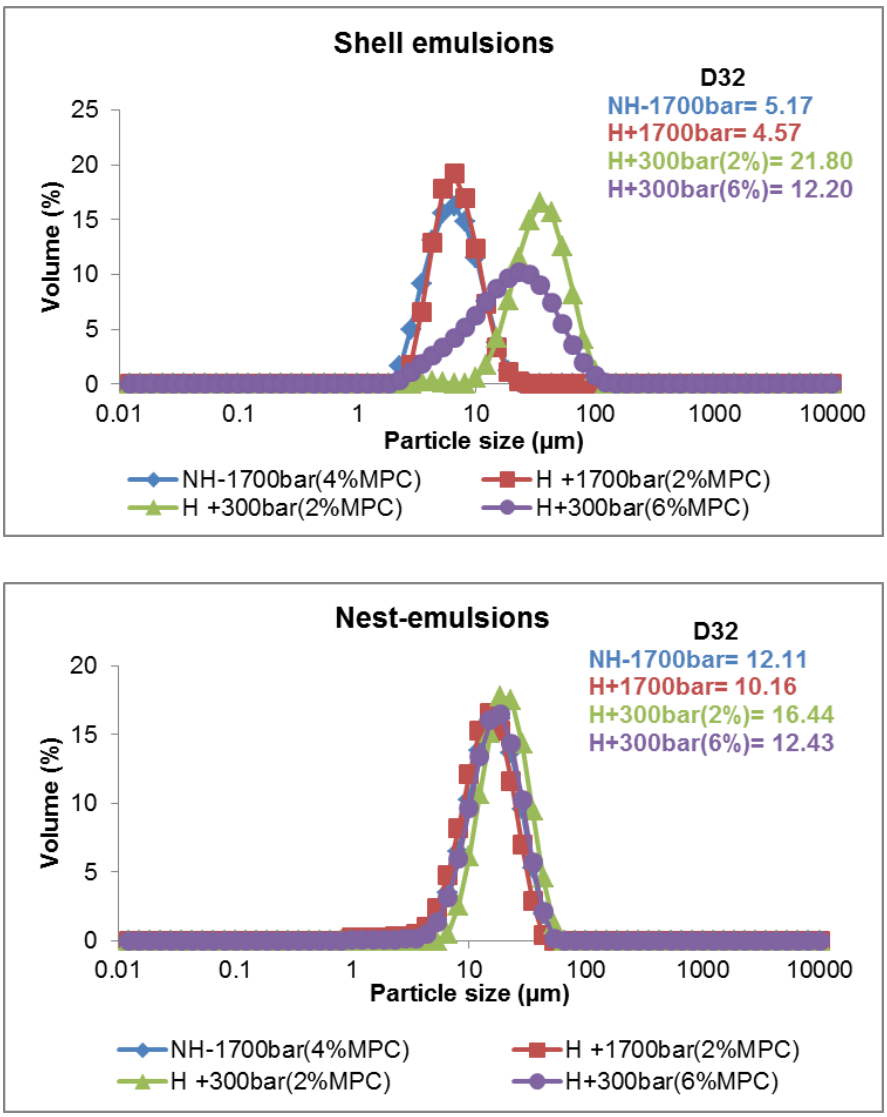

Figure A-1 *Particle size distribution of shell and droplet-stabilised emulsions processed with high calcium MPCs (NH= MPC solution not pre-heated, H= MPC solution pre-heated)*

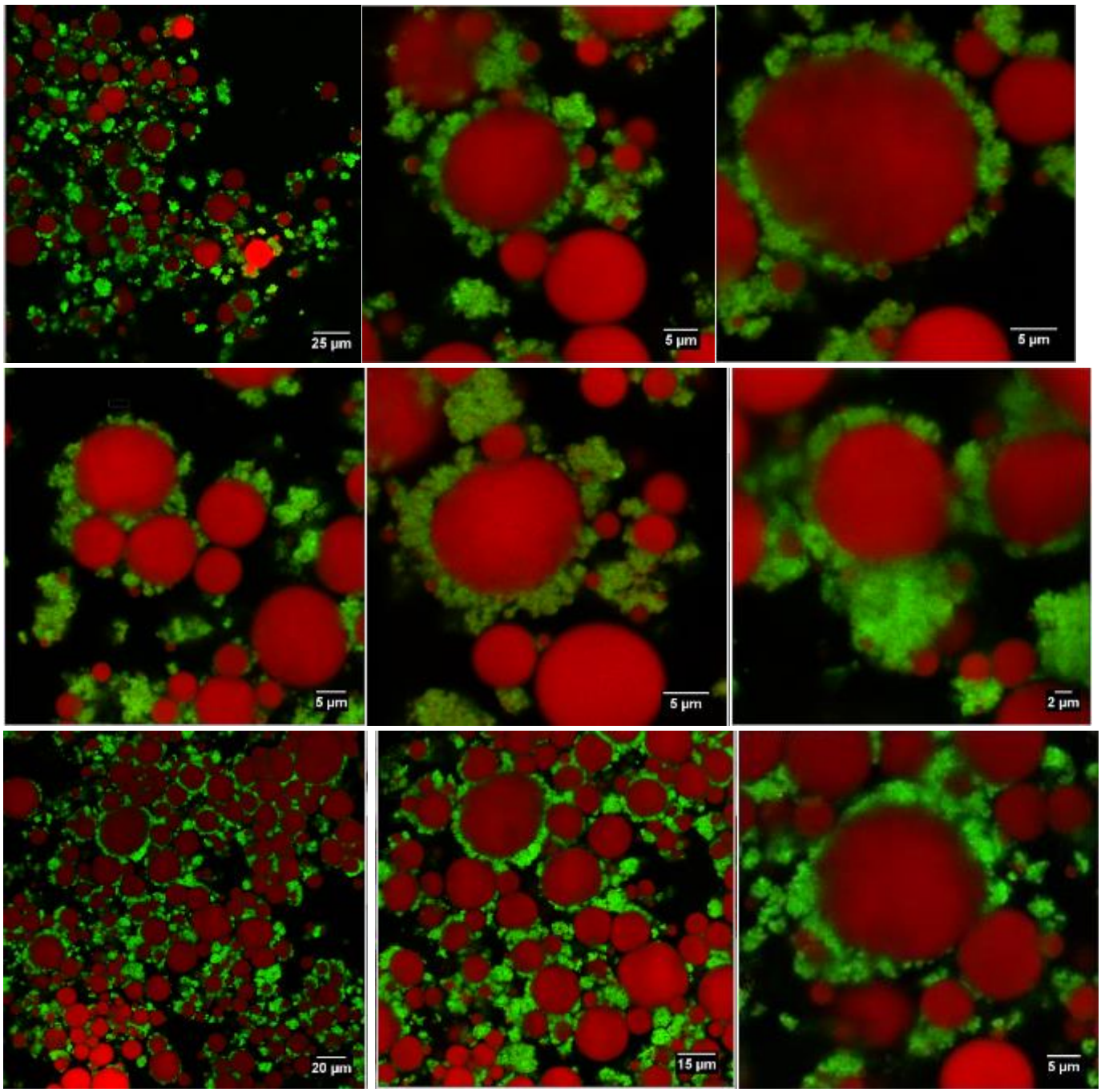

Figure A-2 *Droplet-stabilised emulsions - (10% shell- 4% MPC), MPC solution not-pre-heated processed at 1700 bar (25000 psi).*

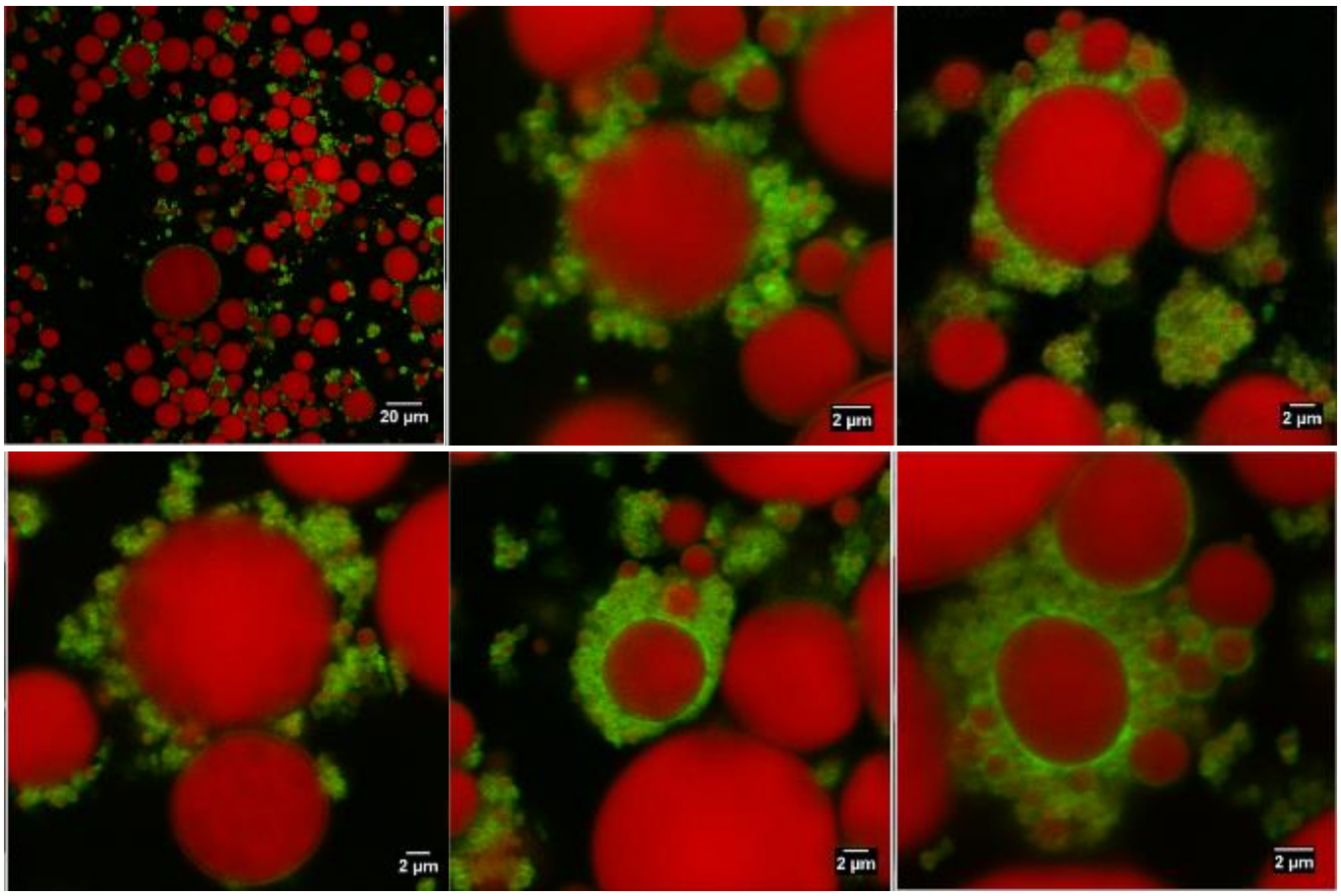

Figure A-3 *Droplet-stabilised emulsions (10% shell-2%MPC); MPC solution pre-heated; processed at 1700 bar (25000 psi).*

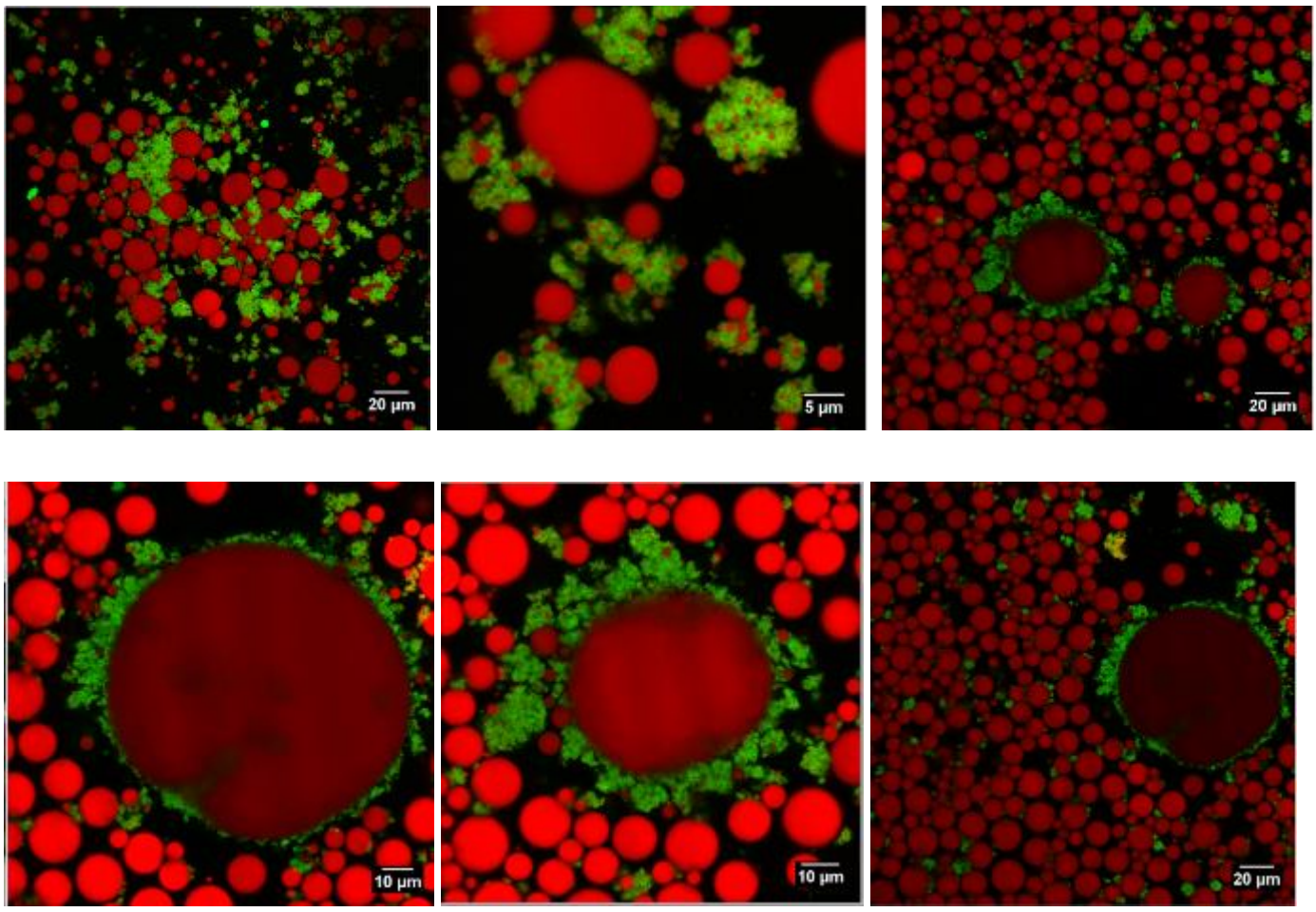

Figure A-4 *Droplet-stabilised emulsions (10%shell- 6%MPC) - MPC solution pre-heated; processed at 300 bar.*

A.2 Crystal morphology in Trimyristin droplet-stabilised emulsions

Confocal microscopy images of trimyristin DSEs and mixed trimyristin and safflower oil processed below and above 56°C showing different crystal morphologies are shown below. X-ray diffractogram of trimyristin shell emulsions and DSEs confirming presence of crystals is also shown below.

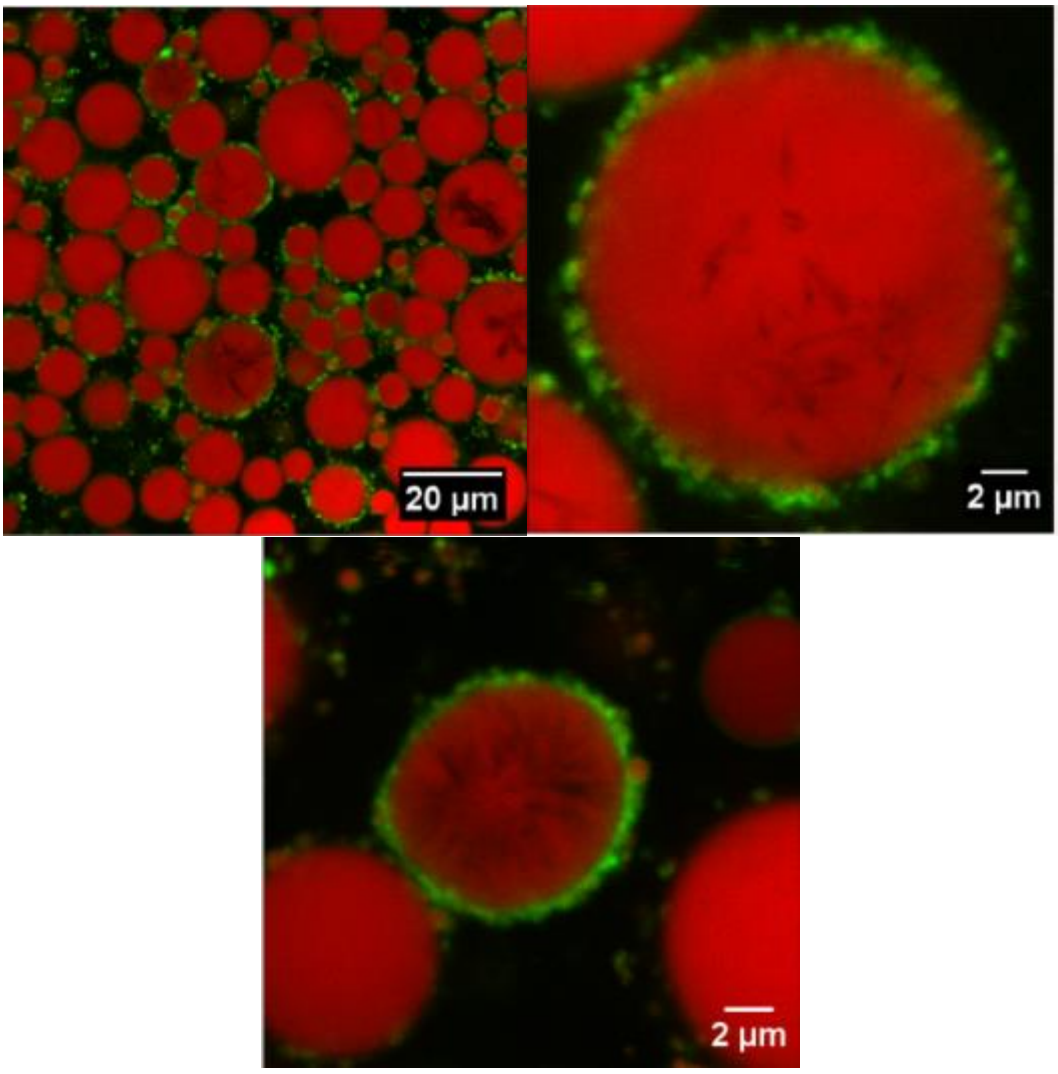

Figure A-5 *Confocal microscopy images of droplets stabilised emulsions with trimyristin surface lipid (processed above melting temperature-NT)*

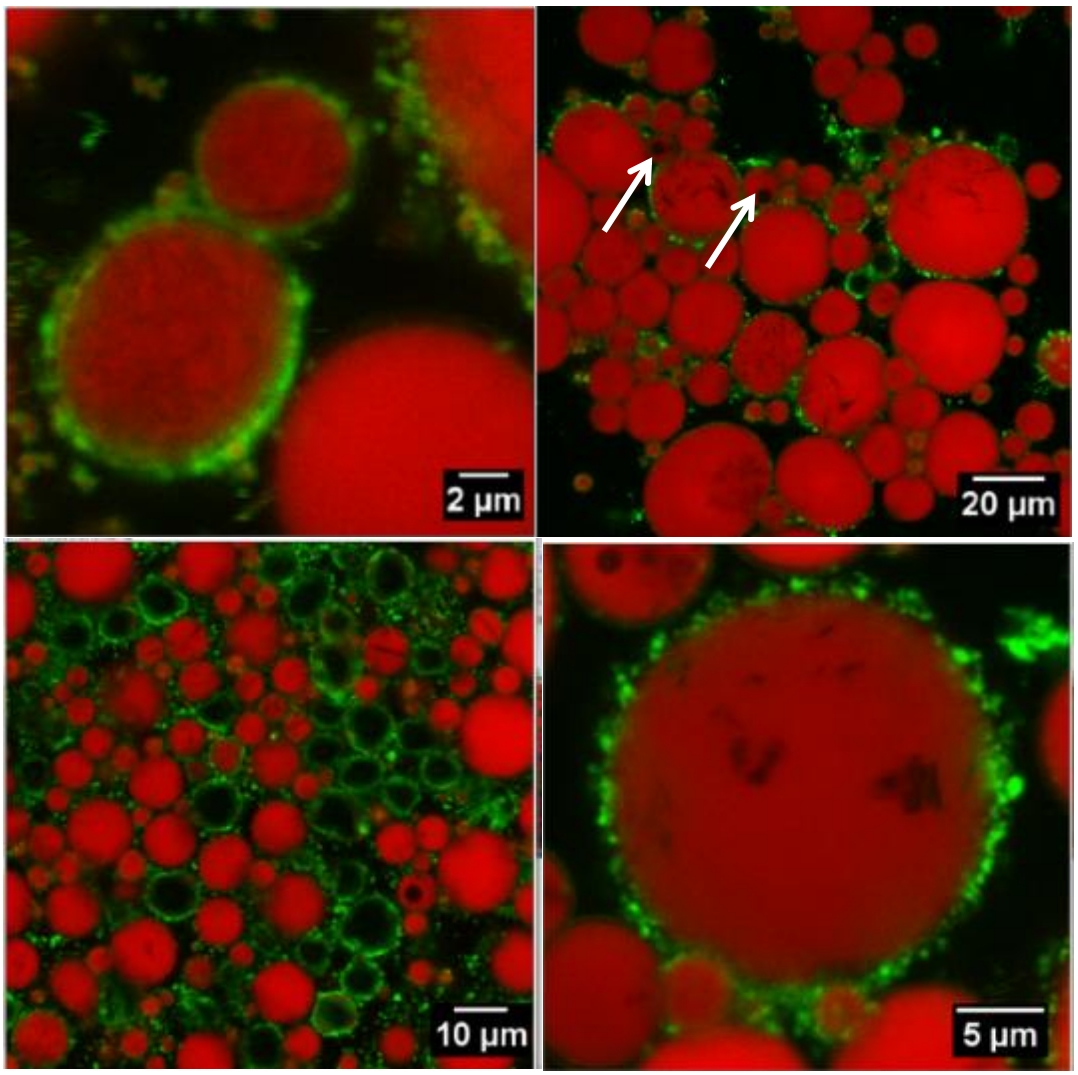

Figure A-6 *Confocal microscopy images of droplets stabilised emulsions with trimyristin surface lipid (processed below melting temperature-NT2) - Arrows show different crystal morphology from emulsion processed above melting temperature*

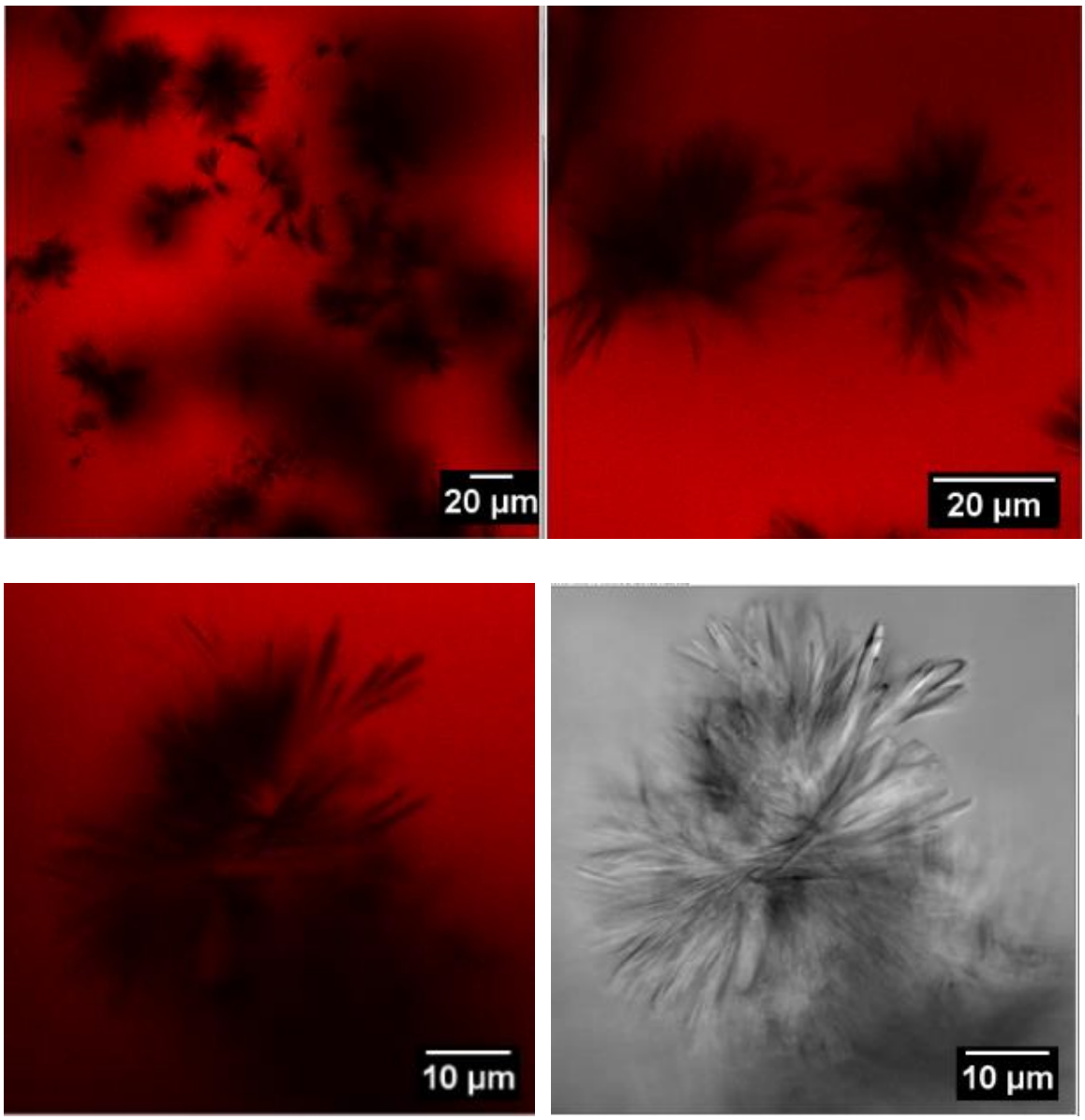

Figure A-7 *Confocal microscopy images of mixed safflower oil and trimyristin (mixture heated to 65°C).*

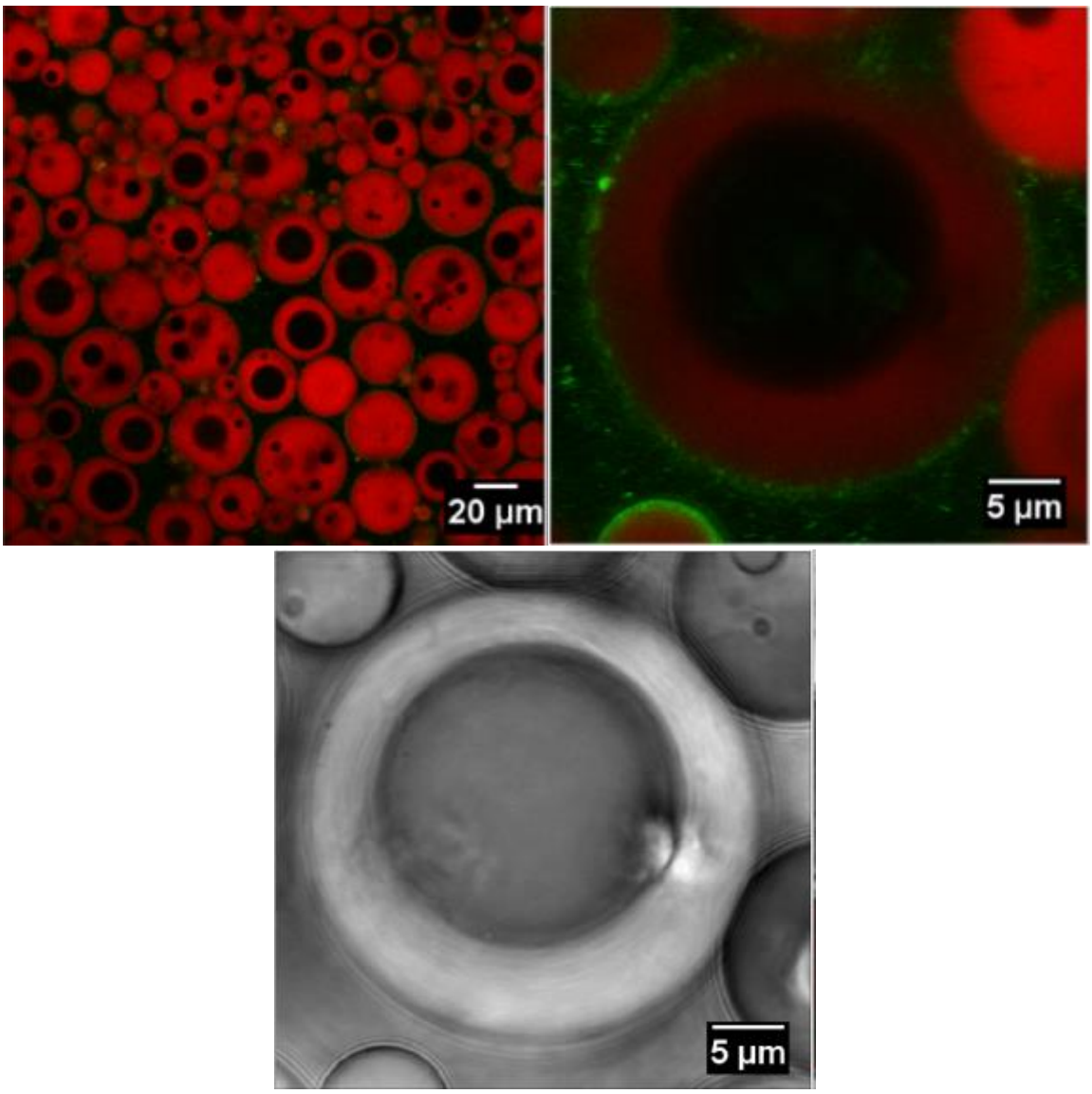

Figure A-8 *Confocal microscopy images of mixed safflower oil and trimyristin coarse emulsion homogenised at ambient temperature.*

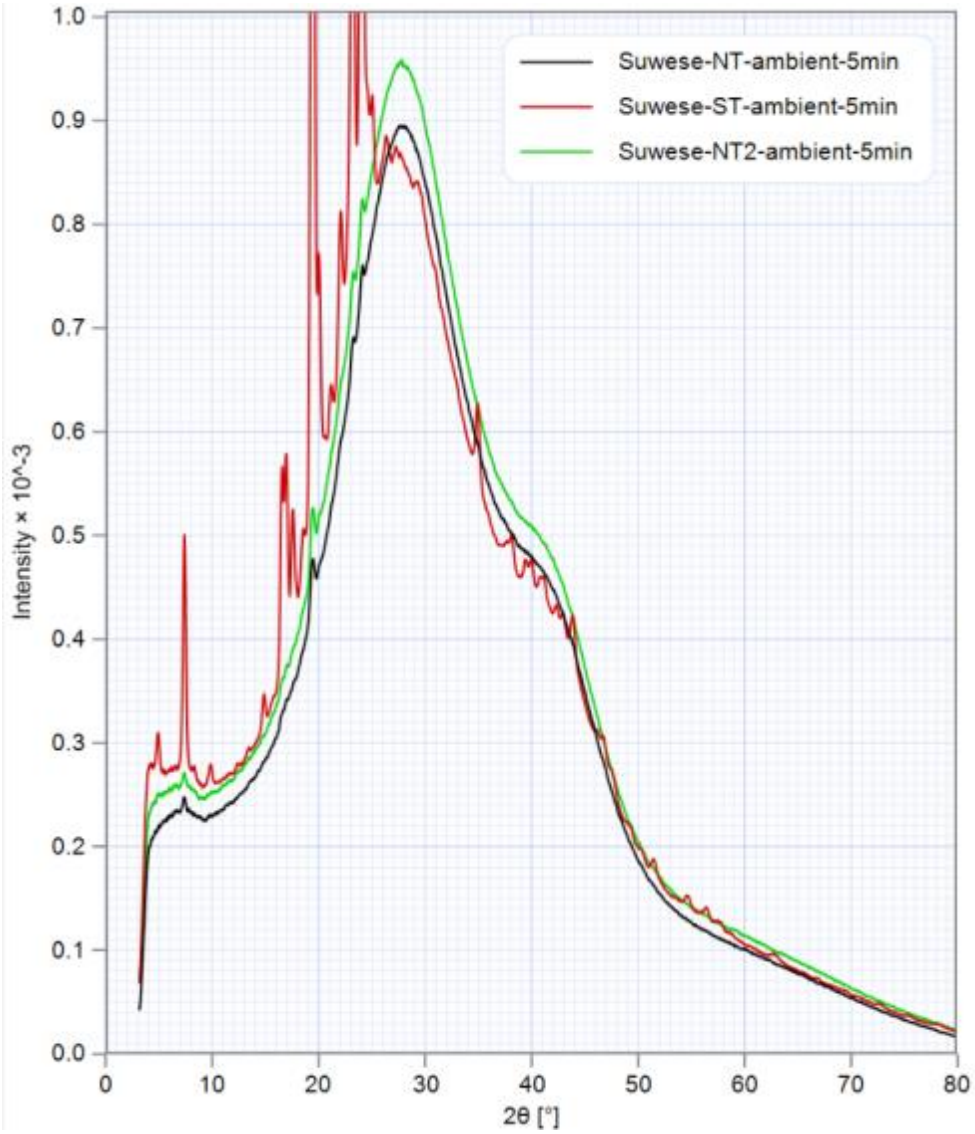

Figure A-9 *X-ray diffractogram of shell and* droplet-stabilised *emulsion- trimyristin surface lipid- ST- shell emulsion; NT- Trimyristin DSEs homogenisation at 65°C; NT2- Trimyristin DSEs homogenisation at ambient temperature.*

Appendix B (chapter 5)

B.1 Accelerated lipid oxidation conditions (Dark Vs Light)

Lipid oxidation rates of DSEs exposed to light in the presence of iron and dark at 25°C in the presence of iron are shown below. Oxidation rates were faster when exposed to light.

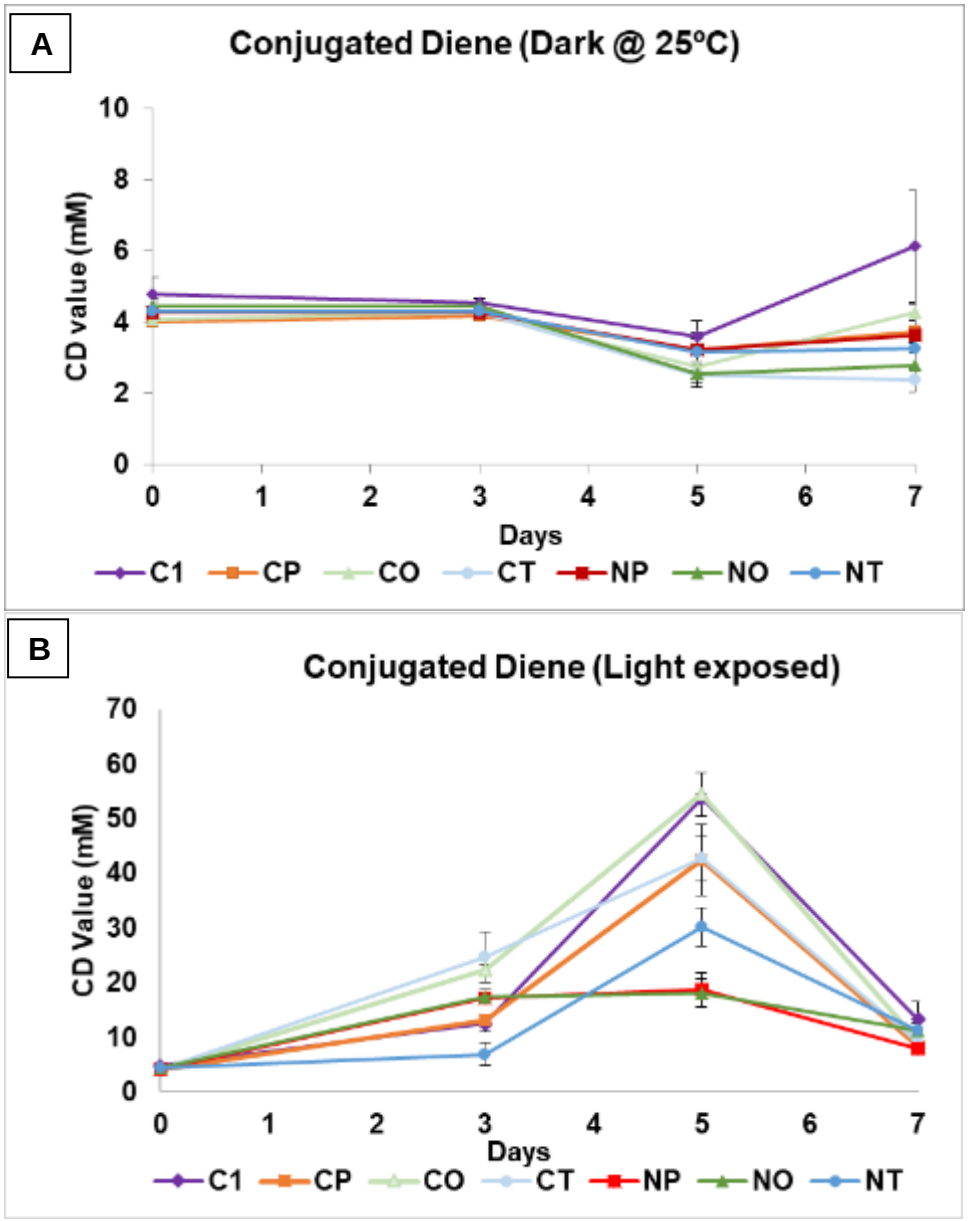

C1= Protein stabilized safflower oil-in-water emulsion; CP= C1+ shell emulsion with palmolein oil surface lipid; CO= C1+ shell emulsion with olive oil surface lipid; CT= C1+ shell emulsion with trimyristin surface lipid; NP= DSE with palmolein oil surface lipid; NO= DSE with olive oil surface lipid; NT= DSE with trimyristin surface lipid.

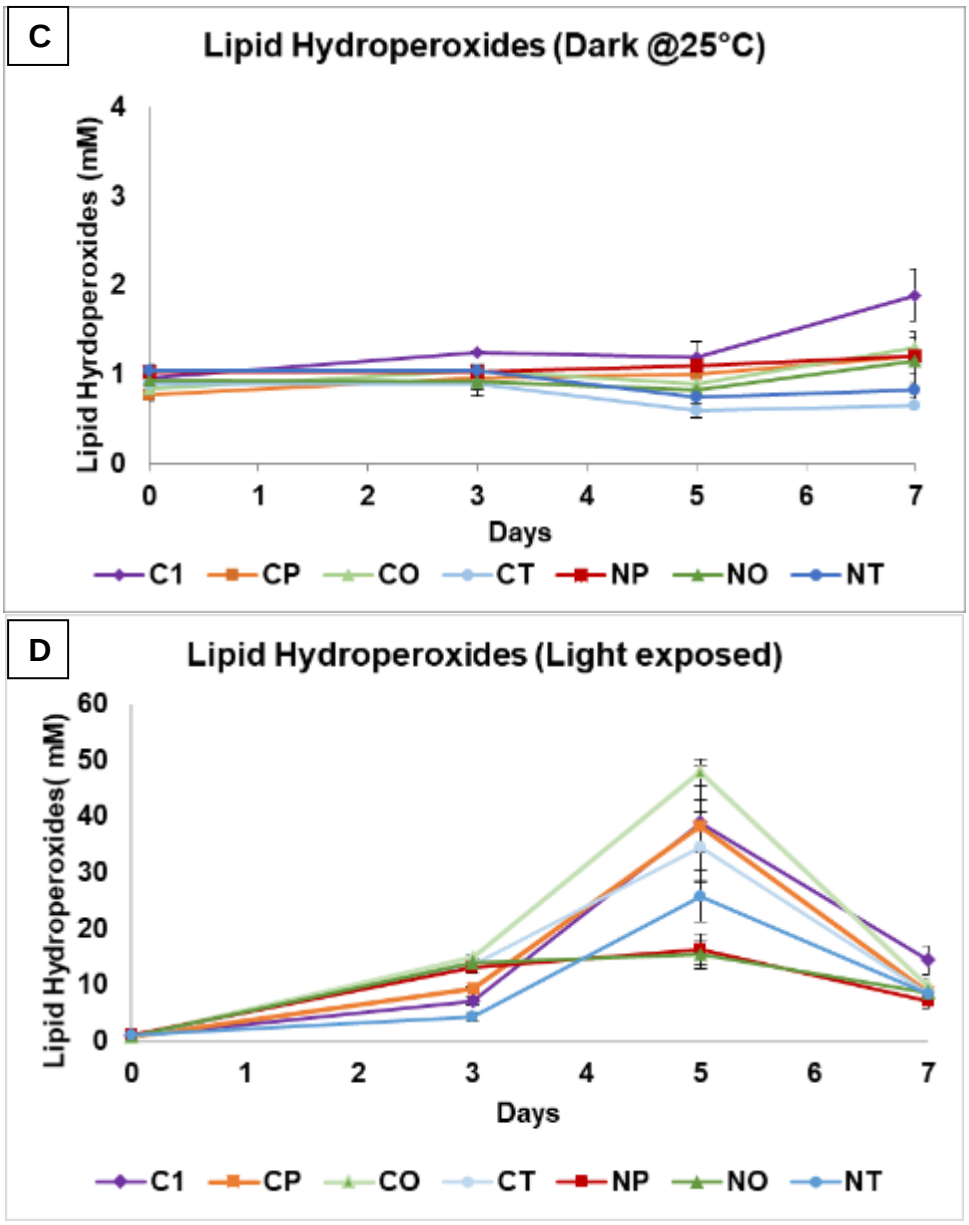

Figure A-10 *Evolution of conjugated dienes (A& B) and lipid hydroperoxides (C & D) in safflower oil core lipid in droplet-stabilised and control emulsions kept in the dark at 25°C and exposed to light in the presence of ferrous iron (100 µM).*

C1= Protein stabilized safflower oil-in-water emulsion; CP= C1+ shell emulsion with palmolein oil surface lipid; CO= C1+ shell emulsion with olive oil surface lipid; CT= C1+ shell emulsion with trimyristin surface lipid; NP= DSE with palmolein oil surface lipid; NO= DSE with olive oil surface lipid; NT= DSE with trimyristin surface lipid.

B.2 Spontaneous adsorption of shell droplets

Confocal microscopy images of composition-matched control showing spontaneous adsorption of shell droplets.

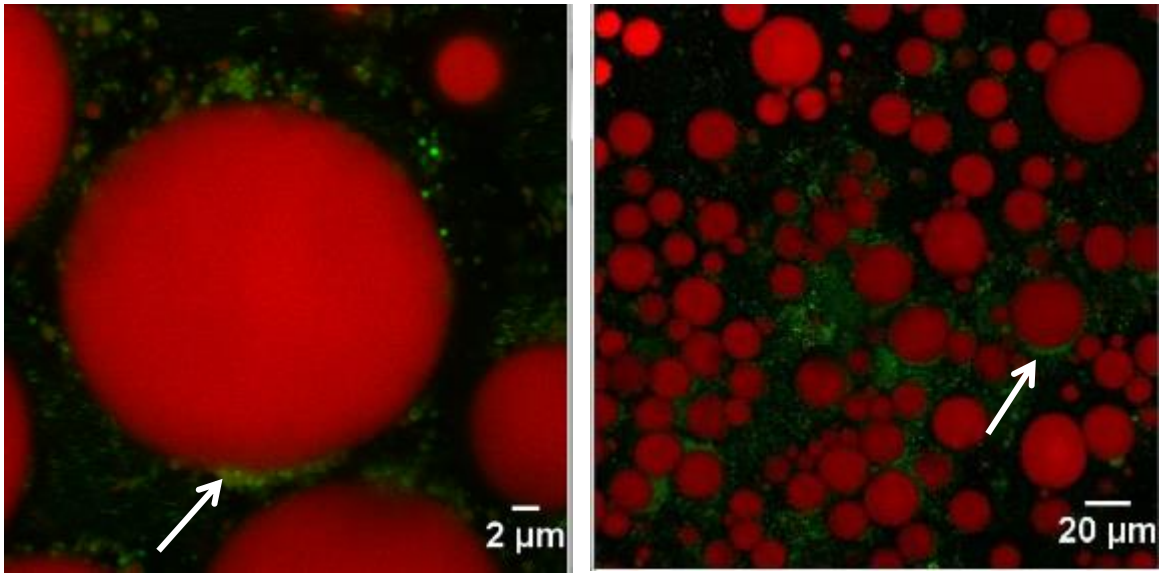

Figure A-11 *Confocal microscopy images of control emulsion with same composition as droplet-stabilised emulsion- Arrows show adsorption of added shell droplets to some core droplets.*

Appendix C (chapter 6)

C.1 Evolution of hexanal in DSEs with BHA (500 ppm)

Comparison of formation of hexanal in olive and trimyristin DSEs with BHA-in-shell and BHA-in-core (BHA-500 ppm) without control.

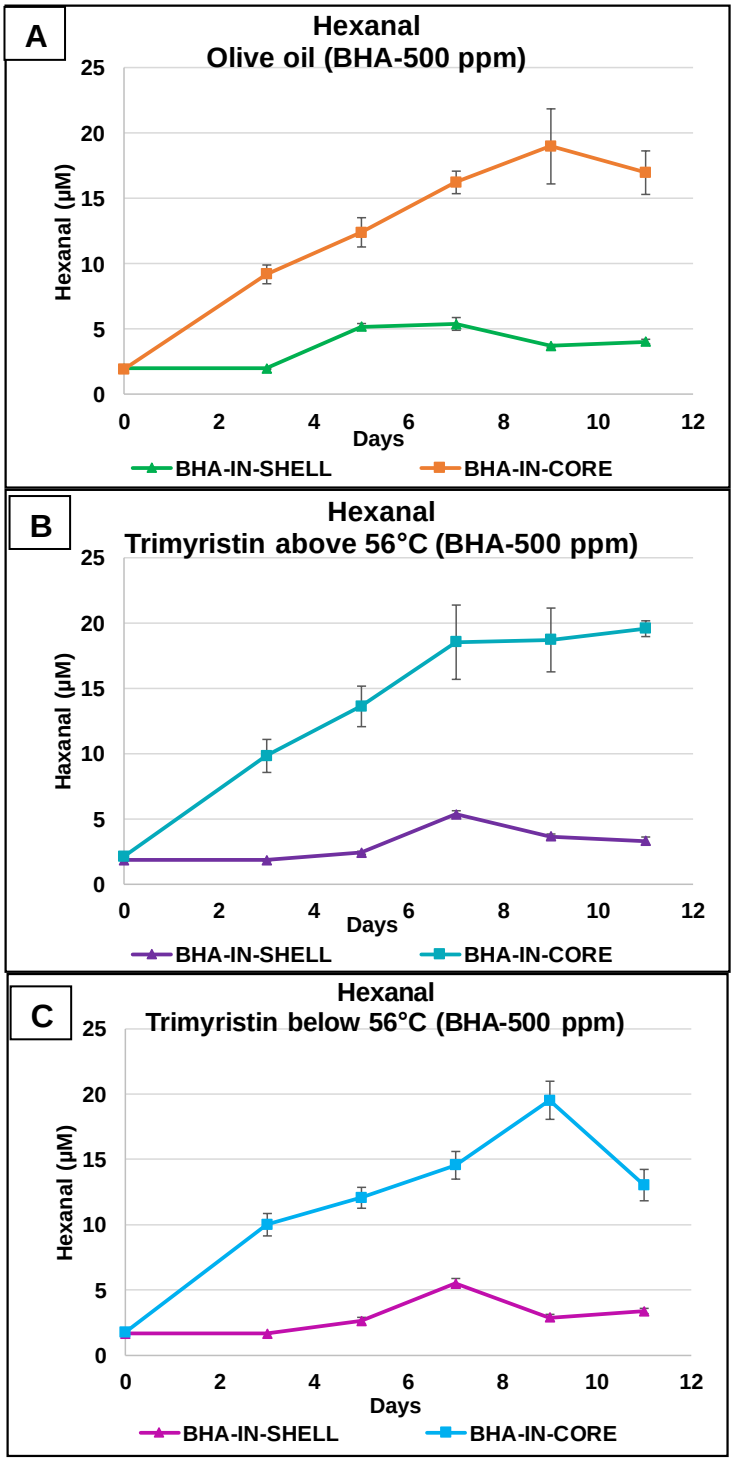

Figure A-12 *Evolution of hexanal in olive (A) and trimyristin (B&C) DSEs with BHA (500 ppm).*

Appendix D (chapter 7)

D.1 Raman spectroscopy of Olive DSEs with BHA (Microscope slides)

Confocal Raman spectra of olive DSEs with BHA-in-shell droplets are shown below. BHA exhibited poor Raman scattering properties compared to beta-carotene.

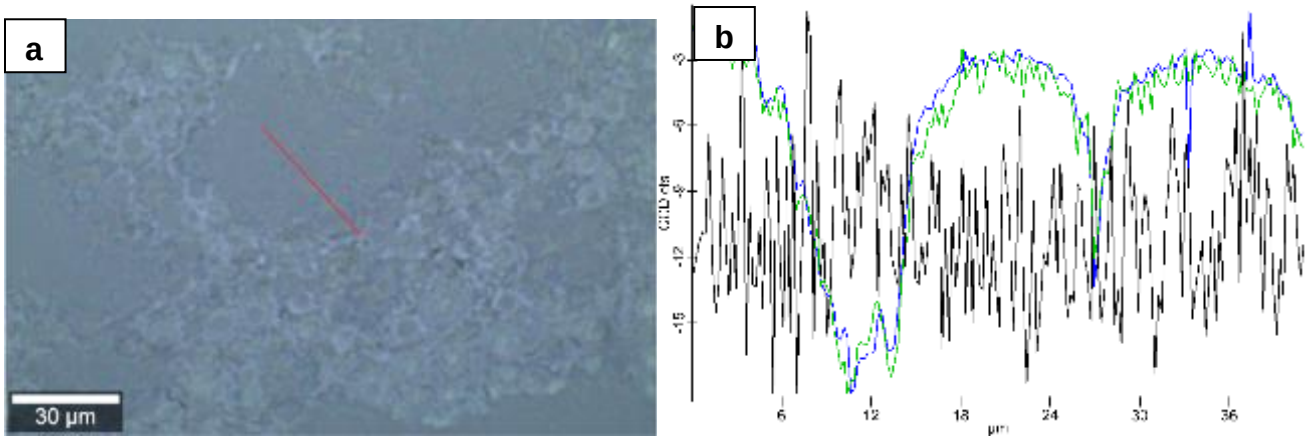

Figure A-13 *Olive DSEs with BHA-in-shell droplets with 182 points. (a) bright field reflectance mode image, (b) peak integral distribution (black trace=BHA; green trace= Olive oil; blue trace= CH group)*

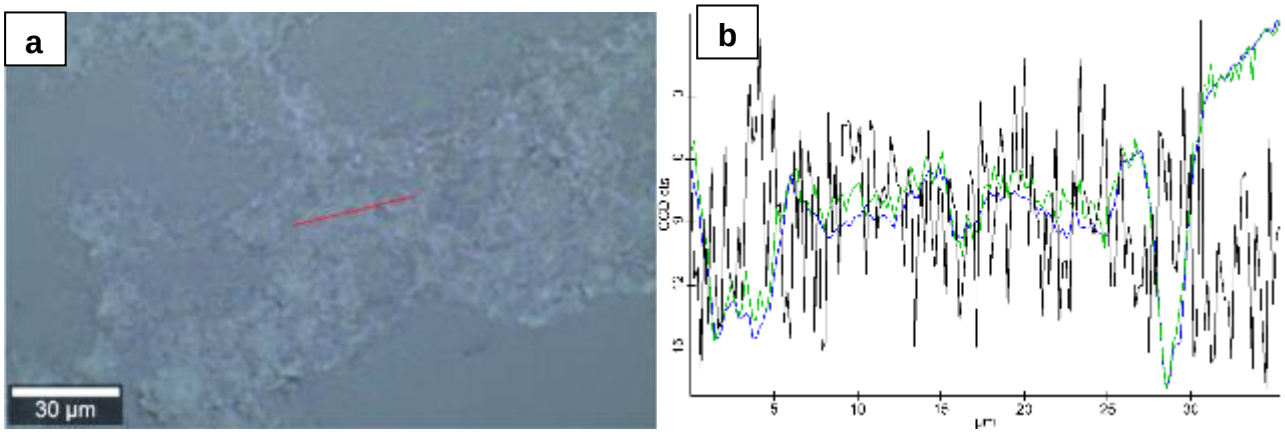

Figure A-14 *Olive DSEs with BHA-in-shell droplets with 172 points. (a) bright field reflectance mode image, (b) peak integral distribution (black trace=BHA; green trace= Olive oil; blue trace= CH group)*

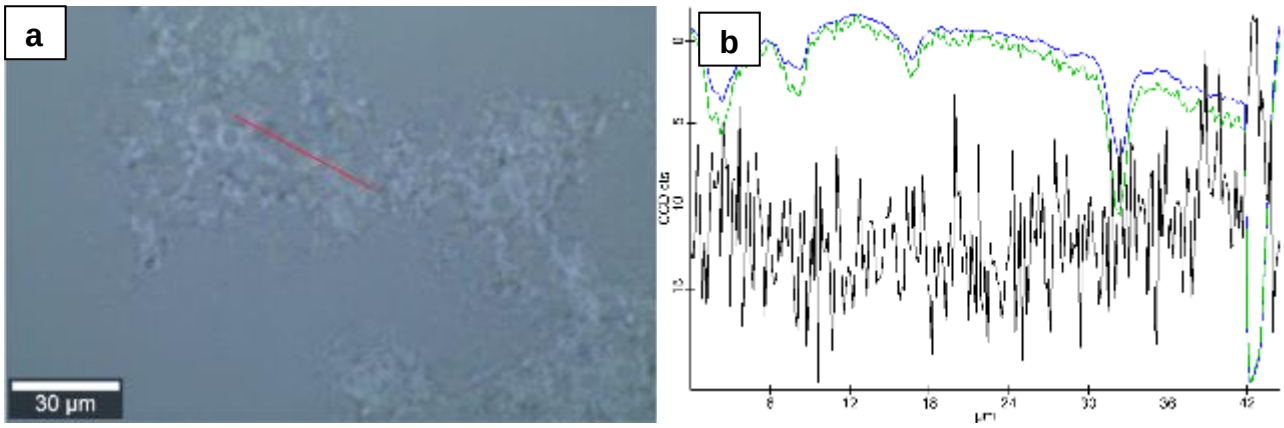

Figure A-15 *Olive DSEs with BHA-in-shell droplets with 255 points. (a) bright field reflectance mode image, (b) peak integral distribution (black trace=BHA; green trace= Olive oil; blue trace= CH group)*